



HAL
open science

Synthèse et caractérisation de capsules multicouches fonctionnelles à base de polysaccharides modifiés

Di Cui

► **To cite this version:**

Di Cui. Synthèse et caractérisation de capsules multicouches fonctionnelles à base de polysaccharides modifiés. Sciences agricoles. Université de Grenoble, 2011. Français. NNT : 2011GRENV025 . tel-00621208

HAL Id: tel-00621208

<https://theses.hal.science/tel-00621208>

Submitted on 9 Sep 2011

HAL is a multi-disciplinary open access archive for the deposit and dissemination of scientific research documents, whether they are published or not. The documents may come from teaching and research institutions in France or abroad, or from public or private research centers.

L'archive ouverte pluridisciplinaire **HAL**, est destinée au dépôt et à la diffusion de documents scientifiques de niveau recherche, publiés ou non, émanant des établissements d'enseignement et de recherche français ou étrangers, des laboratoires publics ou privés.

THÈSE

Pour obtenir le grade de

DOCTEUR DE L'UNIVERSITÉ DE GRENOBLE

Spécialité : **Sciences des polymères**

Arrêté ministériel : 7 août 2006

Présentée par

Di CUI

Thèse dirigée par **Rachel/Auzély-Velty**

préparée au sein du **Centre de Recherches sur les
Macromolécules Végétales (CERMAV-CNRS)**
dans l'**École Doctorale de Chimie et Science Vivante**

Synthesis and characterization of functional multilayer capsules based on chemically modified polysaccharides

Thèse soutenue publiquement le «**26 mai 2011**»,
devant le jury composé de :

M. Saïd SADKI

Professeur CEA – CNRS – UJF, Président

Mme. Véronique COMA

Maître de conférences, LCSV, Rapporteur

M. Benoit FRISCH

Docteur, ULP – CNRS, Rapporteur

Mme. Claudine FILIATRE

Professeur, Institut UTINAM – UMR – CNRS, Membre

Mme. Min-Hui LI

Directeur de recherche, Institut Curie – CNRS, Membre

Mme. Catherine PICART

Professeur, INPG - PHELMA de Grenoble, Membre

Mme. Annabelle VARROT

Chargé de recherche, CERMAV – CNRS, Membre

Mme. Rachel AUZELY-VELTY

Professeur, CERMAV-CNRS, Directeur de thèse



To my husband, Yuan,

To my mother,

To my father

Acknowledgments

During the three years of phd study, long hard but interesting, I not only acquired advanced academic knowledge but also gained excellent experience in life.

At first, a great appreciation is to my supervisor, Mme. Rachel AUZELY-VELTY, who brought me into the world of biopolymers and opened the door to the field of drug delivery.

Thanks M. Reduane BORSALI, the director of CERMAV, who gave me the opportunity to work in CERMAV and always helped me whenever I needed.

Sincerely appreciations are to all members of the jury of my defense for the time that they spent in evaluating my work and all interesting remarks: M. Saïd SADKI (Président), Mme. Véronique Coma (Reporter), M. Benoit Frisch (Reporter), Mme. Claudine FILIATRE (Examiner), Mme. Min-hui, LI (Examiner), Mme. Catherine PICART (Examiner) and Mme. Annabelle VARROT (Examiner).

Thanks the French government for the funding during my phd study.

A special appreciation is to Anna SZARPAK for her selfless given, the precise experience in the synthesis and characterization of capsules. I benefited a lot from the collaboration and discussions with her.

Thanks Catherine PICART for availability of QCM-D and invaluable advices during my PhD study, also thanks to Thomas, Claire and Kefeng.

I am also appreciated to Isabelle PIGNOT-PAINTRAND, Amandine DURAND-TERRASON, Frédéric CHARLOT, Isabelle JEACOMINE, Eric BAYMA, Marie-France MARAIS, Anne IMBERTY, Christophe TRAVELET and Sonia ORTEGA-MURILLO for their technique supporting in my phd work. Specially thanks Isabelle PIGNOT-PAINTRAND for her expert suggestions in microscopy.

Thanks Annabelle VARROT, Christophe DETREMBLEUR (Belgium), Christine JEROME (Belgium), Sandrine LENOIR (Belgium) and Hilde MELLEGARD (England) for their help in the antibacterial assessments. Specially thanks Sandrine for her kind reception during my diary days in Belgium.

I am appreciated Bjorn E. CHRISTENSEN (Norway), who provided the measurement of SEC and give me the scientific advices in polymers characterization.

Thanks Bruno DE GEEST for his expert opinions in synthesis and characterization of capsules as well as the satisfying collaboration in the biological studies of capsules. Specially thanks for his participation in my defense.

Thanks all members of CERMAV for giving me a kind, friendly and open atmosphere in the lab. Specially thanks the young colleagues in our groups, Catherine, Shirin, Caroline, H  l  ne, Xia, Jing, Agathe, Emilie, Julie and Jimmy, with whom I enjoyed a lot.

The last but the most important appreciation is to all members in my family, my parents and my husband. Without for their firm support and the selfless love, I can not arrive here. I love you.

Abstract

This work focused on the design of functional capsules made of chemically modified polysaccharides. The layer-by-layer capsules have attracted great interest due to their advanced multifunctionality, which can be advantageously used for pharmaceutical and biomedical applications. Polysaccharides, which are generally biocompatible and biodegradable, are very attractive materials for the construction of bio-related multilayer systems. Considering the intrinsic antibacterial properties of chitosan (CHI), this polysaccharide was selected and quaternized to prepare in physiological conditions contact-killing capsules by combination with hyaluronic acid (HA). The relationship between the antibacterial activity of the quaternized chitosan derivatives (QCHI) and that of QCHI-based capsules was investigated. Then, in order to encapsulate small hydrophobic drugs within the wall of capsules, alkylated derivatives of HA were used as the negatively charged partner of QCHI for the capsules formation. The encapsulation of the hydrophobic dye, Nile red (NR), in the hydrophobic shell of capsules was determined. At last, to release the payload under mild conditions was studied by synthesizing rapidly degradable capsules composed of hydrolysable cationic dextran derivatives and HA. The degradation of the layer-by-layer assemblies, both multilayer films and microcapsules is discussed.

Key words: layer-by-layer, polysaccharides, microcapsules, antibacterial activity, hydrophobic drug encapsulation, biodegradability

Résumé

Ce travail de thèse porte sur la conception de capsules fonctionnelles à base de polysaccharides chimiquement modifiés. Les capsules couche par couche connaissent actuellement un essor important lié à leur multifonctionnalité pouvant être avantageusement mise à profit dans les domaines pharmaceutique et biomédical. Les polysaccharides, généralement biocompatibles et biodégradables, constituent des matériaux de choix pour la construction de systèmes multicouches. Compte tenu des propriétés antibactériennes intrinsèques du chitosane (CHI), ce polysaccharide a été choisi puis quaternisé afin de préparer dans des conditions physiologiques des capsules par complexation avec l'acide hyaluronique (HA), capables de tuer les bactéries par simple contact. La relation entre l'activité antibactérienne des dérivés quaternisés du chitosane (QCHI) et celle des capsules préparées à partir de QCHI a été étudiée. En outre, afin d'encapsuler des médicaments hydrophobes dans la paroi des capsules, des dérivés alkylés du HA ont été utilisés en tant que partenaire chargé négativement du QCHI pour la formation des capsules. L'encapsulation d'une sonde fluorescente hydrophobe, le Nile rouge (NR), dans le réservoir hydrophobe des capsules a été réalisée avec succès. Enfin, pour libérer des médicaments encapsulés dans des capsules dans des conditions douces, des capsules rapidement dégradables comprenant des dérivés cationiques hydrolysables du dextrane et de HA ont été préparées. La dégradation des assemblages couches par multicouches a été analysée par différentes approches à la fois à partir de capsules et de films plans.

Mots clés: Déposition couche par couche, polysaccharides, microcapsules, activité antibactérienne, encapsulation de médicaments hydrophobiques, biodégradabilité

Table of contents

General introduction (<i>En</i>)	1
Introduction Générale (<i>Fr</i>).....	5
References:	8

Chapter 1 Antibacterial activity of chitosan (CHI) and its derivatives. Application to the synthesis of contact-killing multilayer films 9 |

1	Résumé (<i>Fr</i>)	11
1.1	Introduction	13
1.2	Mode of action to inhibit the growth of bacteria.....	16
1.3	Factors influencing the antibacterial activity of CHI.....	16
1.3.1	Antibacterial activity of native CHI on different bacteria types	17
1.3.2	Effect of experimental conditions	20
1.3.2.1	Concentration of CHI	20
1.3.2.2	pH of the medium.....	21
1.3.2.3	Other factors.....	22
1.3.3	Effect of the nature of CHI.....	23
1.3.3.1	Role of the intrinsic characteristics of native CHI	23
1.3.3.2	Antibacterial activity of chemically modified CHI derivatives	25
1.4	Antibacterial multilayer films based on CHI	41
1.5	Antibacterial multilayer films based on synthetic polyelectrolytes	43
1.6	Conclusion.....	46
	References:	47

Chapter 2 Contact-killing microcapsules based on quaternized chitosan (QCHI) derivatives 51 |

2	Résumé (<i>Fr</i>)	53
2.1	Introduction	55
2.2	Synthesis and characterization of QCHI derivatives.....	57
2.2.1	Synthesis of QCHI derivatives under different conditions	57
2.2.2	Macromolecular characterization of QCHI derivatives	60
2.2.2.1	Measurement of intrinsic viscosity	60
2.2.2.2	Determination of the molar mass by size exclusion chromatography (SEC)	63
2.2.3	Antibacterial activity	65
2.3	Synthesis of capsules based on the QCHI derivatives	67
2.3.1	Utilization of <i>N</i> -QCHI derivatives as the cationic partners of HA for the synthesis of capsules	67
2.3.1.1	Publication in Advanced Functional Materials ¹²	68
2.3.1.2	Supporting information	91
2.3.1.3	Complementary results.....	94
2.3.2	Utilization of <i>N,O</i> -QCHI derivatives as the cationic partners of HA for the synthesis of capsules	99
2.3.2.1	Syntheses of capsules based on <i>N,O</i> -QCHI derivatives.....	99
2.3.2.2	Antimicrobial activity of (HA/ <i>N,O</i> -QCHI) capsules	105

2.4	Conclusion.....	108
2.5	Complementary experimental part	109
	References:	111

Chapter 3 Hydrophobic shell loading of biopolyelectrolyte capsules 113

3	Résumé (<i>Fr</i>)	115
3.1	Submitted article to Advanced Materials (accepted)	117
3.2	Supporting information	128
3.3	Complementary results.....	131
3.3.1	Factors affecting the feasibility of capsule formation.....	131
3.3.2	Permeability of capsules.....	135
3.3.3	Antibacterial activity of capsules	136
	References:	138

Chapter 4 Synthesis of rapidly degradable gel-like microvectors based on hydrolysable polysaccharides..... 139

4	Résumé (<i>Fr</i>)	141
4.1	Introduction	143
4.2	Synthesis of cationic hydrolysable polysaccharides	148
4.3	Hydrolysis of dextran-DMAE.....	152
4.4	Polyelectrolyte complexation between dextran-DMAE and HA.....	155
4.5	Hydrolyze of capsules based on HA/Dextran-DMAE	159
4.5.1	Hydrolysis under neutral conditions	160
4.5.2	Hydrolysis under alkaline conditions.....	162
4.6	Conclusion.....	164
4.7	Experimental part	165
	References:	168

General conclusion and perspectives (*En*) 171

Conclusion générale et perspectives (*Fr*) 175

	Annexes.....	177
	List of Figures	177
	List of Schemes	181
	List of Tables.....	182
	Abbreviations	183
	Symbols.....	183
	List of Instruments	183

General introduction (*En*)

Controlled delivery of hydrophilic and hydrophobic drugs is currently a great challenge in the field of nanobiotechnology. During the past decades, a large variety of micro- and nanocarriers have been developed in order to improve efficiency, availability and toxicity profiles of biotechnological macromolecular therapeutics, such as peptides, proteins and oligonucleotides. The problem of delivery is also crucial for small water-insoluble organic compounds, which constitute a great part of the currently available drugs used in anti-cancer therapy. Besides the well known lipid-based carriers such as liposomes, the development of nanoparticles and emulsion-based nanocapsules has gathered increased interest in the pharmaceutical field and layer-by-layer hollow microcapsules are emerging as a novel potential therapeutic tool. These LbL hollow capsules, also called polyelectrolyte multilayer capsules, possess a fascinating multicompartmental structure, with the possibility to introduce a high degree of functionality within their nanoshell. The latter is constructed by the consecutive adsorption of oppositely charged species onto a spherical sacrificial template. It can consist of various types of polymers, but these have to sustain the core removal step. Interestingly, the shell can be designed to efficiently respond to various environmental changes, allowing the programmed release of active substances contained within the capsule. Recent developments of polyelectrolyte microcapsules in life sciences include the use of polypeptides and polysaccharides as shell components, as these are biocompatible and biodegradable but these require the core to be removed in mild conditions. Nevertheless, polyelectrolyte microcapsules based on polysaccharides are only emerging, due to the inherent difficulties in preparing such capsules, which are related to the “hydrogel-type” and softness of the polysaccharide multilayer films.

In this context, previous work in our laboratory focused on the design of biocompatible and biodegradable capsules based on hyaluronic acid (HA), a natural polysaccharide which plays an important structural and biological role in the living organisms.¹ In spite of its highly hydrated nature and tendency to form soft hydrogel-type multilayer films, capsules consisting of HA and poly(allylamine) (PAH) could be successfully obtained without chemically cross-linking the layers. These capsules were prepared using calcium carbonate particles as sacrificial templates due to their biocompatibility and their ability to be readily dissolved under mild conditions. As the goal was to obtain fully biodegradable capsules, PAH was then replaced by a biocompatible and biodegradable polypeptide, namely poly(L-lysine) (PLL) but

shell cross-linking was required to improve capsule stability. These capsules containing HA could be taken up by the phagocytosing cells and in contrast to other types of capsules, deformed fast inside of cells, which offers perspective of using such capsules as intracellular delivery carriers.

Based on these results, the aim of this work was to prepare capsules made entirely of polysaccharides, combining their biodegradable and biocompatible properties together with specific biological activities. To this end, we selected chitosan (CHI), one of the most abundant natural biopolymers and the only natural polycationic polysaccharide, which is widely used in the biomedical field. To circumvent the inherent drawback of CHI (low solubility in physiological conditions due to its pK_a at 6), which hinders the film build-up at neutral pH as well as causing problems for subsequent core dissolution, we synthesized water-soluble quaternized chitosan (QCHI) derivatives. The latter cationic polymers, showing antibacterial activity, were first used to design antibacterial delivery system based on the contact killing strategy. This strategy seeks to biochemically induce death of bacteria that have adhered to the material surface. Having developed contact killing capsules with good mechanical stability, we next used these water-soluble quaternized chitosan (QCHI) derivatives to prepare capsules that can selectively encapsulate and subsequently deliver poorly water-soluble drugs. For this purpose, we developed a versatile method based on the encapsulation of small hydrophobic molecules in the nanoshell. This relies on the very high affinity of hydrophobic molecules for HA modified with alkyl chains, previously developed in our laboratory². Capsules containing alkylated HA and QCHI were thus shown to efficiently entrap hydrophobic molecules. Since these capsules were made solely on biodegradable polysaccharides derivatives, the simplest strategy to release payload from these capsules was thought to be the enzymatic degradation. However, several studies in our laboratory indicated that the enzymatic degradation of polysaccharide-made capsules requires a rather high concentration of enzyme (500 U/ml), i.e. ~ 250 fold higher than that in human serum. So, in the last part of this work, we proposed to develop fast degradable capsules based on HA and dextran derivatives bearing labile cationic groups. These capsules were expected to be destructed rapidly by polyelectrolyte decomposition and enzymatic degradation of polysaccharides.

This thesis manuscript is divided into four sections:

The first chapter overviews the antibacterial activity of CHI and its derivatives as well as its use for the construction of multilayer films and capsules.

In the second chapter, the synthesis and the characterization of contact-killing capsules based on HA and QCHI derivatives are presented. We first describe the synthesis of water-soluble QCHI derivatives under two different conditions as well as their macromolecular and anti-bacterial properties. We then report on the synthesis of capsules based on QCHI derivatives and analyze in particular the effect of degree of substitution and macromolecular properties of the QCHI derivatives on the size, morphology and permeability of hollow capsules. The antibacterial properties of the capsules based on QCHI derivatives against *E. Coli* are determined.

Chapter 3 deals with capsules based on alkylated HA derivatives and QCHI derivatives. The strategy to obtain stable capsules as well as shell loading using Nile red as a hydrophobic dye is discussed. The permeability and antibacterial properties of the capsules with hydrophobic shells are also determined.

In the chapter 4, the synthetic route to fast degradable capsules based on dextran derivatives bearing labile cationic groups is presented. The cationic dextran derivatives containing carbonate ester groups are prepared under different conditions. The resulting dextran derivatives are then used as a polycationic partner of HA to design gel-like microvectors. The degradability of polymers, the formation and degradability of multilayer films and microvectors based on HA and cationic dextran derivatives are investigated.

Introduction Générale (*Fr*)

La libération contrôlée de médicaments hydrophiles et hydrophobes est actuellement un grand défi dans le domaine des nanobiotechnologies. Au cours des dernières décennies, une grande variété de micro- et nano-transporteurs a été développée afin d'améliorer les profils d'efficacité, de disponibilité et de toxicité de macromolécules biologiquement actives fragiles, tels que des peptides, des protéines et des oligonucléotides. Le problème de la libération est aussi crucial pour les composés organiques de petite taille insolubles dans l'eau, qui constituent une grande partie des médicaments actuellement disponibles utilisés dans la thérapie anti-cancéreuse. Outre les systèmes transporteurs bien connus à base de lipides tels que les liposomes, le développement de nanoparticules et nanocapsules à base d'émulsions a recueilli un intérêt accru dans le domaine pharmaceutique et les microcapsules multicouches creuses apparaissent comme un nouvel outil thérapeutique prometteur. Ces systèmes multicompartiments sont préparés par la technique de dépôt couche-par-couche qui offre la possibilité d'introduire un degré élevé de fonctionnalité au sein de la paroi. Selon cette technique, des polyélectrolytes de charges opposées sont déposés alternativement sur des particules sacrificielles. Fait intéressant, la paroi peut être conçue pour répondre efficacement à divers stimuli extérieurs, permettant la libération programmée de substances actives contenues dans la capsule. Les développements récents de microcapsules de polyélectrolytes liés aux sciences de la vie incluent l'utilisation de polypeptides et de polysaccharides comme constituants de la paroi, car ils sont biocompatibles et biodégradables, mais l'utilisation de ces biopolymères fragiles exige des conditions douces pour dissoudre le cœur. Les microcapsules à base de polysaccharides sont néanmoins encore peu étudiées, du fait des difficultés inhérentes à leur préparation ainsi que de la propriété particulière des polysaccharides à former des films multicouches mous et fortement hydratés.

Dans ce contexte, les travaux antérieurs dans notre laboratoire se sont focalisés sur la conception de capsules biocompatibles et biodégradables à base d'acide hyaluronique (HA), un polysaccharide naturel qui joue des rôles structurel et biologique majeurs dans les organismes vivants.¹ Bien que le HA ait tendance à former des films multicouches ayant un comportement de type gel, des capsules constituées de HA et de poly (allylamine) (PAH) ont pu être obtenues avec succès sans réticuler les couches formant la paroi. Ces capsules ont été préparées en utilisant des particules de carbonate de calcium en tant que supports sacrificiels en raison de leur biocompatibilité et leur capacité à être facilement décomposées dans des

conditions douces. Dans la mesure où le but était d'obtenir des capsules entièrement biodégradables, le PAH a ensuite été remplacé par un polypeptide biocompatible et biodégradable, à savoir la poly(L-lysine) (PLL), mais la réticulation chimique de la paroi s'est avérée nécessaire pour améliorer la stabilité des capsules. Il a été démontré que ces capsules pouvaient être capturées par des cellules phagocytaires et, qu'elles se déformaient rapidement à l'intérieur des cellules, contrairement à d'autres types de capsules à base de polymères synthétiques. Ceci offre des perspectives intéressantes pour la délivrance intracellulaire de médicaments.

Sur la base de ces résultats, l'objectif de ce travail était de préparer des capsules composées entièrement de polysaccharides, en mettant à profit leurs propriétés de biodégradabilité et biocompatibilité et leur activité biologique spécifique. Dans cet objectif, nous avons choisi le chitosane (CHI), qui est l'un des biopolymères naturels les plus abondants et le seul polysaccharide polycationique. Afin de contourner l'inconvénient inhérent au CHI (faible solubilité dans des conditions physiologiques en raison de son pK_a voisin de 6), qui empêche la construction de films multicouches à pH neutre et qui cause des problèmes liés à la dissolution du cœur de carbonate de calcium à $pH < 6$, nous avons synthétisé des dérivés quaternisés du chitosane (QCHI) solubles dans l'eau à pH neutre. Ces dérivés quaternisés, qui présentent une activité antibactérienne, ont tout d'abord été utilisés pour la conception de systèmes transporteurs antibactériens capables de tuer des bactéries par simple contact. Cette stratégie vise en effet à induire la mort biochimique des bactéries qui ont adhéré à la surface du matériau. Après avoir développé des capsules stables à base de HA/QCHI bactéricides, nous avons ensuite utilisé les dérivés QCHI pour préparer des capsules pouvant incorporer de manière sélective des molécules hydrophobes dans leur paroi, laissant la cavité aqueuse libre pour accueillir des molécules hydrophiles. Dans cet objectif, nous avons développé une méthode polyvalente basée sur l'encapsulation de petites molécules hydrophobes dans la paroi. Celle-ci s'appuie sur la très forte affinité de molécules hydrophobes pour l'acide hyaluronique modifié par des chaînes alkyle, précédemment développés dans notre laboratoire². Des capsules à base de HA et de QCHI, capables de piéger de manière efficace des molécules hydrophobes, ont ainsi pu être obtenues. Puisque ces capsules contiennent uniquement des dérivés de polysaccharides biodégradables, la stratégie la plus simple pour libérer les molécules encapsulées apparaît être la dégradation par des enzymes présentes dans le corps. Cependant, plusieurs études dans notre laboratoire indiquent que la dégradation des capsules par la hyaluronidase (qui dépolymérise le HA)

nécessite une concentration relativement élevée de l'enzyme (500 U/ml), soit environ 250 fois supérieure à celle dans le sérum humain. Ainsi, dans la dernière partie de ce travail, nous avons proposé de développer des capsules rapidement dégradables à base de HA et de dérivés du dextrane portant des groupements cationiques labiles. Ces capsules devraient être détruites rapidement par décomplexation des polysaccharides partenaires constituant la paroi ainsi qu'à leur dégradation enzymatique.

Ce manuscrit de thèse est composé de quatre chapitres:

Le premier chapitre donne un aperçu des propriétés antibactériennes du CHI et de ses dérivés ainsi que de son utilisation pour la construction de films et capsules multicouches.

Dans le deuxième chapitre, la synthèse et la caractérisation de capsules à base de HA et de dérivés QCHI capables de tuer les bactéries par simple contact sont présentées. Nous décrivons d'abord la synthèse de dérivés QCHI solubles dans l'eau à pH neutre ainsi que leurs propriétés macromoléculaires et antibactériennes. La synthèse de capsules à base de dérivés QCHI est ensuite abordée, en analysant en particulier l'effet du degré de substitution (DS) et des caractéristiques macromoléculaires des dérivés QCHI sur la morphologie et la perméabilité des capsules creuses. Les propriétés antibactériennes des capsules à base de dérivés QCHI contre *E. Coli* sont discutées.

Le chapitre 3 traite des capsules à base de dérivés alkylés de HA et de dérivés QCHI. La stratégie visant à obtenir des capsules stables ainsi que l'incorporation dans la paroi d'une sonde fluorescente hydrophobe, le « Nile red » sont discutées. Les propriétés de perméabilité et antibactériennes des capsules à parois hydrophobes sont également déterminées.

La synthèse de capsules rapidement dégradables à partir de dérivés de dextrane porteurs de groupements cationiques labiles fait l'objet du chapitre 4. Les dérivés de dextrane sont obtenus par formation de liaisons ester de carbonate selon différentes conditions de synthèse. Ces polymères sont ensuite utilisés en tant que partenaires polycationiques du HA pour concevoir des microvecteurs de type gel. L'hydrolyse des groupements greffés sur le dextrane, la formation et la dégradabilité des films multicouches et microvecteurs à base de HA et de dérivés de dextrane porteurs de groupements cationiques labiles sont analysées à la fin de ce chapitre.

References:

- (1) Szapark, A. *Thesis* 2009.
- (2) Kadi, S. *Thesis* 2007.

Chapter 1

Antibacterial activity of chitosan (CHI) and its derivatives.
Application to the synthesis of contact-killing multilayer films

- *Bibliography review*

Table of contents

1	Résumé (<i>Fr</i>)	11
1.1	Introduction	13
1.2	Mode of action to inhibit the growth of bacteria.....	16
1.3	Factors influencing the antibacterial activity of CHI	16
1.3.1	Antibacterial activity of native CHI on different bacteria types	17
1.3.2	Effect of experimental conditions	20
1.3.2.1	Concentration of CHI	20
1.3.2.2	pH of the medium.....	21
1.3.2.3	Other factors.....	22
1.3.3	Effect of the nature of CHI.....	23
1.3.3.1	Role of the intrinsic characteristics of native CHI	23
1.3.3.2	Antibacterial activity of chemically modified CHI derivatives	25
1.4	Antibacterial multilayer films based on CHI	41
1.5	Antibacterial multilayer films based on synthetic polyelectrolytes	43
1.6	Conclusion.....	46
	References:	47

1 Résumé (*Fr*)

Ce chapitre, situant le travail dans son contexte bibliographique, porte sur les propriétés antibactériennes du chitosane (CHI) et ses dérivés ainsi que son utilisation pour élaborer des films multicouches antibactériens. Le CHI est largement utilisé comme partenaire polycationique dans la construction de films fins par complexation polyanion-polycation. Il constitue le seul polysaccharide d'origine naturel chargé positivement. Ses propriétés de biocompatibilité et biodégradabilité en font par ailleurs un bon candidat pour le développement de biomatériaux. Le CHI présente en outre des propriétés antibactériennes qui ont été mises à profit pour concevoir des revêtements capables de tuer les bactéries par simple contact. L'analyse bibliographique indique que l'efficacité du CHI et de ses dérivés à tuer les bactéries dépend du type de bactérie, de la nature du CHI et de ses dérivés ainsi que des conditions expérimentales. La masse molaire du CHI, son degré d'acétylation, la nature et la position des groupements chimiques greffés ont ainsi un impact important sur les propriétés antibactériennes. L'étude des films à base de CHI suggère que l'effet d'inhibition de films multicouches est non seulement lié à l'activité antibactérienne du CHI, mais aussi aux propriétés antiadhérentes du polyélectrolyte anionique ainsi qu'aux conditions de préparation.

1.1 Introduction

As an advanced multifunctional system, the layer-by-layer (LbL) capsules have attracted great interest for their potential biomedical applications, especially in the administration of drugs.¹⁻⁴ Polysaccharides, due to their biocompatible and biodegradable properties, have been deemed as one of the most attractive materials for the construction of biomedical-used multilayer systems.⁵

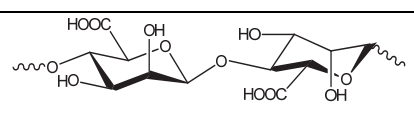
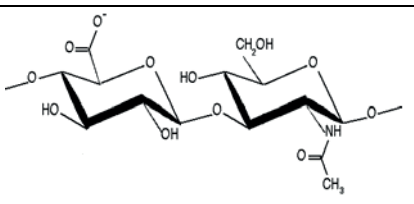
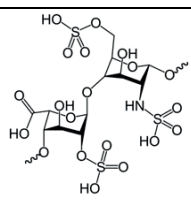
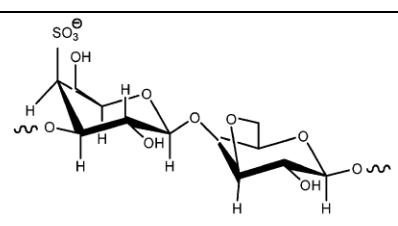
However, the fabrication of polyelectrolyte multilayer capsules based on polysaccharides is difficult. Indeed, as polysaccharides are generally weak polyelectrolytes, the multilayer films made of polysaccharides were always soft, highly hydrated and showed poor mechanical properties compared to those made of synthetic polymers.⁶ This is not favorable for the construction of mechanically stable capsules.

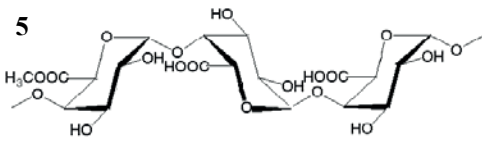
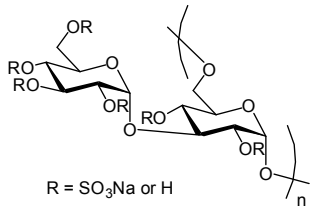
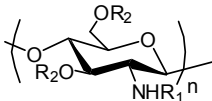
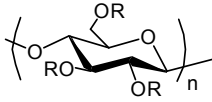
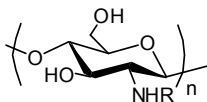
Up to now, only few polysaccharides were used for the synthesis of multilayer assemblies via electrostatic interactions, whose structures are shown in **Table 1.1**.⁷⁻²⁶ It can be noticed that only chitosan (CHI) and its derivatives were used as polycations in these multilayer systems. CHI could be obtained by deacetylation of chitin, which is the structural element in the exoskeleton of crustaceans (such as crabs and shrimp) and cell walls of fungi. Chitin is the 2nd most abundant natural polymer after cellulose. The degree of acetylation (DA) in commercial chitosans is in the range 0 – 0.4. Chitin and its deacetylated derivative, CHI, are the unique cationic polysaccharides in nature. The amino group of CHI has a pK_a value of ~6.5, which leads to a protonation in acidic to neutral solution with a charge density dependent on pH and DA. CHI is biocompatible, biodegradable and shows fantastic biological activities, such as antibacterial activity, permeation enhancing properties, wound-healing activity and immunostimulating properties. Taking these advantages, CHI and its derivatives have been applied in different fields, such as agriculture, water filtration, cosmetic, food industry, and biomedicine, etc.²⁷

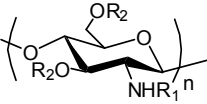
As one of the important biological properties of CHI is its antibacterial activities, CHI and its derivatives have been paid much attention for their applications in the design of contact-killing surface. In order to better understand the relationship between the antibacterial activity of CHI and that of the multilayer assemblies made of CHI and its derivatives, in this chapter, we provide an overview on the antibacterial activities of CHI and the multilayer films based on CHI. We at first describe the mode of antibacterial action of CHI, and then analyze the factors affecting its antibacterial activities from the sides of bacteria, nature of CHI,

experiment conditions as well as chemical modifications. The studies about the multilayer films made of CHI and other polyelectrolytes presenting antibacterial properties are discussed at the end of this part.

Table 1.1: Structures of polysaccharides used for the synthesis of multilayer assemblies via electrostatic interaction and the pK_a values of their functional groups.

Polysaccharides		Chemical structure	pK_a
Polyanions	Alginate ⁷⁻¹²	<p>1</p>  <p>(1→4)-linked β-D-mannuronate (M) and C-5 epimer α-L-guluronate (G) residues</p>	$\sim 3.38 - 3.65$
	Hyaluronic acid or hyaluronan (HA) ^{13-17,26}	<p>2</p>  <p>(1→4)-linked β-D-glucuronic and (1→3)-linked β-N-acetyl-D-glucosamine residues</p>	$\sim 2.9 \pm 0.1$
	Heparin ¹⁸	<p>3</p>  <p>(1→4)-linked 2-O-sulfated iduronic acid and 6-O-sulfated N-sulfated glucosamine residues</p>	<p>sulfate monoesters and sulfamido groups: $\sim 0.5 \pm 1.5$ carboxylate groups: $\sim 2 - 4$</p>
	Carrageenan ¹⁹⁻²¹	<p>4</p>  <p>(1→3)-linked α-4-sulfated galactose and (1→4)-linked β-3,6-anhydrogalactose residues</p>	~ 2

	<p>5</p>  <p>Pectin²²</p> <p>(1→4)-linked α-D-galactosyluronic acid residues</p>	~ 3.5
	<p>6</p>  <p>Dextran sulfate^{8,23}</p> <p>R = SO₃Na or H</p> <p>Sulfated (1→6)-linked α-D-glucose with random (1→3)-linked α-D-glucose branching</p>	--
	<p>7</p>  <p>Chitosan sulfate²⁴</p> <p>R₁ = H or COCH₃ R₂ = H or SO₃Na</p> <p>Sulfated (1→4)-linked β-D-glucosamine and <i>N</i>-acetyl-D-glucosamine residues</p>	--
	<p>8</p>  <p>Carboxymethyl cellulose (CMC)⁸</p> <p>R = H or CH₂CO₂H</p> <p>(1→4)-linked β-carboxymethyl D-glucose</p>	--
Polycations	<p>9</p>  <p>Chitosan (CHI)⁷⁻ 8,10,18,21-22,24-25</p> <p>R = H or COCH₃</p> <p>(1→4)-linked β-D-glucosamine and <i>N</i>-acetyl-D-glucosamine residues</p>	~ 6

	Carboxymethyl chitosan²²	<p>10</p>  <p> $R_1 = \text{H or COCH}_3$ $R_2 = \text{H or CH}_2\text{COOH}$ </p> <p>Carboxymethyl (1→4)-linked β-D-glucosamine and <i>N</i>-acetyl-D-glucosamine residues</p>	--
--	--	--	----

1.2 Mode of action to inhibit the growth of bacteria

Although CHI has been used as antibacterial agent in different fields for a long time, the exact mechanism is still unknown. The mode of antibacterial actions of CHI proposed in the previous works has been summarized by Lim et al.²⁸, Rabea et al.²⁹ and Li et al.³⁰. Generally, CHI was applied in terms of bacteriostatic or bacteriocidal activity to affect bacterial multiplication. Due to the positively charged amino groups, CHI could be firstly adsorbed onto the negatively charged cell wall of bacteria and then kill bacteria by different strategies. It was found that the CHI could inhibit the bacteria by binding trace metal, water or intracellular constituents or by forbidding the transcription of DNA to RNA inside of cells.³¹⁻³² It also can alter the permeability, even damage the structure of cell membrane to cause the leakage of proteinaceous and other intracellular constituents.^{30,33-36} Another explication was that CHI could form a compact layer to block the transport of nutrients necessary for the cell.³⁷ The researches provided the proofs to support their opinion and all of them seemed reasonable and believable. The disagreement on the mechanism was probably due to the difference on the bacteria species, the nature of CHI and experimental conditions used by these authors. In the following text, we focus on the effect of these three factors on the antibacterial activity of CHI.

1.3 Factors influencing the antibacterial activity of CHI

In order to analyze the influence of different factors on the antibacterial activity of CHI, it is necessary to introduce the common definitions and determination methods used in studies of antibacterial activity.

Minimum Inhibitory Concentration (MIC) and Minimum Bactericidal Concentration (MBC) are two important terms in the antimicrobial activity study. MIC is the lowest concentration of an antimicrobial agent that will inhibit the visible growth of a microorganism after overnight incubation (or much longer time) and MBC is defined as the lowest concentration of antibiotic required to kill the germ. Antimicrobials are usually regarded as bactericidal if the MBC is no more than four times the MIC. Generally, the lower MIC (MBC) values indicate the higher antibacterial activity of materials against bacteria. Of note, the MIC or MBC values obtained by different authors are incomparable since they are strongly affected by the testing method and experimental conditions. Thus, to avoid the conflict brought by the results derived from different work, we do not cite the exact MIC (MBC) values in the discussion of this chapter.

Cell viable-counting method using agar plate and optical density measurement were used most frequently in the antibacterial activity studies, by which the dynamic evolution of the bacterial growth inhibitory effect of materials was able to be monitored as a function of time.

The researches also used other techniques to assess the antibacterial ability of CHI, which included the measurement of the adsorption amount of CHI on cell surface, the permeability of cell membrane and the analysis of Transmission Electron Microscopy (TEM) images of cells after incubated in CHI solutions, etc. Most results obtained by these methods were adopted to interpret the antibacterial mechanism of materials.

1.3.1 Antibacterial activity of native CHI on different bacteria types

Typically, bacteria are classified by shape, ranging from spheres, rods to spirals with a few micrometers in length or diameter. According to the difference in the outermost cell envelope structure and composition, bacteria are also commonly classified as Gram positive (Gram(+)) and Gram negative (Gram(-)) bacteria by Gram staining. Gram(+) bacteria possess a thick multilayered peptidoglycan cell wall, embedded with teichoic acid polymers, whereas Gram(-) bacteria exhibit a relatively thin cell wall consisting of a single peptidoglycan layer surrounded by a second lipid membrane (outer membrane) rich of lipopolysaccharide (**Figure 1.1**).³⁸

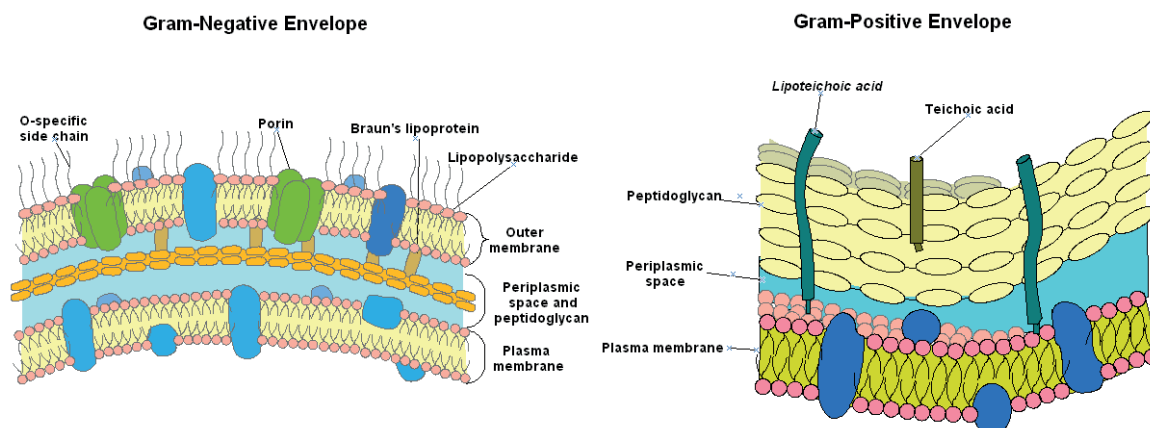


Figure 1.1: The cell envelope structure of bacteria designated by a Gram strain.

Up to now, more than 20 Gram bacteria have been used in the antibacterial study of CHI by different authors, which were listed in **Table 1.2**. Here, we only present the results published from 2000 and in each article at least 5 bacteria species were tested and compared.

Table 1.2: Gram bacteria applied in the test of antibacterial activity of CHI.

Gram (+)	Gram (-)
<i>Staphylococcus aureus</i> ^{21,35-36,39-59}	<i>Escherchia coli</i> ^{30,32,34-35,39-44,46-48,51,53-66}
<i>Streptococcus faecalis</i> ^{35,67}	<i>Samonella typhimurium</i> ^{34,39,42,61}
<i>Streptococcus saprophyticus</i> ^{39,68}	<i>Enterococcus faecalis</i> ^{21,36}
<i>Streptococcus mutans</i> ^{33,39,69}	<i>Pseudomonas fluorescens</i> ^{61,70}
<i>Streptococcus epidermidis</i> ³⁹	<i>Pseudomonas aeruginosa</i> ^{34-35,39,62}
<i>Listeria monocytogenes</i> ^{61,70}	<i>Vibrio parahaemolyticus</i> ⁶¹
<i>Bacillus megaterium</i> ⁶¹	<i>Pseudomonas aureofaciens</i> ⁷¹
<i>Bacillus cereus</i> ^{61,70}	<i>Photobacterium phosphoreum</i> ⁷⁰
<i>Bacillus subtilis</i> ³⁹	<i>Enterobacter aerogenes</i> ⁷⁰
<i>Bacillus bifidum</i> ⁷¹	<i>Enterobacter agglomerans</i> ⁷⁰⁻⁷¹
<i>Lactobacillus plantarum</i> ⁶¹	<i>Salmonella typhi</i> ³⁹
<i>Lactobacillus brevis</i> ³²	
<i>Lactobacillus bulgaricus</i> ^{39,61}	

<i>Lactobacillus casei</i> ³⁹	
<i>Lactobacillus sakei subsp. carnosum</i> ⁷⁰	
<i>Lactobacillus fermentum</i> ³⁹	
<i>Lactobacillus curvatus</i> ⁷⁰	
<i>Brochothrix thermosphacta</i> ⁷⁰	
<i>Pediococcus acidilactici</i> ⁷⁰	
<i>Micrococcus luteus</i> ³⁹	

Chung et al. investigated the inhibitory effect of CHI with DA of 0.05 and 0.25 to the growth of bacteria by analyzing the adsorption amount of CHI on the surface of cells. It was found that the adsorption of CHI on the cell wall of *P. aeruginosa*, *S. typhimurium* and *E. coli* (Gram(-) bacteria) was higher than that of *S. faecalis* and *S. aureus* (Gram(+) bacteria) in the presented order. In his work, the antibacterial activity of CHI was found to be related with the amount of CHI adsorption onto the cell surface.

No et al. tested the antibacterial activity of CHI against 7 Gram (+) bacteria (*L. monocytogenes*, *B. megaterium*, *B. cereus*, *S. aureus*, *L. brevis*, *L. bulgaricus* and *L. plantarum*) and 4 Gram (-) bacteria (*E. coli*, *P. fluorescens*, *S. typhimurium* and *V. parahaemolyticus*). They observed that the inhibitory effect of CHI on the growth of Gram bacteria differed from each other according to the nature of bacteria and the molar mass of CHI. Gram(+) bacteria were more susceptible than Gram(-) bacteria to CHI with weight average molar mass (Mw) above 28 000 g/mol and that with Mw below 22 000 g/mol.

Gerasimenko et al. also investigated antibacterial activity against different species of bacteria. They found that the rate of cell death decreased as the following order: *B. bifidum* > *E. agglomerans* > *B. subtilis* > *P. aeruginosa* > *E. coli* after incubation in CHI solution (viscosity average molar mass (Mv) of CHI in range of 5 ~ 27 000 g/mol, DA 15%) in 1 hour. Among them, *B. bifidum* and *B. subtilis* belong to Gram(+) bacteria, while the others are the Gram(-) bacteria.⁷¹

In the article of Devlighere et al., based on some previous work and combining them with their own results, they concluded that Gram(-) bacteria seemed to be very sensitive to CHI while the sensitivity of the Gram(+) bacteria varied greatly.⁷⁰

In the work of Jeon et al, it was found that the CHI inhibited the growth of 4 Gram(-) and 5 Gram(+) bacteria with different efficacy, which was related to the molar mass of CHI.³⁹

It can be noticed that in these studies the growth of all these bacteria was more or less inhibited by CHI and most bacteria in the same class exhibited a similar sensitivity to CHI. Indeed, the sensitivity of bacteria to CHI was found to be strongly affected by the chemical and physical properties of cell envelope, the main difference between Gram(+) and Gram(-) bacteria.^{35,48,68,71-72} However, the recent studies could not provide clear data about the relationship between the antibacterial activity of CHI and the surface characteristics of cell wall. We also found that the conclusion drawn about the comparison of Gram bacteria sensitivity to CHI differed according to the authors. These disagreements may be partly explained by the difference in CHI samples and experimental conditions used in the tests.

Considering on the similar sensitivity of most bacteria of the same class, it implies to select the typical bacteria in the test of antibacterial activity of CHI, thereby to predict the sensitivity of other bacteria. *E. coli* and *S. aureus*, two common bacteria in nature, have been mostly used in the antibacterial study of CHI and its derivatives as the representative bacteria of Gram (-) and Gram (+), respectively. Between them, *E. coli* was used more frequently. Therefore, the works cited in the following text focus on the antibacterial activity of CHI against *E. coli*.

1.3.2 Effect of experimental conditions

Up to now, a variety of experimental conditions has been applied in the antibacterial test. It was found that the concentration of CHI and the pH can strongly influence the inhibitory effect of CHI on bacteria growth.

1.3.2.1 Concentration of CHI

The effect of the concentration on the antibacterial activity could be divided into three stages types: promoting (a→b, Stage I), maintaining constant (b→c, Stage II) and reducing (c→d, Stage III). (**Figure 1.2**).

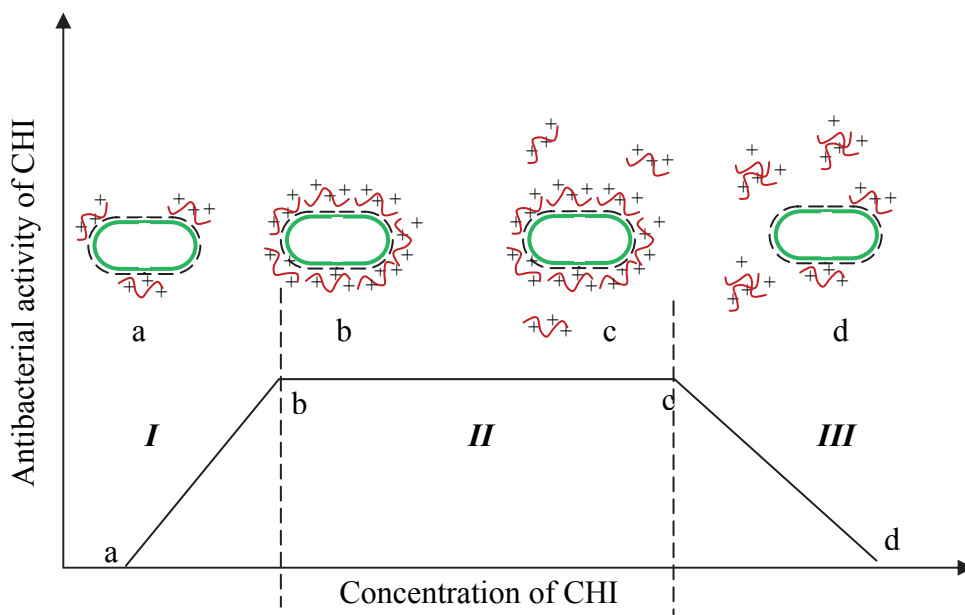


Figure 1.2: Three stages of the variation of the antibacterial activity of CHI as a function of the concentration changes of CHI.

In the promoting stage, the antibacterial activity of CHI is enhanced as more CHI can be adsorbed on the cell wall with the increase of the concentration on CHI.^{33,43-44} Once the concentration is high enough to reach the saturating adsorption (due to the electrostatic repulsion between CHI chains), the antibacterial activity will be not varied with concentration, which is the constant stage.⁴⁴ If the CHI is too concentrated, it will form aggregates, which impairs adsorption on the cell wall, resulting in the reduction of antibacterial activity. This is the reducing stage. The critical concentration in these three stages was different according to the authors. In fact, as the concentration is one of the factors affecting the antibacterial activity of CHI, the value deeply depends on other parameters, such as the nature of CHI and pH, as discussed below.

1.3.2.2 pH of the medium

The antibacterial activity of CHI has been investigated in a wide range of pH (from pH 1 to 8.5). It was found that the inhibitory effect of native CHI on the growth of bacteria was related to the pH. As the pH decreases from pH 8.5 to 3, the amount of positively charged amino groups on the CHI is increased, which enhances the inhibitory effect.^{42-43,61} However,

this tendency is not suitable for the extreme acidic pH, i. e, pH 1 and 2. At these pH, the highly charged chains of CHI lead to a strong inter-/intra- electrostatic repulsions, which reduce the adsorption of CHI on the cell wall. Thus, CHI exhibits a lower antibacterial activity compared to that at weak acidic pH.⁴²

1.3.2.3 Other factors

Besides the concentration of CHI and pH, other parameters, such as solvent,^{42,61} ionic strength,⁴² type and concentration of ions^{34,42} and temperature could also affect the antibacterial activities of CHI.

In general, CHI dissolved in an organic acid solvent (i.e. formic acid, acetic acid) was more effective in inhibiting bacterial growth than that dissolved in an inorganic acid solvent (i.e. HNO₃, HCl, H₃PO₄). That is probably because an inorganic acid may play only the role of a proton donor in CHI solutions, which are almost 100% dissociated at pH 5 and 6, while an organic acid may not only play the role of a proton donor (dissociated form) but also of a bactericide (non-dissociated form). The higher antibacterial activity of the organic acid with a higher pK_a indicated that a greater amount of the non-dissociated form of the acid could enter into the bacterial cell and cause the death of cells.⁴²

Higher concentrations of NaCl seemed to be able to improve the antibacterial activity of CHI by screening electrostatic repulsions between CHI chains, but the adding of metal ions decreased the activity.³⁴

The influence of ethylenediaminetetraacetic acid (EDTA) solution on the antibacterial activity of CHI was also investigated. It was found that EDTA had a positive effect on the improvement of antibacterial activity against *E. coli* but a negative effect against *S. aureus*.⁴² In fact, EDTA could act as a chelating agent to complex with Ca²⁺ or Mg²⁺ in the outer membrane of *E. coli*, and then increase the permeability of this membrane. A hypothesis proposed by Chung et al. to explain the decreasing antibacterial activity against *S. aureus* with the adding of EDTA is that most of primary amino groups of CHI were shielded by reacting with the carboxyl groups of EDTA. According to such hypothesis, the complexation ability between CHI/EDTA should be stronger than that between CHI/*S. aureus* and weaker than that between CHI/*E. coli*. Perhaps the later work of Chung et al.³⁵ could support this hypothesis.

They demonstrated that the absorbed amount of CHI on the surface of *S. aureus* was lower than that on *E.coli*.

Of note, an acetic acid solution at pH ~ 5 – 6.5 with 0.15 M NaCl at 37 °C was most frequently adopted in the previous antibacterial activity studies of CHI.

1.3.3 Effect of the nature of CHI

Besides bacteria species and experimental conditions, the nature of CHI plays an essential effect on its antibacterial activity. In the next part, we will develop the roles intrinsic characteristics of native CHI as well as its chemical modifications.

1.3.3.1 Role of the intrinsic characteristics of native CHI

The intrinsic characteristics of native CHI that may influence the antibacterial activity include the source⁷¹, the degree of acetylation (DA)^{42-43,48,68,71} and the molar mass^{30,32,43-44,48,61,71}.

Although the antibacterial activity of CHI was firstly reported to be dependent on its Mw in 1989 by Uchida et al⁷³, the relationship between them has not been recognized yet. This may be because most studies only involved one or a few different Mw of CHI. Studies of the antibacterial activity against *E .coli* with a wild range of Mw of CHI are summarized in **Table 1.3**. Some discrepancies concerning the effect of Mw were found according to the different authors.

The work of No et al.⁶¹ and Gerasimenko et al.⁷¹ showed an enhanced antibacterial activity of CHI as the molar mass decreased in the range 1000 - 22000 g/mol (Mw) and 6000 - 27000 g/mol (Mv), respectively (**Table 1.3 Entries No. 2 and 3**). In contrast, Qin et al.⁴⁸, Liu et al.³² and Jeon et al.³⁹ found a promoted inhibitory effect of CHI with the increase of Mw ranging from 1400 to 17000, 3000 to 8000 and 1000 to 10000 g/mol, respectively (**Table 1.3 Entries No. 1, 6 and 7**). In addition, Jeon indicated that the Mw of chitoooligosaccharides required for the inhibition of microorganism is higher than 10 000 g/mol.

Table 1.3 : The effect of molar mass on the antibacterial activity of CHI against *E. coli* according to different authors. (Mw: weight average molar mass; Mv: viscosity average molar mass)

Entry No.	Reference	Solvent	Conc. of CHI (g/L)	Molar mass (kg/mol) in the order of antibacterial activity (efficiency)
1	Qin et al. ⁴⁸	Sterilized water at pH 7.0	1	(Mw)130=78=48>17>400>2.8>1.4
2	No et al. ⁶¹	1% (v/v) acetic acid	1	(Mw) 746>471>1671>224>1106>28
			10	(Mw) 1>2>4>7>10>22
3	Gerasimenko et al. ⁷¹	0.1 M acetate buffer at 6.5	5	(Mv) 6>12>27>5
4	Zheng et al. ⁴⁴	Aqueous solution at pH 5.5	2.5	(Mv) 5>48.5>72.4>129=166=305 (no antibacterial activity with the last 3 Mv)
			5	(Mv) 48.5>5>166=305>72.4>129
			7.5	(Mv) 5=48.5=129>166>72.4=305
			10	(Mv) 5=48.5=72.4=129=166=305 (<i>E.coli</i> completely killed with all Mv)
5	Li et al. ³⁰	1% (v/v) acetic acid	5	(Mw) 50>3>1000
6	Liu et al. ³²	2M acetic acid	--	(Mw) 96.1>51.1>8>3=274>650>1080
7	Jeon et al. ³⁹	0.05 M acetate buffer at 6.0	10	(Mw) 650>10>5>1

For CHI with Mv between 27000 and 1000000 g/mol, the effect of Mw is very complicated and irregular. Based on the results in **Table 1.3**, it was found that the CHI with Mv around 50000 ~ 130000 g/mol exhibited higher antibacterial activity than samples with other molar mass in most cases (**Table 1.3 Entries No. 1, 4 and 5**). Liu et al.³² found that the inhibitory effect of CHI increased at first with the Mw up to 96100 g/mol, then decreased with the Mw up to 650 000 g/mol (**Table 1.3 Entry No. 6**). However, No et al.⁶¹ showed that the inhibitory effect of CHI was promoted with the increase of Mw (from 224000 to 746000 g/mol) (**Table 1.3 Entry No. 2**).

The CHI with the Mw higher than 1000000 g/mol showed lower antibacterial activity than those with other Mw, which was confirmed by No et al.⁶¹, Li et al.³⁰ and Liu et al.³² (**Table 2 Entry No. 2, 5 and 6**). Interestingly, the reduction of antibacterial activity caused by CHI with a Mw of 1671000 g/mol was lower than that with a Mw of 1106 000 g/mol, reported by No and his coworkers⁶¹.

From these studies, the antibacterial activity of CHI indeed was found to vary with Mw, but no clear conclusion can be drawn about the range of Mw more favorable for the antibacterial activity of CHI. In fact, the antibacterial mechanism of CHI varies with the hydrodynamic radius of the chain, which is related to the Mw. We can hypothesize that: the chitooligosaccharides (i.e. Mw ~ 775 g/mol) were unable to play the role of antibacterial agent since they were too small to stably deposit on the surface of cell wall; the CHI with low Mw (i.e. Mw ~ 1000 – 27 000 g/mol) could kill the bacteria by penetrating the cell envelope to activate in the inner of the cell; the CHI with medium Mw (Mw ~ 28 000 – 746 000 g/mol) inhibited the growth of bacteria by altering the permeability of cell wall resulting in the leakage of intracellular components and the CHI with high Mw (Mw ~ 1000 000 g/mol) caused the death of bacteria by forming a intensive layer, thereby blocking the transport of nutrients. Unfortunately, few study precisely investigated the relationship between Mw (or hydrodynamic radius of CHI chain) and permeability of cell walls. It can be also noticed that the effect of Mw on the antibacterial activity of CHI could be changed with other parameters, such the DA, substituent and experiment conditions, which may lead to uncorrelated results obtained in the literature.

DA is another essential parameter to affect the antibacterial activity of CHI. Compared to CHI (DA less than 0.5), the chitin (DA higher 0.5) usually showed weaker or no antibacterial activity, which had been confirmed in different works. Chung et al.³⁵ reported the adsorbed amount of CHI with DA 0.05 on the *E. coli* and *S. aureus* was more than that of CHI with 0.25. Since a higher adsorbed amount of CHI always corresponded to a better effect on the bacterial growth inhibition, this result meant that the antibacterial activity of CHI increased with the decrease of DA of CHI. This conclusion is consistent with that obtained by Liu et al.⁶⁰, who determined the antibacterial activity of CHI with the DA varied from 0.04 to 0.26. Gerasimenko et al.⁷¹ also found when the DA of CHI (Mw 4 000 g/mol) increased from 0.15 to 0.45, the death rate of *E. coli* decreased. In fact, the interaction between CHI and cell membrane can be enhanced by increasing the amount of amino groups on the chain of CHI, therefore, the inhibitory effect of CHI to the growth of bacteria increases.

1.3.3.2 Antibacterial activity of chemically modified CHI derivatives

Compared to the good performance of native CHI on the inhibition of bacteria growth under acidic condition, the antibacterial activity of CHI at neutral pH is lower mainly due to its poor solubility under this condition. To improve the solubility of CHI at neutral pH, various chemically modified CHI derivatives have been designed and some of them showed the distinguished antibacterial activity. According to the charge of the grafted groups, the CHI derivatives could be divided into anionic, neutral and cationic derivatives. In the following part, we will discuss the antibacterial activity of these CHI derivatives.

a) CHI derivatives with anionic groups

The derivatives of CHI with anionic groups are shown in **Figure 1.3**. For facilitating the expression of CHI derivatives structure, we use the format of “R_m, R_n, ... = a or b, ...” in this chapter. This format means that both the composition of R_m and R_n can be whether a or b

Until now, 3 different kinds of acidic groups, composed of carboxylic acid^{32,41,52-54,60,67}, sulfate^{46,74} and phosphate⁷⁴, have been successfully grafted on the chains of CHI.

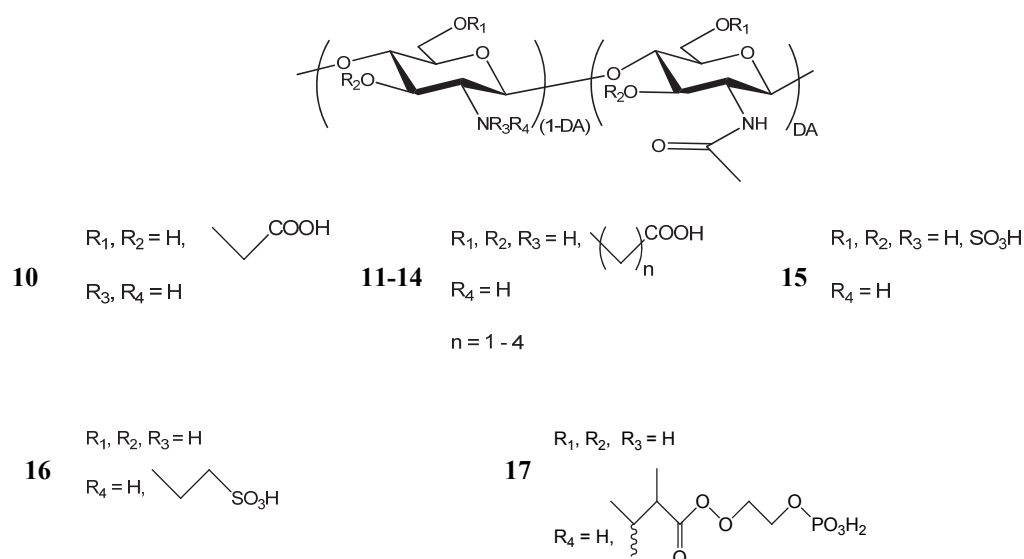


Figure 1.3: Structure of CHI derivatives with anionic groups (**10** *O*- carboxymethyl CHI, **11**, **n=1** *N,O*-carboxymethyl CHI, **12**, **n=2** *N,O*-carboxyethyl CHI, **13**, **n=3** *N,O*-carboxypropyl CHI, **14**, **n=4** *N,O*-carboxybutyl CHI, **15** *N, O*-sulfate CHI, **16** *N*-vinylsulfate CHI, and **17** *N*-(2-methacryloyl oxyethyl) phosphate CHI).

O- and *N,O*-carboxyalkyl CHI derivatives **11-14** were prepared using a carboxyalkylation agent, such as chloroacetic acid, chloropropionic acid and omega-halogen derivative of butane acid in alkaline medium (NaOH 42%, w/v) at 0 ~ 30 °C or in a mixture of 10M NaOH and isopropanol at high temperature (~ 60 - 70 °C), respectively.^{32,53} Compared to native CHI, the solubility of carboxyalkyl CHI derivatives was more or less improved by carboxyl moieties depending on the DS and the carbon number in the alkyl segment.^{53-54,60,67} The improved solubility allowed to investigate the antibacterial activity of these derivatives at neutral pH.

Liu et al. investigated the antibacterial activity of carboxymethyl CHI substituted on the different position in acidic medium (2M acetic acid).⁶⁰ In his work, *N,O*-carboxymethyl CHI **11** did not exhibit any antibacterial activity against *E. coli*; whereas *O*-carboxymethyl CHI **10** did and higher than the native CHI. The absence of antibacterial activity of *N,O*-carboxymethyl CHI **11** was explained by the consumption of the amine groups of CHI for the synthesis, which decreased the number of positive charges along the chains. Since *O*-carboxymethyl CHI **10** was synthesized only on the hydroxyl groups, the number of amino groups was equal to that of CHI. The author suggested that the promoted antibacterial activity of *O*-carboxymethyl CHI **10** was probably due to the increased number of positively charged amino groups activated by carboxyl groups via inter-/intra-molecular interaction. However, this explication seems not clear, because this work was carried out in acidic condition, when the amino groups were almost protonated by the proton dissociated from acid and no further study was carried out to support this hypothesis. In the work of Cai et al, the inhibitory effect of *N,O*-carboxyethyl CHI **12** to the growth of *E. coli* and *S. aureus* was much higher than that of native CHI at pH 7.0.⁵³ In the other case, *N,O*-carboxypropyl CHI **13** were found to show a similar antibacterial activity against *E. coli* and higher activity against *S. aureus* compared to the native CHI at pH 5.5.⁵⁴ It was very interesting to find that although the amino groups were substitutioned, the antibacterial activity of the derivatives did not decrease. This can be attributed to the hydrophobic property of carboxyalkyl groups (the number of C in alkyl is ≥ 2), which could alter the permeability of the cell wall by hydrophobic interaction, thereby cause the death of cells. Thus, the hydrophobicity of carboxyalkyl group, depending on the length of alkyl segments in the side chain, would be considered as another key to affect the antibacterial activity.

N,O-sulfate CHI **15** was prepared by reacting with chlorosulfonic acid (ClSO₃H) with CHI in dimethylformamide (DMF).⁴⁶ Such modified CHI (S% content ~ 10%) could significantly inhibit the growth of *S.aureus* but exhibited no antibacterial activity against *E.coli*. The

authors suggested that the introduction of the strongly negatively charged sulfate groups on the CHI molecules could convert the polycationic CHI to the polyanionic CHI, which decreased the susceptibility of CHI to *E. coli*.

The other type of sulfate CHI, *N*-vinylsulfate CHI **16**, was prepared by reacting CHI with vinylsulfonic acid in acidic aqueous solution (acetic acid 0.5 %) at 40 °C.⁷⁴ In the same work, *N*-(2-methacryloyl oxyethyl) phosphate CHI **17** was also synthesized by grafting with mono-(2-methacryloyl oxyethyl) phosphate on the primary amino groups of CHI under the same condition. The polymerization of monomers and those grafted on CHI chain was initiated by ceric ammonium nitrate (CAN) in 1N HNO₃ aqueous solution. These two water-soluble CHI derivatives exhibited a fungus-selective antibacterial activity, more or less than CHI, which was considered due to the different structure affinity between the cell wall and CHI derivatives.

b) CHI derivatives with neutral groups

The neutral groups grafted on the chain of CHI could be divided according to their hydrophobic/hydrophilic character. Generally, the hydrophobic groups include the alkyl groups^{46,55,62} and the benzyl groups⁵⁵; the hydrophilic groups consist of mono- and disaccharides^{45,47,55,75} as well as the hydroxyalkyl groups^{32,40,63}.

i. Hydrophobic groups

The *N*-acrylated CHI derivatives **18-22** were prepared by acrylation reaction with anhydrides, such as acetic anhydride and propionic anhydride, etc. in a mixture of acetic acid aqueous/alcohol solution,⁶² whose structures are showed in **Figure 1.4**. Affected by the hydrophobicity of alkyl chain and benzyl molecule, the solubility of these derivatives was always lower than the native CHI.

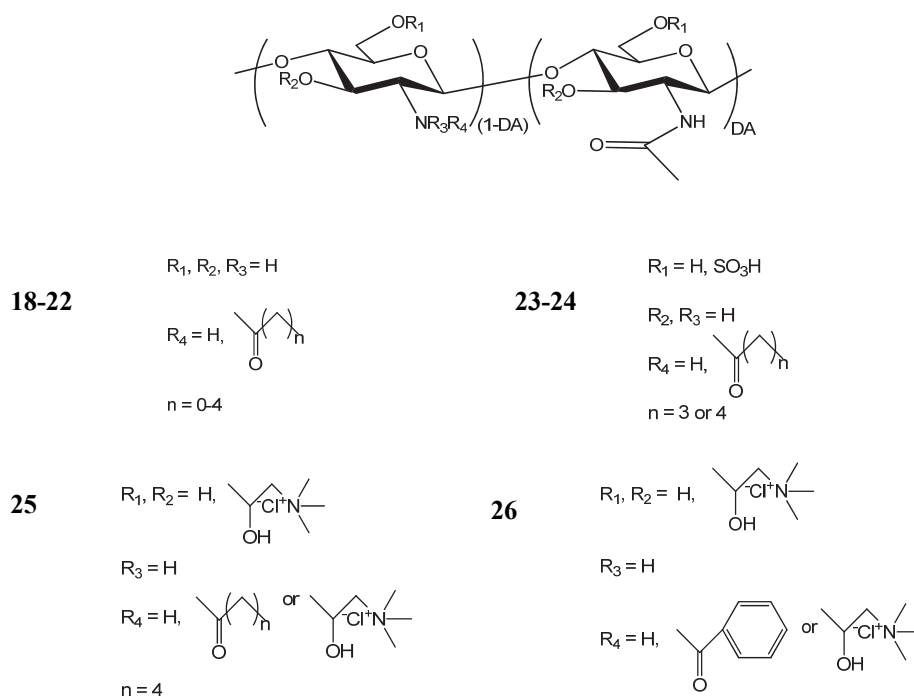


Figure 1.4: Structure of CHI derivatives with hydrophobic neutral groups (**18**, $n=0$ *N*-acetyl CHI, **19**, $n=1$ *N*-propionyl CHI, **20**, $n=2$ *N*-butyl CHI, **21**, $n=3$ *N*-vinyl CHI, **22**, $n=4$ *N*-hexanoyl CHI, **23** (*N,O*-sulfate)-*N*-propanoyl CHI, **24** (*N,O*-sulfate)-*N*-hexanoyl CHI, **25** (*N,O*-quaternized)-*N*-benzyl CHI and **26** (*N,O*-quaternized)-*N*-octyl CHI).

It was found by Hu et al. that the antibacterial activity of CHI and its *N*-acrylated derivatives (DS ~ 0.5) at pH 5.4 decreased as the following order: CHI > *N*-hexanoyl CHI **22** > *N*-propionyl CHI **19** \geq *N*-acetyl CHI **18**; in addition, the *N*-acetylated CHI derivatives showed a non-linearly DS dependent antibacterial activity.⁶² The lower inhibitory effect of *N*-acrylated CHI derivatives compared to the native CHI could be explained by the decrease of the positively charged density due to *N*-substitution reaction, in which the amino groups were partly converted to the amide groups. The influence of the length of alkyl chains to the antibacterial activity was contributed to the self-aggregation of *N*-acrylated CHI derivatives suggested by authors. By investigating the viscosity of concentrated solutions of *N*-acrylated CHI derivatives, they suggested that the higher viscosity of *N*-hexanoyl CHI **22** and the lower viscosity of *N*-acetyl CHI **18** and *N*-propionyl CHI **19** than the native CHI revealed the formation of intermolecular and intramolecular hydrophobic interaction respectively (**Figure 1.5**). As the intramolecular aggregation formed, which is the predominate interaction in the dilute regime, the hydrophobic part associated in the inner and the positively charged amino

groups were exposed to the outer. Thus, the density of protonated amino groups increased; thereby the antibacterial activity was promoted (**Figure 1.6**). In this work, the stronger association was created by the *N*-acryl CHI bearing longer alkyl chain and a higher DS (~ 0.5). Considering on the favorable effect of hydrophobic groups on the antibacterial activity on CHI derivatives grafted with negatively charged groups, we can consider that the improved activity with the increasing length of alkyl groups on the *N*-acrylated CHI chains can be also attributed to the enforced hydrophobic interactions between cell wall and polymers chains besides the electrostatic interactions proposed by Hu et al.⁶²

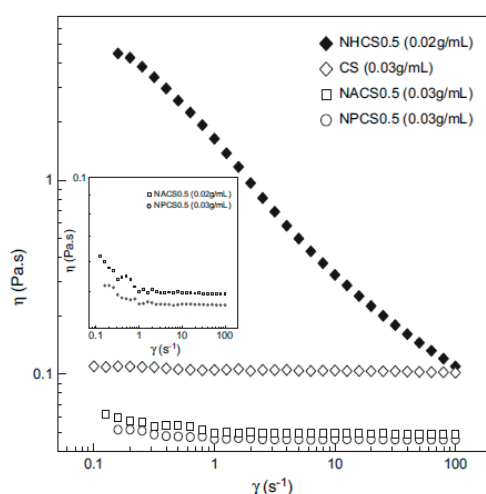


Figure 1.5: Comparison of rheological behaviors of CHI and its *N*-acrylated CHI derivatives. (solvent: 0.3 M HAc-0.05M NaAc; T =25 °C).⁶²

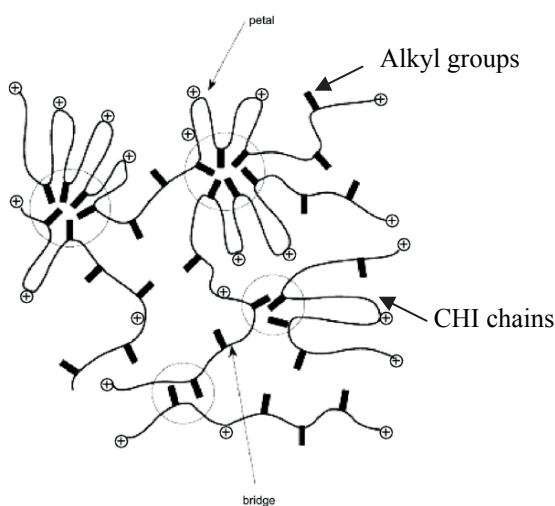


Figure 1.6: Schematic representation of intramolecular aggregates and intermolecular cross-links of *N*-acrylated CHIs with desired amount of hydrophobic alkyl chains (a small loop in a micelle is called “petal” and a subchain connecting two junctions on different chains is call “bridge”).⁶²

Similar effect of the length of alkyl chain and the DS was observed by Hung et al, who firstly grafted the sulfate groups to improve the solubility of CHI, and then introduced the alkyl groups.⁴⁶ These CHI derivatives are named as (*N,O*-sulfate)-*N*-acrylated CHI derivatives **23-24**, whose structures are showed in **Figure 1.4**. The double modified CHI derivatives showed a good antibacterial activity against *E. coli*, which was not found in the case of *N,O*-sulfate CHI **15**. In addition, the (*N,O*-sulfate)-*N*-hexanoyl CHI **24** was more effective than (*N,O*-sulfate)-*N*-propanoyl CHI **23**. Although such result corresponded to the regular of *N*-acryl CHI derivatives, the explications to the effect of alkyl chains were different. In this work, the author attributed the promoted antibacterial activity to the increase of the hydrophobic interaction between cell envelope and hydrophobic domain on the chain of CHI derivatives. This hypothesis is based on the antibacterial mechanism of synthetic polymers bearing hydrophobic groups and the lipid emulsion of CHI.⁷² However, the dependence of antibacterial activity against *E.coli* of (*N,O*-sulfate)-*N*-acrylated CHI derivatives on the degree of acrylation was not linear, which might result from the cooperation of the sulfate groups and the alkyl groups.

Another type of *N*-acrylated CHI derivatives were prepared by acrylation reaction followed by a step of quaternization using glycidyl trimethylammonium chloride (GTMAC) in alkaline milieu reported by Sajomsang et al⁵⁶. The quaternization used here was to improve the solubility of CHI derivatives and thereby to investigate their antibacterial activity at neutral pH. The structures of these CHI derivatives are presented in **Figure 1.4**. It was found that the (*N,O*-2-hydroxypropyl-trimethylammonium)-*N*-benzyl CHI ((*N,O*-quaternized)-*N*-benzyl CHI) **26** (degree of quaternization (DQ) ~ 0.92 and degree of acrylation ~ 0.11) inhibited more *E. coli* and *S. aureus* than the (*N,O*-quaternized)-*N*-octyl CHI **25** (DQ ~ 0.91, degree of acrylation ~ 0.10), whose antibacterial activity is similar to the *N,O*-quaternized CHI (DQ ~ 0.93). Although the benzyl and octyl groups did not evidently improve the antibacterial activity of CHI derivatives as described in other work, at least it did not show a negative effect. Considering on the high antibacterial activity of CHI derivatives predominately initiated by the quaternary groups, discussed later, the less obviously promotion by hydrophobic groups in this work could be acceptable.

ii. Hydrophilic groups

The CHI derivatives bearing hydrophilic groups, such as mono-/disaccharides, called *N*-mono-/disaccharides linked CHI derivatives, were prepared by a reductive animation reaction.

The reaction was carried out by mixing the CHI with aldehydo mono and disaccharides in acetic acid aqueous solution, with presence of sodium cyanoborohydride (NaCNBH₃).⁵⁶ The structures of these derivatives are showed in **Figure 1.7**.

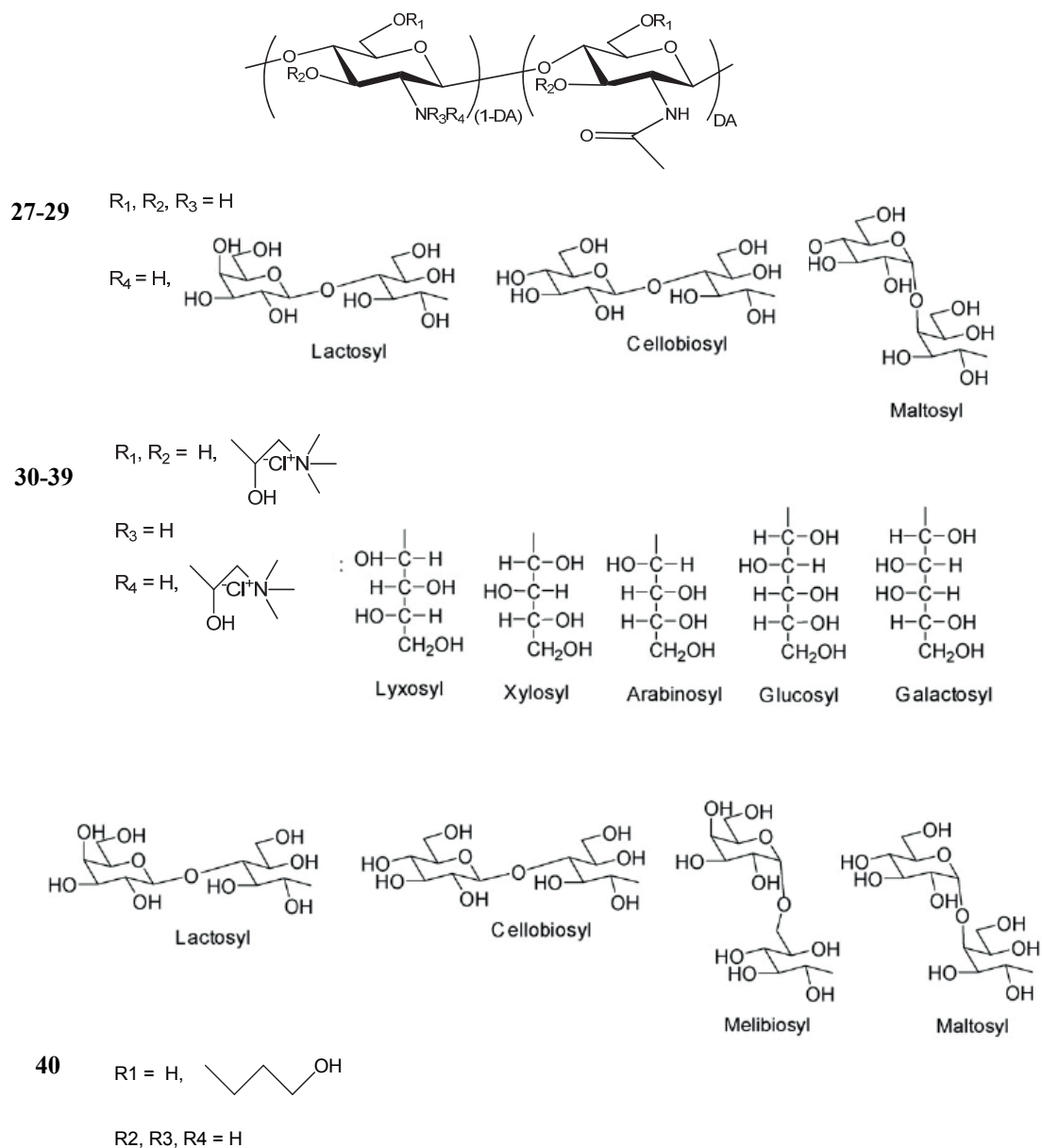


Figure 1.7: Structure of CHI derivatives with hydrophilic neutral groups (**27** *N*-lactosyl CHI, **28** *N*-cellobiosyl CHI, **29** *N*-maltosyl CHI, **30** *N,O*-quaternized CHI, **31** (*N,O*-quaternized)-*N*-lyxosyl CHI, **32** (*N,O*-quaternized)-*N*-xylosyl CHI, **33** (*N,O*-quaternized)-*N*-arabinosyl CHI, **34** (*N,O*-quaternized)-*N*-glucosyl CHI, **35** (*N,O*-quaternized)-*N*-galactosyl CHI, **36** (*N,O*-quaternized)-*N*-lactosyl CHI, **37** (*N,O*-quaternized)-*N*-cellobiosyl CHI, **38** (*N,O*-quaternized)-*N*-melibiosyl CHI, **39** (*N,O*-quaternized)-*N*-maltosyl CHI and **40** *O*-hydroxyethyl CHI).

Since the *N*-disaccharides linked CHI derivatives showed a better solubility than the *N*-monosaccharide CHI derivatives and the native CHI, their antibacterial activity was studied much more. Chen et al. demonstrated that the *N*-lactosyl CHI **27** (DS ~ 0.3 - 0.4) could inhibit the growth of *S. aureus*.⁴⁵ This result is consistent with that obtained by Yang et al.⁴⁷, who found that *N*-lactosyl, *N*-cellobiosyl and *N*-maltosyl CHI derivatives **27-29** (DS ~ 0.3 - 0.4) could inhibit the growth of *E. coli* and *S. aureus* in a wide range of pH (from 5.0 to 7.5) and the *N*-lactosyl CHI **27** were less susceptible than others. At pH > 6.0, *N*-disaccharides linked CHI derivatives could kill more bacteria than the native CHI, but at pH < 6.0, the opposite result was obtained. In addition, it was noticed that the antibacterial activity against *E. coli* of *N*-disaccharides CHI derivatives was improved by increasing the pH of antibacterial test. However, the effect of pH to the growth inhibition of *S. aureus* was not remarkable. The more efficient antibacterial activity of *N*-disaccharides CHI derivatives at higher pH may result from the improved solubility after modification.

The effect of mono-/disaccharides groups on the antibacterial activity of CHI derivatives was also investigated by Sajomasang et al.⁵⁵ using more complicated CHI derivatives, (*N,O*-quaternized)-*N*-mono-/disaccharides linked CHI derivatives **31-39**, which were synthesized by coupling mono-/disaccharides with CHI at first, then grafting GTMAC in alkaline medium. The solubility study demonstrated that the CHI derivatives grafted with disaccharides **31-35** showed a better affinity to water than those grafted with monosaccharide **36-39**. At neutral pH the antibacterial activity of (*N,O*-quaternized)-*N*-mono-/disaccharides linked CHI derivatives **31-39** with lower DS (DS < 0.2, DQ ~ 0.92) was lower than that of *N,O*-quaternized CHI **30** (DQ ~ 0.93), similar to that of *N,O*-quaternized CHI (DQ ~ 0.80). In addition, (*N,O*-quaternized)-*N*-mono-/disaccharides linked CHI derivatives with higher DS (DS ~ 0.28 – 0.4) inhibited much less bacteria than those with lower DS. The above results indicated the hydrophilic mono-/disaccharides groups did not favor to the antibacterial activity of *N,O*-quaternary CHI.

Besides *N*-mono-/disaccharides linked CHI derivatives, the *O*-hydroxyethyl CHI **40** is another kind of CHI derivative bearing the hydrophilic groups. It was prepared by reacting chloroethanol or propylene oxide in alkaline medium.^{41,63} This kind of CHI derivatives always showed a similar antibacterial activity to the native CHI due to the identical amount of amino groups, which has been pointed by Lui et al.³²

c) CHI derivatives with cationic groups

Since it is recognized that the positively charged amino groups play an essential role on the antibacterial activity of CHI, amount of researches have been done to improve the water-solubility and the antibacterial activity by grafting cationic groups, such as primary amino groups, secondary amino groups, tertiary amino groups and quaternary ammonium groups, etc.

i. Primary amino groups

The CHI derivatives bearing amino groups were prepared by different methods, whose structures are shown in **Figure 1.8**.

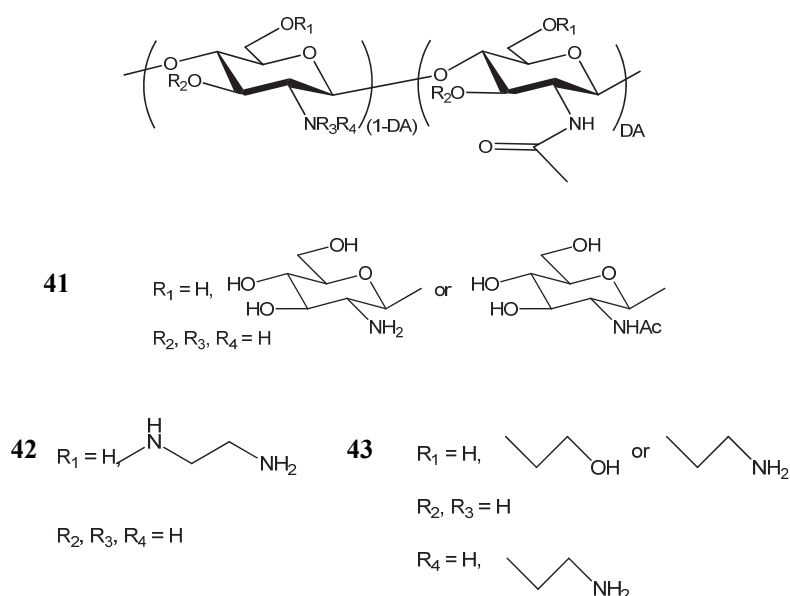
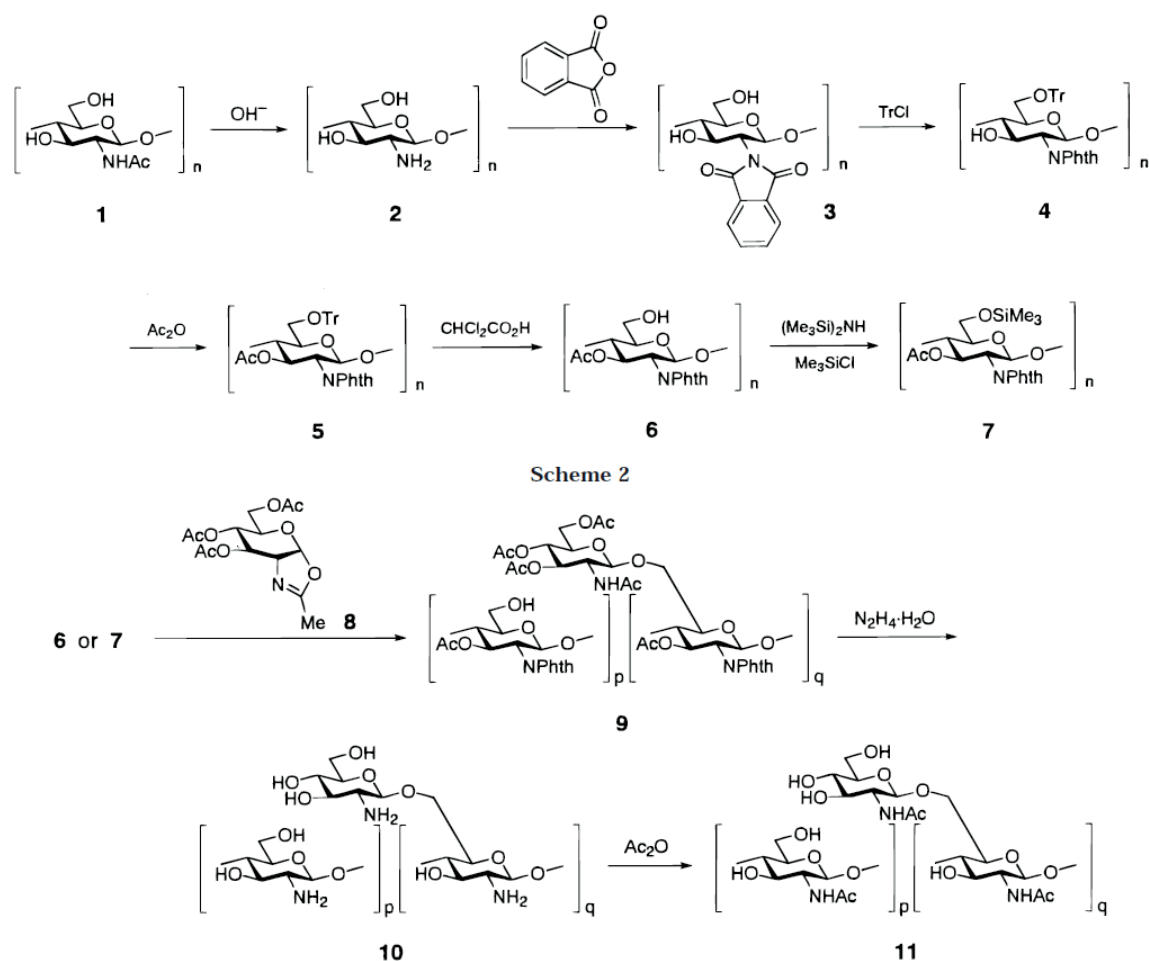


Figure 1.8: Structure of CHI derivatives modified with amino groups (**41** *O*-chitin or *O*-chitosan CHI, **42** *O*-ethyldiamine CHI and **43** (*O*-hydroxyethyl)-*N,O*-ethylamine CHI).

O-chitin/chitosan CHI **41** was synthesized by a complicated process as described in **Scheme 1.1**.⁶⁴ Such CHI derivatives are soluble in water at neutral pH and showed a little higher antibacterial activity against *E. coli* than the native CHI reported in other work at pH 5.8.⁷⁶



Scheme 1.1: Synthetic pathway of *O*-chitin/chitosan CHI.⁶⁴

O-ethylenediamine CHI **42** was prepared by introducing the ethylenediamine group on the hydroxyl groups of CHI using parabenzoquinone (pBQ) as activation agent.⁷⁷ The antibacterial activity of such cationic CHI was investigated at pH 5.5. It was found that its antibacterial activity was higher than the native one, and increased with the DS.

A more complex multifunctional CHI derivatives bearing primary amino groups in the side chain is (*O*-hydroxyethyl)-*N,O*-ethyleneamine CHI **43**. It was obtained by grafting the chloroethylamine hydrochloride onto the chains of *O*-hydroxyethyl CHI in the mixture of isopropanol/alkaline solution (NaOH 42%, w/v). It was found that as the content of amine groups increased, the solubility and the antibacterial activity were evidently promoted.⁶³

ii. Tertiary amino groups

The CHI derivatives grafted with tertiary amino groups were synthesized by aminoalkylation using chlorodialkylaminoethylene as the source of amine in alkaline medium. The structures of these derivatives are shown in **Figure 1.9**. The antibacterial activity of these derivatives was much higher than that of the native CHI at pH 5.5 and increased in the following order: *O*-diethylaminoethyl CHI **46** < *O*-aminoethyl CHI **44** < *O*-dimethylaminoethyl CHI **45**. Je et al. suggested two reasons for the promoted antibacterial activity: 1). the introduction of amino functional groups on hydroxyl groups increased the content of positive charges: 2). the hydrophobic interaction between cell wall and polysaccharides chains was enhanced due to the hydrophobic moieties of substituted groups.⁷⁸

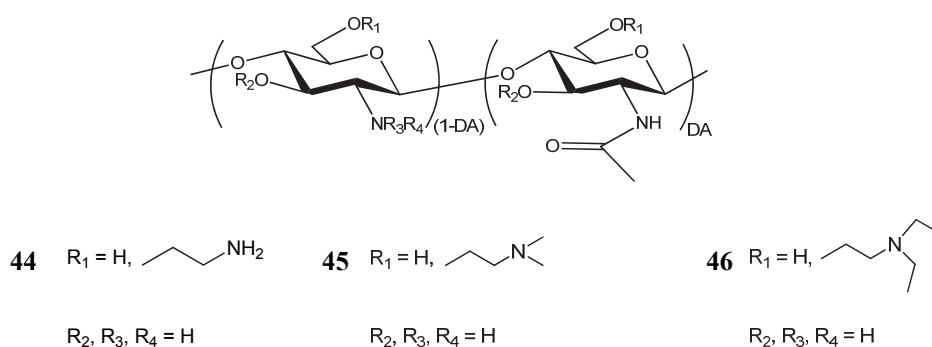


Figure 1.9: Structure of CHI derivatives containing tertiary amide groups (**44** *O*-aminoethyl CHI, **45** *O*-dimethylaminoethyl CHI and **46** *O*-diethylaminoethyl CHI).

iii. Quaternary ammonium groups

The quaternary CHI derivatives could be obtained by 2 different routes: 1 by methylation reaction using methyl iodide (CH_3I) to transfer the primary amino, secondary or tertiary amide groups to quaternary ammonium groups and 2 by introducing the quaternary ammonium groups directly on the chains of CHI.

1) Cationic CHI derivatives obtained by methylation

The structures of the CHI derivatives obtained by methylation are presented in **Figure 1.10**.

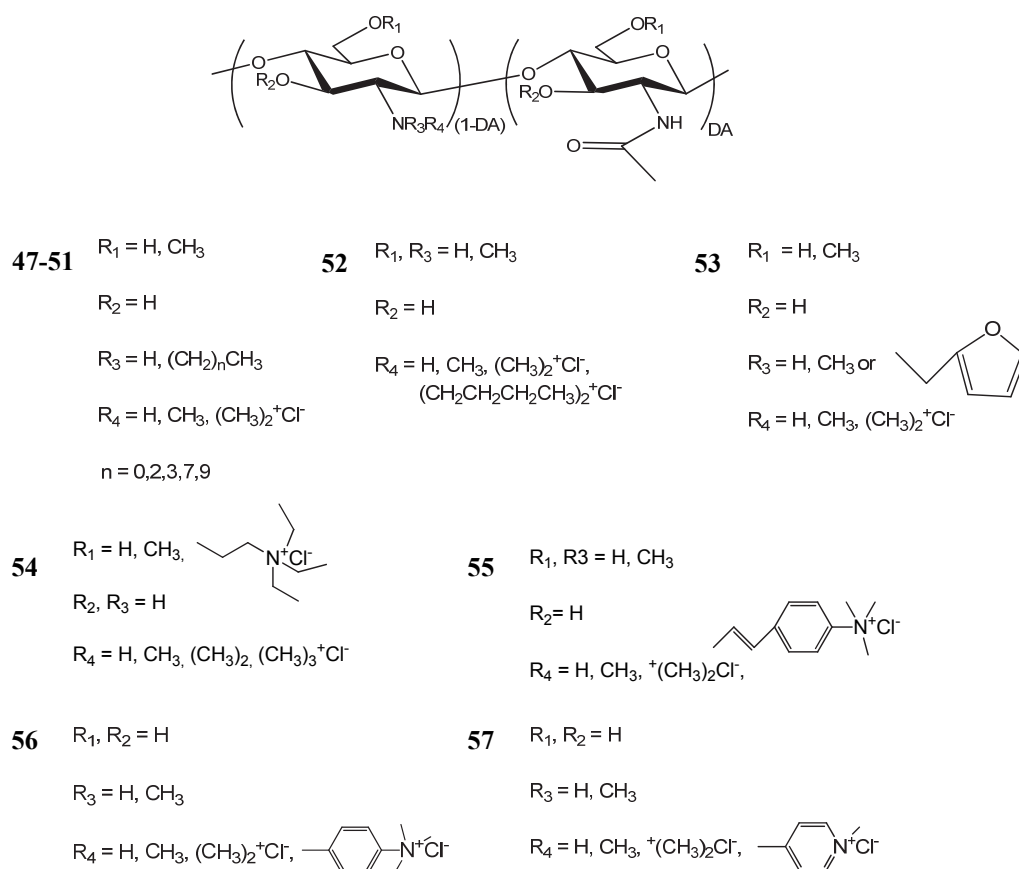


Figure 1.10: Structure of cationic CHI derivatives obtained by methylation (**47** (*O*-methyl)-*N,N,N*-trimethyl CHI, **48** (*O*-methyl)-*N,N*-dimethyl-*N*-propyl CHI, **49** (*O*-methyl)-*N,N*-dimethyl-*N*-butyl CHI, **50** (*O*-methyl)-*N,N*-dimethyl-*N*-octyl CHI, **51** (*O*-methyl)-*N,N*-diimethyl-*N*-dodecyl CHI, **52** (*O*-methyl)-*N*-methyl-*N,N*-dibutyl CHI, **53** (*O*-methyl)-*N,N*-dimethyl-*N*-furfuryl CHI, **54** *O*-triethylaminoethyl CHI, **55** (*O*-methyl)-*N*-(4-trimethylaminocinnamyl) CHI, **56** (*O*-methyl)-*N*-(4-trimethylaminobenzyl) CHI and **57** (*O*-methyl)-*N*-(4-methylpyridyl) CHI).

The most simply cationic methylated CHI derivatives, (*O*-methyl)-*N,N,N*-trimethyl CHI **47** were prepared by methylation reaction using CH_3I , NaI and NaOH in *N*-methyl-2-pyrrolidone (NMP) or a dimethylformamide (DMF)/water mixture.⁵⁰ The methyl groups were grafted randomly both hydroxyl and amino groups and formed *O*-methyl, *N*-methyl, *N,N*-dimethyl and *N,N,N*-trimethyl groups on the chains of CHI. It was found by Runarsson et al. that this kind of derivatives showed antibacterial activity against *S. aureus* at both pH 5.5 and pH 7.2, but the native CHI only functioned at lower pH. It is worth mentioning that the inhibitory effect of the CHI derivative with high amount of *N,N,N*-trimethyl groups (DQ ~

70%) at pH 7.2 was more effective than the native one at pH 5.5. Otherwise, it was noticed that the antibacterial activity of these derivatives also depended on the amount of quaternary ammonium groups. With the increasing number of quaternary groups, the antibacterial activity of the CHI derivatives decreased at pH 5.5, but increased at pH 7.2. This indicated that at pH 5.5, the effect of protonated amino groups was predominate, while at pH 7.2 only *N,N,N*-trimethyl groups positively contributed to the antibacterial activity. The linear correlation between antibacterial activity and percentage of *N,N,N*-trimethyl groups at pH 5.5 meant that the contribution of *N*-methyl groups (secondary amino groups) and *N*-dimethyl groups (tertiary amino groups) was similar to the amino groups (primary amino groups).⁵⁰

The cationic CHI derivatives could be prepared also by grafting secondary amino groups via a reductive amination reaction reacting with alkylaldehydes at pH 4.5 using NaBH₄ as a reducing agent, followed by a step of *N,O*-methylation with the CH₃I. This kind of CHI derivatives were named as *N,N*-dimethyl-*N*-alkyl CHI derivatives **48-51** and **53**. It was found that the antibacterial activity of this kind of CHI derivatives was higher than that of the native one and depended on the DQ, the length of alkyl chain and the hydrophobicity of grafted molecule.^{50,58-59,66,79} Generally, the substituent effect on the promotion of antibacterial activity is as the following order: (*O*-methyl)-*N,N*-dimethyl-*N*-dodecyl CHI **51** > (*O*-methyl)-*N,N*-dimethyl-*N*-octyl CHI **50** > (*O*-methyl)-*N*-methyl-*N*-dibutyl CHI **49** > (*O*-mehtyl)-*N,N*-dibutyl CHI **52** > CHI at pH 6.0 reported by kim et al. The difference between the antibacterial activity of (*O*-methyl)-*N,N*-dimethyl-*N*-propyl CHI **48**, (*O*-mehtyl)-*N,N*-dimethyl-*N*-furfuryl CHI **53** and (*O*-methyl)-*N,N,N*-trimethyl CHI **47** was not remarkable at weak acidic and neutral pH.⁶⁶ Otherwise, although several work demonstrated the positive effect of DQ on the improvement of the antibacterial activity of (*O*-mehtyl)-*N,N*-dimethyl-*N*-alkyl CHI derivatives **48-51** and **53**, it was also noticed by Sajomsang et al. that too much quaternary ammonium groups might induce the decrease of such activity due to the strong electrostatic repulsions of chains with more charges.⁶⁵

O-triethylaminoethyl CHI **54** was prepared by converting the tertiary amino groups of the *O*-diethylaminoethyl CHI **46** to the quaternary ammonium groups via methylation reaction. After the modification, the inhibitory effect of to the growth of *S. aureus* was improved, but that to the growth of *E. coli* was not observed.⁵⁷

The quaternary ammonium CHI derivatives containing aromatic and pyridyl groups were synthesized by reductive amination reaction grafting with aldehydes using NaCNBH₃ as a reductive agent in acetic acid solution followed by a step of methylation.⁶⁵ These CHI

derivatives, (*O*-methyl)-*N*-(4-trimethylaminocinnamyl) CHI **55**, (*O*-methyl)-*N*-(4-trimethylaminobenzyl) CHI **56** and (*O*-methyl)-*N*-(4-methylpyridyl) CHI **57**, also showed good antibacterial activity against *E. coli* and *S. aureus* at neutral pH.^{56,65} To assess the influence of the quaternary groups to the antibacterial activity, the CHI derivatives were compared considering the effect of the degree of total substitution (the sum of aromatic (or pyridyl) groups and *N,N,N*-trimethyl groups, DS_T). It was found that the antibacterial activity decreased in the order of *N*-(4-trimethylaminocinnamyl) CHI **55** (DS_T ~ 0.65) > *N,N,N*-trimethyl CHI **47** (DS_T ~ 0.64) ≈ *N*-(4-methylpyridyl) CHI **57** (DS_T ~ 0.70) > *N,N,N*-trimethyl CHI **47** (DS_T ~ 0.28 or 0.31) > *N*-(4-trimethylaminobenzyl) CHI **56** (DS_T ~ 0.33) > *N*-(4-methylpyridyl) CHI (DS_T ~ 0.30) **57**. Thus, longer side chains and more cationic groups seemed to enhance the antibacterial activity of this kind of CHI derivatives.

2) Cationic CHI derivatives obtained by grafting quaternary ammonium groups

Although the CHI derivatives prepared by 2 steps reaction are soluble in neutral water and showed a good antibacterial activity, it is difficult to control their properties due to the variety of substituent on the chains. Over the last decade, amount of researches were devoted to modify the synthesis process to obtain the quaternized CHI with reproducible properties. In the next part, two main kinds of quaternized CHI (**Figure 1.11**) together with their antibacterial activity will be presented.

The quaternized CHI (QCHI) derivatives **58-63** are common cationic modified CHI derivatives synthesized via an open-ring process of epoxy group.^{69,80-86} The grafted position could be easily controlled by varying the pH of reaction. The QCHI showed a better solubility over a wide range of pH and exhibited significant antibacterial activity against *E. coli* and *S. aureus* at neutral pH (~ pH 7–7.4). It was found that the antibacterial activity of *N*-substituted QCHI was improved with the increase of the DS and the hydrophobicity of substituent.⁵³ The latter could be achieved by increasing the length of alkyl chain in the quaternary ammonium group or replacing the alkyl chain by a more hydrophobic one. For instance, QCHI with tributyl groups and dimethylbenzyl groups **62-63** at the end of side chain were more effective to kill the bacteria compared to that with trimethyl groups **59**.⁵³

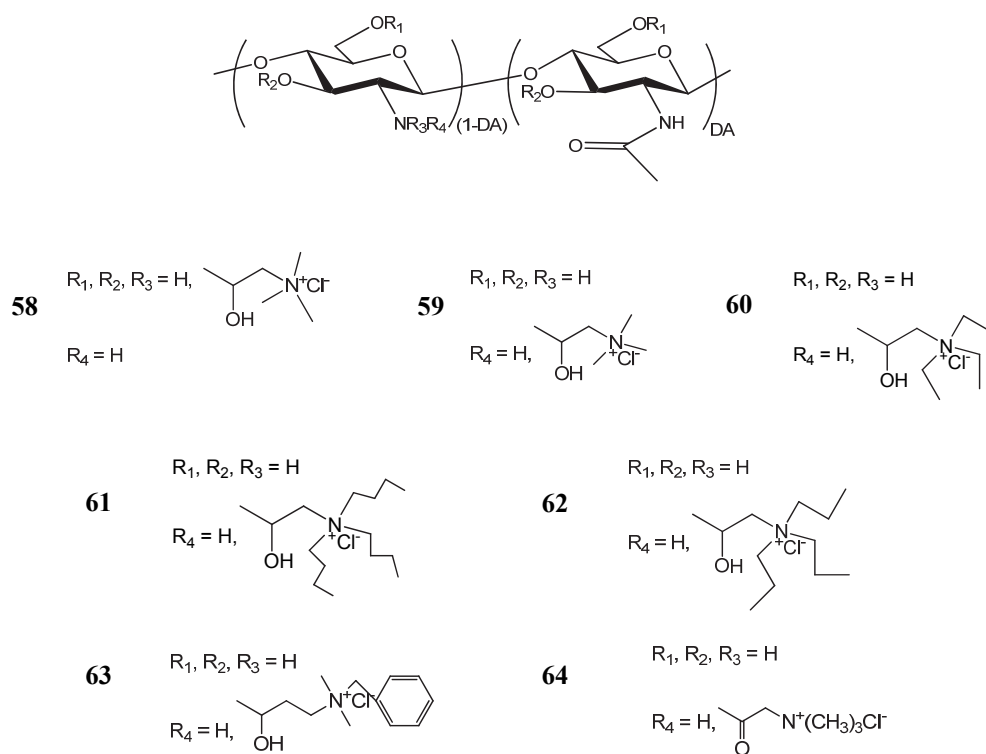


Figure 1.11: Structure of CHI derivatives modified with quaternized groups (**58** *N,O*-hydropropyltrimethyl CHI, **59** *N*-hydropropyltrimethyl CHI, **60** *N*-hydropropyltriethyl CHI, **61** *N*-hydropropyltripropyl CHI, **62** *N*-hydropropyltributyl CHI and **63** *N*-hydropropyldimethylbenzyl CHI and **64** *N*-betainate CHI).

N-betainate CHI derivatives **64** were prepared in 5 reaction steps of reaction with a process of protection and deprotection of the amino and primary hydroxyl groups.⁸⁷⁻⁸⁸ It was found that such CHI derivatives showed little antibacterial activity at pH 7.2 and a decreased activity with the increased of the DS at pH 5.5.⁵¹ The decreased antibacterial activity with the increase of DS was explained by the consumption of the more reactive amine groups with another less reactive one.

Overall, the effect of substituent on the antibacterial activity of modified CHI derivatives is very complicated. Although it is impossible to compare the results obtained by different authors in parallel due to the different experimental conditions and test methods, it still could be concluded that the length of the side chains, the nature of the charge, the degree of substitution, the hydrophobic/hydrophilic property of the substituent and the grafted position

work together. Otherwise, the hydrophilic/hydrophobic balance and the intra/intermolecular interactions caused by the chemical modification also contribute to the antibacterial activity.

1.4 Antibacterial multilayer films based on CHI

According to Rubner *et al.* in their recent review on the design of antibacterial surfaces and interfaces using polyelectrolyte multilayers (PEM),⁸⁹ there are three chief strategies to achieve this goal: adhesion resistance, biocide leaching and contact killing strategies (**Figure 1.12**). In the first approach, the aim is to reduce the capacity of bacteria to adhere at early stages. It often relies on the use of superhydrophobic surfaces.⁹⁰ In the second approach, which is also the oldest one, cytotoxic compounds are released and diffuse over time from the delivery system. Antibacterial peptides⁹¹⁻⁹² and silver ions^{49,93-95} fall into this category.⁹⁶ They have proven to be efficient in reducing the number of bacteria onto functionalized PEM films.^{49,91-95} Finally, the contact killing strategy seeks to biochemically induce death of bacteria that have adhered to the material surface.⁹⁷

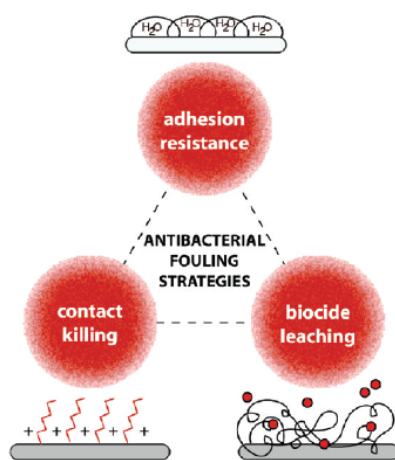


Figure 1.12: Three chief strategies to design an antibacterial surface.⁸⁹

CHI, due to its intrinsic properties as discussed above, appears thus as a good candidate for the design of contact killing films.

Generally, the multilayer films were obtained by alternatively depositing the oppositely charged polyelectrolytes on the substrates as shown in **Figure 1.13**, whose properties could be easily altered by changing the synthesis condition and materials. Although several polyanions

have been used as the partner of CHI for the construction of multilayer films, the antibacterial activity study of these multilayer assemblies was only emerged.^{17-18,21-22,25,98-100}

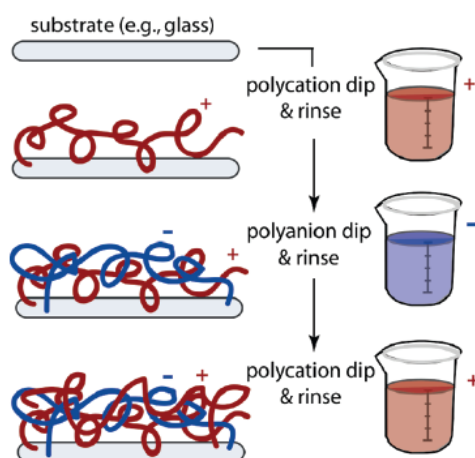


Figure 1.13: Process of the construction the polyelectrolyte multilayers (PEM) films by layer-by-layer technique.⁸⁹

Generally, the antibacterial activity of these multilayer films strongly depends on the nature of CHI and also its negative charged partner. The multilayer films ended by polyanions inhibit less or do not inhibit the growth of bacteria than those ended by CHI.

In PBS, κ -Carrageenan terminated (CHI/ κ -Carrageenan) multilayer films caused very little death of *E. faecalis*, and the viability of the adhering bacteria was very close to the one found on glass (control). Oppositely, on CHI terminated multilayers, a higher proportion of bacteria were dead after 1 h of contact. The result implies that despite the CHI loose some antibacterial function due to the deprotonation of amino groups in solution at pH 6.5-7.15, moderate antibacterial efficacy remains on the surface of multilayer films under physiological conditions, i.e., in PBS and at pH 7.0. CHI/ κ -carrageenan multilayers combine CHI as a rather weak polyelectrolyte with the strong polyelectrolyte carrageenan. Under physiological conditions, the sulfate groups of carrageenan are completely dissociated and can form ion pairs $-O-SO_3^-/-H_3^+N-$ with amino groups of CHI that can stabilize its cationic charge over broader pH range and contribute to its antibacterial activity at elevated pH values.²¹

The investigation of antibacterial activity of multilayer films containing CHI and pectin demonstrated these films could inhibit the growth of bacteria and their antibacterial activity increased with the increase of the deposition number of CHI layers.²²

In another case, reported by Yuhua Feng et al., the (CHI/Keggin-type polyoxometalate (POM) **65**)_n (n=30) and CHI casting multilayer films inhibited the growth of *E. coli*, but the (CHI/ α -SiW₁₂)_n (n=30) did not. The antibacterial activity of (CHI/ α -POM₁₂)_n (n=30) multilayer was explained probably due to the redox property of α -POM₁₂ which may oxidize the cell membrane and inhibit the growth of bacteria.²⁵

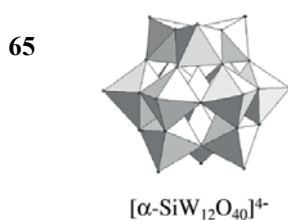


Figure 1.14: Structures of Keggin-type polyoxometalate (POM) (α -[SiW₁₂O₄₀]⁴⁻(α -SiW₁₂)).²⁵

Besides the nature of polyelectrolyte, it was found that the assembly pH could affect the antibacterial activity of PEM film as well. The number of viable bacteria on the (heparin/CHI)₆ multilayer films assembled at pH = 3.8, 2.9 and 6.0 decreased by 68%, 58% and 46% respectively. This phenomenon could be explained by the different amount of CHI adsorbed on the films at different pH.¹⁸

Considering the above studies, it could be imaged that the antibacterial activity is mainly influenced by both the nature of polyelectrolyte and the surface properties of films, including charge density, hydrophobicity, roughness and rigidity. Thus, the PEM films based on polycations other than CHI may also have the possibility to inhibit the growth of bacteria by contact killing, provided that the surface has suitable properties. In the following context, PEM films with contact-killing antibacterial activity are presented.

1.5 Antibacterial multilayer films based on synthetic polyelectrolytes

The structures of the polyelectrolyte pairs used in PEM films are shown in **Figure 1.15**. Some of these PEM films inhibited the growth of bacteria due to the antibacterial property of

polyocations, whereas the others exerting the bacterial growth inhibition effect for the specific properties of PEM surface.

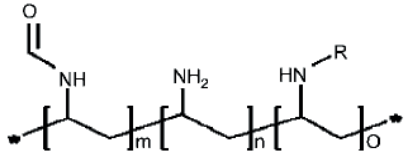
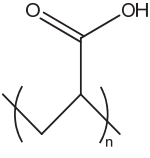
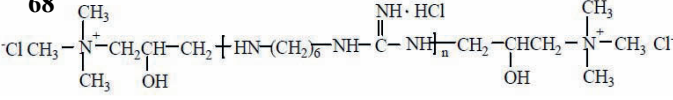
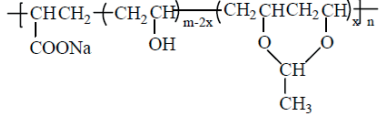
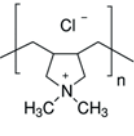
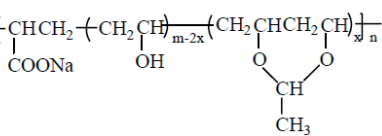
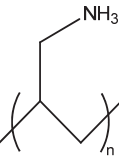
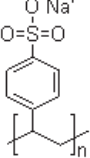
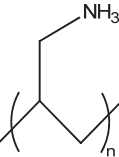
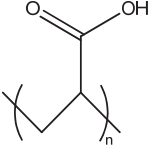
Ref	Polycation	polyanion
101	<p>66</p>  <p>N-hexanoyl-polyvinylamine (C₆-PVAm, R = C₆)</p>	<p>67</p>  <p>poly(acrylic acid) (PAA)</p>
102	<p>68</p>  <p>Cationic poly(hexamethylene guanidine hydrochloride) (CPHGH)</p>	<p>69</p>  <p>poly(vinyl alcohol)/sodium acrylate (APVA-co-AANa)</p>
102	<p>70</p>  <p>poly(diallyldimethylammonium chloride) (PDADMAC)</p>	<p>69</p>  <p>poly(vinyl alcohol)/sodium acrylate (APVA-co-AANa)</p>
103-104	<p>71</p>  <p>poly(allylamine hydrochloride) (PAH)</p>	<p>72</p>  <p>poly(styrene sodium sulfate) (PSS)</p>
103-104	<p>71</p>  <p>poly(allylamine hydrochloride) (PAH)</p>	<p>67</p>  <p>poly(acrylic acid) (PAA)</p>

Figure 1.15: Pairs of polyelectrolyte polymers used in the PEM films showing the antibacterial activity.

The (*N*-hexanoyl-polyvinylamine (C₆-PVAm) **66**/poly(acrylic acid) (PAA) **67** PEM-treated cellulose films showed an increasing capacity to contact-kill *E. coli* with increasing number of polymeric bilayer (between 3 and 6 layers of cationic polymers because of the hydrophobicity of C₆-PVAm.¹⁰¹

Cellulose fibers assembled with thermally sensitive PEM films based on poly(diallyldimethylammonium choride) (PDADMAC) **70**/poly(vinyl alcohol)-co-sodium acrylate (APVA-co-AANa) **69** and cationic poly(hexamethylene guanidine hydrochloride) (CPHGH) **68**/APVA-co-AANa **69** showed high antibacterial activity. The former inhibited 100 % the growth of *E. coli* and *S. aureus* in 1 hour, being more effective than the latter, which inhibited 51.38 % of *E. coli* and 99.9% of *S. aureus* respectively. The antibacterial activity of these films was considered to be related to the quaternary ammonium groups.¹⁰²

The (poly(allylamine hydrochloride) (PAH) **71**/poly(acrylic acid) (PAA) **67**) PEM films and (PAH **71**/poly(styrene sodium sulfate (PSS) **72**) PEM films terminated with PAH built up by Lichter et al. exhibited antibacterial activity against *E. coli* and *S. epidermidis* by adjusting the pH. These films were assembled at high pH (pH > 8.5) and subsequently immersed at low pH (pH < 4.0) and underwent a reversible pH-dependent transition. This transition can create PEMs with drastically different chain mobility restrictions (as indicated by hydrated swelling levels) and free cationic charge (charges not coupled with an anionic polymer), two factors that greatly influence microbiocidal abilities (**Figure 1.16**).¹⁰³⁻¹⁰⁴

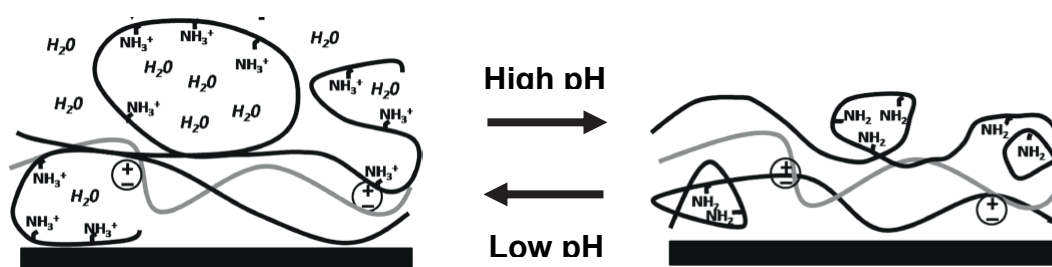


Figure 1.16: The simulation mechanism of reversible pH-dependent transition behavior of (PAH/PAA) and (PAH/PAA) PEM films. At lower pH, the films swells due to strongly electrostatic repulsion of the protonated amino groups; at higher pH, the non-protonated amino groups form the microhydrophobic domains, which cause the formation of rather thinner films. Once these films are washed at neutral pH, the protonated amino groups highly concentrate on the surface of the films just undergoing the incubation step at lower pH and bring out the antibacterial activity.¹⁰⁴

1.6 Conclusion

The antibacterial activity of CHI and its derivatives has been investigated in different work. It was found that this activity depends on the bacteria species, the nature of CHI and its derivatives and the experimental conditions. From the literature, the inhibitory effect of native CHI is caused by the protonated amino groups. However, as the pK_a of native CHI is \sim pH 6, few amino groups are converted to positively charged groups at neutral pH, which limits the antibacterial application of CHI. Therefore, it is important to optimize antibacterial activity by modulating the physico-chemical characteristics of polysaccharides. Since the antibacterial activity of CHI and its derivatives may strongly depend on its macromolecular and structural characteristics (Mw, DA and substituent, etc.), two main strategies have emerged to improve the antibacterial activity of CHI at neutral pH. One is decreasing the Mw or DA of CHI; the other one is grafting tailored functional groups on CHI chains, such as mannosyl groups and quaternary ammonium groups. It was noticed that the modified CHI derivatives showed distinguished susceptibility to bacteria according to the grafting groups. The grafting location, the nature of charges, the hydrophobicity and the structure of substituent were found to affect the antibacterial activity. Among all CHI derivatives, the (*O*-methyl)-*N,N*-dimethyl-*N*-alkyl CHI and *N,O*- or *N*-quaternized CHI (*N,O*- or *N-Q*CHI) showed outstanding inhibitory effect on the growth of *E.coli* and *S. aureus*.

Due to the intrinsic antibacterial activity and cationic property of CHI in weak acidic solution, the PEM films based on the native CHI have been synthesized as contact-killing antibacterial surface by layer-by-layer technique. It was found that the antibacterial activity of these films was not only related to the inhibitory effect of CHI, but also depended on the antibacterial property of polyanions, the strength of charges on anionic polyelectrolytes and the preparation conditions. Although the PEM films made of synthetic polymers also showed antibacterial activity, CHI-made PEM films are more attractive in biomedical applications due to the biocompatible biodegradable properties of polysaccharides.

References:

- (1) De Geest, B. G.; Sanders, N. N.; Sukhorukov, G. B.; Demeester, J.; De Smedt, S. C. *Chemical Society Reviews* **2007**, *36*, 636.
- (2) Kim, B.-S.; Choi, J.-W. *Biotechnology and Bioprocess Engineering* **2007**, *12*, 323.
- (3) Wang, Y.; Angelatos, A. S.; Caruso, F. *Chemistry of Materials* **2008**, *20*, 848.
- (4) Peyratout, C. S.; Daehne, L. *Angewandte Chemie, International Edition* **2004**, *43*, 3762.
- (5) Rinaudo, M. *Polym. Int.* **2008**, *57*, 397.
- (6) Picart, C. *Current Medicinal Chemistry* **2008**, *15*, 685.
- (7) Zhao, Q.; Han, B.; Wang, Z.; Gao, C.; Peng, C.; Shen, J. *Nanomedicine* **2007**, *3*, 63.
- (8) Qiu, X.; Leporatti, S.; Donath, E.; Moehwald, H. *Langmuir* **2001**, *17*, 5375.
- (9) Strand, B. L.; Morch, Y. A.; Espevik, T.; Skjak-Braek, G. *Biotechnology and Bioengineering* **2003**, *82*, 386.
- (10) Ye, S.; Wang, C.; Liu, X.; Tong, Z.; Ren, B.; Zeng, F. *J. Controlled Release* **2006**, *112*, 79.
- (11) Tiourina, O. P.; Sukhorukov, G. B. *Int. J. of Pharmaceutics* **2002**, *242*, 155.
- (12) Schüler, C.; Caruso, F. *Biomacromolecules* **2001**, *2*, 921.
- (13) Lee, H.; Jeong, Y.; Tae, G. P. *Biomacromolecules* **2007**, *8*, 3705.
- (14) Szarpak, A.; Pignot-Paintrand, I.; Nicolas, C.; Picart, C.; Auzely-Velty, R. *Langmuir* **2008**, *24*, 9767.
- (15) Szarpak, A.; Cui, D.; Dubreuil, F.; De Geest, B. G.; De Cock, L. J.; Picart, C.; Auzely-Velty, R. *Biomacromolecules* **2010**, *11*, 713.
- (16) Schneider, A.; Richert, L.; Francius, G.; Voegel, J.-C.; Picart, C. *Biomedical Materials* **2007**, *2*, S45.
- (17) Richert, L.; Lavallo, P.; Payan, E.; Shu, X. Z.; Prestwich, G. D.; Stoltz, J.-F.; Schaaf, P.; Voegel, J.-C.; Picart, C. *Langmuir* **2004**, *20*, 448.
- (18) Fu, J.; Ji, J.; Yuan, W.; Shen, J. *Biomaterials* **2005**, *26*, 6684.
- (19) Schoeler, B.; Delorme, N.; Doench, I.; Sukhorukov, G. B.; Fery, A.; Glinel, K. *Biomacromolecules* **2006**, *7*, 2065.
- (20) Jung, B.-D.; Hong, J.-D.; Voigt, A.; Leporatti, S.; Dähne, L.; Donath, E.; Möhwald, H. *Colloids and Surfaces A: Physicochemical and Engineering Aspects* **2002**, *198-200*, 483.
- (21) Bratskaya, S.; Marinin, D.; Simon, F.; Synytska, A.; Zschoche, S.; Busscher, H. J.; Jager, D.; van der Mei, H. C. *Biomacromolecules* **2007**, *8*, 2960.
- (22) Elsabee, M. Z.; Abdou, E. S.; Nagy, K. S. A.; Eweis, M. *Carbohydrate Polymers* **2008**, *71*, 187.
- (23) Balabushevich, N. G.; Tiourina, O. P.; Volodkin, D. V.; Larionova, N. I.; B., S. G. *Biomacromolecules* **2003**, *4*, 1191.
- (24) Berth, G.; Voigt, A.; Dautzenberg, H.; Donath, E.; Moehwald, H. *Biomacromolecules* **2002**, *3*, 579.
- (25) Feng, Y.; Han, Z.; Peng, J.; Lu, J.; Xue, B.; Li, L.; Ma, H.; Wang, E. *Materials Letters* **2006**, *60*, 1588.
- (26) Kujawa, P.; Schmauch, G.; Viitala, T.; Badia, A.; Winnik, F. M. *Biomacromolecules* **2007**, *8*, 3169.
- (27) Rinaudo, M. *Prog. Polym. Sci.* **2006**, *31*, 603.

- (28) Lim, S.-H.; Hudson, S. M. *Journal of Macromolecular Science, Polymer Reviews* **2003**, *C43*, 223.
- (29) Rabea, E. I.; Badawy, M. E. T.; Stevens, C. V.; Smagghe, G.; Steurbaut, W. *Biomacromolecules* **2003**, *4*, 1457.
- (30) Li, X.-f.; Feng, X.-q.; Yang, S.; Fu, G.-q.; Wang, T.-p.; Su, Z.-x. *Carbohydrate Polymers* **2010**, *79*, 493.
- (31) Tharanathan Rudrapatnam, N.; Kittur Farooqahmed, S. *Critical reviews in food science and nutrition* **2003**, *43*, 61.
- (32) Liu, X.; Song, L.; Li, L.; Li, S.; Yao, K. *Journal of Applied Polymer Science* **2007**, *103*, 3521.
- (33) Choi, B.-K.; Kim, K.-Y.; Yoo, Y.-J.; Oh, S.-J.; Choi, J.-H.; Kim, C.-Y. *International Journal of Antimicrobial Agents* **2001**, *18*, 553.
- (34) Helander, I. M.; Nurmiäho-Lassila, E. L.; Ahvenainen, R.; Rhoades, J.; Roller, S. *International Journal of Food Microbiology* **2001**, *71*, 235.
- (35) Chung, Y.-c.; Su, Y.-p.; Chen, C.-c.; Jia, G.; Wang, H.-l.; Wu, J. C. G.; Lin, J.-g. *Acta Pharmacologica Sinica* **2004**, *25*, 932.
- (36) Raafat, D.; Giraud, L.; Gerente, C.; Le Cloirec, P. *Applied and environmental microbiology* **2007**, *28*, 1357.
- (37) Tokura, S.; Ueno, K.; S., M.; Nishi, N. *Macromolecular symposium* **1997**, *120*, 1.
- (38) Lichter, J. A.; Van Vliet, K. J.; Rubner, M. F. *Macromolecules (Washington, DC, United States)* **2009**, *42*, 8573.
- (39) Jeon, Y.-J.; Park, P.-J.; Kim, S.-K. *Carbohydrate Polymers* **2000**, *44*, 71.
- (40) Xie, W.; Xu, P.; Wang, W.; Liu, Q. *Carbohydrate Polymers* **2002**, *50*, 35.
- (41) Xie, W.; Xu, P.; Wang, W.; Liu, Q. *Journal of Applied Polymer Science* **2002**, *85*, 1357.
- (42) Chung, Y.-C.; Wang, H.-L.; Chen, Y.-M.; Li, S.-L. *Bioresource Technology* **2003**, *88*, 179.
- (43) Strand, S. P.; Varum, K. M.; Ostgaard, K. *Colloids and Surfaces, B: Biointerfaces* **2003**, *27*, 71.
- (44) Zheng, L.-Y.; Zhu, J.-F. *Carbohydrate Polymers* **2003**, *54*, 527.
- (45) Chen, Y.-L.; Chou, C.-C. *Food Microbiology* **2004**, *22*, 29.
- (46) Huang, R.; Du, Y.; Zheng, L.; Liu, H.; Fan, L. *Reactive & Functional Polymers* **2004**, *59*, 41.
- (47) Yang, T.-C.; Chou, C.-C.; Li, C.-F. *International Journal of Food Microbiology* **2005**, *97*, 237.
- (48) Qin, C.; Li, H.; Xiao, Q.; Liu, Y.; Zhu, J.; Du, Y. *Carbohydrate Polymers* **2006**, *63*, 367.
- (49) Li, Z.; Lee, D.; Sheng, X.; Cohen, R. E.; Rubner, M. F. *Langmuir* **2006**, *22*, 9820.
- (50) Runarsson, O. V.; Holappa, J.; Nevalainen, T.; Hjalmsdottir, M.; Jaervinen, T.; Loftsson, T.; Einarsson, J. M.; Jonsdottir, S.; Valdimarsdottir, M.; Masson, M. *European Polymer Journal* **2007**, *43*, 2660.
- (51) Holappa, J.; Hjalmsdottir, M.; Masson, M.; Runarsson, O.; Asplund, T.; Soininen, P.; Nevalainen, T.; Jaervinen, T. *Carbohydrate Polymers* **2006**, *65*, 114.
- (52) Anitha, A.; Divya Rani, V. V.; Krishna, R.; Sreeja, V.; Selvamurugan, N.; Nair, S. V.; Tamura, H.; Jayakumar, R. *Carbohydrate Polymers* **2009**, *78*, 672.
- (53) Cai, Z.-S.; Song, Z.-Q.; Yang, C.-S.; Shang, S.-B.; Yin, Y.-B. *Polymer Bulletin (Heidelberg, Germany)* **2009**, *62*, 445.

- (54) Naberezhnykh, G. A.; Bakholdina, S. I.; Gorbach, V. I.; Solov'eva, T. F. *Russian Journal of Marine Biology* **2009**, *35*, 498.
- (55) Sajomsang, W.; Gonil, P.; Tantayanon, S. *International Journal of Biological Macromolecules* **2009**, *44*, 419.
- (56) Sajomsang, W.; Gonil, P.; Saesoo, S. *European Polymer Journal* **2009**, *45*, 2319.
- (57) Kim, C.-H.; Kim, S.-Y.; Choi, K.-S. *Polymers for Advanced Technologies* **1997**, *8*, 319.
- (58) Kim, C. H.; Choi, J. W.; Chun, H. C.; Choi, K. S. *Polymer Bulletin (Berlin)* **1997**, *38*, 387.
- (59) Ignatova, M.; Starbova, K.; Markova, N.; Manolova, N.; Rashkov, I. *Carbohydrate Research* **2006**, *341*, 2098.
- (60) Liu, X.; Guan, Y.; Yang, D.; Li, Z.; Yao, K. *Journal of Applied Polymer Science* **2001**, *79*, 1324.
- (61) No, H. K.; Young Park, N.; Ho Lee, S.; Meyers, S. P. *International Journal of Food Microbiology* **2002**, *74*, 65.
- (62) Hu, Y.; Du, Y.; Yang, J.; Tang, Y.; Li, J.; Wang, X. *Polymer* **2007**, *48*, 3098.
- (63) Xie, Y.; Liu, X.; Chen, Q. *Carbohydrate Polymers* **2007**, *69*, 142.
- (64) Kurita, K.; Kojima, T.; Nishiyama, Y.; Shimojoh, M. *Macromolecules* **2000**, *33*, 4711.
- (65) Sajomsang, W.; Tantayanon, S.; Tangpasuthadol, V.; Daly, W. H. *Carbohydrate Polymers* **2008**, *72*, 740.
- (66) Jia, Z.; Shen, D.; Xu, W. *Carbohydrate Research* **2001**, *333*, 1.
- (67) Muzzarelli, R.; Tarsi, R.; Filippini, O.; Giovanetti, E.; Biagini, G.; Varaldo, P. E. *Antimicrobial Agents and Chemotherapy* **1990**, *34*, 2019.
- (68) Andres, Y.; Giraud, L.; Gerente, C.; Le Cloirec, P. *Environmental Technology* **2007**, *28*, 1357.
- (69) Kim, J. Y.; Lee, J. K.; Lee, T. S.; Park, W. H. *International Journal of Biological Macromolecules* **2003**, *32*, 23.
- (70) Devlieghere, F.; Vermeulen, A.; Debevere, J. *Food Microbiology* **2004**, *21*, 703.
- (71) Gerasimenko, D. V.; Avdienko, I. D.; Bannikova, G. E.; Zueva, O. Y.; Varlamov, V. P. *Applied Biochemistry and Microbiology (Translation of Prikladnaya Biokhimiya i Mikrobiologiya)* **2004**, *40*, 253.
- (72) Murata, H.; Koepsel, R. R.; Matyjaszewski, K.; Russell, A. J. *Biomaterials* **2007**, *28*, 4870.
- (73) Uchida, Y.; Izume, M.; Ohtakara, A. *G.Skjak-Brock* **1989**, 373.
- (74) Jung, B.-O.; Kim, C.-H.; Choi, K.-S.; Lee, Y. M.; Kim, J.-J. *Journal of Applied Polymer Science* **1999**, *72*, 1713.
- (75) Chen, Y.-L.; Chou, C.-C. *Food Microbiology* **2005**, 29.
- (76) Kurita, K.; Kojima, T.; Munakata, T.; Akao, H.; Mori, T.; Nishiyama, Y.; Manabu, S. *Chen. Lett.* **1998**, *27*, 317.
- (77) Eldin, M. S. M.; Soliman, E. A.; Hashem, A. I.; Tamer, T. M. *Trends Biomater. Artif. Organs* **2008**, *22*, 125.
- (78) Je, J.-Y.; Kim, S.-K. *Journal of Agricultural and Food Chemistry* **2006**, *54*, 6629.
- (79) Guo, Z.; Xing, R.; Liu, S.; Zhong, Z.; Ji, X.; Wang, L.; Li, P. *Int. J. Food Microbiology* **2007**, 214.
- (80) Seong, H.-S.; Whang, H. S.; Ko, S.-W. *Journal of Applied Polymer Science* **2000**, *76*, 2009.

- (81) Cho, J.; Justin, G.; Piquette-Miller, M.; Allen, C. *Biomacromolecules* **2006**, *7*, 2845.
- (82) Wu, J.; Wei, W.; Wang, L.-Y.; Su, Z.-G.; Ma, G.-H. *Biomaterials* **2007**, *28*, 2220.
- (83) Wu, J.; Su, Z.-G.; Ma, G.-H. *Int. J. Pharmaceutics* **2006**, *315*, 1.
- (84) Shi, X.-W.; Du, Y.-M.; Li, J.; L., S. X.-.; Yang, J.-H. *J. Microencapsulation* **2006**, *23*, 405.
- (85) Li, H.; Yumin, D.; Wu, X.; Zhan, H. *Colloids Surf., A: Physicochem. Eng. Aspects* **2004**, *242*, 1.
- (86) Lim, S.-H.; Hudson, S. M. *Carbohydrate Research* **2004**, *339*, 313.
- (87) Korjamo, T.; Holappa, J.; Taimisto, S.; Savolainen, J.; Jaervinen, T.; Moenkkoenen, J. *European Journal of Pharmaceutical Sciences* **2008**, *35*, 226.
- (88) Holappa, J.; Nevalainen, T.; Soninien, P.; Elomaa, M.; Safin, R. *Macromolecules* **2004**, *37*, 2784.
- (89) Lichter, J. A.; Van Vliet, K. J.; Rubner, M. F. *Macromolecules* **2009**, *42*, 8573.
- (90) Genzer, J.; Efimenko, K. *Biofouling* **2006**, *22*, 339.
- (91) Etienne, O.; Picart, C.; Taddei, C.; Haikel, Y.; Dimarcq, J. L.; Schaaf, P.; Voegel, J. C.; Ogier, J. A.; Egles, C. *Antimicrobial Agents and Chemotherapy* **2004**, *48*, 3662.
- (92) Guyomard, A.; De, E.; Jouenne, T.; Malandain, J.-J.; Muller, G.; Glinel, K. *Advanced Functional Materials* **2008**, *18*, 758.
- (93) Fu, J.; Ji, J.; Fan, D.; Shen, J. *Journal of Biomedical Materials Research, Part A* **2006**, *79A*, 665.
- (94) Grunlan, J. C.; Choi, J. K.; Lin, A. *Biomacromolecules* **2005**, *6*, 1149.
- (95) Malcher, M.; Volodkin, D.; Heurtault, B.; Andre, P.; Schaaf, P.; Mohwald, H.; Voegel, J.-C.; Sokolowski, A.; Ball, V.; Boulmedais, F.; Frisch, B. *Langmuir* **2008**, *24*, 10209.
- (96) Shi, Z.; Neoh, K. G.; Zhong, S. P.; Yung, L. Y. L.; Kang, E. T.; Wang, W. *Journal of Biomedical Materials Research, Part A* **2006**, *76A*, 826.
- (97) Li, Y.; Leung, W. K.; Yeung, K. L.; Lau, P. S.; Kwan, J. K. C. *Langmuir* **2009**, *25*, 13472.
- (98) Chua, P.-H.; Neoh, K.-G.; Kang, E.-T.; Wang, W. *Biomaterials* **2008**, *29*, 1412.
- (99) Chua, P. H.; Neoh, K. G.; Shi, Z.; Kang, E. T. *Journal of Biomedical Materials Research, Part A* **2008**, *87A*, 1061.
- (100) Yuan, W.; Ji, J.; Fu, J.; Shen, J. *Journal of Biomedical Materials Research, Part B: Applied Biomaterials* **2008**, *85B*, 556.
- (101) Westman, E.-H.; Ek, M.; Waagberg, L. *Holzforchung* **2009**, *63*, 33.
- (102) Pan, Y.; Xiao, H.; Zhao, G.; He, B. *Polymer Bulletin (Heidelberg, Germany)* **2008**, *61*, 541.
- (103) Lichter, J. A.; Thompson, M. T.; Delgadillo, M.; Nishikawa, T.; Rubner, M. F.; Van Vliet, K. J. *Biomacromolecules* **2008**, *9*, 2967.
- (104) Lichter, J. A.; Rubner, M. F. *Langmuir* **2009**, *25*, 7686.

Chapter 2

Contact-killing microcapsules based on quaternized chitosan (QCHI) derivatives

Table of contents

2	Résumé (<i>Fr</i>)	53
2.1	Introduction	55
2.2	Synthesis and characterization of QCHI derivatives.....	57
2.2.1	Synthesis of QCHI derivatives under different conditions	57
2.2.2	Macromolecular characterization of QCHI derivatives	60
2.2.2.1	Measurement of intrinsic viscosity	60
2.2.2.2	Determination of the molar mass by size exclusion chromatography (SEC)	63
2.2.3	Antibacterial activity	65
2.3	Synthesis of capsules based on the QCHI derivatives	67
2.3.1	Utilization of <i>N</i> -QCHI derivatives as the cationic partners of HA for the synthesis of capsules	67
2.3.1.1	Publication in <i>Advanced Functional Materials</i> ¹²	68
2.3.1.2	Supporting information	91
2.3.1.3	Complementary results.....	94
2.3.2	Utilization of <i>N,O</i> -QCHI derivatives as the cationic partners of HA for the synthesis of capsules	99
2.3.2.1	Syntheses of capsules based on <i>N,O</i> -QCHI derivatives.....	99
2.3.2.2	Antimicrobial activity of (HA/ <i>N,O</i> -QCHI) capsules	105
2.4	Conclusion.....	108
2.5	Complementary experimental part.....	109
	References:	111

2 Résumé (Fr)

Ce chapitre est consacré à la synthèse de microcapsules multicouches constituées uniquement de polysaccharides, capables de tuer des bactéries par simple contact. Ces capsules sont obtenues par assemblage couche-par-couche d'acide hyaluronique (HA) de dérivés quaternisés du chitosane (QCHI) solubles dans l'eau à pH neutre ayant différents degrés de substitution (DS). Les dérivés QCHI sont modifiés soit sélectivement au niveau de la fonction amine du chitosane (*N*-QCHI) soit de façon aléatoire à la fois au niveau de la fonction amine et des hydroxyles (*N,O*-QCHI) selon les conditions de réactions utilisées. Celles-ci consistent à faire réagir le chitosane avec le chlorure de glycidyltriméthylammonium (GTMAC) en milieu aqueux acide homogène ou en milieu aqueux neutre hétérogène. En faisant varier le rapport molaire GTMAC/CHI, des DS allant de 0,31 à 0,66 ont été obtenus pour les dérivés *N*-QCHI, préparés en milieu acide. Les dérivés *N,O*-QCHI, préparés en milieu neutre, ont été isolés avec des DS supérieurs à 1. Étonnamment, deux produits différents ont été obtenus dans des conditions neutres hétérogènes : l'un est isolé à partir de surnageant du milieu réactionnel (*N,O*-QCHIIa), l'autre est récupéré dans la partie insoluble (*N,O*-QCHIIb). Les propriétés macromoléculaires des dérivés QCHI, incluant la viscosité intrinsèque et la masse molaire, M_w ont été analysées par différentes techniques. L'activité antibactérienne des dérivés QCHI contre les bactéries Gram(+) et (-), a également été étudiée. Les dérivés QCHI et l'acide hyaluronique (HA) ont ensuite été utilisés pour la synthèse selon la technique de dépôt couche par couche de microcapsules dans des conditions physiologiques en utilisant des particules de CaCO_3 comme supports biocompatibles. Concernant, les capsules à base de dérivés *N*-QCHI, nous avons constaté que leur morphologie est étroitement liée au DS du *N*-QCHI. Ceci a été attribué à des propriétés de complexation polyélectrolyte différentes avec le HA. Le DS s'est avéré être également un paramètre clé pour contrôler l'activité antibactérienne de *N*-QCHI contre *E.Coli*. Concernant les capsules composées de dérivés de *N,O*-QCHI, leur morphologie varie avec la nature du dérivé selon qu'il provient du surnageant (*N,O*-QCHIIa) ou du précipité (*N,O*-QCHIIb). Malgré une grande différence en ce qui concerne la morphologie, les capsules à base de *N,O*-QCHIIa de DS=1,33 ont montré une activité antibactérienne contre *E.Coli* similaire à celles à base de *N,O*-QCHIIb de DS=1,1. L'activité antibactérienne de ces capsules s'est avérée être plus faible que les capsules préparées avec les dérivés *N*-QCHI de DS=0,66, mais plus élevée que les autres capsules obtenues à partir des dérivés *N*-QCHI de DS < 0,55. Ce résultat indique que l'aptitude des

capsules à inhiber la croissance de bactéries dépend non seulement du DS du QCHI, mais est aussi lié à d'autres facteurs, tels que les caractéristiques macromoléculaires des dérivés QCHI, la densité de charge. L'aptitude des capsules à tuer les bactéries par simple contact a été confirmée par microscopie confocale (CLSM) et microscopie électronique à transmission (TEM). Du fait de leur activité antibactérienne, les capsules contenant des dérivés QCHI offrent un avantage distinct pour transporter des médicaments notamment pour le traitement de certaines infections bactériennes.

2.1 Introduction

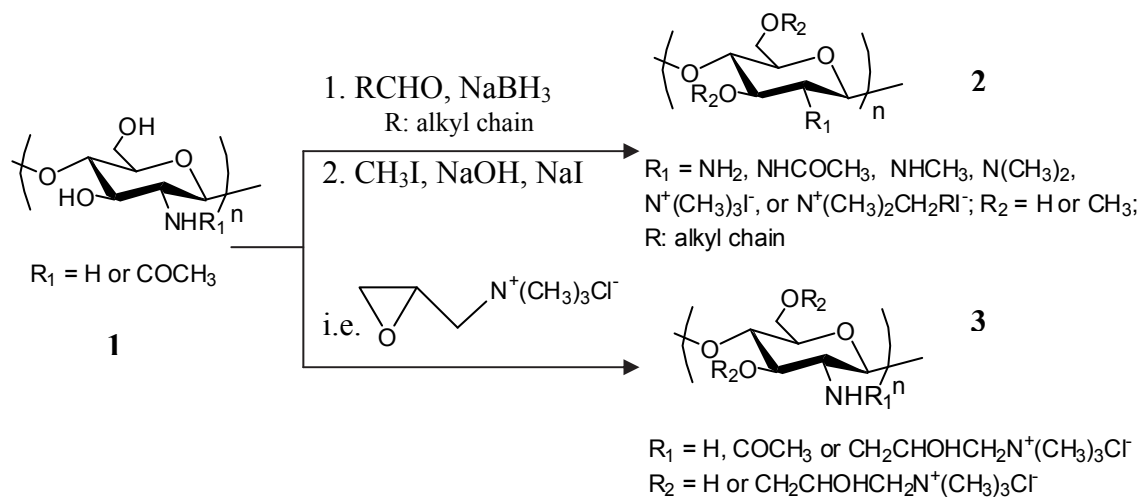
The aim of this work was to synthesize contact-killing multilayer capsules based fully on polysaccharides. The contact-killing strategy seeks to biochemically induce the death of bacteria that adhered to the material surface. The multilayer capsules are prepared by a layer-by-layer assembly of oppositely charged polyelectrolytes on a sacrificial colloidal template, followed by a step of core removal. Based on previous work in our laboratory showing the ability to prepare stable capsules containing hyaluronic acid (HA) as a negatively charged polysaccharide using CaCO_3 particles as template under mild conditions, we proposed to use chitosan (CHI) **1** as a polycationic partner of HA for the synthesis of polysaccharide capsules exhibiting contact killing activity due to the intrinsic antibacterial properties of CHI as reviewed in Chapter 1. However, CHI cannot be used for the synthesis of capsules, since the weak acidic conditions, used for dissolving the native CHI due to its poor water solubility above $\text{pH} \sim 6.5$, can induce the dissolution of CaCO_3 particles. Thus, the synthesis of water-soluble CHI derivatives was required.

Nowadays, a great of work has been done to modify the properties of CHI. Among all modifications, quaternization has been the most efficient method to improve the water solubility of CHI over a wide pH range. In addition, the QCHI derivatives exhibited good antimicrobial activity compared to the native ones at neutral pH. Taking these advantages, QCHI derivatives have been used in the fabrication of fibres, hydrogels and filtration papers applied in different fields, such as pharmaceuticals, cotton industry and water filtration.¹⁻²

Until now, two different strategies have been adopted to obtain such CHI derivatives as shown in **Scheme 2.1**: 1) grafting an alkyl chain onto the amino group of CHI via a reductive amination reaction, and then, converting the resulting secondary amino group to quaternary ammonium group by methylation with methyl iodide;¹⁻⁴ 2) directly introducing quaternary ammonium groups onto the CHI backbone by a ring-opening reaction using an epoxide molecule.⁵⁻¹¹

The former one is a two step reaction. It allows grafting long alkyl chains onto the primary amine groups of CHI. But the random substitution of methyl, dimethyl and trimethyl groups induced by *N,O*-methylation creates a complicated structure of CHI derivatives **2** and thereby it is difficult to exactly determine the amount of various substituted groups. In contrast, the latter strategy is simple. The reaction affords in one step only one type of quaternized groups grafted on the chain of CHI; in addition, by changing reaction conditions, it is possible to

selectively modify CHI on the amino groups. These advantages not only favor the investigation of the influence of the degree of substitution (DS), but also of the grafted position on the properties of CHI derivatives.



Scheme 2.1: Strategies for the synthesis of QCHI derivatives reported in the literature (**1** chitosan (CHI), **2** and **3** quaternized chitosan derivatives (QCHI derivatives) prepared by different ways).

Therefore, we synthesized QCHI derivatives **3** according to the second method using glycidyltrimethylammonium chloride (GTMAC) **4** under acidic⁵⁻⁶ and neutral^{8,11} conditions as described in the literature. The macromolecular properties of the resulting derivatives, such as the intrinsic viscosity and the molar mass, were characterized by different techniques of macromolecular physico-chemistry. The antimicrobial activity of QCHI derivatives against Gram positive (Gram(+)) and Gram negative (Gram (-)) bacteria was also investigated. Then, capsules were synthesized based on HA and various QCHI derivatives and characterized respectively according to the different modification conditions of QCHI derivatives. The capsules made of QCHI derivatives obtained under acidic conditions (*N*-QCHI derivatives) were firstly discussed. Most of this part of work, such as the synthesis, morphology and biological activities, has been reported in **Advanced Functional Materials**¹². We completed with the study of permeability, biodegradability and antimicrobial activity of capsules. Then, the capsules composed of QCHI derivatives obtained under neutral conditions (*N,O*-QCHI derivatives) were concerned. We investigated the morphology and the permeability of capsules, as well as their antimicrobial activities.

2.2 Synthesis and characterization of QCHI derivatives

2.2.1 Synthesis of QCHI derivatives under different conditions

Chitosan with Mw 372 000 g/mol was selected for the synthesis of capsules. This sample is characterized by a degree of acetylation (DA) of 0.09 derived from the digital integration of the anomeric and methyl proton signals of the ^1H NMR spectrum of chitosan (**Figure 2.1**).

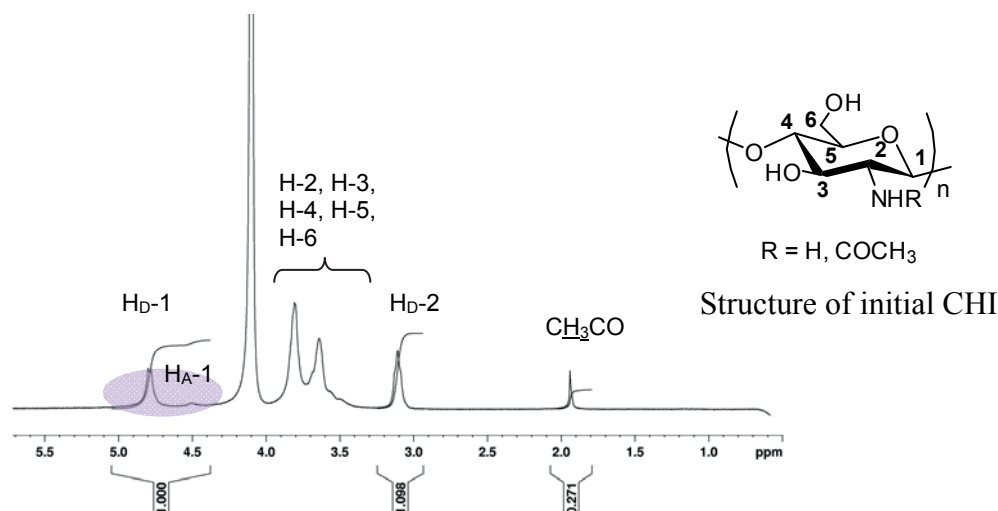
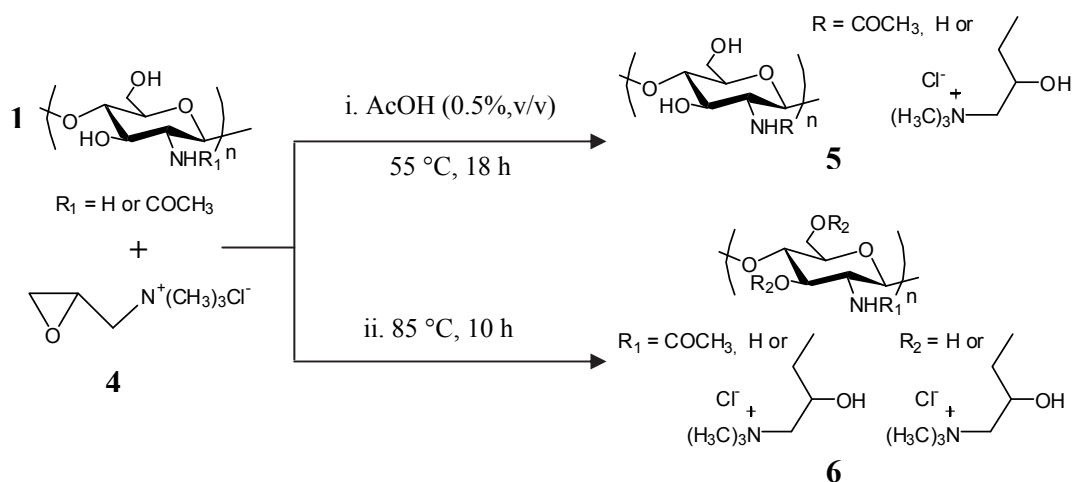


Figure 2.1: ^1H NMR spectra of initial CHI (400 MHz, $\text{D}_2\text{O} + \text{DCl}$, 80 °C, $C_p \sim 6$ g/L).

As mentioned above, we prepared the QCHI derivatives by reaction with GTMAC **4** under two different conditions, acidic homogenous aqueous conditions and neutral heterogeneous aqueous conditions, as shown in **Scheme 2.2**. These QCHI derivatives are named as *N*-substituted QCHI derivatives (*N*-QCHI derivatives) **5** and *N,O*-substituted QCHI derivatives (*N,O*-QCHI derivatives) **6** according to the modification positions on the CHI chain. In fact, the weak acidic homogenous aqueous conditions not only favor the random substitution of the sugar units in the CHI chain, but also the selective grafting on the primary amine groups. However, limited by the degree of acetylation (DA) of initial CHI (DA = 0.09), the degree of substitution (DS) could not exceed 0.91. To obtain the QCHI derivatives with higher DS, neutral conditions were applied since they allow to modify both the hydroxyl and amino groups. Interestingly, two products were isolated in the reaction performed under neutral conditions, which has never been reported in other work. One product with higher DS (*N,O*-QCHIa) was directly purified from the supernatant of the reaction medium; the other one with lower DS (*N,O*-QCHIb) was recovered in the precipitate formed during the reaction. The precipitate would be dissolved in aqueous solution at pH 5 and then purified. The products

obtained after this step showed a good solubility in water even at pH 9. The recovery of two different derivatives from one reaction may be related to the heterogeneous reaction conditions and the molar mass of initial CHI. Nevertheless, it is worth noting that all reactions were perfectly reproducible.



Scheme 2.2: Synthetic pathway for the preparation of the QCHI derivatives (**5** *N*-QCHI derivatives and **6** *N,O*-QCHI derivatives).

The conditions of reaction, the DS and water solubility of all products are given in **Table 2.1**. The DS of the QCHI derivatives samples was derived by conductimetric titration of Cl⁻ ions with AgNO₃. As can be seen from **Table 2.1**, the DS of *N*-QCHI derivatives prepared under acidic conditions did not exceed ~ 0.66, despite of using high molar ratio of GTMAC/CHI (~ 8/1); on the other hand, the DS of *N,O*-QCHIIa,b derivatives obtained at neutral pH by using a lower ratio of GTMAC/CHI (~ 6/1) could be higher than 1. The higher DS of *N,O*-QCHIIa,b confirmed that the substitution at neutral pH occurs on the hydroxyl groups in addition to the amine group. The water solubility of the QCHI derivatives was tested under neutral condition (pH 6.5) and alkaline condition (pH 9) respectively. By introducing cationic quaternary ammonium groups on the main chain of CHI, the water solubility of CHI at any pH was evidently improved. The QCHI derivatives with DS ≥ 0.24 were water-soluble at pH 6.5 and those with DS ≥ 0.31 dissolved even at pH 9. We also investigated the solubility of the QCHI derivatives at pH 6.5 in the aqueous solution with 0.15 M NaCl, which are the conditions adopted in the construction of microcapsules using CaCO₃ particles as a template. It was found that in the presence of salt, *N*-QCHI1 (DS = 0.24) turned to be insoluble at pH 6.5, while the others retained good solubility under the same conditions.

This result means that the QCHI derivatives with $DS \geq 0.31$ can be used in the preparation of capsules. The decreased solubility of *N*-QCHI1 in water at pH 6.5 containing salt can be explained by screening effect provided by the added salt. This reduces electrostatic repulsions between the QCHI chains, leading to aggregation of polymer chains.

Table 2.1: QCHI derivatives with different DS and water-solubility prepared under different reaction conditions.

Reference	Reaction medium	GTMAC: CHI ^a	DS ^b	Water solubility ^c		
				pH 6.5	pH 9	pH 6.5 with 0.15 M NaCl
Initial CHI	-	-	-	-	-	-
<i>N</i> -QCHI0	Acidic aqueous solution	0	0	-	-	-
<i>N</i> -QCHI1		2:1	0.24	+	-	-
<i>N</i> -QCHI2		3:1	0.31	+	+	+
<i>N</i> -QCHI3		4:1	0.39	+	+	+
<i>N</i> -QCHI4		6:1	0.55	+	+	+
<i>N</i> -QCHI5		8:1	0.66	+	+	+
<i>N,O</i> -QCHI1a	Neutral aqueous solution	1.5:1	0.64	+	+	+
<i>N,O</i> -QCHI1b			0.12	-	-	-
<i>N,O</i> -QCHI2a		3:1	0.93	+	+	+
<i>N,O</i> -QCHI2b			0.42	+	+	+
<i>N,O</i> -QCHI3a		6:1	1.33	+	+	+
<i>N,O</i> -QCHI3b			1.10	+	+	+

^amolar ratio; ^bdetermined by conductimetric titration and ^ctested at room temperature ($C_p = 5$ g/L) and verified by naked eyes: “-” means insoluble; “+” means completely soluble.

The ¹H NMR analysis allowed us to confirm the introduction of quaternary ammonium groups on CHI as well as to ascertain the substitution position (**Figure 2.2**). The identification of most proton and carbon signals of one-dimensional spectra of *N*-QCHI2 was precisely reported in the part of NMR spectroscopy of supporting information in publication in **Advanced Functional Materials**¹². The analysis of NMR spectra of *N*-QCHI2 confirmed the selective grafting of quaternary ammonium groups on the primary amine groups of CHI under acidic conditions. Compared to the ¹H NMR spectrum of *N*-QCHI2, an evident peak at 4.75 ppm was observed in the spectrum of *N,O*-QCHI3a and *N,O*-QCHI3b, respectively, corresponding to the H1 signal of the glucosamine units. (**Figure 2.2**) These peaks demonstrated that part of primary amine groups did not take part in the quaternization reaction under neutral conditions. This indicated that the higher DS of *N,O*-QCHI derivatives must be introduced by the random quaternization on both hydroxyl and primary amino groups.

In addition, compared to the signal observed in the δ range of 2.4 ~ 3.1 ppm in the ^1H NMR spectrum of *N*-QCHI2, that in the same range observed in the ^1H NMR spectra of *N,O*-QCHI3a and *N,O*-QCHI3b appears broader. This can be related to the random substitution of the $-\text{OH}$ group in the sugar unit.

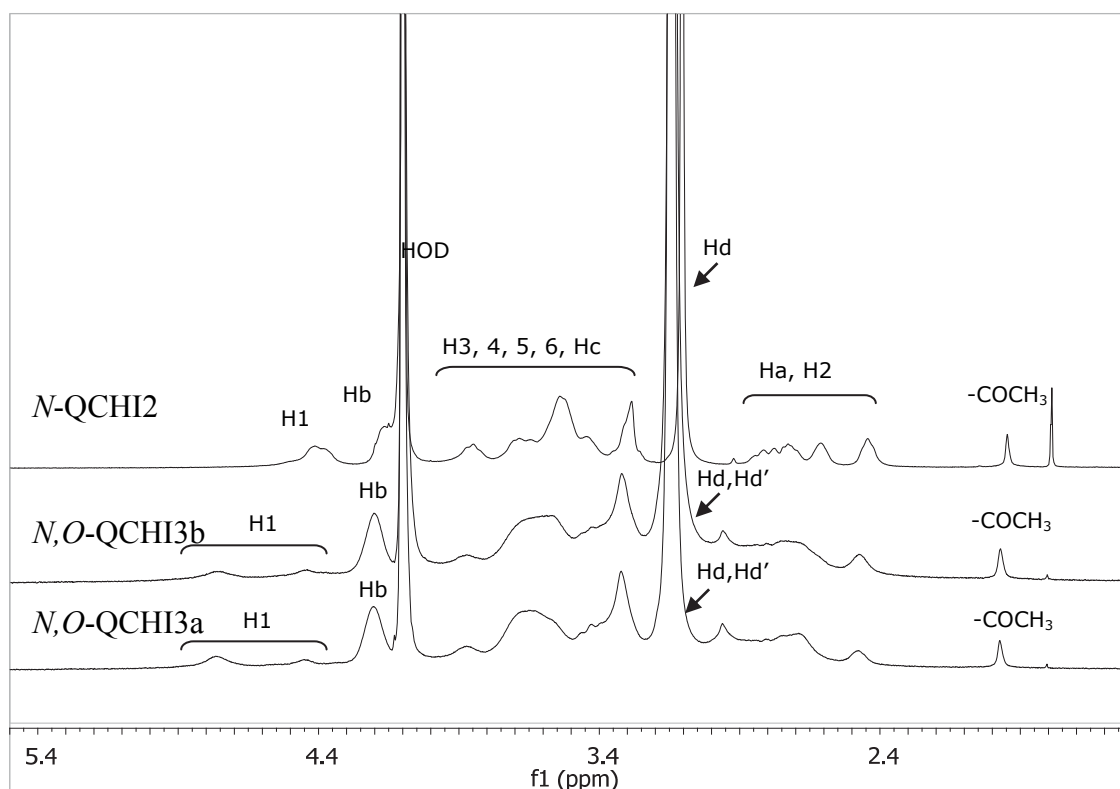
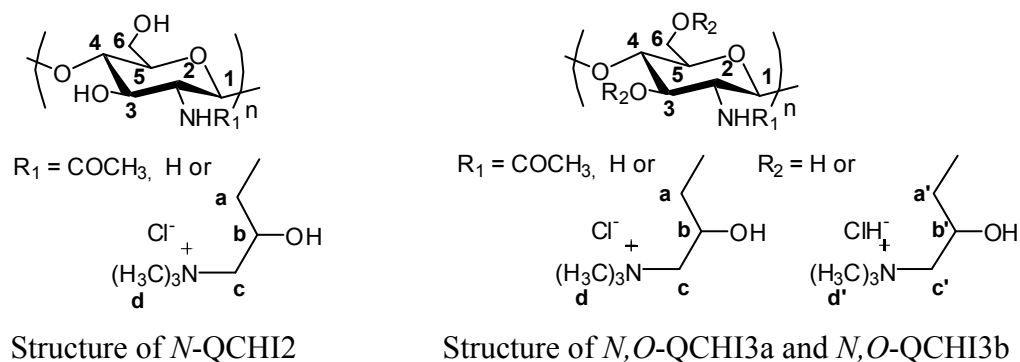


Figure 2.2: ^1H NMR spectra of *N*-QCHI and *N,O*-QCHI derivatives (400 MHz, D_2O , 80 °C, $C_p \sim 6$ g/L).

2.2.2 Macromolecular characterization of QCHI derivatives

2.2.2.1 Measurement of intrinsic viscosity

The reduced viscosity, η_{red} ($\eta_{\text{red}} = (\eta - \eta_0)/\eta_0 c$, with η_0 , the viscosity of the solvent), of CHI and its *N*-QCHI and *N,O*-QCHI derivatives was determined as a function of polymer concentration, c , in a good solvent of chitosan (0.3 M AcOH/0.1 M AcONa) at 25 °C. AcONa was added in order to limit the electrostatic repulsions of the polyelectrolyte chains.

The linear plots of η_{red} vs. c with different slop and intercept are presented in **Figure 2.3**. From the dependence of η_{red} on c , the intrinsic viscosity $[\eta]$ and the Huggins constant k_H could be derived using the Huggins equation (1):

$$\eta_i / c = [\eta] + k_H [\eta]^2 c \quad \text{Equation (1)}$$

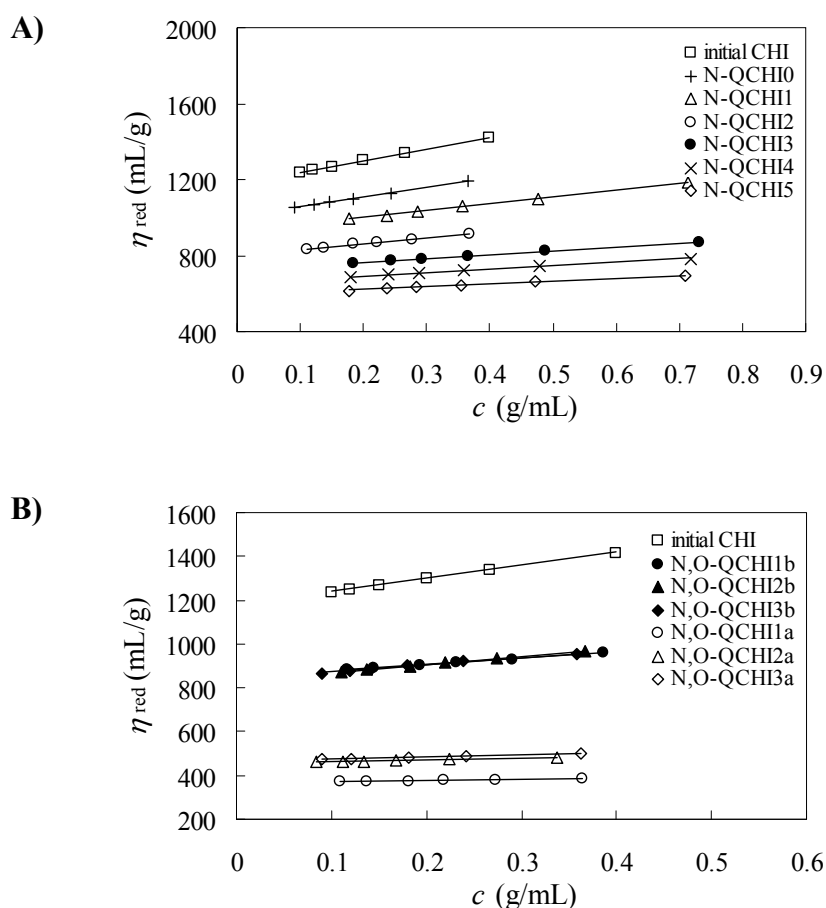


Figure 2.2: The reduced viscosity of CHI and its derivatives determined as a function of polymer concentration in aqueous 0.3 M AcOH/0.1 M AcONa solution at 25 °C: A) initial CHI and its *N*-QCHI derivatives and B) initial CHI and its *N,O*-QCHI derivatives.

The results about $[\eta]$ and k_H of CHI and its derivatives are summarized in **Table 2.2** and **Table 2.3**. As can be seen from these **Tables**, the values of k_H in all cases are lower than 0.5, which suggests that the polymer-solvent interactions are good.

Table 2.2: The intrinsic viscosities $[\eta]$ and Huggins constant k_H derived from the measurement of reduced viscosities of the *N*-QCHI derivatives.

Reference	DS ^a	$[\eta]$ (mL/g)	k_H
Initial CHI	0	1179	0.43
<i>N</i> -QCHI0	0	1008	0.48
<i>N</i> -QCHI1	0.24	932	0.40
<i>N</i> -QCHI2	0.31	800	0.48
<i>N</i> -QCHI3	0.39	726	0.38
<i>N</i> -QCHI4	0.55	657	0.42
<i>N</i> -QCHI5	0.66	592	0.42

^adetermined by conductimetric titration

Table 2.3: The intrinsic viscosities $[\eta]$ and Huggins constant k_H derived from the measurement of reduced viscosities of the *N,O*-QCHI derivatives.

Reference	DS ^a	$[\eta]$ (mL/g)	k_H
<i>N,O</i> -QCHI1a	0.64	467	0.43
<i>N,O</i> -QCHI2a	0.94	451	0.43
<i>N,O</i> -QCHI3a	1.33	363	0.46
<i>N,O</i> -QCHI1b	0.12	840	0.47
<i>N,O</i> -QCHI2b	0.42	831	0.49
<i>N,O</i> -QCHI3b	1.10	849	0.39

^adetermined by conductimetric titration

To explore the relationship between $[\eta]$ and the DS of QCHI derivatives, $[\eta]$ was plotted as a function of the DS of *N*-QCHI, *N,O*-QCHIa and *N,O*-QCHIb in **Figure 2.3**. The dependence of $[\eta]$ on DS in the case of *N*-QCHI derivatives (**Figure 2.3A**) was discussed in the publication in **Advanced Functional Materials**. The comparison of $[\eta]$ of *N*-QCHI0 (blank) with that of initial CHI confirmed that some degradation occurred under acidic conditions. However, the dramatic decrease of $[\eta]$ with the increase of DS could not be explained by the degradation of CHI chains, as similar synthetic conditions used for all *N*-QCHI derivatives. As the value of $[\eta]$ reflects the hydrodynamic volume of the polymer chain in aqueous solution, we hypothesized that the decrease of $[\eta]$ of *N*-QCHI derivatives might be attributed to the loose hydrophobic interactions between the $-N^+(\text{CH}_3)_3$ groups along the CHI chains.

However, we did not observe similar variations of $[\eta]$ as a function of DS in the case of *N,O*-QCHI derivatives (**Figure 2.3B**). In fact, the $[\eta]$ of *N,O*-QCHI derivatives was strongly influenced by their isolated part of reaction medium other than DS. The $[\eta]$ values of *N,O*-QCHIb derivatives recovered from the precipitate of reaction medium are similar, ~ 840 mL/g, nearly the twice of those of *N,O*-QCHIa derivatives, which were obtained in the supernatant of reaction medium. The DS-independence of $[\eta]$ in the case of the *N,O*-QCHI derivatives reflects a weak influence of chemical modification on the apparent hydrodynamic volume (V_h) of *N,O*-QCHI derivatives isolated from the same part of reaction medium. The higher $[\eta]$ of *N,O*-QCHIb derivatives compared to that of *N,O*-QCHIa derivatives suggested the increase of V_h , which will be confirmed by the following study.

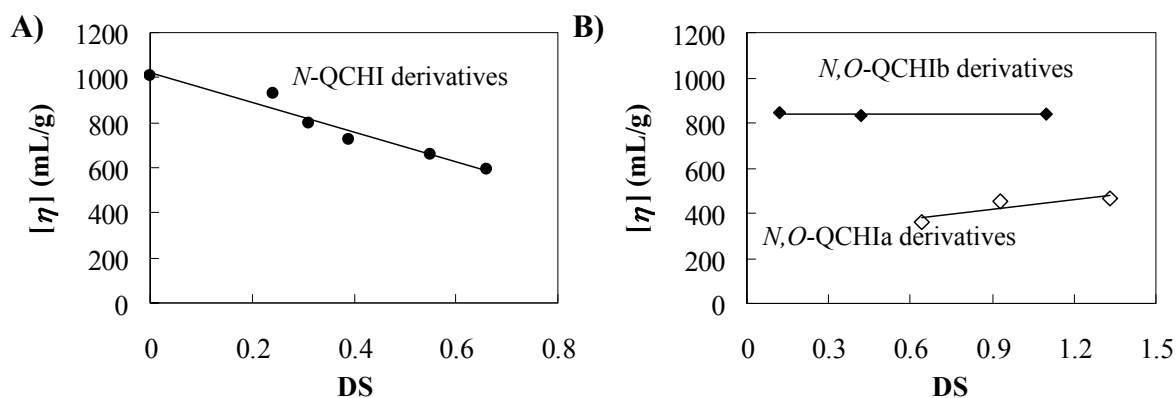


Figure 2.3: Plots of intrinsic viscosities of QCHI derivatives as a function of DS: A) for the *N*-QCHI derivatives and B) for the *N,O*-QCHI derivatives.

2.2.2.2 Determination of the molar mass by size exclusion chromatography (SEC)

The weight average molar mass (M_w) and weight average intrinsic viscosity ($[\eta]_w$) of almost *N*-QCHI derivatives and *N,O*-QCHIa,b derivatives with the highest DS (*N,O*-QCHI3a and *N,O*-QCHI3b) were determined by SEC-MALLS equipped with a viscosity detector in NH_4OAc buffer (pH 4.5, 0.2 M NH_4OAc). The results are shown in **Table 2.4**. To minimise the experimental error, the humidity of all tested samples was firstly measured by thermalgravimetry analysis (TGA) and also given in **Table 2.4**. The humidity is defined as the percentage of the content of water in the sample. As can be seen from **Table 2.4**, the lower M_w of *N*-QCHI0 compared to initial CHI demonstrates the degradation of CHI chains under acidic conditions, which is consistent with the conclusion obtained from the viscosity study by capillary viscometry. In addition, we notice that as the DS of *N*-QCHI derivatives

increases, the Mw of *N*-QCHI derivatives increase, but the $[\eta]_w$ decreases. The calculation of the theoretical Mw of QCHI samples by multiplying the Mw of repeating units of *N*-QCHI derivatives with the weight average degree of polymerization (DP_w) of *N*-QCHI0 demonstrates that the increase of Mw can be related to the attachment of a heavy substituent onto the main chain of polysaccharides as well as the increase of DP_w. The decrease of $[\eta]_w$ with increasing DS is consistent with the relationship between $[\eta]$ and DS obtained from the previous viscosity study.

Table 2.4: The degree of substitution (DS), humidity, weight-average molar mass (Mw), molar mass of the repeating units (M_{RU}), theoretical molar mass (theoretical Mw), weight-average degree of polymerization (DP_w) and weight-average intrinsic viscosity ($[\eta]_w$) of CHI and its derivatives.

Reference	DS ^a	Humidity ^b (%)	Mw ^c (g/mol)	M _{RU} ^d (g/mol)	Theoretical Mw ^d (g/mol)	DP _w ^f	$[\eta]_w$ ^e (mL/g)
Initial CHI	0	10	372 000	220	372 000	1690	821
<i>N</i> -QCHI0	0	8	301 000	220	301 000	1368	679
<i>N</i> -QCHI1	0.24	11	392 000	262	358 000	1496	643
<i>N</i> -QCHI2	0.31	8	461 000	274	375 000	1682	545
<i>N</i> -QCHI3	0.39	8	596 000	288	394 000	2094	563
<i>N</i> -QCHI5	0.66	11	642 000	336	460 000	1910	517
<i>N,O</i> - QCHI3a	1.33	10	560 000	453		1236	366
<i>N,O</i> - QCHI3b	1.10	10	1 600 000	414		3864	675

^adetermined by conductimetric titration; ^bdetermined by TGA; ^cdetermined by SEC-MALLS; ^dmolar mass of the repeating unit associating (M_{RU}); ^ecalculated from the DP_w of *N*-QCHI0 and the M_{RU} and ^fcalculated from the Mw and the M_{RU}.

A great difference between Mw was noticed for *N,O*-QCHI3a and *N,O*-QCHI3b which supports the viscometry data indicating a higher intrinsic viscosity value for *N,O*-QCHI3b. The higher Mw of *N,O*-QCHI3b may be related to the heterogeneous conditions used for the grafting of cationic groups. Due to the partial solubility of chitosan in ultrapure water, the substitution may have occurred mainly on the surface of the aggregates (**Figure 2.4**). This may result in only partial dissolution of the chitosan chains. Therefore, it can be assumed that

some non-substituted parts of these chains remain associated together leading to an increase of the apparent Mw of the modified chitosan.

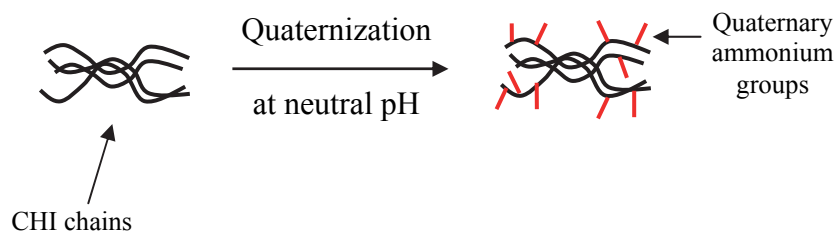


Figure 2.4: Simulation of the grafting position of *N,O*-QCHI3b derivatives.

2.2.3 Antibacterial activity

The antibacterial activity of CHI and its derivatives has been reported in many articles, which have been summarized in the first chapter of thesis. Herein, we investigated the antibacterial activity of the synthesized QCHI derivatives against both Gram positive and negative bacteria by different methods.

1) Gram (-) bacteria – *E. coli*

We analyzed the ability of the *N*-QCHI derivatives to kill *E. coli* cells by the viable-cell counting method. All tests were performed in PBS (pH 7.4) at 37 °C for 4 h. To investigate the effect of the DS on the antimicrobial activity of the *N*-QCHI derivatives, all samples were dissolved at a same molar concentration (1.25 mM). The results have been presented in the publication in **Advanced Functional Materials**¹². It was found that the *N*-QCHI derivatives with DS > 0.5 could completely inhibit the growth of *E. coli* within 4 h and the antimicrobial activity of the *N*-QCHI derivatives increased with the increase of concentration and DS.

The antibacterial activity against *E. coli* of the most substituted *N,O*-QCHI derivatives, i.e. *N,O*-QCHI3a (DS = 1.33) and *N,O*-QCHI3b (DS = 1.10) was investigated under the same conditions to that of the *N*-QCHI derivatives. It is surprising to find that the *N,O*-QCHIa derivative having a DS of 1.33 did not show a higher antibacterial activity than the *N,O*-QCHIb derivative having a DS of 1.10 from (**Figure 2.5A**). Moreover, the latter derivative exhibited an antibacterial activity lower than that of *N*-QCHI5 (DS = 0.66), but higher than that of *N*-QCHI3 (DS = 0.39) (**Figure 2.5B**). These results indicate that the antimicrobial

activity of the QCHI derivatives not only depends on the DS, but also on the position of substitution.

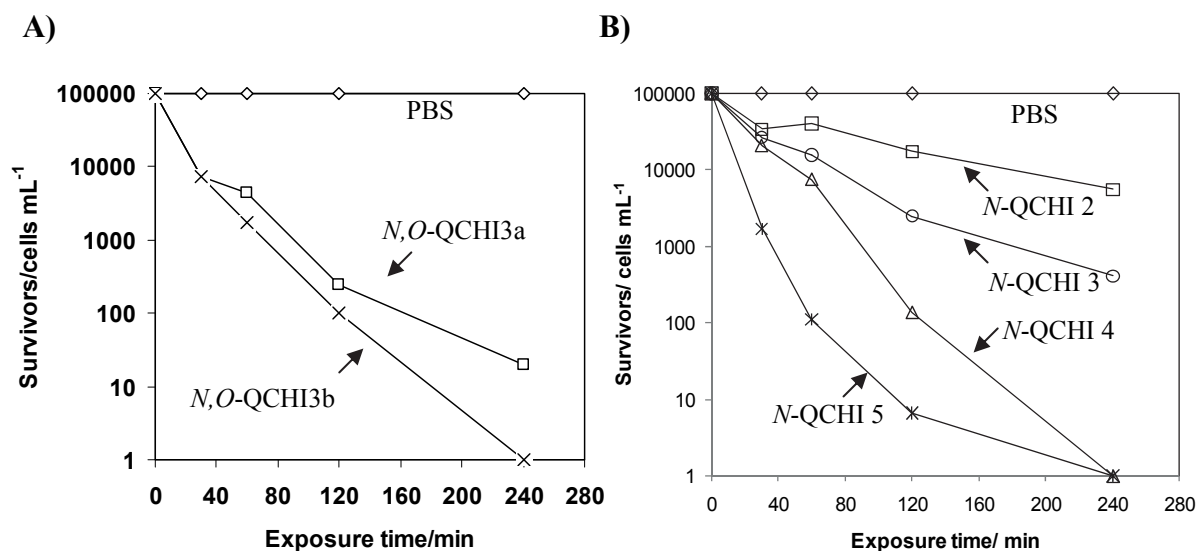


Figure 2.5: Antibacterial activity against *E. coli* of A) the most substituted *N,O*-QCHI derivatives, *N,O*-QCHI3a (DS = 1.33) and *N,O*-QCHI3b (DS = 1.10) and B) the *N*-QCHI derivatives (the DS of *N*-QCHI2-5 correspond to 0.31, 0.39, 0.55 and 0.66, respectively). All QCHI samples were dissolved in PBS at a concentration of 1.25 mM.

2) Gram (+) bacteria - *B. cereus* ATCC 14579

The antimicrobial activity of QCHI derivatives against *B. cereus* was examined also by viable-cell counting method. The Minimum Inhibitory Concentration (MIC) and Minimum Bactericidal Concentration (MBC) of tested QCHI derivatives are shown in **Table 2.5**. As can be seen from **Table 2.5**, the similar value of MIC and MBC means that the QCHI derivatives can be taken as bactericidal. In addition, we observed that the MIC and MBC of the *N*-QCHI derivatives decreased with the increase of DS, except for *N*-QCHI5. This means the moderately substituted *N*-QCHI derivatives (i.e. *N*-QCHI3) are more effective to kill bacteria. Nevertheless, this result should be confirmed by additional experiments. Interestingly, the highly substituted *N,O*-QCHI derivatives have the lowest value of MIC and MBC among all QCHI derivatives. This suggests that the antimicrobial activity of the most substituted *N,O*-QCHI derivatives against *B.cereus* ATCC 14579 was higher than that of the *N*-QCHI derivatives. Furthermore, we noticed that there was no difference between the MIC and MBC values of *N,O*-QCHI3a and *N,O*-QCHI3b, although these derivatives were isolated from different part of reaction medium and exhibited distinguished macromolecular properties.

Table 2.5: The MIC and MBC of QCHI derivatives against *B.cereus* ATCC 14579.

Reference	DS ^a	<i>B. cereus</i> ATCC 14579	
		MIC (mg/ml)	MBC (mg/ml)
<i>N</i> -QCHI1	0.24	0.25 (0.063) ^b	0.25 (0.063) ^b
<i>N</i> -QCHI2	0.31	0.125	0.125
<i>N</i> -QCHI3	0.39	0.063	0.063
<i>N</i> -QCHI5	0.64	1.0 (0.25) ^b	1.0 ^b
<i>N,O</i> -QCHI3a	1.33	0.032	0.032
<i>N,O</i> -QCHI3b	1.10	0.032	0.032

^adetermined by conductimetric titration and ^bexperimental errors

From the above results, we can conclude that the QCHI derivatives can inhibit the growth of both gram (+) and (-) bacteria. More importantly, we found that the antimicrobial activity of these derivatives was influenced by the bacteria species, the DS and the position of substitution of the CHI chains.

2.3 Synthesis of capsules based on the QCHI derivatives

As the synthetic QCHI derivatives showed good water solubility in a wide range of pH and exhibited antimicrobial activity against bacteria, they appeared as interesting candidates for the synthesis of contact-killing capsules. In this part, we mainly present the synthesis and the characterization of capsules based on *N*-QCHI derivatives and *N,O*-derivatives, respectively.

2.3.1 Utilization of *N*-QCHI derivatives as the cationic partners of HA for the synthesis of capsules

Our work concerning the synthesis of capsules based on *N*-QCHI derivatives and their characterizations have been mainly reported in **Advanced Functional Materials**.¹² It was found that the complexation ability between HA and *N*-QCHI derivatives, the morphology and the surface roughness of capsules and the antimicrobial activity of capsules against *E.coli* strongly depends on the DS of *N*-QCHI derivatives. Since these capsules showed good

stability upon storage and exhibited tunable antimicrobial activity, they provide a possibility to delivery drugs while avoiding additional infections. In the following parts, we present the permeability properties of these capsules assessed by analyzing the diffusion the small molecules from the outside to the inside of capsules. We also report on the biodegradability studies of capsules considering their potential biomedical applications. Additionally, the investigation of the DS of the *N*-QCHI derivatives to the antimicrobial activity of capsules is completed.

2.3.1.1 Publication in Advanced Functional Materials¹²

Contact killing polyelectrolyte microcapsules based on chitosan derivatives

By *Di Cui, Anna Szarpak, Isabelle Pignot-Paintrand, Annabelle Varrot, Thomas Boudou, Christophe Detrembleur, Christine Jérôme, Catherine Picart and Rachel Auzély-Velty**

Keywords: Polyelectrolyte capsules, quaternized chitosan, antibacterial activity, polyelectrolyte complexation

ABSTRACT

Polyelectrolyte multilayer microcapsules are made by layer-by-layer (LbL) assembly of oppositely charged polyelectrolytes onto sacrificial colloidal particles, followed by core removal. In this paper, we prepared contact killing polyelectrolyte microcapsules based solely on polysaccharides. To this end, water-soluble quaternized chitosan (QCHI) with varying degree of substitution (DS) and hyaluronic acid (HA) were assembled into thin films. The quaternary ammonium groups were selectively grafted on the primary amine group of chitosan based on its reaction with glycidyltrimethylammonium chloride (GTMAC) under homogeneous aqueous acidic conditions. We found that the morphology of the capsules was closely dependent on the DS of the quaternized chitosan derivatives, suggesting differences in their complexation with HA. The DS was also a key parameter to control the antibacterial activity of QCHI against *Escherichia Coli* (*E. coli*). Thus, capsules containing the QCHI derivative with the highest DS were shown to be the most efficient to kill *E. coli* while

retaining their biocompatibility toward myoblast cells, suggesting their potential as drug carriers able to combat bacterial infections.

1. Introduction

In recent years, among the various naturally occurring polymers, chitosan (CHI) has attracted a special attention in the field of biomaterials due to its excellent biological properties such as biocompatibility, biodegradability, permeation enhancing properties, antibacterial and wound-healing activity.^[1-2] Several studies demonstrated promising applications for this polysaccharide as a material for drug delivery,^[1, 3-4] tissue engineering,^[5] and implantable biomaterials^[6].

One of the interesting properties of chitosan is its antibacterial properties, in particular against Gram-negative and Gram-positive bacteria.^[7-8] Chitosan and its derivatives have been shown to bind to the negatively charged bacterial cell membrane and cause leakage, when in solution or immobilized on surfaces.^[9]

In the design of antibacterial surfaces, polyelectrolyte multilayer films (PEM) that are made by the layer-by-layer (LbL) technique can act as a multifunctional platform. This technique allows depositing thin films on various kinds of supporting materials with a high degree over the control of physico-chemical and biological parameters. According to Rubner *et al.* in their recent review on the design of antibacterial surfaces and interfaces using PEM,^[10] there are three chief strategies to achieve this goal: adhesion resistance, biocide leaching and contact killing strategies. In the first approach, the aim is to reduce the capacity of bacteria to adhere at early stages. It often relies on the use of superhydrophobic surfaces.^[11] In the second approach, which is also the oldest one, cytotoxic compounds are released and diffuse over time from the delivery system. Antibacterial peptides^[12-13] and silver ions^[14-17] fall into this category. They have proven to be efficient in reducing the number of bacteria onto functionalized PEM films.^[12-17] Finally, the contact killing strategy seeks to biochemically induce death of bacteria that have adhered to the material surface.

Chitosan, due to its intrinsic properties, appears thus as a good candidate for the design of contact killing films. To this end, the buildup of films containing chitosan as polycation and either hyaluronan^[18] or heparin^[6] as polyanions has been explored. CHI/HA films assembled at physiological ionic strength (0.15 M NaCl) resisted 80% of *E. coli* attachment^[18] but that study did not address the possible contact killing effect of chitosan. The latter effect was demonstrated by Shen *et al.* who found that variations in assembly pH could influence

strongly the anti-bacterial properties of CHI/heparin films due to differences in density and mobility of chitosan chain segments at the film surface.^[6] However, acidic conditions required for the film construction from native chitosan due to its poor water solubility above pH ~ 6.5 are not compatible with physiological conditions. This drawback greatly limits the practical applications of chitosan-based coatings. Moreover, the obtained films were often not stable enough in neutral aqueous solution and had to be chemically cross-linked. Such difficulties have recently been overcome by synthesizing water-soluble derivatives of chitosan. Bulwan *et al.* thus demonstrated the ability to buildup at physiological pH multilayered chitosan films from a quaternized derivative and a sulfonated carboxymethylchitosan.^[19] The resulting films were shown to be very stable offering new potential biomedical applications. Nevertheless, in spite of the promising antimicrobial activity of quaternized chitosan that was recently observed in solution,^[20] as compared to that of native chitosan, the potential anti-bacterial effect of films made from such derivatives has never been addressed.

Besides delivery from a planar supported film, delivery from a vehicle like a hollow microcapsule could open new applications for antibacterial delivery systems. In particular, polyelectrolyte microcapsules prepared by the LbL deposition technique have attracted a great deal of interest owing to their potential applications in various fields including drug delivery, biotechnology and catalyst research.^[21-25] These capsules are formed by deposition of a LbL film onto a sacrificial template that is dissolved after film deposition. One of the advantages of these multicompartments systems is the possibility to introduce a high degree of multifunctionality within their nanoshell by the nature of the polyelectrolytes and assembly conditions used for their preparation. Polyelectrolyte microcapsules based on polysaccharides are only emerging, due to the inherent difficulties in preparing such capsules, which are related to the “hydrogel-type” and softness of the polysaccharide multilayer films.^[26] In particular, core dissolution is a delicate step and needs to be performed in appropriate and mild conditions for polysaccharides in order to avoid the shell rupture.^[27] Calcium carbonate particles are good sacrificial templates due to their ability to be readily dissolved under mild conditions and only slightly acidic conditions.

Hyaluronan is a highly hydrated natural polysaccharide that has been shown to reduce bacterial adhesion due to its hydrophilicity.^[28] It has already been incorporated into many planar multilayer films^[18, 29-30] but in very few polyelectrolyte microcapsules^[27, 31-32].

Up to date, there are only few examples of antibacterial delivery system based on polyelectrolyte microcapsules. These employed the biocide leaching strategy by either

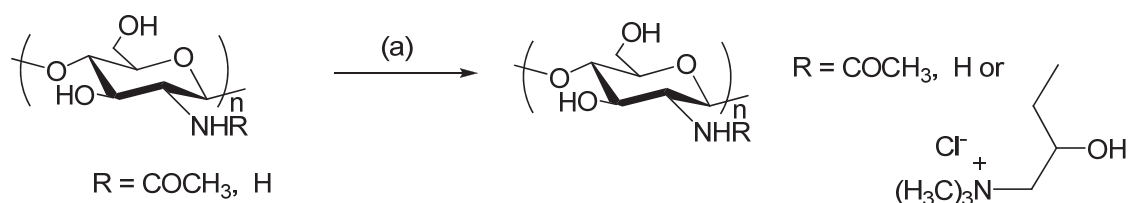
inserting an antibacterial drug, ciproflaxine, in the core or shell of the capsule^[33-34] or by inserting nanoparticles in the shell of the capsules^[35].

To the best of our knowledge, the contact killing strategy has never been attempted using polyelectrolyte microcapsules as delivery system and chitosan as antibacterial polysaccharide.

The goal of our work was to design a new type of polyelectrolyte capsules as antibacterial vehicles by taking advantage of the properties of natural polysaccharides. To this end, we prepared capsules made of HA and water-soluble quaternized chitosan (QCHI) derivatives having different degrees of substitution. The synthesis of these derivatives, described in the first part, is based on a selective quaternization reaction performed on the primary amine function of chitosan. In the second part, we examine the formation of HA/QCHI films on planar surfaces and carbonates cores and analyze the systematic effect of four chitosan derivatives of increasing DS on the size and morphology of hollow capsules. Finally, we compare the antibacterial properties of these chitosan derivatives against *Escherichia Coli* in solution as well as in the microcapsule form.

2. Synthesis of water-soluble quaternized chitosan derivatives.

The quaternized derivatives of chitosan were prepared by reacting chitosan with glycidyltrimethylammonium chloride (GTMAC) under homogeneous aqueous acidic conditions as shown in scheme 1.



Scheme 1 : Quaternization reaction of chitosan. *Reagents and conditions*: a, GTMAC, 0.5 % aqueous AcOH (v/v), 55 °C, 18 h.

Such conditions not only favor the random substitution of the sugar units in the chitosan chain, but also the selective grafting on the primary amine groups.^[36-37] We used ^1H and ^{13}C NMR spectroscopy to confirm the introduction of quaternary ammonium groups on chitosan as well as to ascertain the selective substitution of the primary amine groups (*cf.* Supporting information, Figures S1 and S2). The degree of substitution of the QCHI samples was derived by conductimetric titration of Cl^- ions with AgNO_3 . We selected the latter method for the determination of the DS as partial overlapping of the proton signals of the $-\text{N}^+(\text{CH}_3)_3$ groups with those of chitosan prevented a correct quantification and the long time required to obtain ^{13}C NMR DEPT spectra with good signal-to-noise ratios precluded the analysis of many samples. The characteristics of the QCHI samples prepared in this work are listed in Table 1. All derivatives were prepared under identical reaction conditions of temperature, reaction time and concentration of polymer which were considered to be optimal from studies reported in the literature.^[37] We only varied the mole ratio of GTMAC to chitosan from 3:1 to 8:1 leading to QCHI derivatives with DS values from 0.31 to 0.66. The samples were isolated by a diafiltration process followed by freeze-drying with yields higher than 90 %. The intrinsic viscosity, $[\eta]$, of the products was additionally measured by capillary viscometry to get information about the chain dimensions, as the value of $[\eta]$ reflects the hydrodynamic volume of the polymer chain in aqueous solution. As can be seen from Table 1, the intrinsic viscosity decreases as the DS increases as previously reported in the literature.^[36] These authors attributed the decrease in $[\eta]$ to a higher degradation for the more substituted derivatives. However, as all derivatives have been synthesized under similar reaction conditions, it is difficult to account for a higher degradation for some of them. Interestingly, using pyrene as sensitive fluorescent probe, Amiji et al.^[38] demonstrated contact between native chitosan chains due to intermolecular hydrophobic interactions of the methyl groups of *N*-acetyl glucosamine of the polysaccharide. Thus, in our conditions, the decrease of the macromolecular size and hence, intrinsic viscosity, might be explained by loose hydrophobic interactions between the $-\text{N}^+(\text{CH}_3)_3$ groups along the chitosan chains. This hypothesis appeared to be supported by the peculiar properties of the capsules developed in this work as discussed below.

Table 1. Reaction conditions for the synthesis of quaternized chitosan derivatives and macromolecular characteristics derived from conductivity and viscometry measurements.

Sample	GTMAC/CHI molar ratio[a]	DS[b]	$[\eta]$ [c] mL g ⁻¹
CHI	-	-	1008
QCHI-1	3:1	0.31	800
QCHI-2	4:1	0.39	726
QCHI-3	6:1	0.55	657
QCHI-4	8:1	0.66	582

[a] Coupling reaction performed in 0.5 % aqueous AcOH (v/v) at 55 °C for 18 h ; [b] determined by conductimetry; [c] measured by capillary viscometry in 0.3 M AcOH/0.1 M AcONa, at 25 °C.

3. Fabrication of hollow HA/QCHI capsules.

Multilayer microcapsules were fabricated by layer-by-layer assembly of HA/QCHI onto CaCO₃ particles, followed by core removal. Thus, high M_w HA (M_w = 820 000 g mol⁻¹) and QCHI were alternatively deposited at a concentration of 5 and 2 g L⁻¹ in water containing 0.15 M NaCl at pH 6.5, respectively, which were found to be the optimal conditions. Indeed, using high M_w HA and relatively high concentrations of HA for deposition on the CaCO₃ particles allows to obtain stable capsules with good reproducibility.^[27] Assembly of HA and QCHI derivatives in multilayer films was confirmed by following (HA/QCHI) film deposition on a planar solid substrate by quartz crystal microbalance with dissipation monitoring (QCM-D) (**Fig. 1**). The multilayer film buildup was found to be very similar for all the QCHI of different DS (from DS = 0.31 to 0.66). In addition, a linear growth of the film thickness with the number of layers was evidenced in our working conditions over the range investigated (up to 4 layer pairs). This film growth is consistent with those reported in the literature for HA/CHI films constructed at the same ionic strength for HA samples of low and intermediate molecular weights (31 × 10³ g mol⁻¹ and 360 × 10³ g mol⁻¹, respectively)^[18, 29]. Interestingly, the thickness value of 125 ± 40 nm obtained by others for films made of five layer pairs of HA (M_w = 360 × 10³ g mol⁻¹) and chitosan (160 × 10³ g mol⁻¹)^[29] is similar to the values determined for our (HA/QCHI)₄ films by QCM-D (**Fig. 1B**). After deposition of 4.5 HA/QCHI layer pairs, the LbL coated CaCO₃ particles were incubated in ethylenediaminetetraacetic acid (EDTA, 0.1 M, pH 7.2), affording hollow capsules to be

formed after several washing steps. Figure 2 compares confocal laser scanning microscopy (CLSM) and scanning electron microscopy images (SEM) of (HA/QCHI)_{4,5} capsules prepared from QCHI of different DS.

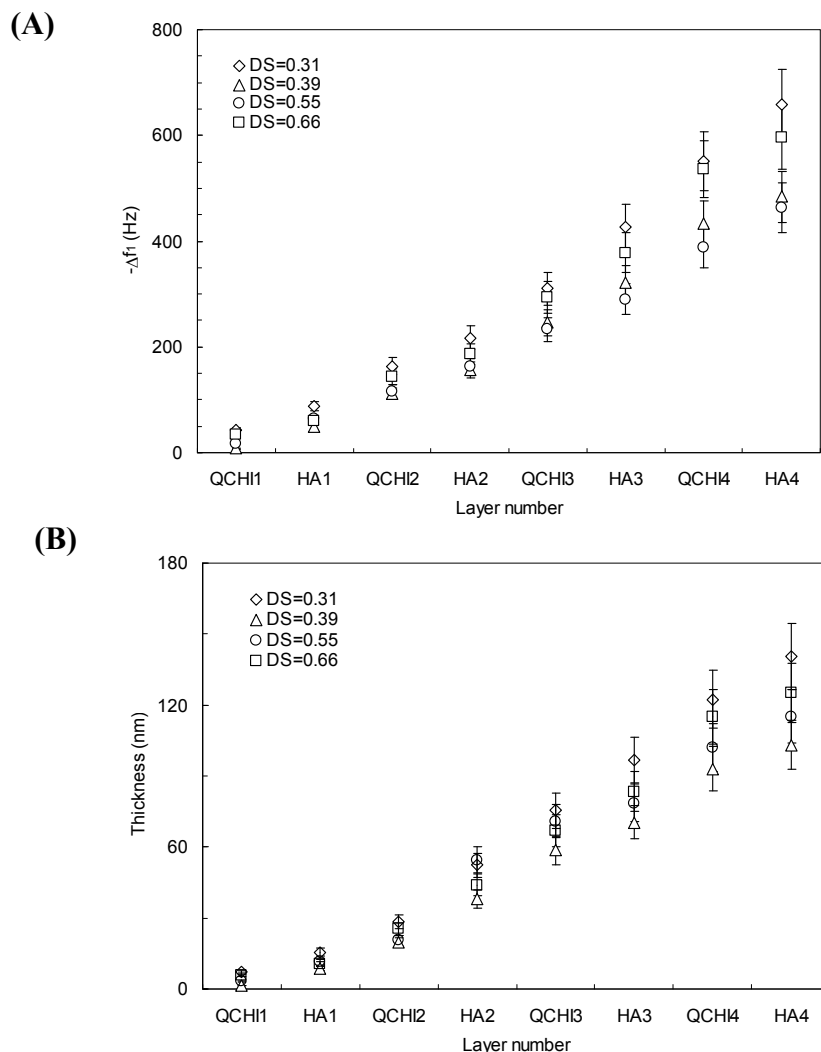


Figure 1: (HA/QCHI) film growth in 0.15 M NaCl (pH 6.5) as measured by QCM-D on gold coated crystals. Differences in the QCM frequency shifts measured at 15 MHz (A) as well as film thickness (B) are plotted for each HA and QCHI deposited layer (for HA at 5 g/L and QCHI at 2 g/L) up to four layer pairs. Data are given for QCHI samples with different DS : (\diamond) 0.31, (Δ) 0.39, (\circ) 0.55 and (\square) 0.66.

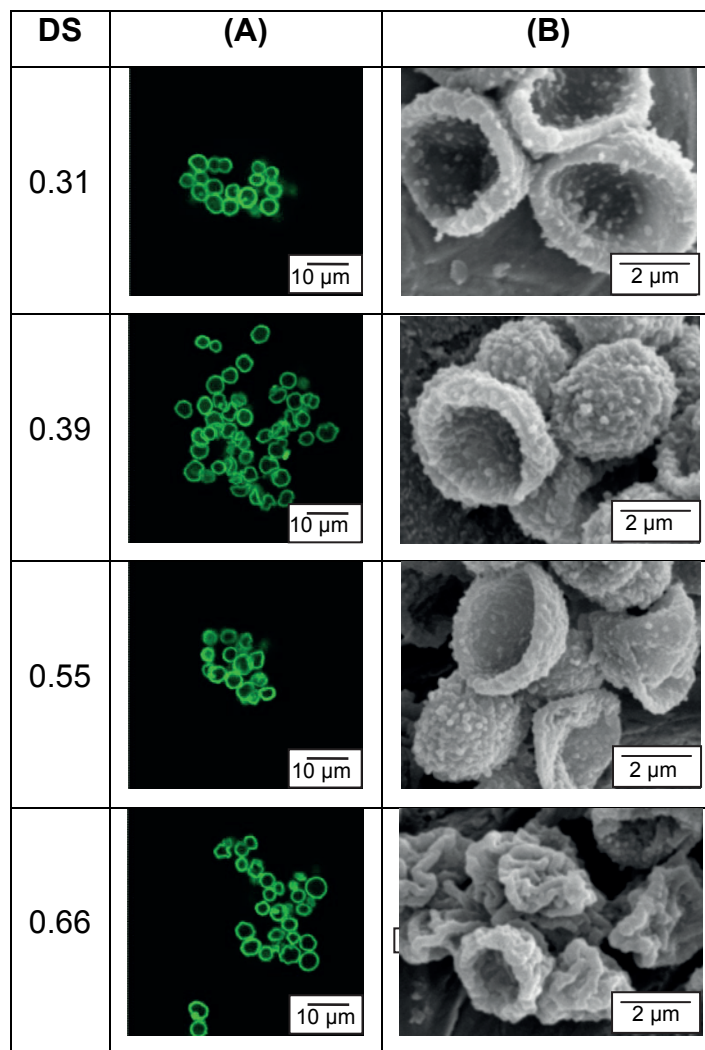


Figure 2: CLSM (A) and SEM (B) images of $(\text{HA}/\text{QCHI})_{4.5}$ microcapsules prepared using QCHI samples having different DS. The LbL assembly was performed using fluorescein isothiocyanate-labeled HA for visualization by CLSM

On CLSM images, the capsules appear in all cases to be spherical with number-average diameters varying between 3.5 and 3.3 μm (calculated for $n \sim 60$ capsules). The SEM images also indicate diameters in the order of $\sim 3 \mu\text{m}$ for the dried capsules, except for those prepared with the high DS of 0.66. Indeed, some shrinkage can be observed from SEM images of these capsules. Noticeably, all types of HA/QCHI capsules exhibited irregularities (grains) on the shell surface, which are particularly visible on the SEM images. To investigate this in more details, we imaged the capsules by atomic force microscopy (AFM) (**Fig. 3**). Capsules did not show the typical folds and creases observed for synthetic polyelectrolyte multilayer

capsules,^[39] but instead were observed to collapse on the substrate in a pancake form upon drying.

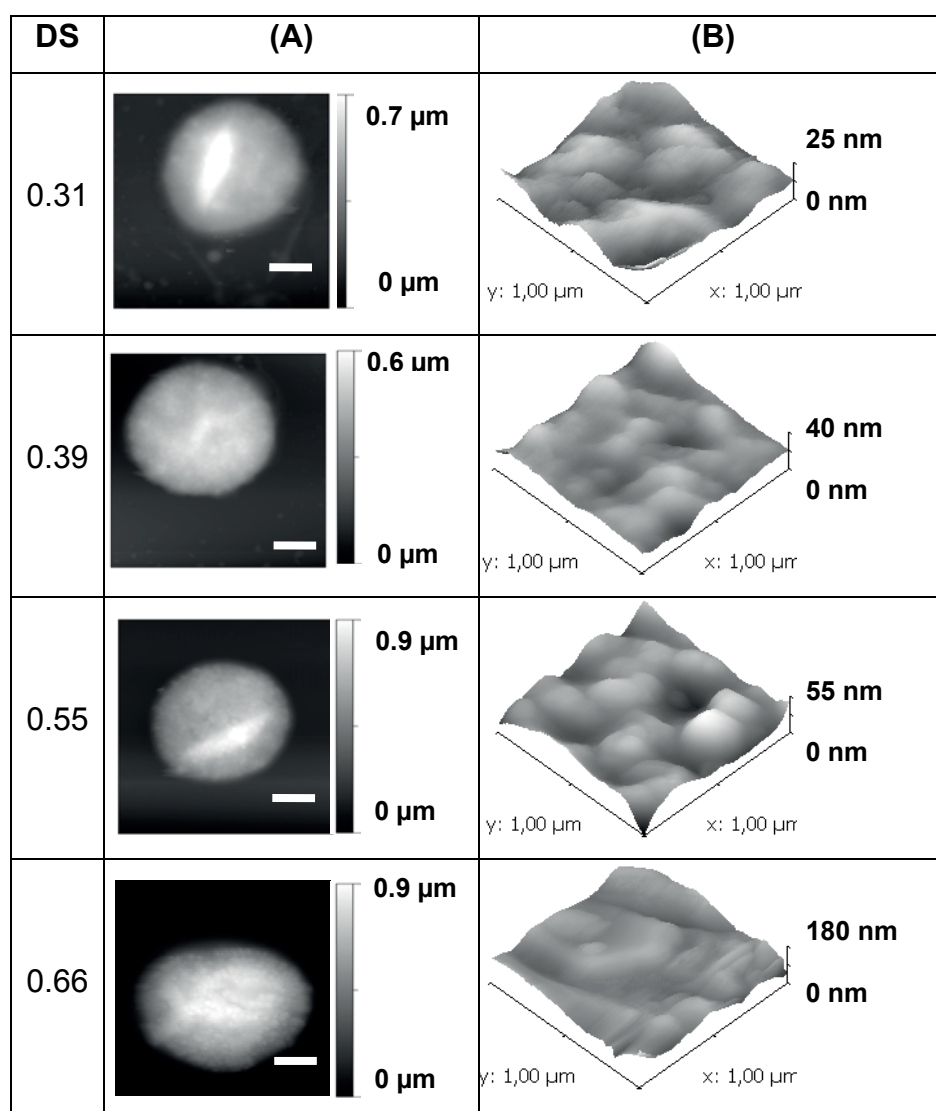


Figure 3: AFM topographical images of microcapsules made of 4.5 layer pairs of HA and QCHI of increasing DS (from top to bottom). All images have the same size : $10 \times 10 \mu\text{m}^2$ for 2D images (A) and $1 \times 1 \mu\text{m}^2$ for 3D images (B). Scale bar is $2 \mu\text{m}$.

The thickness of the polyelectrolyte shell was estimated by following the protocol reported previously by Leporatti *et al.*^[40] Considering that the measured height is twice the thickness of a single microcapsule wall, the thickness of capsules was determined (**Fig. 4A**). It was between 160 to 310 nm depending on the DS of QCHI with no systematic difference.

The high values of capsule thickness obtained by AFM after capsule drying compared to those obtained by QCM-D on hydrated supported films (~120 nm) may probably originate from the difference in the substrates. In the case of CaCO₃ capsules, adsorption is realized on a porous template in which the polyelectrolytes can partially diffuse. This may favor the adsorption of larger polyelectrolyte amounts as compared to a non porous planar surface. The high thickness value may also be related to the irregularity of the capsule surface.

Of note, we found that the capsule's shell roughness increased with increasing the DS of QCHI (**Fig. 4B**). Although no clear experimental proof could support this assumption, we hypothesize that such grains may result from hydrophobic interactions between the quaternary ammonium groups of the QCHI chains, as mentioned above. Indeed, recently, we observed similar grains on planar multilayer films containing hydrophobically modified HA derivatives.^[41] Their size was shown to depend on the length of the grafted alkyl chain and on the DS. The roughness of such films measured by AFM increased from 4.1 nm to 98.2 nm by increasing the hydrophobicity of the polysaccharide. One can notice that the roughness of the less hydrophobic planar films is similar to that found for capsules with DS ranging from 0.31 to 0.55 (i.e 4 to 6 nm), supporting our assumption concerning the nature of the grains.

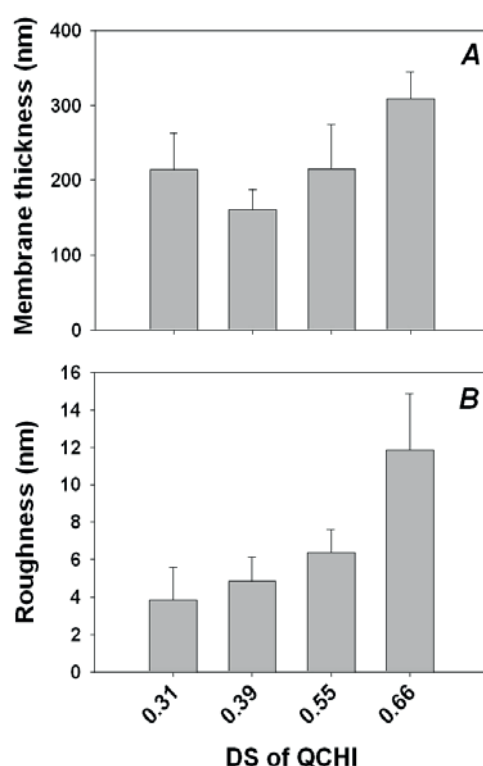


Figure 4: Membrane thickness (A) and average roughness R_a (B) as measured from AFM images as a function of the DS of QCHI for (HA/QCHI)_{4.5} capsules. Data are means \pm SD of three images.

In order to get a better understanding on the role of the DS of QCHI on the HA/QCHI multilayer assembly, we studied the polyelectrolyte complexation by isothermal titration calorimetry (ITC). As polyanion/polycation interactions are usually accompanied by an entropy increase,^[42-44] complexes can be considered “strong” when the polyanion/polycation complexation process is exothermic (negative ΔH) and “weak” when it is endothermic (positive ΔH). In this work, the ITC experiments were carried out by adding aliquots of a solution of HA to a solution of QCHI in the microcalorimeter cell. In all experiments performed with the different QCHI, endothermic heat is produced after each injection of HA, indicating formation of weak polyelectrolyte complexes. The magnitude of the released heat was constant as the chains of HA established a maximum of interactions with the QCHI chains (**Fig. 5**). Indeed, QCHI is in large excess compared to HA, even after ten injections where the final concentration of monomer units of HA is less than 2.5 % that of QCHI. The complexation enthalpy derived from these thermograms after subtraction of the dilution heat is represented in **Fig. 6** as a function of the DS of QCHI. ΔH was always positive and increased with the DS of QCHI. From this figure, we thus assumed that the strength of HA/QCHI polyelectrolyte complexation progressively decreases as the DS of QCHI increases. Such findings may be in relation with the formation of grains, whose size depends on the substitution degree.

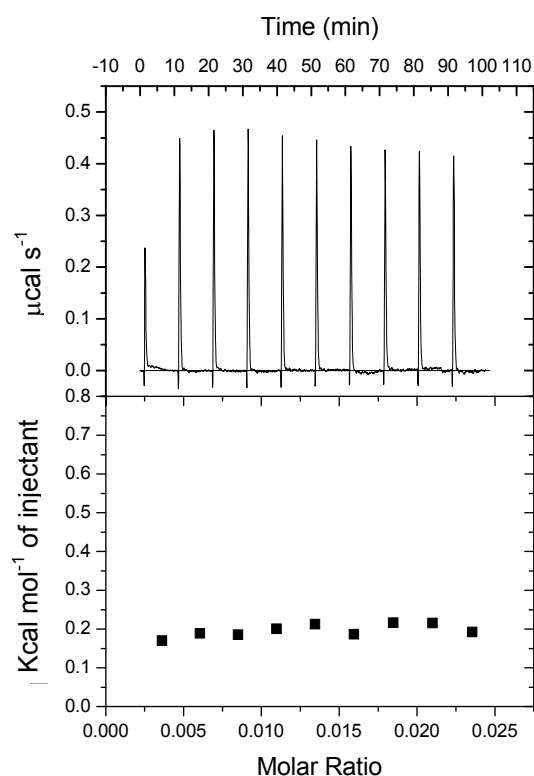


Figure 5: Calorimetric titration of QCHI with HA in Tris-HCl buffer (pH 7.4) containing 0.15 M NaCl at 25 °C. Top : raw data for 10 sequential injections (10 μL per injection except the first one (5 μL)) of the HA solution injected into solutions of QCHI (DS = 0.31); bottom : the integrated curve showing experimental points taking into account heat of dilution.

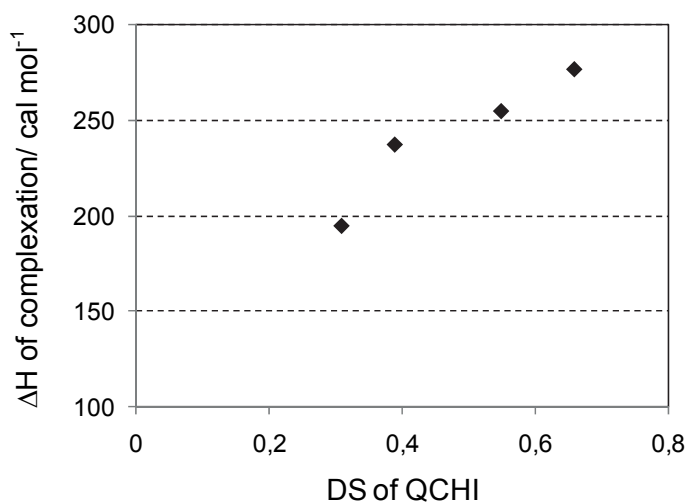


Figure 6: Variation of the enthalpy of HA/QCHI complexation as a function of the DS of QCHI measured in Tris-HCl buffer (pH 7.4) containing 0.15 M NaCl at 25 °C.

4. Antibacterial activity of QCHI and capsules.

As a first approach to study the antibacterial activity of HA/QCHI capsules, we analyzed the ability of the most substituted QCHI (i.e. QCHI-4 having a DS of 0.66) to kill *E. coli* cells by the viable-cell counting method (*cf.* Experimental section). About 10^5 cells mL⁻¹ of the strain were exposed to QCHI-4 at concentrations of 1.25, 0.125, 0.01, 0.001 mM in PBS. We found that 100 % of *E. coli* was killed within 240 min contact when the QCHI-4 concentration was above 0.01 mM (*cf.* Supporting information, Figure S3). From these data, we studied the dependence of the DS of the QCHI derivatives on the antibacterial activity against *E. coli*. As can be seen on Figure 7, all the bacteria were killed within 240 min with the QCHI derivatives having a DS higher than 0.50 (for [QCHI] = 1.25 mM) whereas those with lower DS showed a much lower antibacterial activity. These results are thus in good agreement with those reported by Seong *et al.*^[37] who demonstrated superior antibacterial activity of modified CHI with respect to native CHI, due to the presence of quaternary ammonium groups.

Based on these results, we next examined the antibacterial effect of microcapsules prepared from QCHI-4 and consisting either of 4.5 or 5 (HA/QCHI-4) layer pairs, i.e. ending either by HA or QCHI. From the zeta-potential measurements, (HA/QCHI-4)_{4.5} shells had a

negative value in 0.02 M phosphate buffer at pH 7.4 (-21.09 ± 1 mV) whereas (HA/QCHI-4)₅ shells possessed a positive potential (9.05 ± 2.3 mV).

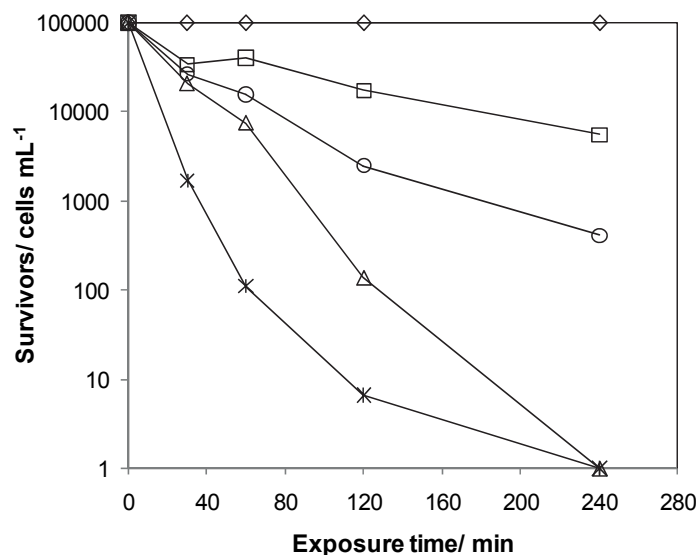


Figure 7: Antibacterial activity against *E. coli* of QCHI derivatives having different DS: (□) 0.31; (○) 0.39; (△) 0.55; (*) 0.66; (◇) control (PBS). The QCHI derivatives were dissolved in PBS at a concentration of 1.25 mM.

As shown in Figure 8, the (HA/QCHI-4)₅ shells terminated by QCHI killed all *E. coli* bacteria within 240 min (for an initial ratio of capsules/bacterial cell of ~ 100), similarly to QCHI-4. Interestingly, in the case of HA-ending capsules, an important fraction of *E. coli* bacteria was also killed within 240 min of contact. Thus, although the HA-ending capsules have a less favorable zeta potential (of the same sign than that of bacteria), they can still approach the bacterial and have a killing effect on them. As the zeta potential is a global measurement and can take into account local heterogeneities at the micrometer scales, we conclude that the surface of these capsules may also contain some positively charged groups that are concentrated in the hydrophobic grains. These results appear to be in line with those reported recently by Corbitt et al.^[45] These authors noted a very effective antibacterial activity of their capsules made of conjugated photoactive polyelectrolytes. They suggested that the heterogeneity of the polyelectrolyte capsules surface, containing both positive charges and hydrophobic groups, may significantly contribute to their ability to attract and bind bacteria.

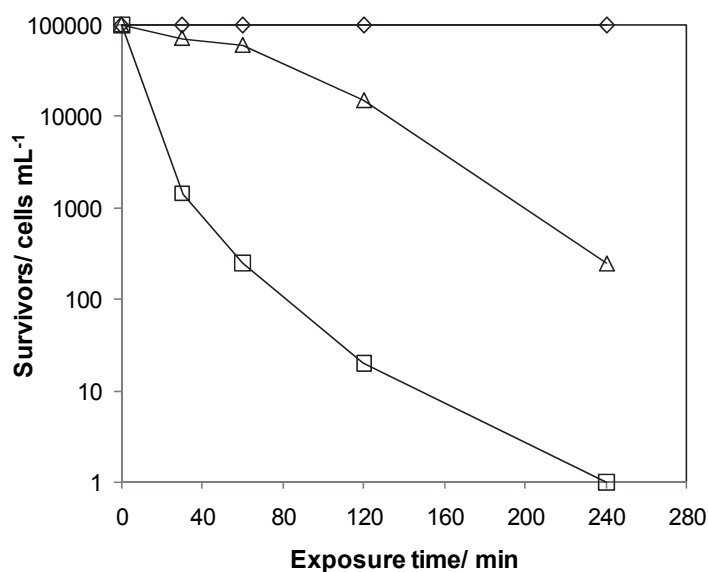


Figure 8: Antibacterial activity against *E. coli* of HA/QCHI microcapsule prepared using QCHI with a DS of 0.66 : (◇) control (PBS); (Δ) (HA/QCHI)_{4.5} microcapsules ending by HA; (□) (HA/QCHI)₅ microcapsules ending by QCHI. In this assay, the ratio capsules/bacteria was ~ 100.

The analysis of bacterial viability by confocal microscopy fully supported our data obtained by the viable-cell counting method. For this study, bacteria were incubated in the presence of HA- or Q-CHI-ended capsules (capsules/bacterial cells ratio ~ 1) and a mixture of DNA-staining dyes. These DNA stains penetrate the cells and produce red and green fluorescence emission for live and dead bacteria. As depicted in **Fig. 9**, images from HA- and QCHI-ended capsules in the presence of bacteria exhibited a green fluorescence at the walls, which is partly related to the unspecific diffusion of the dye in the membrane (as all capsules are green), but also and importantly, which is much stronger at specific locations. We attribute these bright and dense spots to the presence, at the microcapsules surface, of bacteria that have been killed upon contact with the microcapsules. Red-labeled living bacteria can still be observed at the microcapsules' periphery. From these images, (HA/QCHI)₅ capsules ending by QCHI appear to be more effective at killing bacteria. Physical interactions of bacteria with the QCHI-ending microcapsules can be reasonably explained by the attractive electrostatic interactions occurring between the positively charged capsules and negatively charged bacteria.

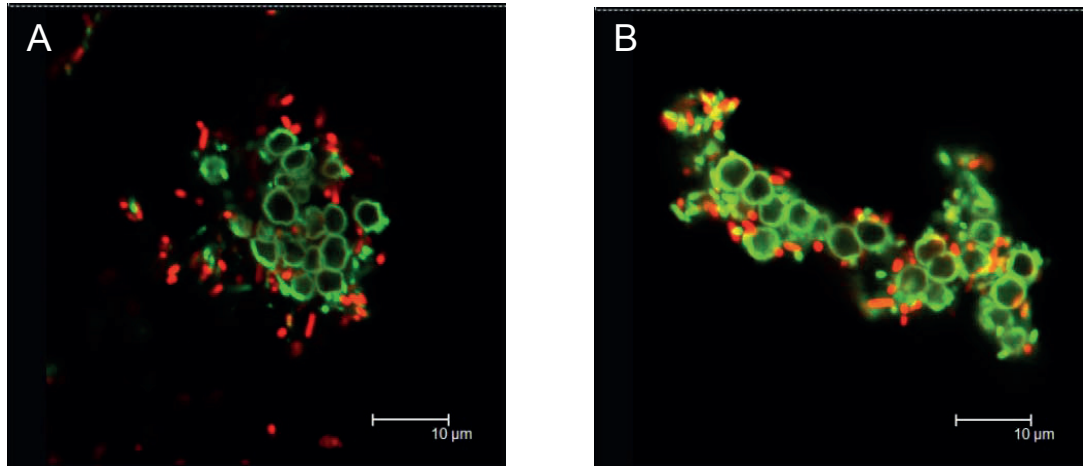


Figure 9: Confocal microscopy images obtained by overlay of the green and red channels : (A) (HA/QCHI)_{4.5} capsules ending by HA and, (B) (HA/QCHI)₅ capsules ending by QCHI after 20 h of co-incubation with *E. Coli* bacteria (capsules/bacterial cells ratio ~ 1). Some diffusion of the green dye within the microcapsule wall was observed. Most bacteria co-incubated with HA-ending capsules were alive (red fluorescence). In contrast, most bacteria associated with QCHI-ending capsules appeared green indicating they have been killed. The intense and dense green spots at the capsules's wall, which is particularly observed in (B) is attributed to the presence of dead bacteria and bacterial debris. Bacteria appeared to be stucked on the QCHI-ending capsules, reflecting the preferential interactions of these capsules with the bacteria.

Finally, we investigated the *in vitro* cytotoxicity of the polysaccharide microcapsules on myoblast cells by introducing an increasing number of capsules in the cell culture (**Fig. 10**). We observed that cell viability was strongly reduced when the microcapsule/cell ratio was ~ 100 (5% of remaining live cells). At a ratio of ~ 50 , 32% of the cells remained viable. At a ratio of ~ 20 capsules/cell, the cytotoxicity was low and 75% of the cells remained viable. Similar toxicity levels were observed by Kirchner et al.^[46] using PSS/PAH based microcapsules on a fibroblast cell line and by De Koker et al.^[47] on bone marrow derived dendritic cells. This shows that it is possible to apply a rather large amount of microcapsules to myoblast cells without affecting their viability.

All together, our results indicate that QCHI derivatives can be successfully employed to build polyelectrolyte multilayer capsules in physiological conditions. Very interestingly, the

QCHI derivatives can retain their antibacterial activity when they are associated with HA in the multilayer :

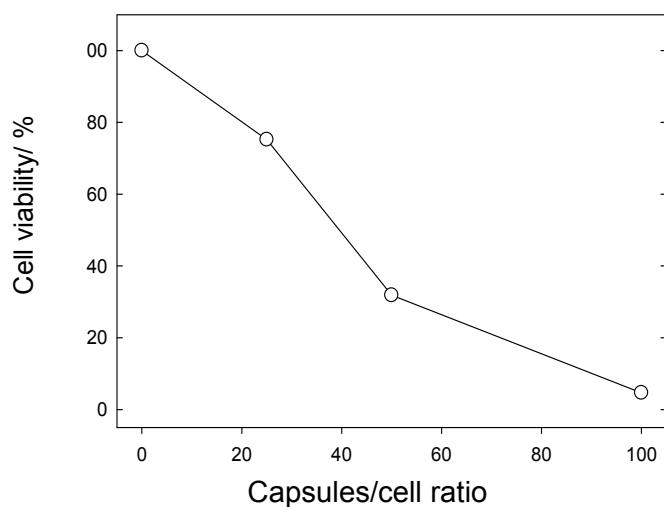


Figure 10. Viability of C2C12 cells incubated with (HA/QCHI)₅ microcapsules. The capsules per number of seeded my

cells is expressed as the number of capsules

5. Conclusions

In this study, we successfully prepared polysaccharide-based hollow microcapsules with contact killing activities. These capsules were entirely made of polysaccharides as polyanion and polycation constituents, i.e. hyaluronic acid and chitosan derivatives bearing quaternary ammonium groups. The latter QCHI derivatives with varying degree of substitution have been prepared using a selective nucleophilic substitution reaction. Thanks to the increased solubility of these derivatives, polyelectrolyte multilayer capsules could successfully be built in physiological conditions and were shown to be stable. We found that the capsules morphology was closely dependent on the DS of the quaternized chitosan. In particular, the roughness of the capsule wall increased with increasing the DS of QCHI. We hypothesized that grains on the capsule surface resulted from loose hydrophobic interactions between the quaternary ammonium groups of the QCHI chains. The DS was found to be a key parameter in the control of the antibacterial activity of QCHI against *E. coli*. Thus, microcapsules containing the QCHI derivative with the highest DS exhibited the highest antibacterial activity. Interestingly, we noticed that capsules ending by QCHI were more efficient than those ending by HA to kill *E. coli* bacteria, although these latter ones had a significant effect.

Finally, we verified that myoblast cells remained viable in the presence of the microcapsules, provided that the capsule/cell ratio remained below ~ 30 .

Such capsules displaying effective cationic contact killing abilities could offer a distinct advantage for the delivery of drugs especially for the treatment of some bacterial infections.

6. Experimental

Materials. Chitosan Protasan with a degree of *N*-acetylation (DA) of 0.09 was kindly provided by FMC BioPolymer AS, Novamatrix (Norway). Its viscosity average molecular weight was determined to be $1.8 \times 10^5 \text{ g mol}^{-1}$ from the intrinsic viscosity measured in 0.3 M AcOH/0.1 M AcONa at 25 °C (assuming $K=0.074$ and $a=0.76$).^[48] Hyaluronic acid under the sodium salt form, having a molar mass of M_w of $820000 \text{ g mol}^{-1}$, was a gift from ARD (Pomacle, France). GTMAC, silver nitrate (AgNO_3), FITC, EDTA, calcium chloride (CaCl_2), sodium carbonate (Na_2CO_3), acetic acid (AcOH), sodium acetate (AcONa), sodium chloride (NaCl), phosphate buffer saline (PBS), tris(hydroxymethyl)aminomethane hydrochloride (Tris-HCl) were purchased from Sigma-Aldrich-Fluka. All chemicals were used without any further purification. FITC-labeled HA was prepared as described previously,^[27] by mixing FITC and HA modified by adipic dihydrazide groups (HA-ADH) in 0.05 M borate buffer, followed by dialysis against pure water. The water used in all experiments was purified by a Millipore Milli-Q Plus purification system, with a resistivity of 18.2 M Ω cm.

Synthesis of the quaternized derivatives of chitosan. Chitosan (0.5 g, 3 mM) was suspended in deionized water (38 mL), and then AcOH (i.e. $\sim 0.5 \%$, v/v) was added. The chitosan-AcOH mixture was stirred overnight at room temperature prior to the dropwise addition of GTMAC in three portions at 2 hours intervals. The mole ratio of GTMAC to chitosan was varied from 3:1 to 8:1 to produce QCHI derivatives with different DS as listed in Table 1. The reaction mixture was stirred at 55 °C for 18 h. It was then diluted with 100 ml distilled water and the pH was adjusted at 7.0 using an aqueous solution of 0.1 N NaOH. The modified chitosan samples were purified by diafiltration through an ultramembrane Amicon YM 30. The diafiltration was stopped when the filtrate conductivity was lower than 10 μS , and the QCHI derivatives were recovered by freeze-drying with yields higher than 90 %.

Capsule preparation. Microcapsules were prepared using calcium carbonate particles as a sacrificial template. CaCO_3 particles were synthesized from solutions of CaCl_2 and Na_2CO_3 as reported in the literature.^[49-50] The CaCO_3 particles were coated layer-by-layer by incubating

them at a concentration 2 % (w/v)^[51] in solutions of QCHI (C_p at 2 g L⁻¹) and HA (C_p at 5 g L⁻¹), both in 0.15 M NaCl (pH 6.5). After shaking for 10 min, the particles were collected by centrifugation and the residual non-adsorbed polyelectrolyte was removed by washing twice with 0.01 M NaCl (pH 6.5).

After the desired number of layers was deposited, the CaCO₃ core was removed by treatment with an aqueous solution of EDTA (0.1 M, pH 7.2). To avoid mechanical damages of “soft” polyelectrolyte shells, the dissolved ions resulting from the decomposition of CaCO₃ were removed by dialysis against pure water, using spectra Por dialysis bags with a molecular weight cut off of 3.5 kDa.

Conductivity measurements. The degree of substitution of the QCHI derivatives was measured by titrating the amount of Cl⁻ ions on the QCHI with aqueous AgNO₃ solution.^[20] The DS is defined as the ratio of mol of reacted GTMAC per mol of repeating unit of chitosan. QCHI (0.025 g) was dissolved in deionized water (50 mL) and titrated with an aqueous solution of AgNO₃ (0.02 M). The DS of QCHI was calculated using equation 1:

$$C_{\text{AgNO}_3} \times V_{\text{AgNO}_3} = (m_{\text{QCHI}} \times \text{DS}) / [\text{DS} \times M_3 + (1-\text{DS}) \times ((1-\text{DA}) \times M_1 + \text{DA} \times M_2)] \quad (1)$$

In this relation, M_1 is the molecular weight of the glucosamine unit, M_2 is the molecular weight of the *N*-acetyl-glucosamine unit, M_3 is the molecular weight of the quaternized unit, and DA is the degree of acetylation of chitosan (0.09).

Dilute solution viscometry. The intrinsic viscosities were determined by measuring viscosity of polymer solutions at low concentrations (< 1 g L⁻¹) with an Ubbelohde capillary viscometer ($\phi = 0.58$ mm) and extrapolating to infinite dilution using the Huggins equation^[52] as described below :

$$\eta_{\text{sp}}/C = [\eta] + k'[\eta]^2 C \quad (2)$$

In this relation, η_{sp} is the specific viscosity, C is the polymer concentration (g mL⁻¹) and k' , the Huggins constant.

Isothermal titration calorimetry. ITC experiments were carried out on a Microcal VP-ITC titration microcalorimeter (Northampton, USA). All titrations were made in 0.01 M Tris-HCl buffer pH 7.4 with 0.15 M NaCl at 25°C. The reaction cell ($V = 1.45$ mL) contained the QCHI solution ($[\text{QCHI}] = 21.3$ mM, calculated from the average molecular weight of the repeating unit). A series of 10 injections of 10 μL from the computer-controlled 300- μL microsyringe at an interval of 10 min of the solution of HA ($[\text{HA}] = 7.4$ mM, calculated from the average molecular weight of the repeating unit) were performed into the QCHI solution while stirring at 300 rpm at 25 °C. The raw experimental data were reported as the amount of

heat produced after each injection of HA as a function of time. The amount of heat produced per injection was calculated by integration of the area under individual peaks by the instrument software, after taking into account heat of dilution.

Films characterization by quartz crystal microbalance with dissipation monitoring. The (HA/QCHI)_i film buildup (where *i* denotes the number of layer pairs) was followed by *in situ* quartz crystal microbalance (QCM with dissipation monitoring, D300, Qsense, Sweden).^[30] The gold-coated quartz crystal was excited at its fundamental frequency (about 5 MHz, $\nu = 1$) as well as at the third, fifth and seventh overtones ($\nu = 3, 5$ and 7 corresponding to 15, 25 and 35 MHz, respectively). Changes in the resonance frequencies Δf and in the relaxation of the vibration once the excitation is stopped were measured at the four frequencies. The QCM-D data have been analyzed using a Voigt based model^[53] implemented in the Qtools software (Q-Sense) using predetermined values for the film density (1009 kg m^{-3}), buffer density (1000 kg m^{-3}) and viscosity ($1 \text{ mPa}\cdot\text{s}$). Three parameters (film thickness, viscosity and shear modulus) are then deduced.

Confocal Laser Scanning Microscopy. Capsules suspensions alone were observed with a Leica TCS SP2 AOBS (Acoustico Optical Bean Splitter) confocal laser scanning system and an inverted fluorescence microscope equipped with an oil immersion objective lens 63 \times . FITC-labeled HA and QCHI were visualized by excitation of the fluorochrome with a 488 nm Argon/krypton laser and the emitted fluorescence was collected between 497 and 576 nm, precisely defined by the AOBS. Live/dead assays were performed using SYTO 60 and SYTOX Green stains (Molecular probes, Invitrogen). These DNA stains produce red ($\sim 670 \text{ nm}$) and green ($\sim 530 \text{ nm}$ emission for live and dead bacteria, respectively). The stains were added as a 1:1 mixture to the samples containing bacteria and capsules ($2 \mu\text{L}$ of mixed stains per 1 mL of suspension) and incubated for 15 min in PBS. Bacterial cells were co-incubated with HA- or QCHI-ended capsules for 20 h (capsules/bacterial cells ratio ~ 1 ; $\sim 10^7$ capsules and cells per mL) and then added with the mixture of stains. Confocal laser microscopy images were acquired on a Leica TCS SP2 AOBS apparatus by excitation of the SYTO Green with a 488 nm Argon/krypton laser and collection of the emitted fluorescence between 513 and 533 nm and by excitation of the SYTO 60 with a 633 He/Ne diode and collection of emitted fluorescence between 676 and 696 nm.

Scanning Electron Microscopy. Drops of capsules suspensions were deposited onto copper stubs and allowed to air drying. The samples were sputtered with Au/Pd for 3 min and observed in secondary electron imaging mode with a Jeol JSM6100 microscope using an accelerating voltage of 8 kV.

Atomic force microscopy. All AFM images were carried out in air with a PicoPlus AFM in tapping mode using tetrahedral tips (OMCL-AC240TM-E tip from Olympus) with a resonance frequency of 75 kHz and a spring constant of 2 N m^{-1} . Capsules deposited on a mica substrate were imaged at line rates of 1 Hz. For surface roughness analysis, $1 \times 1 \mu\text{m}^2$ AFM images were obtained and the arithmetic average roughness R_a was calculated according to:

$$R_a = \frac{1}{N_x N_y} \sum_{i=1}^{N_x} \sum_{j=1}^{N_y} |z_{ij} - z_{mean}| \quad (3)$$

where z_{ij} is the height of a given pixel, z_{mean} is the average height of the pixels, and $N_x = N_y = 512$ are the number of pixels in the x and y directions.

Antibacterial test. The antibacterial activity of the QCHI samples and capsules against the Gram-negative bacterium *E. Coli* was assessed by a viable-cell counting method.^[54] *E. Coli* (DH5 α) was incubated in nutrient broth (Lennox L Broth Base, Invitrogen®, 20 g L^{-1}) at 37°C overnight. Then, $200 \mu\text{L}$ of culture was placed in 100 mL of nutrient broth; the bacterial culture was incubated at 37°C until the culture of *E. Coli* contained c.a. $10^7 \text{ cells mL}^{-1}$ (absorbance at 600 nm equal to 0.6). QCHI was dissolved in 15 mL of PBS (pH 7.4 , $[\text{NaCl}] = 0.137 \text{ M}$) overnight. The solutions of QCHI and suspensions of capsules ($\sim 10^7$ per mL by counting in a Petroff-Hausser counting chamber) were sterilized by UV (254 nm) for 15 min and then placed in the incubator at 37°C for 3 h . $150 \mu\text{L}$ of the bacterial culture was added to these solutions, and in parallel, added to 15 mL of sterilized PBS (control experiment). $100 \mu\text{L}$ of each sample were picked out after $0, 30, 60, 120,$ and 240 min incubation. Decimal serial dilutions (until 10^5) were carried out by mixing $100 \mu\text{L}$ of each sample with $900 \mu\text{L}$ of PBS. From these dilutions, the surviving bacteria were counted by the spread plate method: $100 \mu\text{L}$ of decimal dilutions were spread on a Petri dish that contained LB agar (Lennox L Agar, Invitrogen®, 32 g L^{-1}). The Petri dishes were incubated at 37°C overnight. After incubation, the colonies were counted. The experiments were performed in triplicates.

Cell viability tests. C2C12 cells (< 20 passages, kindly provided by Cécile Gauthier-Rouvière, CRBM, Montpellier, France) were maintained in polystyrene flasks in a 37°C , $5\% \text{ CO}_2$ incubator, and cultured in a 1:1 Dulbecco's Modified Eagle Medium (DMEM)/Ham's F12 medium (growth medium, GM, Gibco, Invitrogen, Cergy-Pontoise, France) supplemented with 10% foetal bovine serum (FBS, PAA Laboratories, Les Mureaux, France), containing 100 U mL^{-1} penicillin G and $100 \mu\text{g mL}^{-1}$ streptomycin (Gibco, Invitrogen, Cergy-Pontoise, France). Cells were subcultured prior to reaching $60\text{-}70\%$ confluence (approximately every 2

days). For the viability experiments, C2C12 cells were seeded at 2×10^4 cells per well in 8-well Labteck chambers in GM. 30 min later, the capsules at different ratio were added in the culture medium. The cells were observed in phase contrast microscopy using a 10X objective under a Zeiss Axiovert 200 (Zeiss, Germany) inverted microscope. After 48 hours, cells were fixed in 3.7 % formaldehyde in PBS followed by 4 min of permeabilization in 0.2 % Triton X-100 in PBS. Nuclei were stained with Hoechst 33342 (Molecular Probes, Invitrogen, France) at $5 \mu\text{g mL}^{-1}$ for 10 min at room temperature. Images were obtained using a CoolSNAP EZ CCD camera and acquired with Metavue software (both from Roper Scientific, Evry, France). The cell number per surface area was then counted and compared to the control conditions (cells on tissue culture polystyrene without capsules in the suspending medium).

Acknowledgements

This work has been supported by the “Agence Nationale pour la Recherche” (grant ANR-07-NANO-002 to RA and CP). We thank Sandrine Lenoir for her technical help in the antibacterial assays. CP is a Junior Member of the “Institut Universitaire de France” whose support is gratefully acknowledged. D.C. and A.S. gratefully acknowledge the MENRT and the E.C. (contract number MEST-CT-2004-503322 of Sixth Framework Programme), respectively, for their thesis grant in CERMAV. C.D. is Senior Research Associate by the National Funds for Scientific Research (F.R.S.-FNRS) and thanks F.R.S.-FNRS for financial support. Supporting Information is available online from Wiley InterScience or from the author.

Received: (March 29, 2010)

Published online: (August 23, 2010)

_ References

- [1]S. Chopra, S. Mahdi, J. Kaur, Z. Iqbal, S. Talegaonkar, F. J. Ahmad, *J. Pharm. Pharmacol.* **2006**, *58*, 1021.
- [2]H. Sashiwa, S. Aiba, *Prog. Polym. Sci.* **2004**, *29*, 887.
- [3]A. S. Pedro, E. Cabral-Albuquerque, D. Ferreira, B. Sarmento, *Carbohydr. Polym.* **2009**, *76*, 501.

- [4] C. Peniche, W. Arguelles-Monal, H. Peniche, N. Acosta, *Macromol. Biosci.* **2003**, *3*, 511.
- [5] R. A. A. Muzzarelli, *Carbohydr. Polym.* **2009**, *76*, 167.
- [6] J. Fu, J. Ji, W. Yuan, J. Shen, *Biomaterials* **2005**, *26*, 6684.
- [7] R. Belalia, S. Grelier, M. Benaissa, V. Coma, *J. Agric. Food Chem.* **2008**, *56*, 1582.
- [8] G. J. Tsai, W. H. Su, *J. Food Prot.* **1999**, *62*, 239.
- [9] E. I. Rabea, M. E. T. Badawy, C. V. Stevens, G. Smagghe, W. Steurbaut, *Biomacromolecules* **2003**, *4*, 1457.
- [10] J. A. Lichter, K. J. Van Vliet, M. F. Rubner, *Macromolecules* **2009**, *42*, 8573.
- [11] J. Genzer, K. Efimenko, *Biofouling* **2006**, *22*, 339.
- [12] O. Etienne, C. Picart, C. Taddei, Y. Haikel, J. L. Dimarcq, P. Schaaf, J. C. Voegel, J. A. Ogier, C. Egles, *Antimicrob. Agents Chemother.* **2004**, *48*, 3662.
- [13] A. Guyomard, E. De, T. Jouenne, J.-J. Malandain, G. Muller, K. Glinel, *Adv. Funct. Mater.* **2008**, *18*, 758.
- [14] J. Fu, J. Ji, D. Fan, J. Shen, *J. Biomed. Mater. Res.* **2006**, *79A*, 665.
- [15] J. C. Grunlan, J. K. Choi, A. Lin, *Biomacromolecules* **2005**, *6*, 1149.
- [16] Z. Li, D. Lee, X. Sheng, R. E. Cohen, M. F. Rubner, *Langmuir* **2006**, *22*, 9820.
- [17] M. Malcher, D. Volodkin, B. Heurtault, P. André, P. Schaaf, H. Möhwald, J.-C. Voegel, A. Sokolowski, V. Ball, F. Boulmedais, B. Frisch, *Langmuir* **2008**, *24*, 10209.
- [18] L. Richert, P. Lavalley, E. Payan, Z. Shu Xiao, G. Prestwich, J.-F. Stoltz, P. Schaaf, J.-C. Voegel, C. Picart, *Langmuir* **2004**, *20*, 448.
- [19] M. Bulwan, S. Zapotoczny, M. Nowakowska, *Soft Matter* **2009**, *5*, 4726.
- [20] S.-H. Lim, S. M. Hudson, *Carbohydr. Res.* **2004**, *339*, 313.
- [21] B. G. De Geest, S. De Koker, G. B. Sukhorukov, O. Kreft, W. J. Parak, A. G. Skirtach, J. Demeester, S. C. De Smedt, W. E. Hennink, *Soft Matter* **2009**, *5*, 282.
- [22] B. G. De Geest, N. N. Sanders, G. B. Sukhorukov, J. Demeester, S. C. De Smedt, *Chem. Soc. Rev.* **2007**, *36*, 636.
- [23] B. G. De Geest, G. B. Sukhorukov, H. Möhwald, *Exp. Opin. Drug Deliv.* **2009**, *6*, 613.
- [24] A. P. R. Johnston, C. Cortez, A. S. Angelatos, F. Caruso, *Curr. Opin. Colloid Interface Sci.* **2006**, *11*, 203.
- [25] C. S. Peyratout, L. Dähne, *Angew. Chem. Int. Ed.* **2004**, *43*, 3762.
- [26] C. Picart, *Curr. Med. Chem.* **2008**, *15*, 685.
- [27] A. Szarpak, I. Pignot-Paintrand, C. Nicolas, C. Picart, R. Auzély-Velty, *Langmuir* **2008**, *24*, 9767.
- [28] C. Cassinelli, M. Morra, A. Pavesio, D. Renier, *J. Biomaterials Sci. Polym. Ed.* **2000**, *11*, 961.
- [29] P. Kujawa, P. Moraille, J. Sanchez, A. Badia, F. M. Winnik, *J. Am. Chem. Soc.* **2005**, *127*, 9224.
- [30] C. Picart, P. Lavalley, P. Hubert, F. J. G. Cuisinier, G. Decher, P. Schaaf, J. C. Voegel, *Langmuir* **2001**, *17*, 7414.

- [31] A. Szarpak, D. Cui, F. Dubreuil, B. G. De Geest, L. J. De Cock, C. Picart, R. Auzély-Velty, *Biomacromolecules*, 2010, *11*, 713.
- [32] H. Lee, Y. Jeong, T. G. Park, *Biomacromolecules* **2007**, *8*, 3705.
- [33] D. Bhadra, G. Gupta, S. Bhadra, R. B. Umamaheshwari, N. K. Jain, *J. Pharm. Sci.* **2004**, *7*, 241.
- [34] Z. Mao, L. Ma, C. Gao, J. Shen, *J. Controlled Release* **2005**, *104*, 193.
- [35] W. S. Choi, H. Y. Koo, J.-H. Park, D.-Y. Kim, *J. Am. Chem. Soc.* **2005**, *127*, 16136.
- [36] J. Cho, J. Grant, M. Piquette-Miller, C. Allen, *Biomacromolecules* **2006**, *7*, 2845.
- [37] H.-S. Seong, H. S. Whang, S.-W. Ko, *J. Appl. Polym. Sci.* **2000**, *76*, 2009.
- [38] M. M. Amiji, *Carbohydr. Polym.* **1995**, *26*, 211.
- [39] W. Tong, C. Gao, H. Möhwald, *Chem. Mater.* **2005**, *17*, 4610.
- [40] S. Leporatti, A. Voigt, R. Mitloehner, G. Sukhorukov, E. Donath, H. Möhwald, *Langmuir* **2000**, *16*, 4059.
- [41] S. Kadi, D. Cui, E. Bayma, T. Boudou, C. Nicolas, K. Glinel, C. Picart, R. Auzély-Velty, *Biomacromolecules* **2009**, *10*, 2875.
- [42] N. Laugel, C. Betscha, M. Winterhalter, J.-C. Voegel, P. Schaaf, V. Ball, *J. Phys. Chem. B* **2006**, *110*, 19443.
- [43] D. P. Mascotti, T. M. Lohman, *Biochemistry* **1992**, *31*, 8932.
- [44] M. T. Record, Jr., M. L. Lohman, P. De Haseth, *J. Mol. Biol.* **1976**, *107*, 145.
- [45] T. S. Corbitt, J. R. Sommer, S. Chemburu, K. Ogawa, L. K. Ista, G. P. Lopez, D. G. Whitten, K. S. Schanze, *ACS Appl. Mater. Interfaces* **2009**, *1*, 48.
- [46] C. Kirchner, A. M. Javier, A. S. Sussha, A. L. Rogach, O. Kreft, G. B. Sukhorukov, W. J. Parak, *Talanta* **2005**, *67*, 486.
- [47] S. De Koker, B. G. De Geest, C. Cuvelier, L. Ferdinande, W. Deckers, W. E. Hennink, S. De Smedt, N. Mertens, *Adv. Funct. Mater.* **2007**, *17*, 3754.
- [48] J. Brugnerotto, J. Desbrières, G. Roberts, M. Rinaudo, *Polymer* **2001**, *42*, 09921.
- [49] A. A. Antipov, D. Shchukin, Y. Fedutik, A. I. Petrov, G. B. Sukhorukov, H. Möhwald, *Colloids Surf. A Physicochem. Eng. Aspects* **2003**, *224*, 175.
- [50] D. V. Volodkin, A. I. Petrov, M. Prevot, G. B. Sukhorukov, *Langmuir* **2004**, *20*, 3398.
- [51] A. I. Petrov, D. V. Volodkin, G. B. Sukhorukov, *Biotechnol. Prog.* **2005**, *21*, 918.
- [52] M. L. Huggins, *J. Am. Chem. Soc.* **1942**, *64*, 2716.
- [53] M. V. Voinova, M. Rodahl, M. Jonson, B. Kasemo, *Phys. Scr.* **1999**, *59*, 391.
- [54] T. J. Franklin, G. A. Snow, Eds., *Biochemistry of Antimicrobial Action*, Chapman and Hall, London 1981.

2.3.1.2 Supporting information

NMR spectroscopy.

^1H and ^{13}C NMR experiments were performed using a Bruker DRX400 spectrometer operating at 400 and 100 MHz, respectively. Bidimensional experiments were acquired using 2K data points and 256 time increments. For the HMQC experiment, the phase sensitive (TPPI) sequence was used and processing resulted in a 1K \times 1K (real-real) matrix. Chemical shifts are given relative to external tetramethylsilane (TMS = 0 ppm) and calibration was performed using the signal of the residual protons of the solvent as a secondary reference. Deuterium oxide was obtained from SDS (Vitry, France). Details concerning experimental conditions are given in the figure captions.

The identification of most proton and carbon signals of the one-dimensional spectra was derived from two-dimensional ^1H - ^1H COSY and ^1H - ^{13}C HMQC experiments, respectively, and literature data¹³. In the one-dimensional ^1H NMR spectrum of QCHI, an intense peak can be observed at 3.11 ppm (Figure S1), corresponding to the proton signals of the $-\text{N}^+(\text{CH}_3)_3$ group. Comparison of the ^{13}C DEPT135 RMN spectrum of initial chitosan with that of quaternized chitosan provided interesting information about the regioselectivity of the quaternization reaction (Figure S2). The splitting of the C2 signal of the glucosamine units of QCHI demonstrates partial substitution of the amine function. In contrast, only one peak can be observed for the C6 signals of the sugar units of QCHI, which suggests no modification of the primary hydroxyl groups. Although no clear conclusion can be drawn from the RMN spectrum regarding the substitution of the C3 secondary hydroxyls, these groups, which are considered to be less reactive than the primary hydroxyl groups, are likely not modified. Since quantitative integration of ^{13}C signals is possible in the case of ^{13}C NMR DEPT experiments, we assessed the DS of QCHI by integration of the C2 signals. It provided a value of 40 % for sample #1 which was closed to that derived by conductimetric titration of Cl^- ions with AgNO_3 .

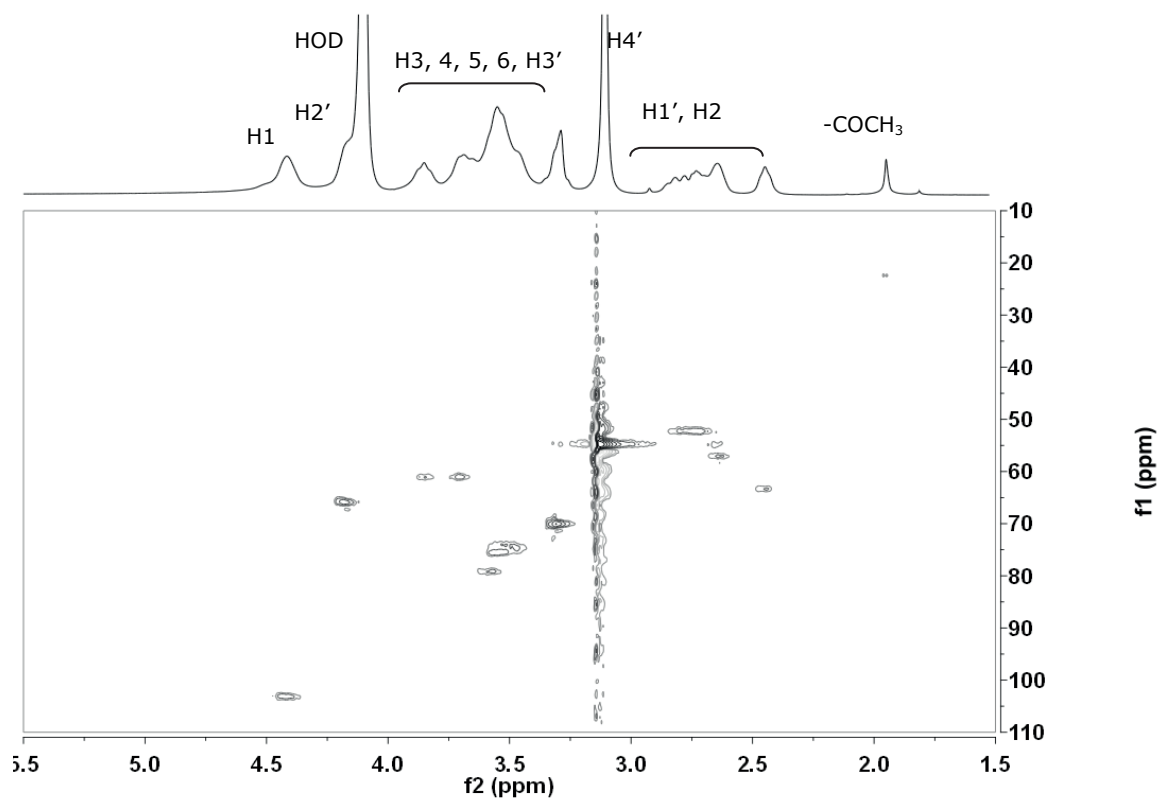
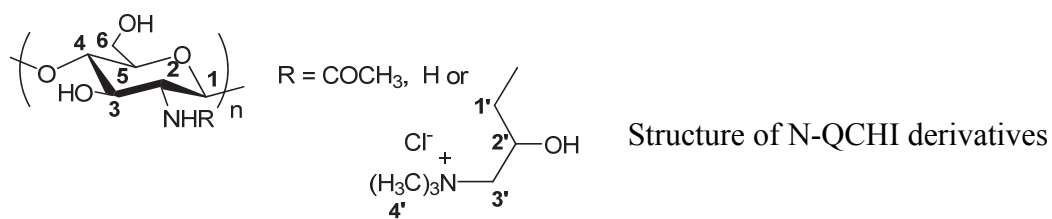


Figure S1: ¹H-¹³C HMQC NMR spectrum (400/100 MHz, 80 °C) of QCHI (DS = 0.31, 6 mg/mL in D₂O) with the one-dimensional ¹H NMR spectrum performed on the same sample (top).

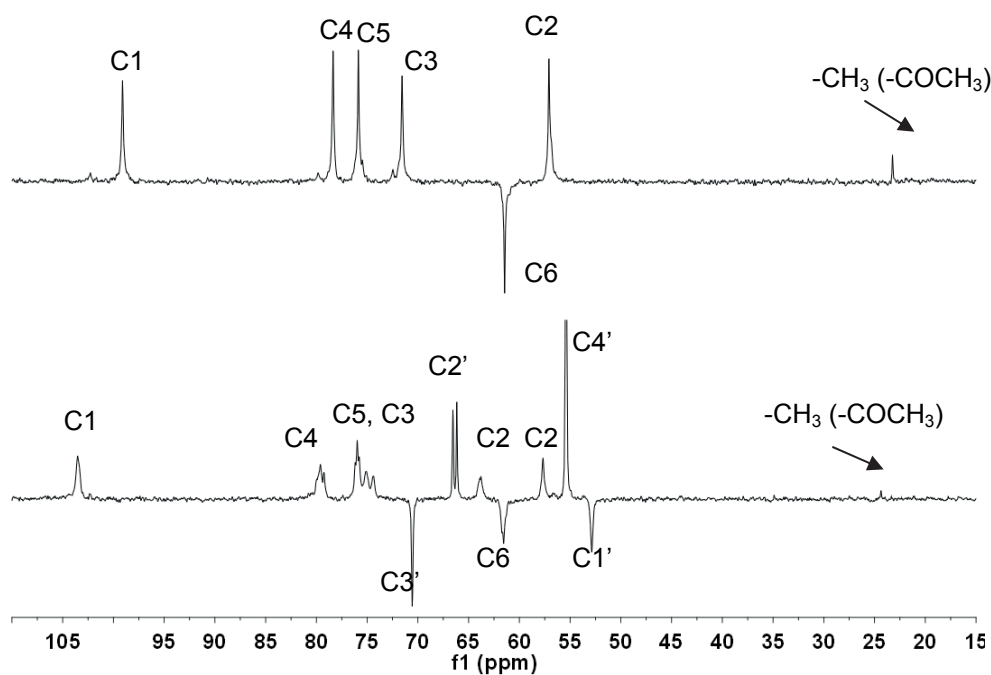


Figure S2: ^{13}C DEPT 135 NMR spectra (100 MHz, 80 °C) of (A) initial chitosan (20 mg/mL in $\text{D}_2\text{O}/\text{DCl}$, pD = 4) and (B) QCHI (DS = 0.31, 20 mg/mL in D_2O).

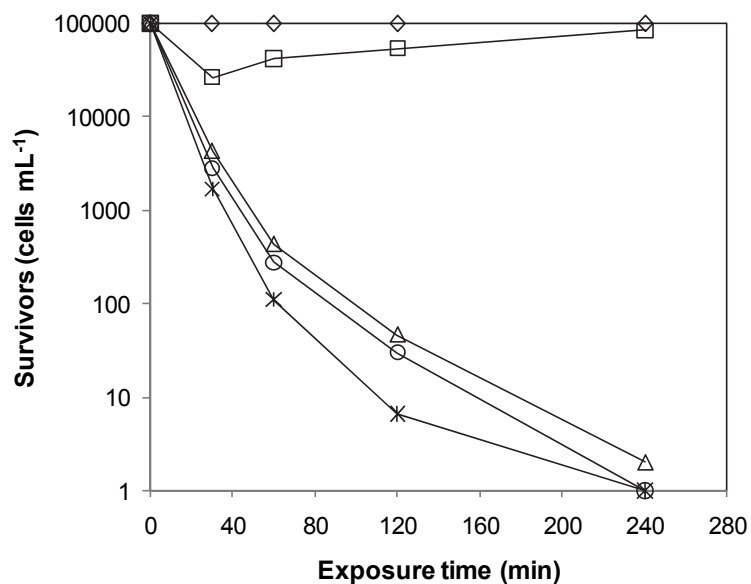


Figure S3. Plots of survivors versus exposure time for QCHI-4 (DS = 0.66) dissolved in PBS at different concentrations : (\diamond) 0 mM (control (PBS)); (\square) 0.001 mM; (Δ) 0.01 mM; (\circ) 0.125 mM; ($*$) 1.25 mM.

2.3.1.3 Complementary results

1) Permeability of capsules

To study the permeability of the capsule shells, we performed experiments by using FITC labelled dextran (Dextran^{FITC}) with different hydrodynamic radius (R_h). The relationship between R_h and the Mw of dextran has been explored in the literature (**Figure 2.6**).¹⁴⁻¹⁶

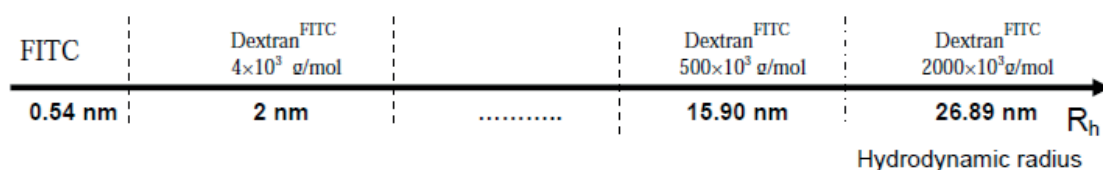


Figure 2.6: Hydrodynamic radius of FITC and FITC labeled dextran molecules (Dextran^{FITC}) at different Mw.¹⁴⁻¹⁶

Depending on the size of diffusing Dextran^{FITC}, the different concentration of molecule inside and within the shells can be obtained, as illustrated in **Figure 2.7**.

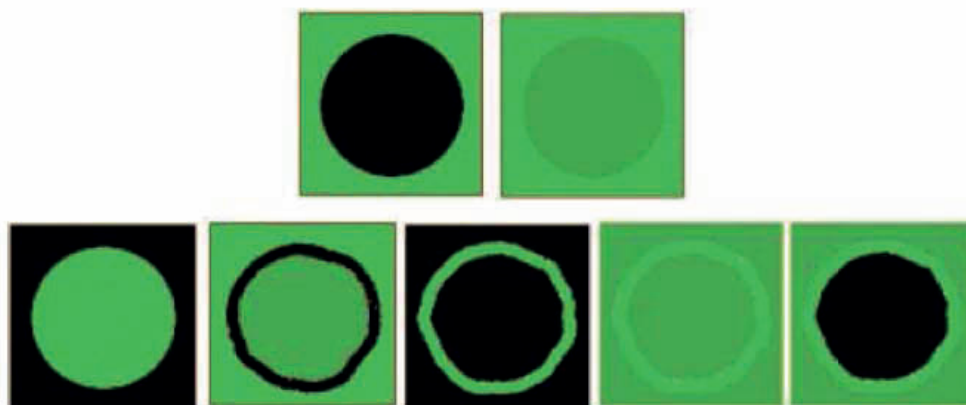


Figure 2.7: Schematic illustration of images of a single suspended shell which can be obtained in the presence of fluorescent probes. The green colour indicates regions of lower or higher fluorescent intensity according to the local concentration distribution of the probe (outside/shell wall/inside). Black regions mean the absence of fluorescent probes.¹⁷

In our permeability experiments, before mixing with diffusing molecules, the hollow capsules were suspended in PBS buffer (pH 7.4) or MES buffer (pH 6.5) overnight. Dextran^{FITC} with different Mw (Dextran^{FITC}-4, -500 and -2000 representing Dextran^{FITC} with

Mw of 4000, 500000 and 2000000 g/mol, respectively) were dissolved in the same buffer at concentrations of 2mg/mL. For the permeability tests in the presence of salt, NaCl was added into the MES buffer to obtain a concentration of 0.15M. Typically, 20 μ L of Dextran^{FITC} solution was mixed with 20 μ L of capsule suspension on a glass slide. After 20min, the capsules were observed under CLSM. As examples, the images of the capsules made of *N*-QCHI2 after 20 min of contact with Dextran^{FITC}-4 and Dextran^{FITC}-2000 were respectively presented in Figure 2.8. The images were analyzed using Leica Confocal Software by the measurement of the light emitted by the capsule interior (I_{int}) and surrounding solution (I_{ext}). The permeability coefficient (I_{int}/I_{ext}) was estimated as an average value from 7-10 capsules.

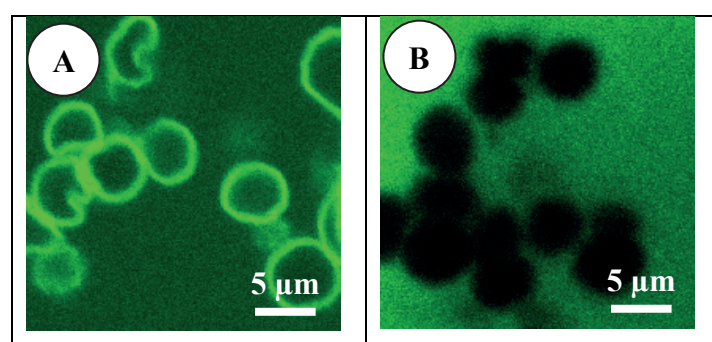


Figure 2.8: CLSM images of capsules based on HA and *N*-QCHI2 (DS = 0.31) obtained after 20 min of contact with Dextran^{FITC}: A) Dextran^{FITC}-4 and B) Dextran^{FITC}-2000.

As can be seen from **Figure 2.9**, the permeability of capsules based on *N*-QCHI derivatives and HA was strongly dependent on the Mw of Dextran^{FITC}, the DS of *N*-QCHI derivatives and the concentration of salt. In the buffer of MES with 0.15 M of salt, all of the (*N*-QCHI/HA)_{4.5} capsules were 100% permeable to Dextran^{FITC}-4, while in the buffer of MES without added salt (only 0.02 M MES), the permeability decreased (**Figure 2.9A**). Under the latter conditions, it was found that the permeability of capsules increased with the increase of DS, except those based on *N*-QCHI5. In fact, the permeability of capsules based on HA and *N*-QCHI5 to Dextran^{FITC}-4 was a little lower than that of capsules based on HA and *N*-QCHI4. The increasing permeability with the increased of the DS of *N*-QCHI derivatives might be due to the weaker complexation ability between HA and *N*-QCHI derivatives with higher DS, which we have been discussed in the publication reported in **Advanced Functional Materials**.¹² In the buffer of PBS, with the increase of the Mw of Dextran^{FITC}, a decreasing permeability of capsules was observed (**Figure 2.9B**).

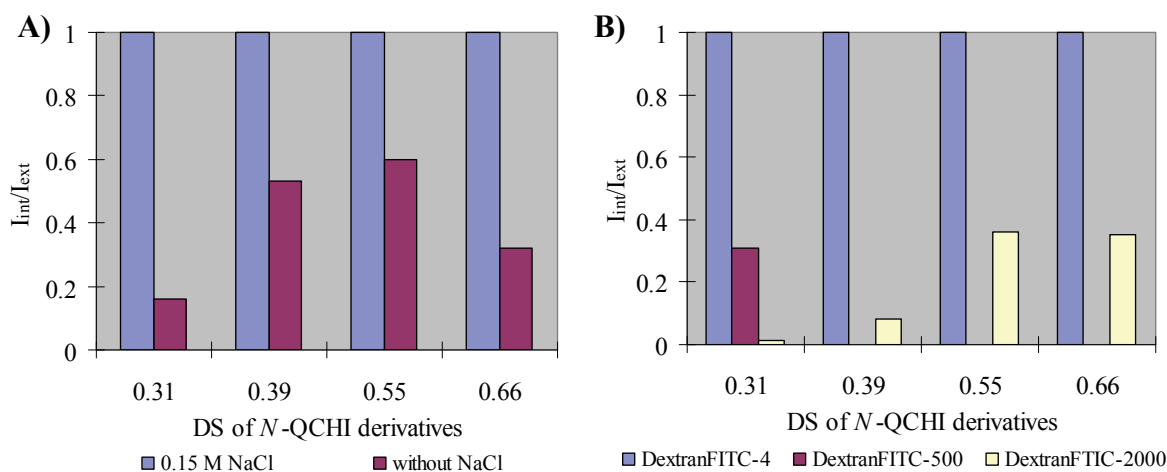


Figure 2.9: Permeability of capsules based on HA and QCHI derivatives: A) effect of the salt on the permeability of capsules to Dextran^{FITC}-4 in MES buffer (pH 6.5) and B) effect of Mw of Dextran^{FITC} on the permeability of capsules in PBS. The *N*-QCHI derivatives with DS of 0.31, 0.39, 0.55 and 0.66 correspond to *N*-QCHI2-5, respectively.

2) Enzymatic degradation

We used CLSM to investigate the enzymatic degradation of capsules based on HA and *N*-QCHI2 (DS = 0.31). 25 μ L of hollow capsule suspension (in PBS) was added to 25 μ L of hyaluronidase solution (1000 U/mL in PBS). The mixtures with final concentration of enzyme of 500U/mL were stored overnight at 37°C. The capsules incubated in PBS and those contacted with hyaluronidase overnight were observed by CLSM respectively (**Figure 2.10**). After overnight contact with hyaluronidase, the capsules based on HA and QCHI still kept their mechanical stability and the change of permeability to Dextran^{FITC}-2000 was not remarkable. However, we could observe the influence of enzyme to the capsules by the high light adsorption of Dextran^{FITC}-2000 in the shell of capsules. This phenomenon perhaps was caused by the slightly enzymatic degradation of HA in the shell of capsules.

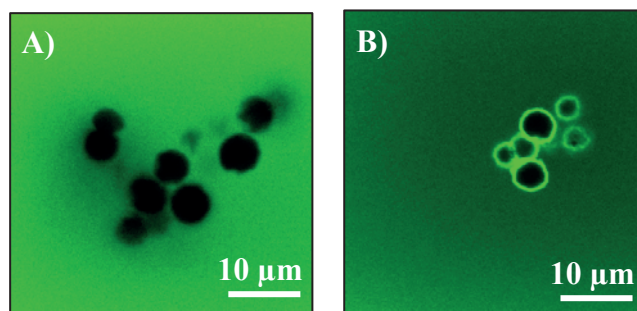


Figure 2.10: Investigation of enzymatic degradation of capsules by CLSM: A) CLSM image of capsules incubated in PBS at room temperature overnight and B) CLSM image of capsules incubated in PBS with contact of hyaluronidase (500 U/mL) overnight.

3) Study of the antimicrobial activity of capsules against *E. coli*

a. Effect of DS of QCHI derivatives on the antimicrobial activity of capsules

In the work published in **Advanced Functional Materials**, we demonstrated that the *N*-QCHI-ended capsules based on HA and *N*-QCHI with the highest DS (*N*-QCHI5, DS = 0.66) showed a similar antimicrobial activity to the solution of *N*-QCHI5.¹² To explore the effect of the DS of *N*-QCHI derivatives on the antimicrobial activity of (HA/*N*-QCHI) capsules, we also determined the inhibitory ability of capsules based on *N*-QCHI with lower DS (*N*-QCHI2, DS = 0.31) by comparing the time required to kill bacteria derived from the viable cell-counting method. It is worth mentioning that to obtain quantitative results, all antimicrobial tests of capsules using this method were carried out under the same conditions. As can be seen from **Figure 2.11**, the capsules containing *N*-QCHI2 exhibited lower antimicrobial activity than those containing *N*-QCHI5. The *N*-QCHI2-ended capsules also showed a similar antimicrobial activity to *N*-QCHI2 solution and these capsules killed more *E. coli* than those ended by HA. These results obtained from the capsules based on QCHI derivatives with lower DS are in good agreement with the results obtained in the previous study. So, we can conclude that the DS of the *N*-QCHI derivatives affects the antimicrobial activity of capsules. An increase of the DS results in a higher killing activity of capsules against *E. coli*.

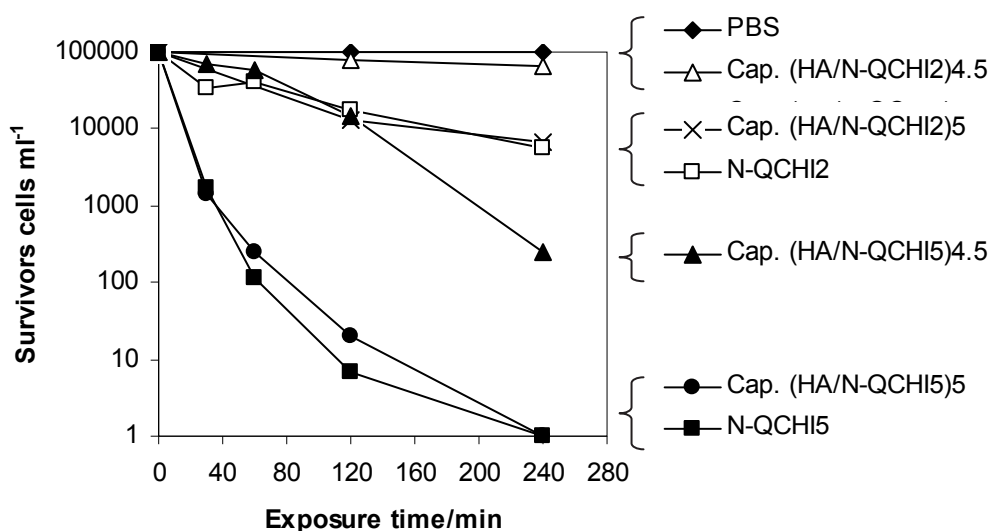


Figure 2.11: Comparison of antibacterial activity of *N*-QCHI derivatives solutions and capsules based on HA and *N*-QCHI derivatives ended by either HA or *N*-QCHI derivatives against *E. coli*. Cap. (HA/*N*-QCHI)_{4.5} and Cap (HA/*N*-QCHI)₅ mean the capsules prepared based on the pair of HA/*N*-QCHI ended by HA and *N*-QCHI, respectively ($C_p \sim 1.25$ mM; Capsules/bacterial cells ratio ~ 100).

b. Mode of action to kill bacteria

From the analysis of bacterial viability, we found that the (HA/*N*-QCHI)₅ capsules killed *E. coli* by a contact-killing process. In this part, we investigated the antimicrobial activity of capsules against *E. coli* by transmission electron microscopy (TEM) to get information about the antimicrobial mechanism of capsules to kill *E. coli*. **Figure 2.12** shows the TEM images of native *E. coli*, *E. coli* mixed with (HA/*N*-QCHI₅ (DS = 0.66)) capsules ended by HA and *N*-QCHI₅ respectively. As can be seen from the image, different to the native *E. coli*, which was full of intercellular components inside of the cell, *E. coli* mixed with HA-ended capsules had some gaps in the cellular inner, whereas little intercellular components was found in the case of *E. coli* mixed with *N*-QCHI₅-ended capsules. In addition, although the inner of cells was almost empty in the last case, the cell wall was not destroyed. These observations indicated that these capsules killed *E. coli* by altering the permeability of cell wall and thereby leading to the leakage of intracellular component, which could be proved by the comparison of the inner of *E. coli* before and after treated with capsules.

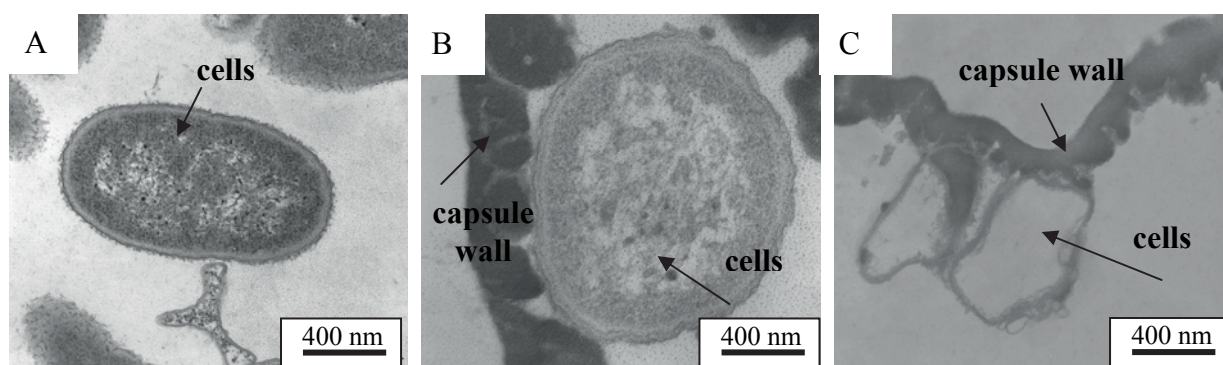


Figure 2.12: Investigation of antimicrobial activity of (HA/*N*-QCHI5) capsules against *E. coli* by TEM: A) *E. coli*; B) HA-ended capsules with *E. coli* and C) *N*-QCHI5-ended capsules with *E. coli*.

2.3.2 Utilization of *N,O*-QCHI derivatives as the cationic partners of HA for the synthesis of capsules

2.3.2.1 Syntheses of capsules based on *N,O*-QCHI derivatives

1) Study of multilayer films built-up

To synthesize the capsules based on *N,O*-QCHI derivatives, at first, we verified the layer-by-layer deposition of different polyelectrolytes by QCM-D. *N,O*-QCHI3a (DS = 1.33) and *N,O*-QCHI3b (DS = 1.11) were used as polycations since they have highest DS. The assembly of HA and *N,O*-QCHI derivatives in multilayer films was confirmed by following (HA/*N,O*-QCHI) film deposition on a gold coated crystal by quartz crystal microbalance with dissipation monitoring (QCM-D). As can be seen from **Figure 2.13**, the frequency shift and the thickness of the (HA/*N,O*-QCHI) films growth exponentially, but different to each other in growth extent. The thickness of the (HA/*N,O*-QCHI3b)₄ films (~ 170 nm) is much higher than that of the (HA/*N,O*-QCHI3a)₄ films (~ 135 nm). This result may be related to the higher molar mass and intrinsic viscosity (reflecting the hydrodynamic volume) measured for the *N,O*-QCHI3b sample, resulting in a higher mass deposited after each adsorption step.

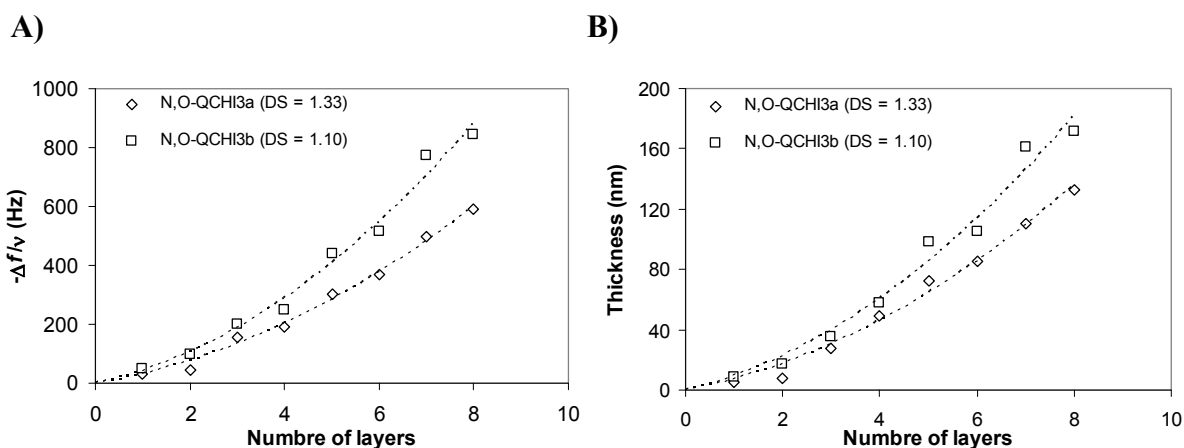


Figure 2.13: (HA/N,O-QCHI) film growth monitored in situ by QCM-D. Differences in A) frequency shifts measured at 15 MHz and B) film thickness are plotted for each HA and N,O-QCHI derivatives deposited layer up to four layer pairs.

2) Synthesis and morphology characterization of capsules

The capsules based on HA/N,O-QCHI3a and HA/N,O-QCHI3b were respectively prepared using the same procedure as used for capsules based on HA/N-QCHI derivatives. The multilayer films coated CaCO₃ particles were observed by TEM in the dried state. As can be seen in **Figure 2.14**, the multilayer film made of 4.5 (HA/N,O-QCHI3a) bilayers was very smooth; in contrast, that made of 4.5 (HA/N,O-QCHI3b) bilayers appeared more irregular. In addition, the thickness of the former was estimated to be ~ 23-36 nm, twice thinner than that of the latter, ~ 50-80 nm. The higher thickness of the (HA/N,O-QCHI3b) multilayer coating has been noticed in the part of the study of multilayer films built-up, in which the thickness of water-containing films was derived from QCM-D measurement.

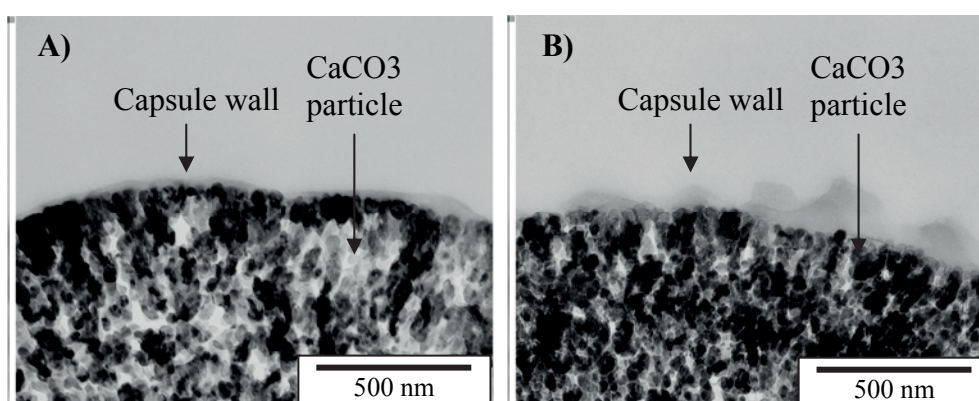


Figure 2.14: TEM images of (HA/N,O-QCHI) multilayer films coated CaCO₃ particles: A) 4.5 (HA/N,O-QCHI3a) bilayers; B) 4.5 (HA/N,O-QCHI3b) bilayers.

Hollow capsules were obtained by removing the cores in the EDTA solution and then washed several times with water. The morphologies of the capsules made of *N,O*-QCHI derivatives with highest DS were investigated in the dried state by SEM, and in aqueous solutions (in PBS, pH 7.4) by CLSM. The possibility of using Dextran^{FITC}-4 as probes to describe the contour of capsules in solution has been mentioned in the Thesis of Anna Szarpak.¹⁸ The images obtained from different techniques were shown in **Figure 2.15**. The capsules based on *N,O*-QCHI3a are small (SEM and CLSM) and shrank (SEM), and such morphology has been found in the SEM image and CLSM image of the capsules based on HA and *N*-QCHI5 (DS = 0.66), while those based on *N,O*-QCHI3b are perfectly spherical in the solution (CLSM), but collapsed in the dried state.

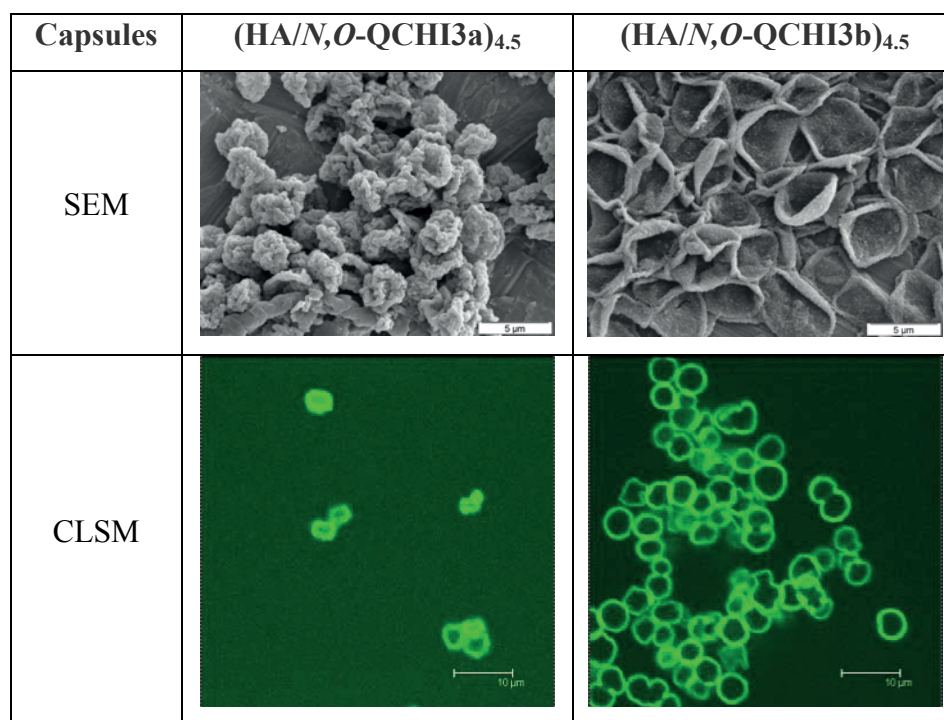


Figure 2.15: Observation of capsules based on HA and *N,O*-QCHI derivatives with 4.5 bilayers by SEM and CLSM.

We determined the size of hollow capsules based on HA and *N,O*-QCHI derivatives and the thickness of their walls by atomic force microscopy (AFM) in their dried state. The folded flat morphology of capsules during the drying process allows the measurements of the wall thickness. From its profile, the difference between the background and the lowest region of walls gives the thickness of capsules shell (**Figure 2.16**). The diameter of these capsules is estimated to be ~ 4 μm for the (HA/*N,O*-QCHI3a)_{4.5} capsules and ~ 5 μm for the (HA/*N,O*-

QCHI3a)_{4,5} capsules. Measured by AFM, The wall thickness of the hollow (HA/N,*O*-QCHI3a)_{4,5} capsules is ~ 110 nm, almost the same as that of the hollow (HA/N,*O*-QCHI3b)_{4,5} capsules (~ 115 nm).

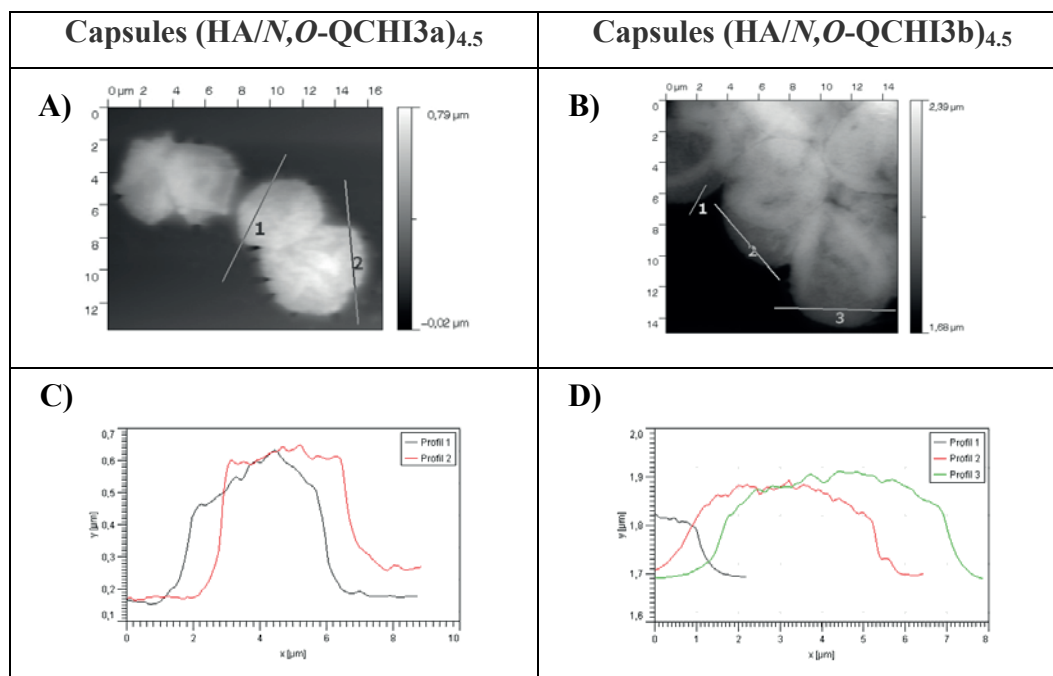


Figure 2.16: AFM images of dried (HA/ N,*O*-QCHI)_{4,5} capsules with corresponding profiles: A) and C) correspond to the (HA/N,*O*-QCHI3a)_{4,5} capsules and B) and D) (HA/N,*O*-QCHI3b)_{4,5} correspond to capsules.

The comparison of the thickness of various (HA/N,*O*-QCHI) coatings measured by different techniques is presented in **Table 2.6**. The similar wall thickness of hollow capsules based on HA and different *N,O*-QCHI derivatives by AFM is not consistent with the conclusion obtained by QCM-D and TEM, which demonstrated that the thickness of multilayer films made of HA/N,*O*-QCHI3b was higher. This is probably due to the shrinkage folded morphology of the capsules made of HA/N,*O*-QCHI3a which affected the measurement by AFM. In addition, we noticed that the thickness of the (HA/N,*O*-QCHI)_{4,5} multilayer films coated on CaCO₃ particles measured by TEM and the thickness of (HA/N,*O*-QCHI)_{4,5} hollow capsules measured by AFM was lower than that of the multilayer films made of the same materials with 4 bilayers determined by QCM-D. The difference in thickness obtained by TEM/AFM and QCM-D can be explained by the dried state of capsules in the former case and the water-containing state of multilayer films in the latter case. It is worth to

mention that as proposed by Szarpark¹⁸ the morphology of the substrate used for the construction of multilayer films can also contribute to the thickness of the capsules wall. However, in our case such influence is not obviously. Compared to the wall thickness values of capsules obtained by TEM, it is found that the values obtained by AFM are much higher. This is probably due to the loss of polymers in the multilayer polyelectrolyte shells of capsules after several washings in the TEM studies or for the negative effect of folded collapse morphology of capsules on the precision of measurements in the AFM studies.

Table 2.6: Comparison of the thickness of (HA/*N,O*-QCHI) coatings measured by different techniques.

	QCM	TEM	AFM
Bilayers	4	4.5	4.5
Substrate	Planar golden-crystal	Porous CaCO ₃ particle	Porous CaCO ₃ particle removal
HA/ <i>N,O</i> -QCHI3a	~ 135 nm	~ 23 – 36 nm	~ 110 nm
HA/ <i>N,O</i> -QCHI3b	~ 170 nm	~ 50 – 80 nm	~ 115 nm

The capsules prepared based on HA and *N,O*-QCHI derivatives with different DS were observed by SEM. As can be seen from Figure 2.17, all water-soluble *N,O*-QCHI derivatives can be used to synthesize mechanically stable hollow capsules and the morphology of these capsules were evidently distinguished according to the series of *N,O*-QCHI derivatives divided by the isolated parts of reaction medium. The capsules based on *N,O*-QCHIa derivatives are smaller and folded; those based on *N,O*-QCH Ib derivatives are bigger and collapsed. The capsules based on *N,O*-QCHI derivatives with highest DS were more homogenous and showed better morphology. Of note, the morphologies of capsules based on *N,O*-QCHI derivatives with lower DS, are also different to those of capsules based on *N*-QCHI derivatives. This observation indicates that the morphology variation of capsules made of QCHI derivatives is not only dependent on the DS of QCHI derivatives, but also on other factors, such as Mw and structure (grafting position).

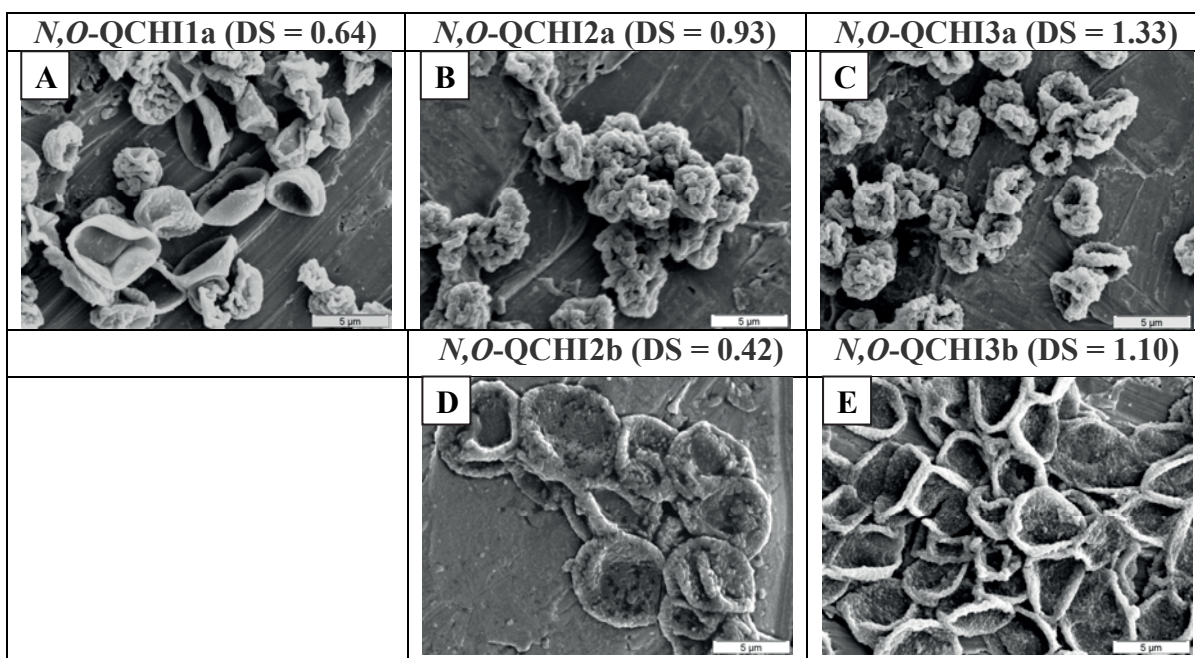


Figure 2.17: SEM images of capsules with 4.5 bilayers prepared based on HA and QCHI derivatives with different DS: A-C). *N,O*-QCHIa and D-E). *N,O*-QCHIb.

2.4.1.2 Permeability of capsules

The permeability of capsules based on HA and *N,O*-QCHI derivatives was investigated and showed in **Figure 2.18**. It is found that the permeability of capsules based on *N,O*-QCHI3a (DS = 1.33) is affected by the concentration of salt whereas that of capsules based on *N,O*-QCHI3b (DS = 1.10) is not. In addition, the capsules composed of *N,O*-QCHI3b (DS = 1.10), has a much lower permeability to Dextran^{FITC}-2000 in PBS than those composed of *N,O*-QCHI3a (DS = 1.33). We suggest that these interesting performance of capsules based on *N,O*-QCHI derivatives on permeability should be related to the different complexation ability and interactions of HA/*N,O*-QCHI derivatives.

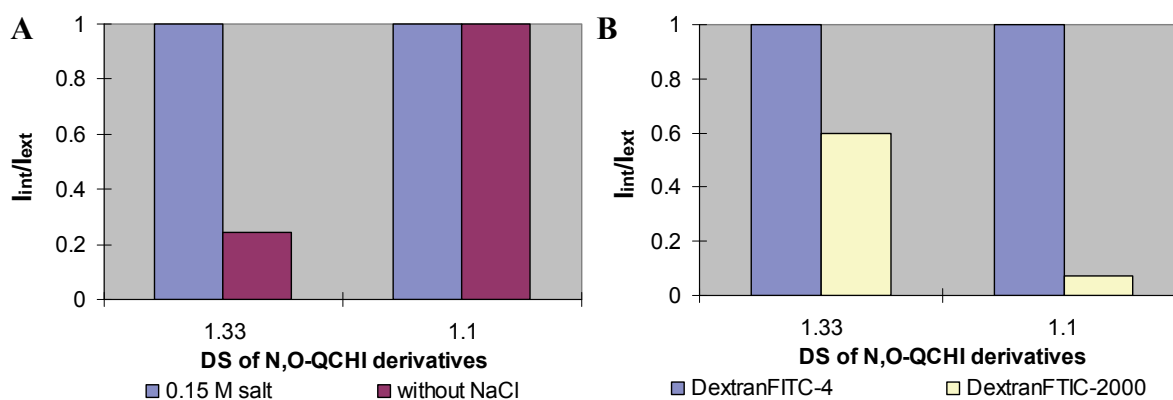


Figure 2.18: Permeability of capsules with 4.5 bilayers prepared based on HA and *N,O*-QCHI derivatives. A) effect of the salt on the permeability of capsules to Dextran^{FITC}-4 in MES buffer (pH 6.5); B) effect of Mw of Dextran^{FITC} on the permeability of capsules in PBS. The *N,O*-QCHI derivatives with DS of 1.33 and 1.10 correspond to *N,O*-QCHI3a and *N,O*-QCHI3b, respectively.

2.3.2.2 Antimicrobial activity of (HA/*N,O*-QCHI) capsules

The antimicrobial activity of capsules based on *N,O*-QCHI derivatives against *E. coli* was determined by viable cell-counting method. The results of antibacterial activity tests are summarized in **Figure 2.19**. It was found that the capsules ended by HA killed less bacteria than those ended by *N,O*-QCHI derivatives. Although these capsules made from *N,O*-QCHI3a and *N,O*-QCHI3b showed different morphology, the antibacterial ability against *E. coli* of them is similar. These results confirm that the polymers used for the built-up of last layers and the DS of QCHI derivatives are the major factors in the antibacterial activity of capsules. In addition, since the antibacterial activity of capsules made of *N,O*-QCHI derivatives with highest DS (DS >1) was not higher than that of capsules made of *N*-QCHI5 (DS = 0.66) and even was lower than that of the solutions of *N,O*-QCHI derivatives, it demonstrates that the antibacterial activity of QCHI-ended capsules does not only depend on the DS .

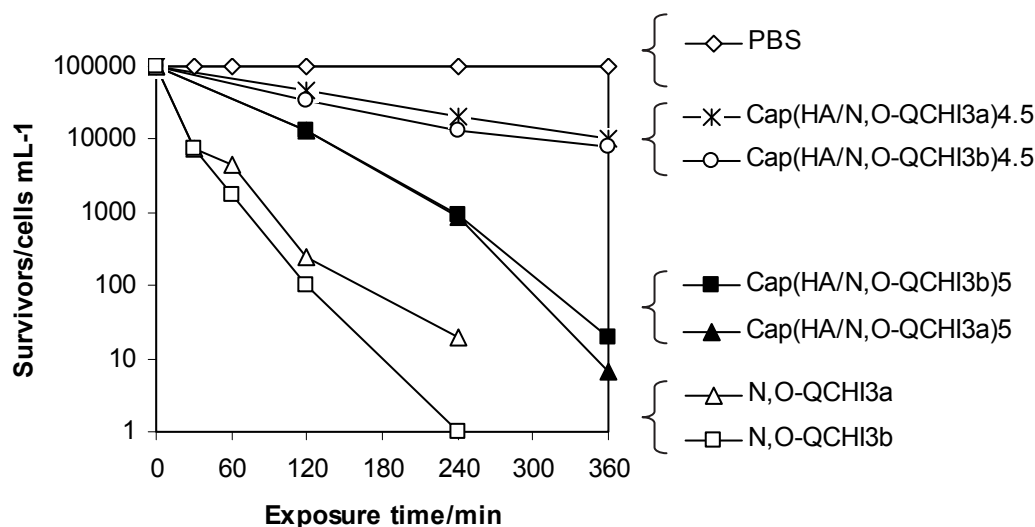


Figure 2.19: Comparison of antibacterial activity of *N,O*-QCHI derivatives solutions and capsules based on HA and *N,O*-QCHI derivatives ended by either HA or *N,O*-QCHI derivatives against *E. coli*. (HA/*N,O*-QCHI)_{4.5} capsules and (HA/*N,O*-QCHI)₅ capsules are terminated by HA and *N,O*-QCHI, respectively. ($C_p \sim 1.25$ mM; Capsules/bacterial cells ratio ~ 100).

We also investigated the antimicrobial activity of capsules based on *N,O*-QCHI derivatives by CLSM and TEM observations (**Figure 2.20**). DNA-staining dyes were used here to distinguish the viability of bacteria. In the CLSM images, the red and green spots correspond to the alive and dead cells, respectively. The shells of capsules were stained by non specific adsorption of dyes. It was found that although the capsules ended by HA presented the negative charges on the surface, *E. coli* still could adhere onto the wall of capsules. But this contact did not induce the fast death of bacteria. The *N,O*-QCHI-ended capsules could adsorb *E. coli* and kill them rapidly. In the TEM images, we can observe that the cells adhering onto the surface of capsules terminated by HA have intracellular components while those adhering onto the surface of QCHI-ended capsules lost almost all of the intracellular components. This observation is consistent with our previous results obtained in the case of capsules based on *N*-QCHI derivatives. Otherwise, in the TEM images, we noticed that there were spots on the surface of cells incubated in the suspension of capsules. Such phenomenon is probably due to the lyse of the surface of capsules resulting from the contact of cell/capsules.

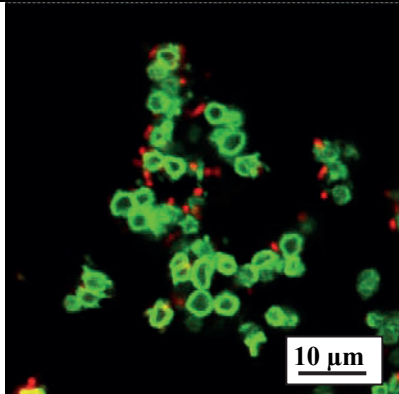
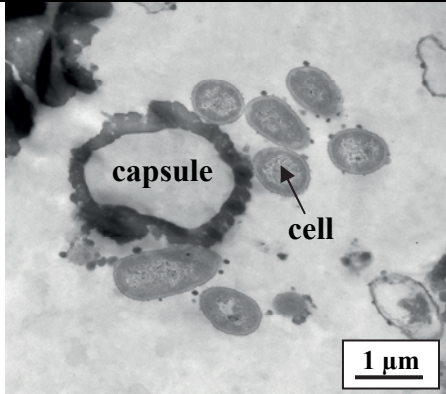
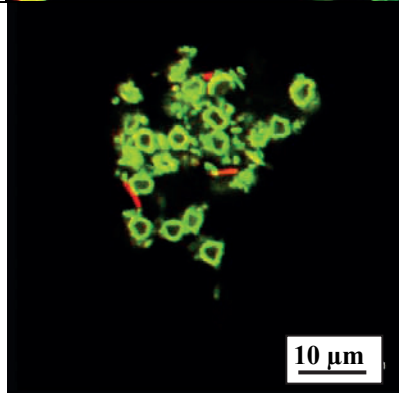
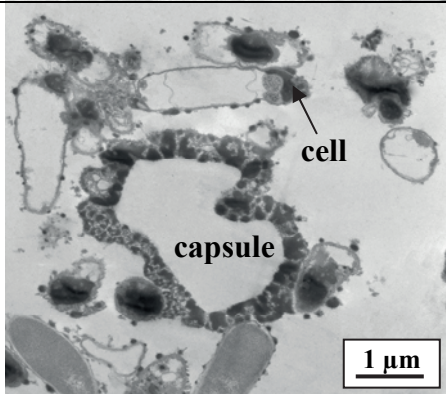
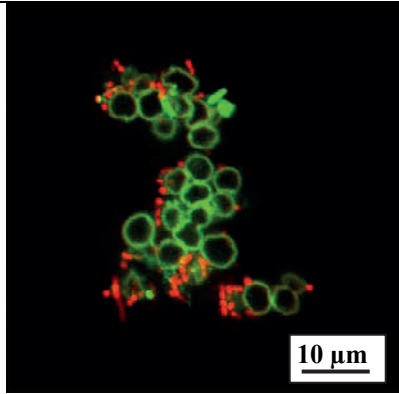
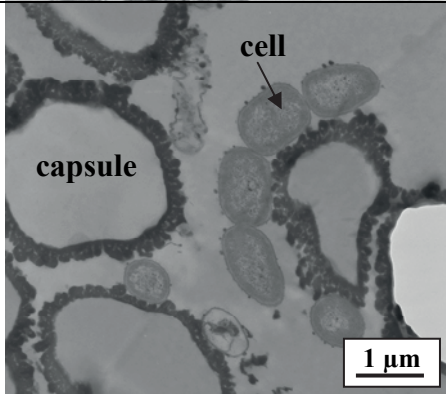
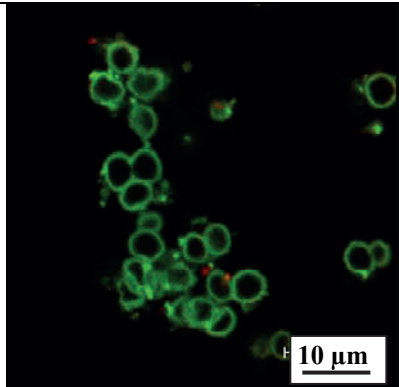
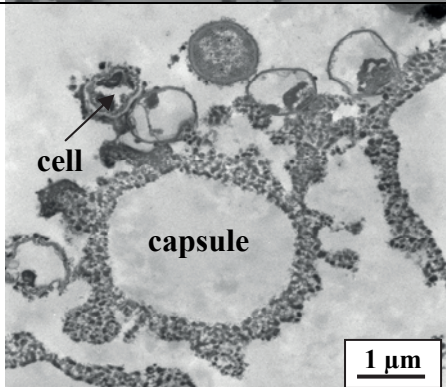
Cap.	Last layer	CLSM	TEM
HA/ <i>N,O</i> -QCHI3a DS = 1.33	HA		
	<i>N,O</i> -QCHI3a		
HA/ <i>N,O</i> -QCHI3b DS = 1.10	HA		
	<i>N,O</i> -QCHI3b		

Figure 2.20: Investigation of antimicrobial activity of capsules based on HA and *N,O*-QCHI derivatives by CLSM and TEM (capsules/bacterial cells ratio ~ 1).

2.4 Conclusion

In order to obtain contact-killing microcapsules based solely on polysaccharides, water-soluble QCHI derivatives were synthesized by reacting CHI with GTMAC in aqueous solutions under different pH conditions. *N*-QCHI derivatives with lower DS were obtained by the selective grafting of quaternary ammonium groups on the primary amine groups of CHI chains under homogeneous acidic conditions, whereas *N,O*-QCHI derivatives with higher DS were obtained by the non-selective modification on hydroxyl and amine groups of CHI chains under heterogeneous neutral conditions. Interestingly, two products were isolated from the supernatant and precipitate of reaction medium performed under neutral conditions, which can be related to the assembly insoluble chains of CHI in the reaction medium at neutral pH. Interestingly, with the increase of DS, the intrinsic viscosity of *N*-QCHI derivatives decreased, while that of *N,O*-QCHI derivatives almost kept constant. This result may be due to the different conditions used for the grafting quaternary ammonium groups onto the CHI chains. The antibacteria activity study of QCHI derivatives against Gram (+) and Gram (-) bacteria demonstrates that the concentration, DS as well as the position of substituent on the CHI chains are the key factors governing the bacterial growth inhibitory effect of QCHI derivatives.

The *N*-QCHI derivatives with $DS > 0.24$ and the *N,O*-QCHI derivatives with $DS > 1$ can be used to form the mechanically stable capsules without cross-linking. The morphologies and antibacterial activities against *E. coli* of these capsules are strongly dependent on the DS and the modification process of QCHI derivatives. By analysing the TEM and CLSM images, it is found that the CHI-based capsules can adsorb *E. coli* onto the capsules wall and killed them by altering the permeability of cell membrane.

Since these capsules still retained the biocompatibility towards myoblast cells, such capsules displaying effective cationic contact-killing antimicrobial abilities could offer a distinct advantage for the delivery of drugs especially for the treatment of some bacterial infections.

2.5 Complementary experimental part

The experimental protocols concerning the synthesis and the characterization of *N*-QCHI derivatives and their corresponding capsules have been reported in publication in **Advanced Functional Materials**. According to them, the structure, DS and intrinsic viscosity of *N,O*-QCHI derivatives, as well as the morphology, film growth and antibacterial activity of their relative capsules were analyzed. In this complementary part, we only present the synthesis of *N,O*-QCHI derivatives and the else characterization techniques, which was not mentioned in publication in **Advanced Functional Materials**..

Materials:

Hyaluronidase (Hase, type VIII, ~300 units/mg, ref H3727), fluorescein isothiocyanate dextran with Mw of 4000, 70000, 500000 and 2000000 g/mol (Dextran^{FITC}-4, -70, -500 and -2000) and 2-(*N*-morpholino) ethanesulfonic acid sodium salt (MES) were purchased from Sigma-Aldrich-Fluka.

Syntheses:

Syntheses of N,O-QCHI derivatives: 0.5 g CHI (protasane) was dispersed in 5 ml distilled water (100mg/mL) overnight. 1.94 g GTMAC was added into the suspension in three portions at 2 hours intervals. After 10 hours' reaction at 85 °C, the clear, yellowish and gel-like product was obtained. This product was poured into 200 ml distilled water. After one night stirring, part of product was soluble. The precipitate was isolated by centrifugation (8000 rpm, 20 min, 20 °C). The product from the supernatant (*N,O*-QCHIa) was directly purified by ultrafiltration, and then freeze-dried; the product from the precipitate (*N,O*-QCHIb) was redissolved before purification, as following steps: at first, the precipitate was dispersed in 200 ml distilled water, 0.1 M HCl was added drop by drop in the suspension in order to dissolve the product and once the product was completely dissolved (at ~ pH 5), 0.1 M NaOH was added to neutralized the solution to pH 7.5. This neutral solution containing *N,O*-QCHIb was purified by ultrafiltration with an ultramembrane Amicon YM 30 and then freeze dried.

Characterization:

Size Exclusion Chromatography (SEC). The molecular weight distribution and the weight-average molar mass were determined by size exclusion chromatography using a Size-exclusion chromatography (SEC) with online multi-angle laser light scattering (MALS) and

viscometry (VISC) measurements were performed as described previously.¹⁹ The fluent was 0.2 M ammonium acetate adjusted to pH 4.5. This gives stable measurements in SEC–MALS.

Transmission Electron Microscopy (TEM). To observe the LbL film deposited on the carbonate particles and the bacterial cells and the capsules after 20 h co-incubation (capsules/bacterial cells ratio ~ 1 ; $\sim 10^7$ capsules and cells per mL), the samples were postfixed with 1% osmium tetroxide in water for 2 h at 4°C, in order to enhance differential contrast between the resin, particles and multilayers. After dehydration by incubation for 20 min in ethanol/water mixtures (7/3, 95/5) and finally twice in ethanol, the samples were infiltrated with ethanol/Lowicryl HM20 resin mixtures (2/3-1/3, 1/3-2/3), for 90 min each. The resin was polymerized at 22°C, allowing preservation the morphology of particles and multilayered assembly, under indirect UV light for 72 h, using the Automatic freeze-substitution System (AFS Leica). Ultrathin sections (70 nm) were prepared with a diamond knife on an UC6 Leica ultramicrotome and collected on carbon-coated 200 μm mesh copper grids. Ultrathin sections were viewed at 80 kV with a Philips CM200 transmission electron microscope. In order to avoid modification of the morphology of samples, we used a resin for the preparation of ultramicrotome sections which can be polymerized under mild conditions, i.e. at room temperature.

Atomic force microscopy (AFM). The wall thickness of (HA/N,O-QCHI)_{4.5} capsules was determined for each batch by AFM imaging of dried capsules by using a Molecular Imaging PicoPlus AFM (now Agilent) in Tapping mode® using Silicon cantilevers (Mikromash NSC15 $f_c = 325$ kHz) from the Nanobio facility in Grenoble.

Antibacterial test against Gram positive (Gram(+)) bacteria. The antibacterial activity of the QCHI samples against Gram-positive bacterium *B. cereus ATCC 14579* was determined according the following protocol. Serial twofold dilution of stock solutions of 4 mg/ml of the chitosans was prepared in MQ water in sterile 96-well round-bottom microtiter plates (Nunc, Roskilde, Denmark). Fresh cultures inoculated from overnight cultures of test strains were grown in Iso-Sensitest Broth (Iso-SB) (Oxoid, Hampshire, England) containing 10 mM MES buffer (Sigma-Aldrich, St. Louis, MO) at pH 6 and 37 °C to an optical density at 600 nm (OD₆₀₀) of around 0.5. 100 μl volumes were added to each well in equal volume to the chitosan solution, yielding a bacterial test concentration of approximately 10^5 cells/ml. The microplates were incubated at 37 °C for 20 ± 1 h and minimum inhibition concentration (MIC) was read as the lowest concentration of chitosan inhibiting visible bacterial growth. Minimum bactericidal concentration (MBC) assays were performed by plating 100 μl aliquots from the

wells onto blood agar plates and incubating at 37 °C for 20 h. The MBC was defined as the lowest concentration reducing the inoculum by $\geq 99.9\%$ after 20 ± 1 h.

References:

- (1) Jonker, C.; Hamman, J. H.; Kotzé, A. F. *Int. J. of Pharmaceutics* **2002**, 238, 205.
- (2) Guo, Z.; Xing, R.; Liu, S.; Zhong, Z.; Ji, X.; Wang, L.; Li, P. *Carbohydr. Res.* **2007**, 342, 1329.
- (3) Jia, Z.; Shen, D.; Xu, W. *Carbohydr. Res.* **2001**, 333, 1.
- (4) Guo, Z.; Liu, H.; Chen, X.; Ji, X.; Li, P. *Bioorganic & Medicinal Chemistry Letters* **2006**, 16, 6348.
- (5) Seong, H.-S.; Whang, H. S.; Ko, S.-W. *Journal of Applied Polymer Science* **2000**, 76, 2009.
- (6) Cho, J.; Justin, G.; Piquette-Miller, M.; Allen, C. *Biomacromolecules* **2006**, 7, 2845.
- (7) Wu, J.; Wei, W.; Wang, L.-Y.; Su, Z.-G.; Ma, G.-H. *Biomaterials* **2007**, 28, 2220.
- (8) Wu, J.; Su, Z.-G.; Ma, G.-H. *Int. J. Pharmaceutics* **2006**, 315, 1.
- (9) Shi, X.-W.; Du, Y.-M.; Li, J.; L., S. X.-.; Yang, J.-H. *J. Microencapsulation* **2006**, 23, 405.
- (10) Li, H.; Yumin, D.; Wu, X.; Zhan, H. *Colloids Surf., A: Physicochem. Eng. Aspects* **2004**, 242, 1.
- (11) Lim, S.-H.; Hudson, S. M. *Carbohydrate Research* **2004**, 339, 313.
- (12) Cui, D.; Szarpak, A.; Pignot-Paintrand, I.; Annabell, V.; Boudou, T.; Determbleur, C.; Jérôme, C.; Picart, C.; Auzély-Velty, R. *Advanced functional materials* **2010**, 20, 3303.
- (13) Lim, S.-H.; Hudson, S. M. *Carbohydrate Research* **2004**, 339, 313.
- (14) Andrieux, K.; Lesieur, P.; Lesieur, S.; Ollivon, M.; Cécile, G.-M. *Analytical chemistry* **2002**, 74, 5217.
- (15) Armstrong, J. K.; Wenby, R. B.; H.J., M.; T.C., F. *Biophysical Journal* **2004**, 87, 4259.
- (16) Fowlkes, J. D.; Hullander, E. D.; Fletcher, B. L.; Retterer, S. T.; Melechko, A. V.; Hensley, D. K.; Simpson, M. L.; Doktycz, M. Z. *Nanotechnology* **2006**, 17, 5659.
- (17) Berth, G.; Voigt, A.; Dautzenberg, H.; Donath, E.; Möhwald, H. *Biomacromolecules* **2003**, 3, 579.
- (18) Szapark, A. *Thesis* **2009**.
- (19) Vold, I. M. N.; Kristiansen, K. A.; Christensen, B. E. *Biomacromolecules* **2006**, 7, 2136.

Chapter 3

Hydrophobic shell loading of biopolyelectrolyte capsules

Table of contents

3	Résumé (<i>Fr</i>)	115
3.1	Submitted article to Advanced Materials (accepted)	117
3.2	Supporting information	128
3.3	Complementary results.....	131
3.3.1	Factors affecting the feasibility of capsule formation	131
3.3.2	Permeability of capsules.....	135
3.3.3	Antibacterial activity of capsules	136
	References:	138

3 Résumé (Fr)

Ce chapitre décrit la synthèse de capsules constituées uniquement de polysaccharides, capables d'incorporer sélectivement dans leur paroi de petites molécules hydrophobes. La paroi des capsules est formée d'un film multicouche comportant des nanocavités hydrophobes, qui se forment grâce à l'appariement de dérivés alkylés d'acide hyaluronique (HAC10) et de dérivés du chitosane quaternisés. Leur auto-assemblage est réalisé très simplement en milieu aqueux selon la technique de dépôt couche-par-couche en utilisant des particules de CaCO_3 comme support colloïdal biocompatible et biodégradable. Ce support est ensuite dissous dans des conditions douces pour conduire à la formation de capsules. Il a été constaté que la stabilité des capsules est fortement affectée par la masse molaire et le degré de substitution (DS) des polysaccharides modifiés. Des capsules stables sont ainsi obtenues à partir de HAC10 ayant un masse molaire $M_w \sim 200\ 000\text{g/mol}$ et un DS de 0,2, et de chitosane quaternisé (*N,O*-QCHI) de DS relativement élevé (DS ~ 1.1 -1.3).

Ces polysaccharides modifiés possèdent une forte affinité pour les molécules hydrophobes, avec lesquels ils peuvent être pré-complexés. Une sonde fluorescente, le Nile Red (NR), peut ainsi être piégée de façon sélective dans la paroi des capsules.

La propriété semi-perméable de capsules (HAC10/*N,O*-QCHI)₅, mise en évidence avec du dextrane^{FITC}, suggère en outre la possibilité d'encapsuler également des macromolécules hydrophiles dans la cavité aqueuse.

Enfin, compte tenu de l'activité antibactérienne des dérivés QCHI et des capsules à base de HA et des dérivés QCHI (Chapitre 2), l'effet inhibiteur de la croissance bactérienne des capsules à base de HA10C10/*N,O*-QCHI a été étudié. Les capsules (HA20C10/*N,O*-QCHI)₅ montrent une activité antibactérienne plus faible que les capsules (HA/*N,O*-QCHI)₅.

3.1 Submitted article to *Advanced Materials* (accepted)

Hydrophobic shell loading of biopolyelectrolyte capsules

By *Di Cui, Jing Jing, Thomas Boudou, Isabelle Pignot-Paintrand, Stefaan De Koker, Bruno G. De Geest, Catherine Picart,* and Rachel Auzély-Velty**

Keywords: microcapsules • polysaccharides • hydrophobic drugs • layer-by-layer • dendritic cells

Controlled delivery of hydrophilic and hydrophobic drugs is currently a great challenge in the field of nanobiotechnology. Microparticulate drug carriers can shield the drug from degradation, improve its biodistribution and facilitate targeted delivery. The problem of delivery is especially crucial for water-insoluble organic compounds, which constitute a great part of the currently available drugs, whether anti-inflammatory, anti-cancer.^[1] In the field of vaccine delivery also, there is an increased interest in the use of hydrophobic immune modulating compounds. Besides the well known lipid-based carriers such as liposomes,^[2] the development of nanoparticles^[3] and emulsion-based nanocapsules^[4] has gathered increased interest in the pharmaceutical field and layer-by-layer-based hollow microcapsules are emerging as a novel potential therapeutic tool^[5]. These LbL-based hollow capsules, also called polyelectrolyte multilayer capsules consist of two distinct compartments: the multilayer shell and the cavity. The shell is assembled through consecutive adsorption of oppositely charged species onto a spherical sacrificial template. It can consist of various types of polymers, but these have to sustain the core removal step. Recent developments of polyelectrolyte microcapsules in life sciences include the use of polypeptides and polysaccharides as shell components,^[6] as these are biocompatible and biodegradable but these require the core to be removed in mild conditions^[7]. The cavity, which is obtained after dissolution of the core material, represents the aqueous part of the capsules in which a range of materials can be encapsulated, including peptides,^[8] proteins^[9] or nucleic acids^[10]. These compounds can be loaded by means of different strategies (“post-loading” and “pre-loading”) and released upon well-defined stimuli, including changes in pH, ionic strength or temperature, as well as light irradiation or enzymatic degradation.^[5a, 5c] While these are promising steps towards the development of next-generation carriers of active biomacromolecules, developing a robust method to prepare capsules that can selectively encapsulate and subsequently deliver poorly water-soluble drugs still represents a challenge. Indeed, the structure of LbL capsules consisting of an aqueous cavity surrounded by a

hydrophilic multilayer shell poses difficulties to incorporate hydrophobic drug molecules. To date, four main strategies have been proposed for loading water-insoluble compounds into LbL capsules. The first method consists of filling the cavity of pre-formed hollow capsules with an oil phase containing the drug.^[11] The second approach is to solubilize the hydrophobic drug in the core of sodium dodecyl sulfate (SDS) or polymeric micelles, which are then assembled layer-by-layer onto a sacrificial template.^[12] The third technique is to embed liposomes within the multilayer capsule, resulting in hybrid carrier capsosomes^[13]. Finally, mesoporous silica templates loaded with hydrophobic drugs were used as decomposable template.^[14] However, these methods have limitations associated with the necessity of an oil phase,^[11] the problem related to stability and/or cytotoxicity of micelles,^[12] or very harsh buffers (hydrofluoric acid and ammonium fluoride) conditions for core removal in the case of silica templates^[14].

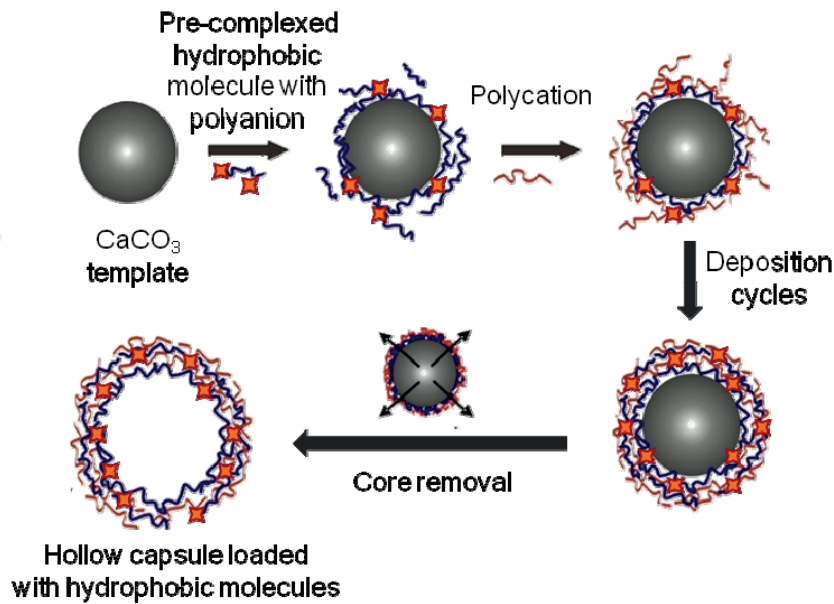
In the present work, we describe an original and versatile approach to selectively encapsulate a water-insoluble molecule in the nanoshell of multilayered microcapsules. The microcapsules are prepared under mild conditions and consist exclusively of polysaccharides, using hyaluronic acid (HA) and a chitosan (CHI) derivative that water-soluble at physiological pH as components of the nanoshell. We further show that hydrophobic molecules can be delivered intracellularly in dendritic cells. Our approach relies on the very high affinity of hydrophobic molecules for alkylated hyaluronic acid.^[15] We recently demonstrated that this chemically modified HA is able to assemble in layer-by-layer films with the polypeptide poly(L-lysine) as polycation.^[15] Furthermore, these films specifically incorporated hydrophobic molecules within hydrophobic nanodomains formed by the alkyl chains grafted onto the HA backbone. Here, the keys to our strategy is (**Fig. 1A**): i) the specific and stable entrapment of hydrophobic molecules within the LbL film by pre-complexation of hydrophobic molecules with the chemically modified HA and ii) the ability of the hydrophobic nanoshell to form a stable hollow microcapsule after core decomposition in mild conditions and to retain selectively the hydrophobic molecule in the nanoshell.

The unique physico-chemical and biological properties of chitosan^[16] and hyaluronic acid^[17] used for multilayer film construction, and the close control over drug loading by pre-complexation of hydrophobic molecules with alkylated HA makes these capsules versatile candidates as drug delivery vehicle. To our knowledge, this is the first report utilizing biocompatible natural polyelectrolytes to design LbL capsules as carriers for hydrophobic drugs.

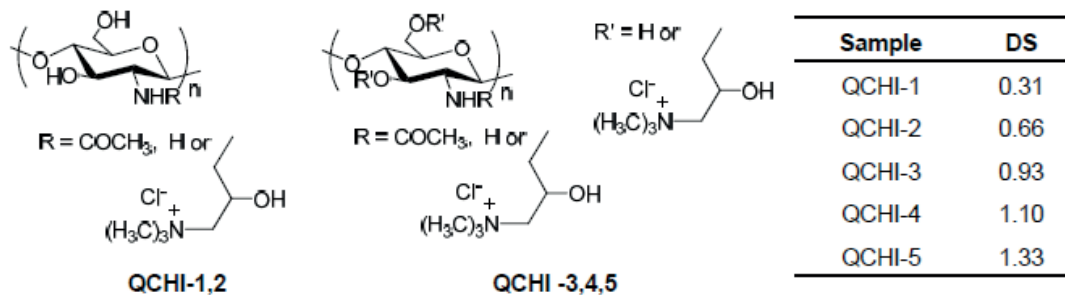
To circumvent the inherent drawback of CHI (low solubility in physiological conditions due to its pK_a at 6), which hinders the film build-up at neutral pH as well as causing problems for subsequent core dissolution, we synthesized soluble quaternized chitosan (QCHI) derivatives. The quaternary ammonium groups were grafted onto chitosan based on its reaction with glycidyltrimethylammonium chloride (GTMAC) under acidic^[18] or neutral^[19] conditions leading to derivatives having degrees of substitution (DS, number of mole of substituent, i.e. quaternary ammonium group, per mole of repeating unit) over a large range, from 0.31 to 1.33 (**Fig. 1B**). Under acidic conditions, chitosan was selectively modified through the primary amine group. The DS of the resulting QCHI varied between 0.31 to 0.66. The QCHI derivatives having higher DS were synthesized under neutral conditions, also substituting some hydroxyl groups in addition to the amine group, which allowed to obtain a DS higher than 1. Decylamino hydrazide derivatives of HA (HAxC10) ($x = 100 \times DS$ with DS = 0.10 or 0.20) were used as polyanionic partners (**Fig. 1C**) due to their high affinity for hydrophobic molecules.^[15] These derivatives will be called hereafter alkylated HA.

In a first step, we tested the ability of the different quaternized CHI and alkylated HA self-assemblies to entrap the poorly soluble dye Nile Red (NR)^[20] and to reveal the presence of hydrophobic nanodomains. To this end, NR was pre-complexed with the alkylated HA derivatives and the fluorescence of the (QCHI/HAxC10) films was followed step-by-step (**Fig. 2**). The effective assembly of the polysaccharide derivatives in multilayer films was also confirmed by following their sequential deposition on a planar solid substrate by quartz crystal microbalance with dissipation monitoring (QCM-D) (**Fig. SI 1**). Films with the highest substitution degree (DS 1.3) exhibited the largest frequency shifts and slightly higher dissipation values. Thus, films with high DS are slightly more viscoelastic. As can be seen in **Fig. 2**, the fluorescence of the films containing the HA20C10 derivative (having a DS of 0.20) appeared systematically much higher than that of HA10C10 (having a DS of 0.10), suggesting that the former HA derivative incorporate much more NR. Note that the DS of QCHI had also an impact, although of lesser extent, on the incorporation of NR. We found that NR incorporation increased with the DS of QCHI with the fluorescence signal being maximal for the DS of 1.1 and 1.3. This effect was particularly visible for the QCHI derivatives assembled with HA20C10. It might be attributed to the presence of methyl groups of the QCHI quaternary ammonium moieties, which may contribute to loose hydrophobic interactions with HAxC10. Importantly, these data show that the NR content can be tuned in a very simple manner by varying the type of QCHI and HA derivatives as well as the number of deposited layers.

A)



B) Quaternized Chitosan derivatives



C) Alkylated (C10) derivatives of hyaluronic acid

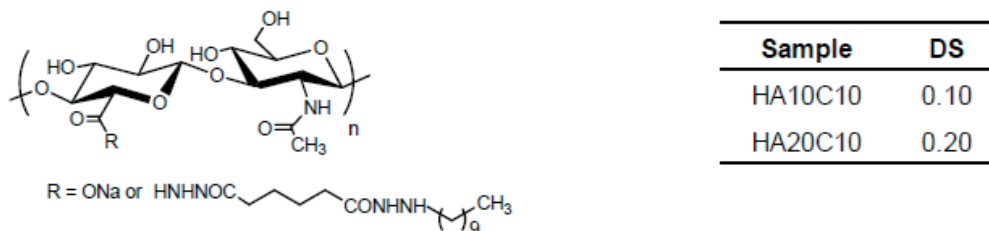


Figure 1. Design strategy of the microcapsules with hydrophobic nanoshells and chemically modified polysaccharides. A) CaCO₃ microparticles are coated with alternating layers consisting, as polyanion, of a pre-complexed hydrophobic molecule (orange) with hydrophobically modified HA (blue) and as polycation, of quaternized chitosan (brown). After dissolution of the CaCO₃ core by EDTA, hollow capsules containing the hydrophobic molecules in the nanoshell are obtained, the hydrophobic molecule being specifically trapped in the nanoshell. B) Chemical structure of the quaternized chitosan derivatives used in this study, with a DS over a large range from 0.31 to 1.33. C) Chemical structure of the hydrophobically modified HA with a decylaminohydrazide (C10) chain (alkylated HA). Two DS of 0.10 and 0.20 have been selected.

In a second step, we investigated the possibility to form hollow microcapsules with the different QCHI and HA_xC10 derivatives. To this end, the LbL films were deposited on calcium carbonate microparticles as the sacrificial core template to prepare capsules [21]. These microparticles can be easily dissolved under mild conditions by treatment with an aqueous solution of ethylenediaminetetraacetic acid (EDTA)^[7]. In a previous work, we successfully applied this method to prepare HA-based polyelectrolyte capsules with native unmodified HA.^[7]

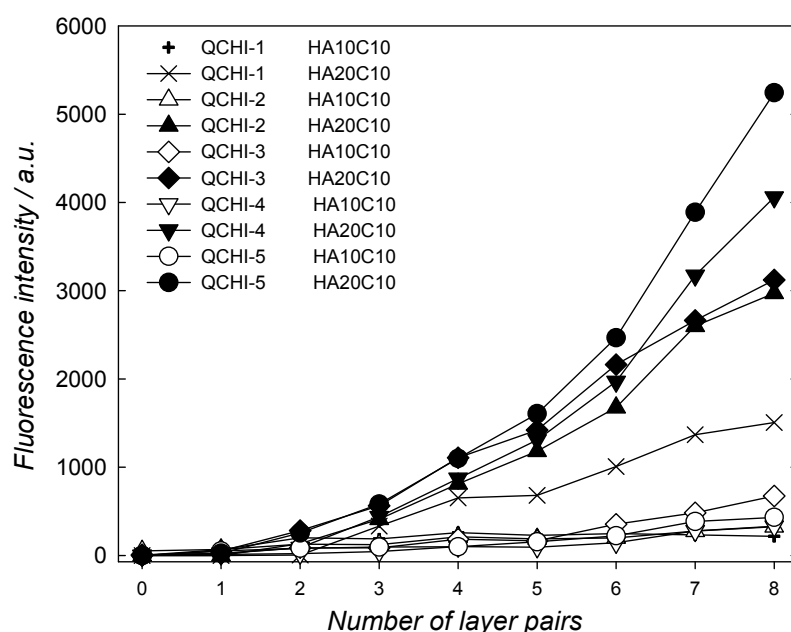


Figure 2. Nile red incorporation in planar (QCHI/HA_xC10) films. Fluorescence intensity of Nile Red incorporated in (QCHI/HA10C10) and (QCHI/HA20C10) planar films for the 5 different QCHI samples of increasing DS (derivatives shown in **Fig. 1B and 1C**), as a function of the number of deposited layer pairs.

We noted that the HA10C10 derivative revealed to be inefficient to produce stable capsules after core removal. In contrary, with the HA20C10 derivative, we successfully obtained capsules, with however some differences in the yield (intact vs broken capsules) depending on the DS of QCHI. SEM observations evidenced that capsules prepared from QCHI with a low DS (0.31-0.66) were isolated in much lower amounts (**Fig. 3A**) compared to those containing the QCHI derivatives of DS close or higher than 1 (**Fig. 3B**). Note that the capsules made from QCHI-4 of DS 1.10 exhibited a very smooth surface. This was indeed confirmed by AFM observations, which enabled us to estimate the nanoshell thickness (~ 110 nm) with a roughness R_a of ~5 nm (**Fig. SI 2**). Observations of the NR containing capsules

made of five (HA20C10/QCHI-4) layer pairs in PBS solution by CLSM confirmed their spherical shape with a size of $5.0 \pm 0.4 \mu\text{m}$ and highly homogeneous red capsule shells (**Fig. 3C**). Importantly, the intensity profile along a diameter confirmed the selective incorporation of NR in the hydrophobic shell, with no trace of NR in the core of the capsule (**Fig. 3D**), as well as its impressive stability after core removal.

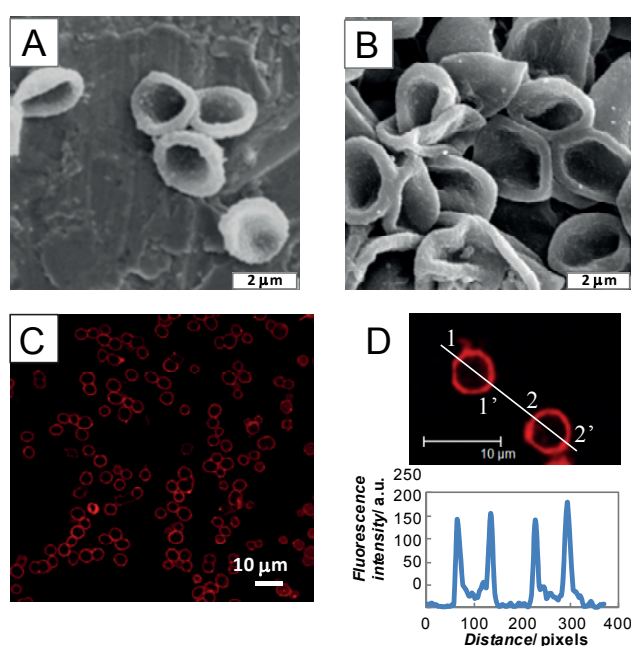


Figure 3. Microscopic observations of the microcapsules with hydrophobic nanoshells. SEM observations of the dried hollow microcapsules made of 5 layer pairs with QCHI of different DS: (A) QCHI-2 (B) QCHI-4). C) Confocal microscopy images of (HA20C10/QCHI-4)₅ microcapsules exhibiting a highly localized red fluorescence in their nanoshell due to the specific entrapment of Nile Red molecules in hydrophobic nanodomains. D) Magnified image of two microcapsules and corresponding fluorescence intensity profiles along their diameter, confirming the selectivity of NR incorporation in the nanoshell.

To quantify the effective loading of NR in the hydrophobic nanoshell, we measured the amount of NR effectively loaded by UV spectrometry after NR extraction from the capsules with ethanol. Using a calibration curve for NR in ethanol (**Fig. SI 3**), we deduced a mean NR mass per capsule of $0.17 \pm 0.06 \text{ pg}$. A simple calculation of the “effective concentration” of NR in the nanoshell can be deduced, knowing the capsule (diameter $\sim 5 \mu\text{m}$) and the shell thickness ($\sim 110 \text{ nm}$). We found an effective concentration of $\sim 64 \text{ mM}$, which represents a ~ 6400 fold increase in NR concentration upon loading in the shell as compared to its initial “feeding” concentration of $10 \mu\text{M}$. Thus, the capsules with hydrophobic nanoshell constitute a

powerful tool to locally deliver a high concentration of drug. Note that we also found that NR in the nanoshell is very stable after several days in PBS without any burst release (**Fig. SI 4**).

Finally, to serve as drug carrier we evaluated whether these hydrophobic nanoshells could be internalized by phagocytic cells. Therefore, we incubated the capsules *in vitro* with dendritic cells. Dendritic cells are professional antigen presenting cells and are the primary target for vaccine delivery. Moreover, several poorly water soluble molecules have been reported to act as immunomodulator, which allows one to steer the type of immune response towards humoral and/or cellular immunity as well as antibody isotype switching. **Fig. 4** shows a confocal microscopy image of dendritic cells (DC) that internalized the hydrophobic nanoshells. These images show that polysaccharide-based LbL, which are normally used to deliver hydrophilic macromolecules (such as proteins), can also be employed to deliver intracellularly hydrophobic compounds.

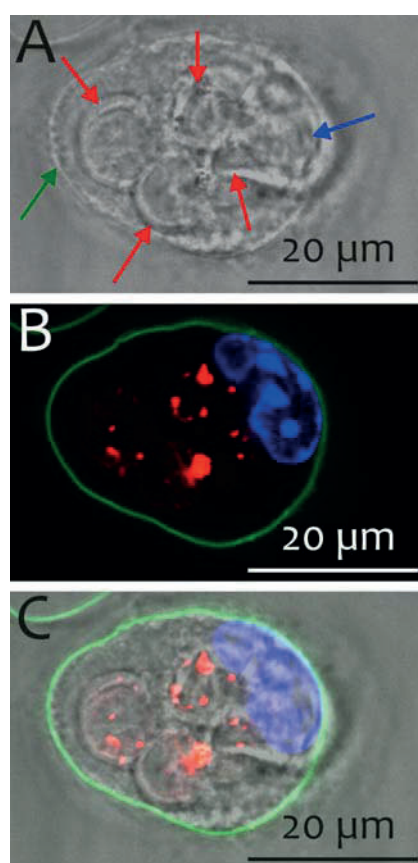


Figure 4. Confocal microscopy images of a dendritic cell that has internalized hydrophobic nanoshells. The cell membrane was stained with alexa488 conjugated cholera toxin subunit B (green fluorescence) and cell nuclei were stained with HOECHST (blue fluorescence). The (A) image shows the DIC channel – a green arrow indicates the cell membrane, red arrows indicate internalized nanoshells and the blue arrow indicates the cell nucleus. The (B) image shows the overlay of the blue, green and red channel and the (C) image shows the overlay of the blue, green, red and DIC channel.

In conclusion, a versatile method based on the encapsulation of small hydrophobic molecules in the nanoshell of polysaccharide-based microcapsules is reported. This relied on the layer-by-layer assembly in mild aqueous conditions at physiological pH of chemically modified natural polysaccharides. Microcapsule formation in aqueous conditions was successful and highly efficient for the films made of the most highly substituted polysaccharides samples (i.e. QCHI_{DS >1} and HA20C10). Furthermore, these hydrophobic nanofilms and nanoshells exhibited the highest trapping capacity for hydrophobic model drug NR, as probed by its fluorescence. Notably, the microcapsules with hydrophobic shell specifically trapped NR in their nanoshell. In addition, they exhibited a very high stability in a physiological medium. Given the versatility of the LbL assembly to produce nanoshells and the durability of drug entrapment, these hydrophobic polysaccharide nanoshells open new avenues for applications in nanomedicine, as hydrophobic drug-carrier systems as well as coatings of medical devices or implantable biomaterials. Our future studies will aim to further exploit the properties of such powerful microcapsules for the simultaneous multi-delivery of several types of hydrophilic and hydrophobic drugs. Moreover, taking advantage of the recently reported spaying approach^[22] for the fabrication of polyelectrolyte microspheres which mimic the composition and properties of multilayered capsules, we also plan in the future to apply this single-step all aqueous methodology to prepare capsules from alkylated HA with high encapsulation efficiency.

Experimental

Materials: Chitosan Protasan with a degree of *N*-acetylation (DA) of 0.09 and a molar mass of M_w of 372000 g mol⁻¹ was kindly provided by FMC BioPolymer AS, Novamatrix (Norway). Hyaluronic acid under the sodium salt form, having a molar mass of M_w of 200000 g mol⁻¹, was purchased from MEDIPOL Distribution. GTMAC, EDTA, calcium chloride (CaCl₂), sodium carbonate (Na₂CO₃), acetic acid (AcOH), sodium chloride (NaCl), phosphate buffer saline (PBS) and, all other chemicals were purchased from Sigma-Aldrich-Fluka. The water used in all experiments was purified by a Millipore Milli-Q Plus purification system, with a resistivity of 18.2 MΩ cm. The quaternized derivatives of chitosan were prepared by reacting chitosan with glycidyltrimethylammonium chloride (GTMAC) under aqueous acidic or neutral conditions according to procedures previously reported^[18-19]. The decylamino hydrazide derivatives of hyaluronic acid (HAxC10) were synthesized as previously described^[15].

Polysaccharide capsules preparation and quantification of NR incorporated in capsules: Microcapsules were prepared using calcium carbonate particles as a sacrificial template. CaCO_3 particles were synthesized from solutions of CaCl_2 and Na_2CO_3 as reported in the literature [21, 23]. HAxC10 derivatives were pre-complexed with NR by adding few μL of a NR stock solution (1 mg mL^{-1} or 3.1 mM in ethanol) in the HAxC10 solutions at 1 g L^{-1} in order to have a final NR concentration of $10 \mu\text{M}$. The CaCO_3 particles were coated layer-by-layer by incubating them at a concentration 2% (w/v)^[24] in solutions of QCHI (C_p at 2 g L^{-1}) and HAxC10/NR (C_p at 1 g L^{-1}), both in 0.15 M NaCl (pH 6.5). After shaking for 10 min, the particles were collected by centrifugation and the residual non-adsorbed polyelectrolyte was removed by washing twice with 0.01 M NaCl (pH 6.5). After the desired number of layers was deposited, the CaCO_3 core was removed by treatment with an aqueous solution of EDTA (0.1 M , pH 7.2). To avoid mechanical damages of “soft” polyelectrolyte shells, the dissolved ions resulting from the decomposition of CaCO_3 were removed by dialysis against pure water, using spectra Por dialysis bags with a molecular weight cut off of 3.5 kDa .

Film characterization by microfluorimetry and measurement of NR absorbance: For the measurement of NR incorporation by pre-complexation, (QCHI/alkylated HA)₈ films were directly fabricated into 96-well plates (3 wells per condition). Alkylated HA derivatives were pre-complexed with NR by adding few μL of a NR stock solution (1 mg mL^{-1} or 3.1 mM in ethanol) in the HA solutions at 2 g L^{-1} in order to have a final NR concentration of $10 \mu\text{M}$. Briefly, $50 \mu\text{L}$ of QCHI (2 g/L in PBS) were introduced into each well and let adsorbed for 8 min. Wells were then washed twice with the rinsing solution and $50 \mu\text{L}$ of alkylated HA (2 g L^{-1} in PBS) were introduced in each well, let adsorbed for 8 min and subsequently rinsed. The process was repeated until the desired number of layer was reached. The fluorescence of the plates was directly measured after each HA-NR deposition step (after the rinsing step) using a fluorescence microplate reader (Infinite 1000, Tecan, Austria) with excitation and emission wavelengths set at $590 \pm 5 \text{ nm}$ and $650 \pm 5 \text{ nm}$ respectively. To estimate the absolute NR concentration, we realized a calibration curve for the absorbance of NR in ethanol, measured at 590 ± 2.5 as a function of NR concentration.

Nile extraction from capsules and quantification. The amount of NR incorporated in the capsules was determined by fluorescence intensity measurements after extraction of NR from capsules with ethanol according to the following procedure. The suspension of capsules ($200 \mu\text{L}$) in PBS was centrifugated (4000 rpm , 4 min , $20 \text{ }^\circ\text{C}$) and the supernatant was removed.

After addition of ethanol (0.5 mL), the suspension was again centrifugated (4000 rpm, 4 min, 20 °C) and the supernatant containing NR was recovered. This process was repeated two times to ensure a full extraction of NR from the microcapsules. The solutions were then pulled and analyzed using the fluorescence microplate reader (see above). The total concentration of NR in solution was determined using a calibration curve established from solutions of NR in EtOH at increasing concentrations (**Fig. SI 3**). The concentration of NR per capsule was then derived knowing the NR concentration in solution and the number of capsules per mL of suspension, which was determined using a Petroff-Hausser counting chamber. Two independent measurements have been performed for each capsule batch, on three different batches.

DC uptake experiments: DCs were generated from mouse bone marrow as earlier reported^[9a] and seeded in Lab-Tek (Nunc, Thermo Scientific) 8 chambered coverglasses. 10 µl capsule suspension was added to the DCs. After 2h incubation, the cells were fixed in an aqueous 4 % formaldehyde solution overnight. Subsequently the cells were washed 3 times with PBS and stained with Cy5 conjugated cholera toxin subunit B (5 µg mL⁻¹) and HOECHST 33258 (2 µg mL⁻¹).

Supporting information

Supporting Information is available online from Wiley InterScience or from the author.

Acknowledgements

The authors thank Judith Mähner for technical help with the fluorescence measurements. This work was financially supported by the “Agence Nationale pour la Recherche” (grant ANR-07-NANO-002 to RAV and CP). D.C. gratefully acknowledges the MESR for a PhD fellowship. RAV and C.P. are indebted to the Institut Universitaire de France for financial support.

- [1] a)A. Agarwal, Y. Lvov, R. Sawant, V. Torchilin, *J. Controlled Release* **2008**, *128*, 255; b)R. C. Smith, M. Riollano, A. Leung, P. T. Hammond, *Angew. Chem., Int. Ed.* **2009**, *48*, 8974.
- [2] B. Haley, E. Frenkel, *Urol. Oncol. Semin. Orig. Invest.* **2008**, *26*, 57.
- [3] a)A. Kumari, S. K. Yadav, S. C. Yadav, *Colloids Surf., B* **2010**, *75*, 1; b)K. S. Soppimath, T. M. Aminabhavi, A. R. Kulkarni, W. E. Rudzinski, *J. Controlled Release* **2001**, *70*, 1.

- [4] a)N. T. Huynh, C. Passirani, P. Saulnier, J. P. Benoit, *Int. J. Pharm.* **2009**, *379*, 201; b)C. E. Mora-Huertas, H. Fessi, A. Elaissari, *Int. J. Pharm.* **2010**, *385*, 113.
- [5] a)L. L. del Mercato, P. Rivera-Gil, A. Z. Abbasi, M. Ochs, C. Ganas, I. Zins, C. Soennichsen, W. J. Parak, *Nanoscale* **2010**, *2*, 458; b)A. N. Zelikin, *ACS Nano* **2010**, *4*, 2494; c)L. J. De Cock, S. De Koker, B. G. De Geest, J. Grooten, C. Vervaet, J. P. Remon, G. B. Sukhorukov, M. N. Antipina, *Angew. Chem., Int. Ed.* **2010**, *49*, 6254.
- [6] B. G. De Geest, S. De Koker, G. B. Sukhorukov, O. Kreft, W. J. Parak, A. G. Skirtach, J. Demeester, S. C. De Smedt, W. E. Hennink, *Soft Matter* **2009**, *5*, 282.
- [7] A. Szarpak, I. Pignot-Paintrand, C. Nicolas, C. Picart, R. Auzély-Velty, *Langmuir* **2008**, *24*, 9767.
- [8] a)S.-F. Chong, A. Sexton, R. De Rose, J. Kent Stephen, N. Zelikin Alexander, F. Caruso, *Biomaterials* **2009**, *30*, 5178; b)R. De Rose, A. N. Zelikin, A. P. R. Johnston, A. Sexton, S.-F. Chong, C. Cortez, W. Mulholland, F. Caruso, S. J. Kent, *Adv. Mater.* **2008**, *20*, 4698.
- [9] a)S. De Koker, B. G. De Geest, S. K. Singh, R. De Rycke, T. Naessens, Y. Van Kooyk, J. Demeester, S. C. De Smedt, J. Grooten, *Angew. Chem., Int. Ed.* **2009**, *48*, 8485; b)P. Rivera-Gil, S. De Koker, B. G. De Geest, W. J. Parak, *Nano Lett.* **2009**, *9*, 4398.
- [10] a)U. Reibetanz, C. Claus, E. Typlt, J. Hofmann, E. Donath, *Macromol. Biosci.* **2006**, *6*, 153; b)C. Schuler, F. Caruso, *Biomacromolecules* **2001**, *2*, 921; c)D. G. Shchukin, A. A. Patel, G. B. Sukhorukov, Y. M. Lvov, *J. Am. Chem. Soc.* **2004**, *126*, 3374.
- [11] S. Sivakumar, V. Bansal, C. Cortez, S.-F. Chong, A. N. Zelikin, F. Caruso, *Adv. Mater.* **2009**, *21*, 1820.
- [12] a)U. Manna, S. Patil, *J. Phys. Chem. B* **2008**, *112*, 13258; b)Y. Zhu, W. Tong, C. Gao, H. Möhwald, *Langmuir* **2008**, *24*, 7810.
- [13] L. Hosta-Rigau, B. Stadler, Y. Yan, E. Collins Nice, J. K. Heath, F. Albericio, F. Caruso, *Adv. Funct. Mater.* **2010**, *20*, 59.
- [14] Y. Wang, Y. Yan, J. Cui, L. Hosta-Rigau, J. K. Heath, E. C. Nice, F. Caruso, *Adv. Mater.* **2010**, *22*, 4293.
- [15] S. Kadi, D. Cui, E. Bayma, T. Boudou, C. Nicolas, K. Glinel, C. Picart, R. Auzély-Velty, *Biomacromolecules* **2009**, *10*, 2875.
- [16] R. A. A. Muzzarelli, C. Muzzarelli, *Adv. Polym. Sci.* **2005**, *186*, 151.
- [17] G. D. Prestwich, J.-w. Kuo, *Curr. Pharm. Biotechnol.* **2008**, *9*, 242.
- [18] a)J. Cho, J. Grant, M. Piquette-Miller, C. Allen, *Biomacromolecules* **2006**, *7*, 2845; b)D. Cui, A. Szarpak, I. Pignot-Paintrand, A. Varrot, T. Boudou, C. Detrembleur, C. Jerome, C. Picart, R. Auzély-Velty, *Adv. Funct. Mater.* **2010**, *20*, 3303.
- [19] a)S.-H. Lim, S. M. Hudson, *Carbohydr. Res.* **2004**, *339*, 313; b)H.-S. Seong, H. S. Whang, S.-W. Ko, *J. Appl. Polym. Sci.* **2000**, *76*, 2009.
- [20] A. Guyomard, B. Nysten, G. Muller, K. Glinel, *Langmuir* **2006**, *22*, 2281.
- [21] D. V. Volodkin, A. I. Petrov, M. Prevot, G. B. Sukhorukov, *Langmuir* **2004**, *20*, 3398.
- [22] M. Dierendonck, S. De Koker, C. Cuvelier, J. Grooten, C. Vervaet, J.-P. Remon, B. G. De Geest, *Angew. Chem., Int. Ed.* **2010**, *49*, 8620.
- [23] A. A. Antipov, D. Shchukin, Y. Fedutik, A. I. Petrov, G. B. Sukhorukov, H. Möhwald, *Colloids Surf., A* **2003**, *224*, 175.
- [24] A. I. Petrov, D. V. Volodkin, G. B. Sukhorukov, *Biotechnol. Progress* **2005**, *21*, 918.

Received: ((will be filled in by the editorial staff))

Revised: ((will be filled in by the editorial staff))

Published online: ((will be filled in by the editorial staff))

3.2 Supporting information

Films characterization by quartz crystal microbalance with dissipation monitoring. The (QCHI/HA20C10)_i film buildup (where *i* denotes the number of layer pairs) was followed by *in situ* quartz crystal microbalance (QCM with dissipation monitoring, D300, Qsense, Sweden). The gold-coated quartz crystal was excited at its fundamental frequency (about 5 MHz, $\nu = 1$) as well as at the third, fifth and seventh overtones ($\nu = 3, 5$ and 7 corresponding to 15, 25 and 35 MHz, respectively). Changes in the resonance frequencies Δf and in the relaxation of the vibration once the excitation is stopped ΔD were measured at the four frequencies.

Atomic force microscopy. AFM images of the dried microcapsules were carried out in air with a PicoPlus AFM in tapping mode using tetrahedral tips (OMCL-AC240TM-E tip from Olympus) with a resonance frequency of 75 kHz and a spring constant of 2 N m^{-1} . Capsules deposited on a mica substrate were imaged at line rates of 1 Hz. For surface roughness analysis, $1 \times 1 \mu\text{m}^2$ AFM images were obtained and the arithmetic average roughness R_a was calculated according to:

$$R_a = \frac{1}{N_x N_y} \sum_{i=1}^{N_x} \sum_{j=1}^{N_y} |z_{ij} - z_{mean}| \quad (1)$$

where z_{ij} is the height of a given pixel, z_{mean} is the average height of the pixels, and $N_x = N_y = 512$ are the number of pixels in the *x* and *y* directions.

Measurement of NR release from capsules over time. The suspension of capsules (5 mL) in PBS was divided in 5 samples, corresponding to 5 different time periods from 0 to 8 days, noted D0, D2, D4, D6, and D8 respectively). The D0 sample, consisting in 200 μL of capsules suspension freshly prepared, was treated as described in the experimental section to determine the amount of NR incorporated. This process was performed in duplicate in order to confirm the values. The D2, D4, D6 and D8 samples (each consisting of 1 mL of capsules suspension) were introduced in Spectra/Por® dialysis membranes (6-8 kDa cutoff) and the samples were immersed in PBS (200 mL). Each sample was washed four times with PBS (200 mL) during 2 days. For each sample (D2, D4, D6 and D8), 200 μL of capsules suspension were taken up and underwent a treatment similar to the D0 sample for determination of the amount of NR in the capsules. These processes were performed in duplicate. The analysis of NR contained in the capsules as a function of time demonstrates only a minor release of the dye in spite of the

washing steps with PBS, as shown in **Fig. SI 4**. This demonstrates the high stability of the entrapment of the hydrophobic molecule in the nanoshell.

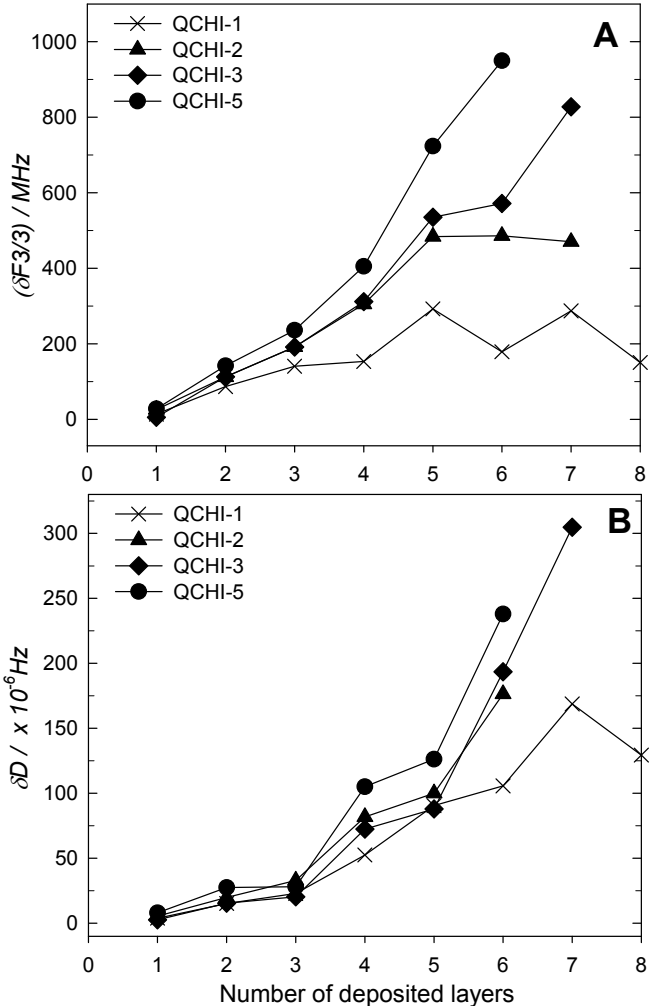


Figure SI 1 : (QCHI/HA20C10) film growth in PBS (pH 7.4) as measured by QCM-D on gold coated crystals. Differences in the QCM frequency shifts (A) and in the dissipation (B) measured at 15 MHz are represented as a function of the number of deposited layers. All QCHI concentrations and HA20C10 were of 2 mg/mL.

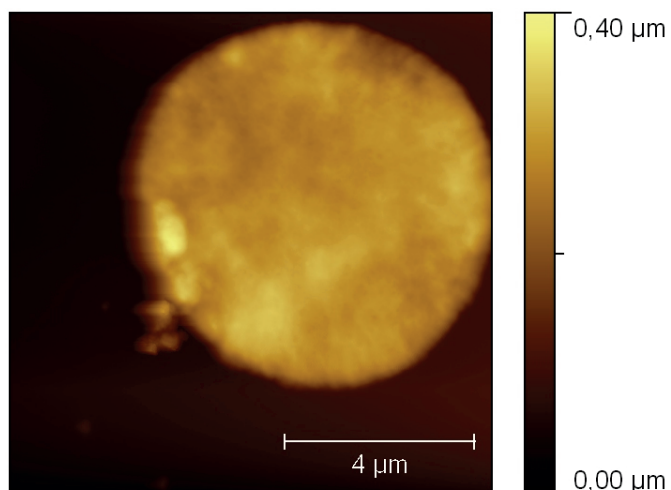


Figure SI 2. AFM topographical image of a microcapsule made of 4.5 layer pairs of (QCHI-4/HA20C10)_{4.5} layers. Image size is $10 \times 10 \mu\text{m}^2$.

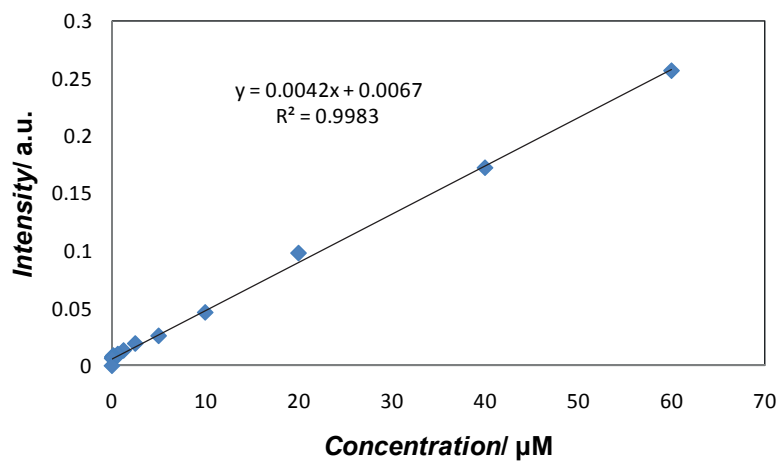


Figure SI 3. Calibration curve for the absorbance of Nile Red in ethanol (measured at 590 nm) as a function of its concentration in solution.

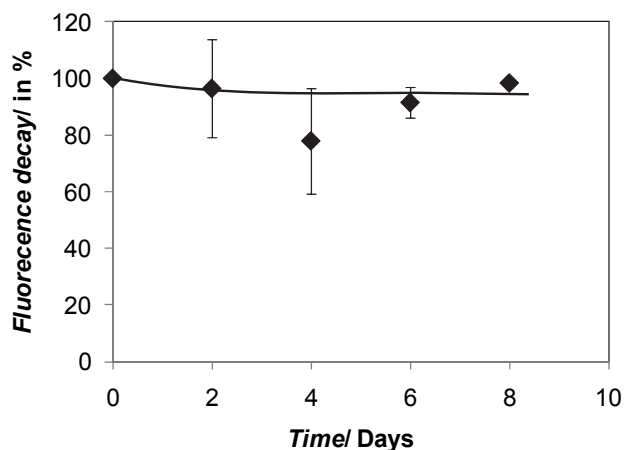


Figure SI 4. Fluorescence intensity measurements of NR intensity remaining in $(\text{HA20C10/QCHI-4})_5$ microcapsules over a 8 day period of immersion in PBS. The minor decrease in fluorecence indicates that the stability of NR in the hydrophobic nanodomains is very high.

3.3 Complementary results

3.3.1 Factors affecting the feasibility of capsule formation

During the synthesis of capsules for the encapsulation of small hydrophobic molecules, we found that the feasibility to construct this kind of capsules was affected by many factors. Herein, we only discuss the influence of the intrinsic properties of materials, such as Mw, viscosity, and DS of decyl-grafted HA derivatives ($\text{HA}_x\text{C10}$), apart from the DS of QCHI derivatives, which have been presented in the submitted article.

In chapter 2, we successfully built contact-killing microcapsules based on HA and QCHI derivatives. HA with a high Mw ($\sim 820\,000$ g/mol) was used for the formation of capsules. Based on this result, we firstly constructed the capsules from HA20C10 with a Mw of $\sim 820\,000$ g/mol and QCHI derivatives. HA20C10 was selected due to the excellent performance of its solution to incorporate the hydrophobic dye nile red (NR) in hydrophobic macrodomains of alkyl chains.¹ However, these derivatives were too viscous to be used in the fabrication of capsules, even at low concentration (1 mg/mL). The CaCO_3 particles incubated in the solution of HA20C10 could not be separated from the suspension by a mild centrifugation process. Thus, we used HA20C10 with a lower Mw ($\sim 200\,000$ g/mol). Whereas capsules based on HA with a Mw of $\sim 200\,000$ g/mol and QCHI derivatives were deformed after the dissolution of cores, it was surprising to see that hollow capsules based on

HA20C10 with a similar Mw exhibited a regular spherical shape and stability upon storage. The successful formation of capsules may be attributed to the higher viscosity of HA20C10 compared to the native HA and the double interactions, hydrophobic and electrostatic interactions, in the multilayer shells.

We also tried to synthesize capsules by using decyl-grafted HA derivatives with lower DS (Mw ~ 200 000 g/mol). By varying the molar ratio of HA/decanal, HA10C10 and HA18C10 were synthesized under the similar reaction conditions to HA20C10 as described by Kadi et al.¹⁻². We used ¹H NMR analysis to determine the DS of these samples by integration of the methyl protons of the decyl chain and anomeric protons of HA (**Figure 3.1**). The DS of these samples derived from ¹H NMR spectrum and corresponding molar ratio of HA/decanal used in the synthesis are presented in **Table 3.1**. Of note, due to the accuracy of ¹H NMR analysis (~ 10 %), the difference in the DS of HA18C10 and HA20C10 is not remarkable.

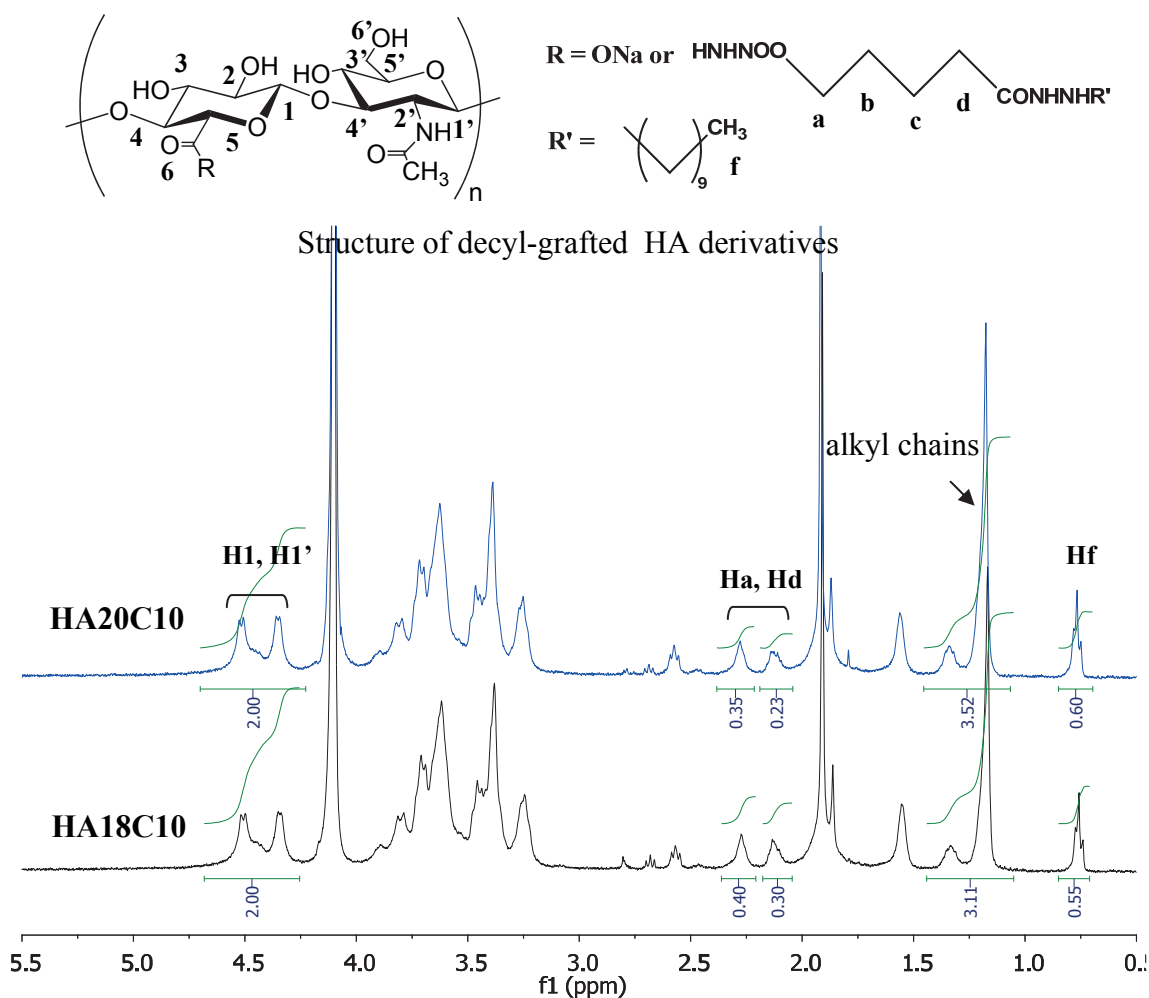


Figure 3.1: Comparison of ¹H spectra of HA18C10 and HA20C10 (400 MHz, D₂O, 80 °C, C_p ~ 6 g/L).

Table 3.1: Decyl-grafted HA derivatives with different DS synthesized by varying the molar ratio of HA/decanal.

Reference	HA/decanal ^a	DS ^b
HA10C10	1/0.16	0.1 ± 0.01
HA18C10	1/0.30	0.18 ± 0.018
HA20C20	1/0.34	0.2 ± 0.02

^a molar ratio and ^b determined by ¹H NMR analysis

Thus, to compare the macromolecular properties of HA18C10 and HA20C20, we performed rheological experiments from their solutions in PBS at a concentration of 10 g/L, corresponding to the semidilute regime of the parent HA (Ref). The dynamic rheological analysis demonstrated that these solutions behave like a highly elastic physical gel ($G' > G''$), over the entire range of frequencies covered (**Figure 3.2**). In addition, the G' and G'' values of the HA20C10 solution are much higher than those of the HA18C10 solution, although the DS of these two samples derived from ¹H NMR study are nearly similar. This result is consistent with that obtained by Kadi et al., who observed higher values of the G' and G'' for the HAxC10 derivatives with higher DS.¹ The higher values of the modulus G' and the formation of a physical hydrogel are due to the formation of hydrophobic domains of decyl chains playing the role of physical junctions.

The morphology of capsules based on *N,O*-QCHI3a and HAxC10 with different DS (HA10C10, HA18C20 and HA20C20) were observed in the dried state by SEM and in solution by CLSM, respectively (**Figure 3.3**). To visualize the capsules in solution by CLSM, NR was entrapped in the shell of capsules. As can be seen from the images, the capsules made of *N,O*-QCHI3a and HA20C10 show a spherical morphology, while the capsules containing HA18C10 were partly damaged and those containing HA10C10 were completely destructed. This result underlines the importance of alkyl chains in the capsules formation. A little decrease of the DS of HAxC10 derivatives has the risk to induce the damage of capsules.

Therefore, to ensure the successful construction of this kind of capsules, it was necessary to carefully analyze the physicochemical properties of decyl-grafted HA derivatives by different techniques. Rheometry was found to be particularly useful to interpret our experimental results.

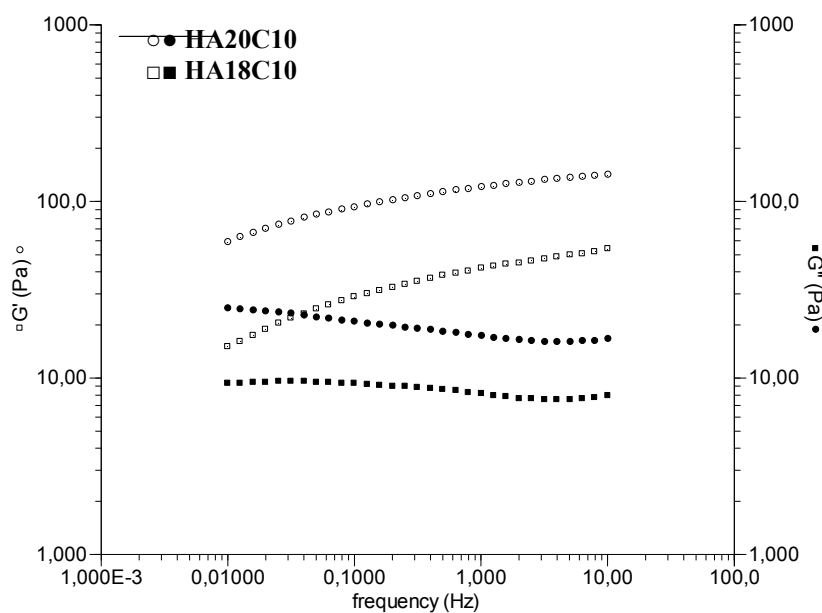


Figure 3.2: Comparison of the storage and loss moduli as a function of frequency for the solutions of HA18C10 and HA20C10 (10 g/L in PBS at 25 °C).

	(HA10C10/N,O-QCHI3a) ₅ capsules	(HA18C10/N,O-QCHI3a) ₅ capsules	(HA20C10/N,O-QCHI3a) ₅ capsules
SEM			
CLSM			

Figure 3.3: SEM and CLSM images of capsules based on *N,O*-QCHI3a and decyl-grafted HA derivatives with different DS. In all cases, NR was loaded in the nanoshell during the process of capsules construction by pre-complexation with decyl-grafted HA derivatives.

3.3.2 Permeability of capsules

In order to load different hydrophobic or/and hydrophilic molecules both in the multilayer shells and the cavity of capsules, we investigated the permeability of the (HA20C10/*N,O*-QCHI)₅ capsules by the observation of the Dextran^{FITC} diffusion from outside of capsules to inside under CLSM as described in **Chapter 2**. The results are presented in **Figure 3.4**. It can be seen that in general, the permeability of (HA20C10/*N,O*-QCHI)₅ capsules depends on the Mw of Dextran^{FITC} as well as the concentration of salt in the medium, which has been found in the permeability studies of multilayer capsules prepared from initial HA. These results suggest the possibility to encapsulate hydrophilic macromolecules in the aqueous cavity of capsules and then control the release by altering the concentration of salt in the medium.

Of note, the permeability of (HA20C10/*N,O*-QCHI3a)₅ capsules towards Dextran^{FITC}-4 was little influenced by salt concentration, similar to that of the capsules based on HA20C10/*N,O*-QCHI3b, but different to that of capsules based on HA/*N*-QCHI derivatives and HA/*N,O*-QCHI3a (see **Chapter 2: Figure 2.9A** and **Figure 2.18A**). In fact, the permeability of latter two kinds of capsules towards Dextran^{FITC}-4 decreased with the increase of salt concentration. The different effect of salt concentration on permeability probably can be related to the hydrophobic interaction occurring between the layers.

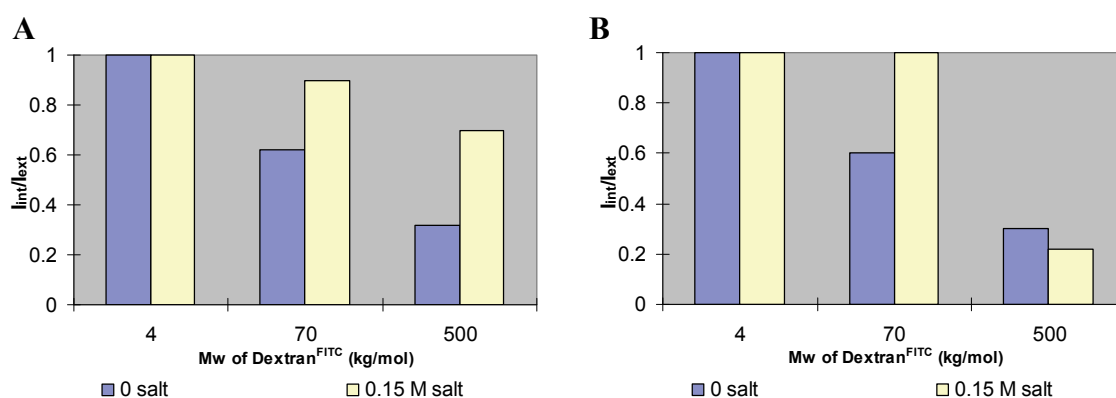


Figure 3.4: Permeability of capsules based on HA20C10 combining *N,O*-QCHI derivatives, A) *N,O*-QCHI3a and B) *N,O*-QCHI3b, respectively, towards Dextran^{FITC} with different Mw in the phosphate buffer (at pH 6.5, $C_{phosphate} \sim 0.01M$) with and without the adding of NaCl ($C_{NaCl} \sim 0.14 M$).

3.3.3 Antibacterial activity of capsules

As the QCHI derivatives and the capsules made of HA and QCHI derivatives showed an antibacterial activity against *E. coli* (Chapter 2), we also investigated the inhibitory effect of capsules containing HA20C20 and *N,O*-QCHI derivatives with highest DS (*N,O*-QCHI3a (DS = 1.33) and *N,O*-QCHI3b (DS = 1.10)) on the growth of bacteria by the viable cell-counting method and the analysis of cell viability, respectively, as described in **Chapter 2**. The results obtained by viable cell counting method are presented in **Figure 3.5**. The capsules based on HA20C20 and different *N,O*-QCHI derivatives exhibited a similar antibacterial activity, however, their activity was lower than that of the capsules based on initial HA. One explanation for the decrease of antibacterial activity of HA20C10 made capsules may be that quaternary ammonium groups of *N,O*-QCHI derivatives bind to HA10C10 not only through the electrostatic interactions but also via the hydrophobic interactions. As a result, the amount of free quaternary ammonium groups presenting on the surface of capsules reduced. Otherwise, although the hydrophobicity of capsules surface was considered as one of the factors affecting their antibacterial activity, in our case, the lower antibacterial activity of capsules containing HA20C10 indicates that the inhibitory effect of quaternary ammonium groups is predominate.

The cell viability study confirms that the capsules based on HA20C10 and *N,O*-QCHI derivatives killed *E. coli* also by the contact-killing strategy since almost all bacteria were adsorbed on the shell of capsules (**Figure 3.6**). DNA-staining dyes were used here to distinguish the viability of bacteria. In the CLSM images, the red and green spots correspond to the alive and dead cells, respectively. Additionally, the color of the shell of the capsules containing HA20C10 is found to be red, while that of the capsules made of initial HA is green. This difference is probably caused by specific/non-specific adsorptions of different DNA dyes within the capsules shells depending on the hydrophilic hydrophobic nature of the shells.

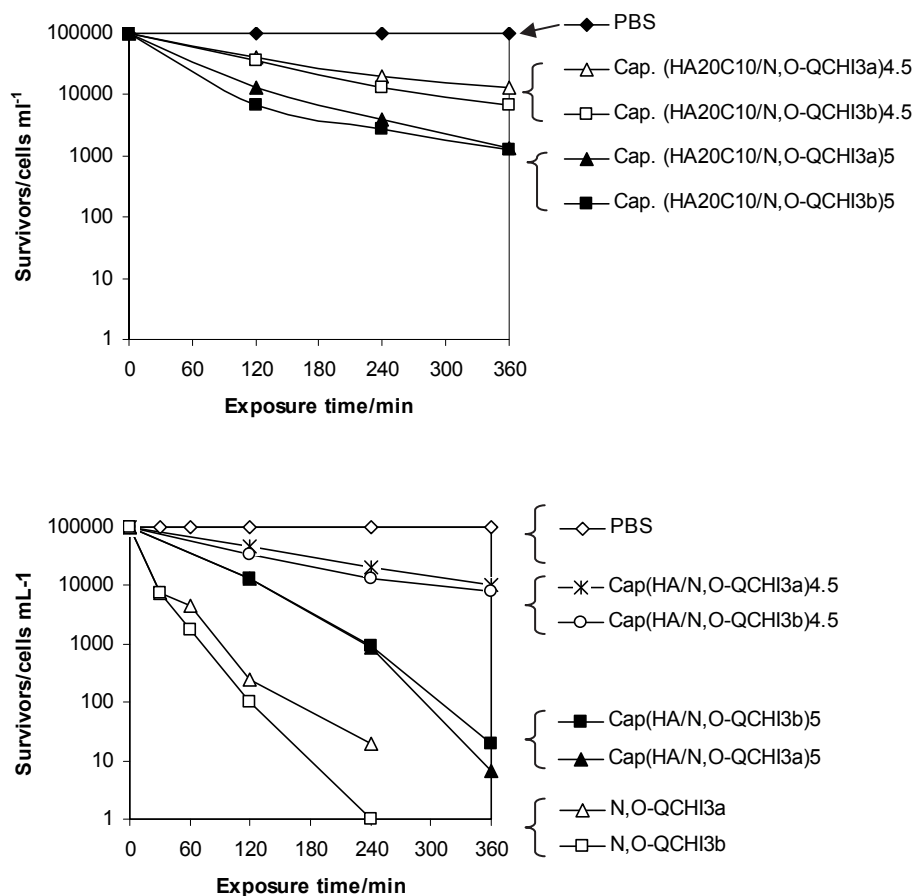


Figure 3.5: Comparison of antibacterial activity of capsules based on *N,O*-QCHI derivatives combining A) HA20C10 and B) HA ended by against *E. coli* (Capsules/bacterial cells ratio ~ 100).

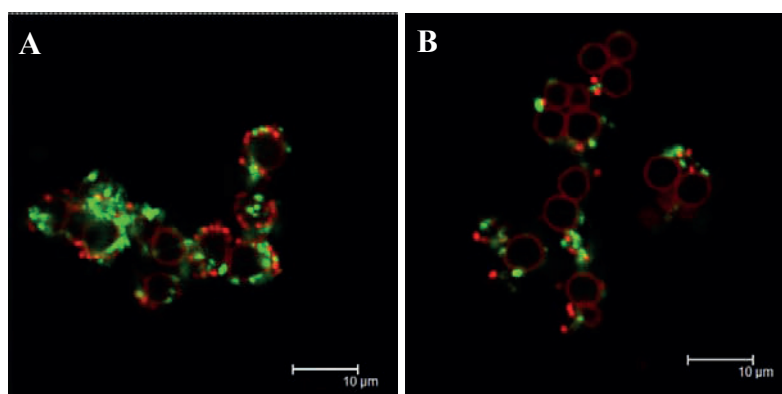


Figure 3.6: Investigation of antibacterial activity of capsules based on HA and *N,O*-QCHI derivatives by CLSM (capsules/bacterial cells ratio ~ 1): A) (HA20C10/*N,O*-QCHI3a)₅ capsules and B) (HA20C10/*N,O*-QCHI3b)₅ capsules.

References:

- (1) Kadi, S.; Cui, D.; Bayma, E.; Boudou, T.; Nicolas, C.; Glinel, K.; Picart, C.; Auzély-Velty, R. *Biomacromolecules* **2009**, *10*, 2875.
- (2) Kadi, S. *Thesis* **2007**.

Chapter 4

Synthesis of rapidly degradable gel-like microvectors based on hydrolysable polysaccharides

Table of contents

4	Résumé (<i>Fr</i>)	141
4.1	Introduction	143
4.2	Synthesis of cationic hydrolysable polysaccharides	148
4.3	Hydrolysis of dextran-DMAE	152
4.4	Polyelectrolyte complexation between dextran-DMAE and HA	155
4.5	Hydrolyze of capsules based on HA/Dextran-DMAE	159
4.5.1	Hydrolysis under neutral conditions	160
4.5.2	Hydrolysis under alkaline conditions	162
4.6	Conclusion.....	164
4.7	Experimental part	165
	References:	168

4 Résumé (Fr)

Ce chapitre porte sur la conception de capsules multicouches capables de se dégrader rapidement par hydrolyse chimique et enzymatique des polysaccharides constituant la paroi, permettant ainsi la libération contrôlée de médicaments. L'obtention de telles capsules a reposé sur la synthèse de dérivés du dextrane porteurs de groupements cationiques labiles par couplage du diméthylaminoéthanol (DMAE) avec le dextrane via des liaisons carbonates. L'analyse par RMN ^1H a montré que ces dérivés sont hydrolysés rapidement à pH physiologique et à 25 °C mais beaucoup plus lentement à pH 6,5. Dans la mesure où les capsules sont préparées à cette valeur de pH, les dérivés dextrane-DMAE ont donc par la suite été utilisés pour la synthèse de capsules par complexation avec l'acide hyaluronique (HA). Après avoir mis en évidence la formation de films multicouches plans par complexation entre le HA et le dextrane-DMAE par microbalance à cristal de quartz (QCM), des capsules à base de HA et dextrane-DMAE ont été synthétisées en utilisant des particules sphériques de CaCO_3 comme support sacrificiel à pH 6,5 (tampon phosphate) et à 25°C. Les particules de CaCO_3 recouvertes par 4,5 paires de couches HA/dextrane-DMAE et les capsules creuses obtenues après dissolution du coeur ont été observées par microscopie électronique à balayage (MEB) et microscopie confocale à balayage laser (CLSM). Le film sec de HA/dextrane-DMAE présent à la surface des particules de CaCO_3 apparaît poreux et relativement épais (épaisseur moyenne estimée à environ 0,5 μm). Les capsules creuses ont une structure coquille-cavité en solution, mais leur coquille n'est pas parfaitement sphérique. Les particularités observées pour ces capsules ont été attribuées à la faible complexation entre le HA et le dextrane-DMAE. La dégradation des films multicouches et des capsules à base de HA et de dextrane-DMAE a été par la suite étudiée dans diverses conditions et par différentes techniques. Il a été remarqué que le taux de dégradation des films multicouches et des capsules était beaucoup plus lent que celui du dextrane-DMAE quelles que soient les conditions. La dégradation du film $(\text{HA/dextrane-DMAE})_4$ a été évaluée à partir des variations de fréquence mesurées par QCM. Après huit jours d'incubation dans le PBS à pH 7,4 et à 25°C, une dégradation d'environ 48 % du film a été déterminée. Un mécanisme en trois temps a été proposé pour la dégradation du film. La dégradation des capsules $(\text{HA/dextrane-DMAE})_{4,5}$ a été étudiée à pH neutre et à pH basique par CLSM, microscopie électronique à transmission (TEM) et FT-IR. Il a été constaté que les capsules incubées à pH 10,5 à 25°C sont complètement détruites en trois jours, mais celles incubées à pH 7,4 à 37°C

conservent leur structure coquille-cavité plus d'une semaine. Comme l'hydrolyse du dextrane-DMAE est plus rapide à pH physiologique et à 37°C qu'en milieu basique à 25 °C, il a été proposé que la destruction des capsules en milieu basique à 25 °C était non seulement causée par l'hydrolyse de dextrane-DMAE, mais aussi par la déprotonation des groupes DMAE à pH élevé.

4.1 Introduction

In the last decade, the layer-by-layer-microcapsules have attracted a particular attention due to their promising applications in drug delivery. By modulating the nature of the polymers and the template, the morphology and properties of capsules, such as the size of capsules, the shell thickness and the permeability of the wall can be easily varied. In addition, due to the multicompartemental structure of such carriers, capsules with tailored properties can be designed based on the chemical modification of polymers.¹⁻³ Up to now, many hydrophilic drugs have been loaded in the capsules cavities. These components could be released by enlarging the permeability or/and destructing the capsules, in response to stimuli, such as pH, ion strength and concentration,⁴ temperature,⁵ solvent polarity,⁶ biomolecules⁷ and physical light,⁸ etc.

Recently, degradable capsules based on either hydrolysable polymers or enzymatic degradable polymers have attracted much attention for their specific performance in the field of drug release.⁹⁻¹⁰ Once in contact with body tissues, such capsules may be taken up by cells and degraded intracellularly or can degrade and release their content into the extracellular space without varying the external conditions.¹¹ In fact, in the past decade the degradable materials made of biodegradable polymers, such as nanoparticles, nanogels, micelles, liposomes and films, etc. have been widely studied for the biomedical, pharmaceutical, agricultural and packaging applications.¹² However, very little research concerned degradable multilayer films and capsules for drug delivery. Most of these studies were reported previously by the groups of Picart (films),¹³⁻¹⁷ Lynn (films),¹⁸⁻²⁵ Auzély (capsules)⁹ and De Geest (capsules)^{10,26}.

Two approaches have been reported to design degradable films and capsules.

The first approach consists of using biodegradable polysaccharides, particularly hyaluronic acid (HA), which were realized by the group of Picart and Auzely, respectively. HA is an anionic biocompatible polysaccharide and could be degraded rapidly with the presence of enzyme, such as hyaluronidase.²⁷ Kadi et al. found that the concentration of hyaluronidase required for a 50 % decrease in the viscosity of HA aqueous solution at 10 g/L (Mw between 200 000 and 600 000 g/mol) within 1 hour at 37 °C in PBS was less than ~5 U/ml and this concentration of hyaluronidase corresponding to the biodegradability of HA was related to its molar mass.²⁸

Based on HA with an Mw of 400 000 g/mol, Picart et al. constructed 2 kinds of multilayer films combined with different cationic polyelectrolyte, poly(L-lysine) (PLL) and chitosan (CHI), respectively. They found that the (HA/PLL)₂₄ films could be degraded for a period of 10 ~ 15 hours in contact with Hyaluronidase (500 U/ml) at 37 °C, whereas (HA/CHI)₂₄ films were degraded within few hours under the same condition.¹³⁻¹⁵ They attributed the faster degradation rate of HA/CHI films than HA/PLL films to the different nature of polycations.¹⁷ Although these films exhibited good enzymatic biodegradability, they might be not suitable for rapid degradation in the human body since the hyaluronidase concentration required for the degradation of these films was too high compared to that in the human serum (~ 2.6 U/ml)²⁹. The in vivo biodegradability study of these films was also carried out. It was found that the (HA/PLL)₂₄ films did not show any biodegradability, but interestingly, the (HA/CHI)₂₄ films could be degraded in few hours similar to the performance in vitro biodegradability study with the presence of enzyme. Although the HA/CHI films showed a good biodegradability, their soft morphology and poor mechanical properties limits the applications. To improve the mechanical strength of the films, the chemical cross-linking was applied. Such rigid mechanical stable cross-linked films were found to be less susceptible to degradation. Only superficial attack was visible on the surface of the HA/CHI films in contact with enzyme observed by confocal laser scanning microscopy (CLSM) and the degradation time in the vivo degradability study prolonged from few hours to several days once cross-linked.¹⁶

Concerning capsules, only few studies have focused on their biodegradability.⁹⁻¹⁰ De Geest et al. synthesized capsules based on poly-L-arginin (pARG) and dextran sulfate (DEXS) and they found this kind of capsules degraded within 2 hours in contact with 1mg/ml pronase at 37 °C in Tris buffer (pH 7.4). Another kind of capsules was prepared by Sarpark et al. based on HA and polyallyamine hydrochloride (PAH).³⁰ Such (HA/PAH)_{4.5} capsules were mechanically stable due to the strong complexation between HA and PAH. It was found that these capsules were highly resistant to enzymatic degradation (500 U/ml) at 37 °C in 0.02 M MES buffer (pH 7.4 without salt). After overnight contacting with hyaluronidase, the permeability of (HA/PAH)_{4.5} capsules towards dextran^{FITC}-4 (Mw ~ 4000 g/mol) varied from ~ 4 % to ~ 6 %. Furthermore, stable hollow microcapsules composed of HA and PLL were obtained by adding a step of chemical cross-linking after the deposition of multilayers. While the non-crosslinked native (HA/PLL)_{4.5} microcapsules showed a shrinkage morphology after dissolution of cores and were destroyed overnight by the hyaluronidase (500 U/ml) at 37 °C

in the same buffer; the cross-linked ones retained their morphology and only their permeability towards dextran^{FITC}-4 changed from ~ 5% to ~ 61 %, as determined by CLSM images. This result indicated increased resistance of capsules to enzymatic hydrolysis due to chemical cross-linking. Moreover, in chapter 2, we synthesized the capsules based on fully polysaccharides, HA and QCHI, whose biodegradability was also tested at 37 °C in PBS in contact with hyaluronidase (500 U/mol). As observed by CLSM, the capsules kept their morphology. As discussed in Chapter 2, we did not observe the remarkable increase of the permeability towards of dextran^{FITC}-2000 (Mw ~ 2000 000 g/mol), which might be explained by the high hydrodynamic radius of such molecule.

The second approach to obtain the degradable multilayer films or capsules relies on the use of hydrolysable polymers. The work of Lynn et al. and De Geest et al. fall down into this strategy. They constructed multilayer films and capsules based on poly(β -amino ester) and poly(carbonate ester), respectively. The structures of these degradable cationic polymers were shown in **Figure 4.1**.

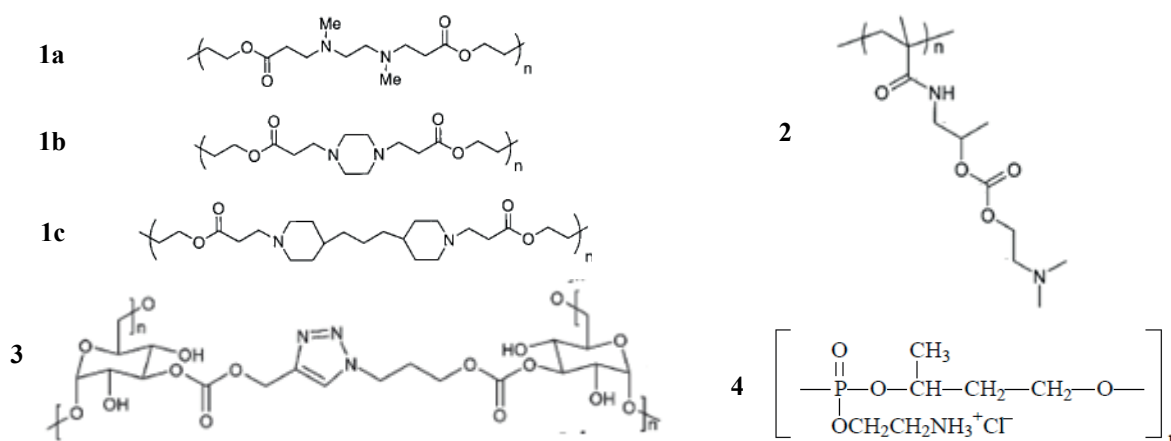


Figure 4.1: Structure of hydrolysable polymers used for the fabrication of multilayer films and capsules: **1a**, **1b** and **1c** belong to the family of poly(β -amino ester), **2** and **3** are the polymers containing carbonate ester groups and **4** is poly(2-aminoethyl propylene phosphate) (PPE-EA).

Lynn et al. synthesized a series of cationic degradable polymers containing amino ester groups **1a**, **1b** and **1c**.³¹ These polymers degraded more quickly at pH 7.4 than pH 5.1 at 37 °C in the buffer. Generally, they could be completely degraded in less than ~ 5 hours at pH 7.4, whereas 50 % degraded for a period of ~7-8 hours at pH 5.1. In addition, the

degradability of polymers was found to be related to their chemical structure. Taking advantage of their hydrolysable properties and cationic charged nature, the thin multilayer films were prepared for the tunable drug release by Wood et al.¹⁸ The anionic polysaccharide, Heparin, low molar mass heparin and chondroitin sulfate were chosen as the partner of poly(β -amino ester) **1c**. Similar to poly(β -amino ester) **1c**, the degradation rate of these thin films was more rapid in basic environment. They completely degraded within 20 hours at pH 7.4 and more than 8 days at pH 6.2 presented by the linearly decreasing films thickness.

Hydrolysable capsules were initially prepared by De Geest et al. based on poly(styrene sulfonate) (PSS) and poly(hydropropyl methacrylamide dimethylaminoethyl) (p(HPMA-DMAE) **2**, a hydrolysable synthetic polymer, whose estimated half-life time (time used for hydrolysing 50 % carbonate ester groups) is \sim 12 hours at 37 °C in PBS (pH 7.4).^{10,32} The capsules containing the polymer bearing cationic labile groups could be completely destroyed in \sim 48 hours in PBS at 37 °C, different to the non-degradable capsules based on synthetic polymers, PSS and poly(allyamine hydrochloride) (PAH). Later, degradable hydrogel capsules based on dextran propargyl carbonate and dextran azidopropyl carbonate were reported by the same groups for the delivery of drugs²⁶. Such hydrogel microcapsules released 50% FITC-dextran for about 7 to 10 days according to the degree of substitution of dextran derivatives. In this work, the release of FITC-dextran was caused by the increasing permeability, which was altered by the decrease of multilayer wall cross-linking due to the chemical hydrolysis of the dextran carbonate derivatives **3**.

Besides the above studies, Lu et al. also synthesized hydrolysable multilayer films based on plasmid DNA and poly(2-aminoethyl propylene phosphate) (PPE-EA) **4**. PPE-EA **4** is a kind of hydrolysable polymers. After 10 days incubation in PBS at 37 °C it degraded to oligomers and failed to bind plasmid DNA.³³ The degradation of PPE-EA-made multilayer film was measured via the determination of the release of DNA. It was found that the DNA was released 55% in 25 days and 80 % in 60 days under the same conditions.³⁴

Overall, from these works, we can see that the mechanically stable films and capsules composed of biodegradable polysaccharides almost showed slow degradation rate in contact with enzyme at a high concentration. The hydrolysable multilayer systems based on synthetic polymers exhibited variable degradation properties according to the nature of polymers, but they lacked biocompatibility.

Thus, the aim of our work is to design a new kind of biocompatible degradable capsules based fully on polysaccharides, one of them bearing labile cationic groups. These capsules may be decomposed rapidly by polyelectrolyte decomplexation and enzymatic degradation of polysaccharides. To our knowledge, no work combining these two concepts has been reported up to now.

The hydrolysable cationic polysaccharide derivatives are synthesized by grafting labile cationic groups onto the main chain of polysaccharides. In the literature, several cationic molecules have been grafted onto the chain of polymers to obtain cationic derivatives and only two of them, dimethylaminoethanol (DMAE) and glycine betaine, could form labile groups through carbonate ester groups and ester groups, respectively. Starch modified with glycine betaine was found to be stable for several days upon storage at room temperature. The cationic hydrolysable polymer p(HPMA-DMAE) could degrade 50 % at 37 °C in ~ 12 hours at pH 7.4 and in ~ 380 hours at pH 5.1. It was reported that the carbonate ester groups were more susceptible to the degradation.³⁵ Thus, we synthesized cationic labile polysaccharides containing carbonate ester groups. Dextran **5**, hydroxyethyl cellulose (HEC) **6** and guar **7** were selected as the potential candidates for the synthesis of degradable cationic polysaccharides by a 2-step coupling reaction (**Figure 4.2**). The resulting dextran-DMAE derivatives were then used as a polycationic partner of HA to design gel-like microvectors. The degradability of polymers, multilayers formation and microvectors based on HA/dextran-DMAE were analyzed.

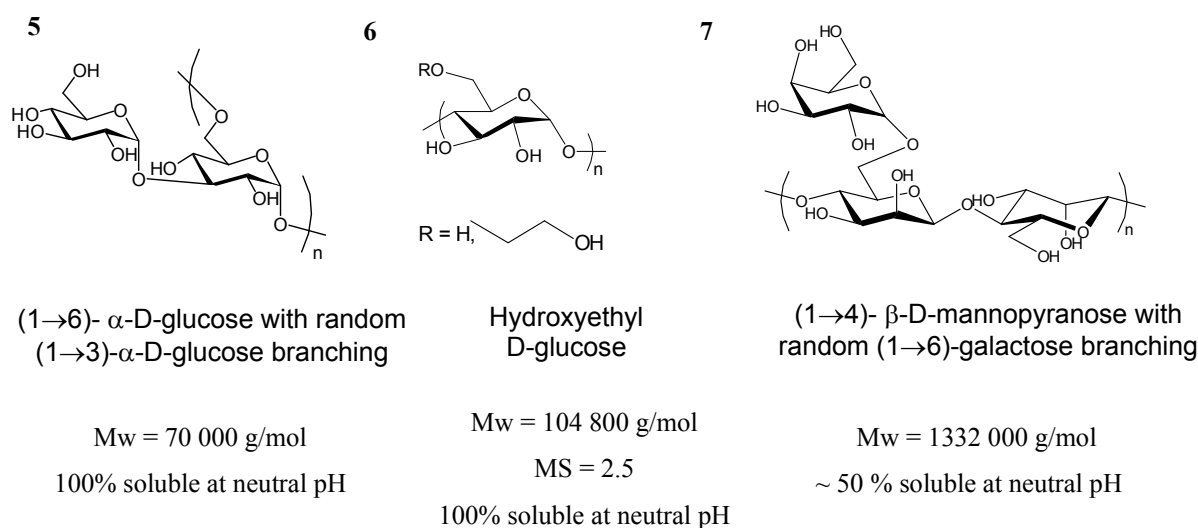
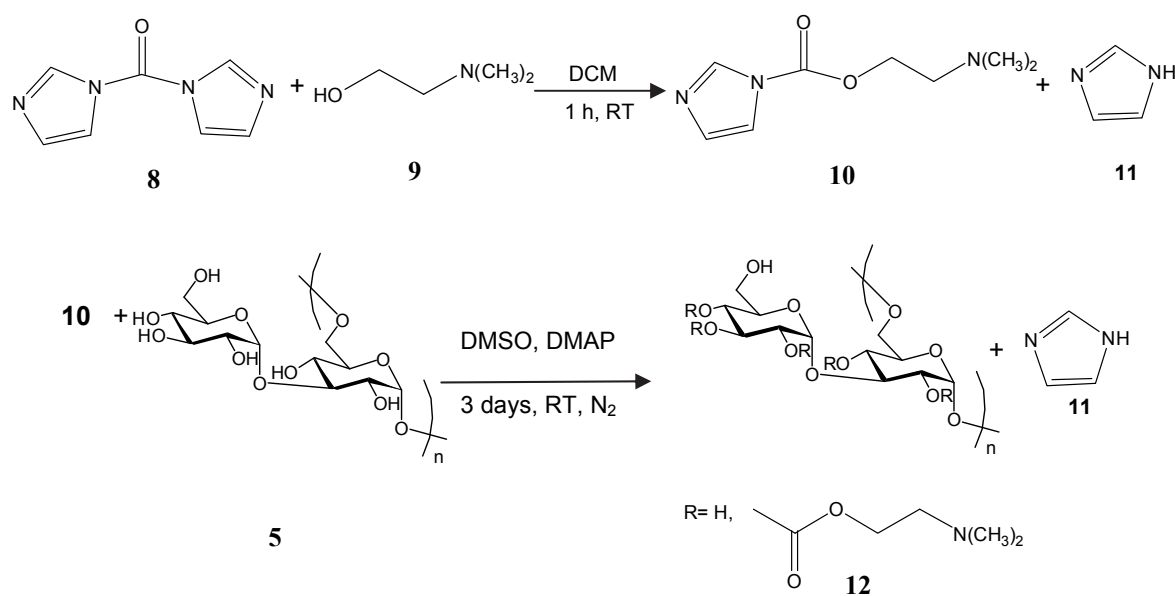


Figure 4.2: Structure of the neutral polysaccharides used to prepare hydrolysable polycations: **5** dextran, **6** HEC and **7** Guar.

4.2 Synthesis of cationic hydrolysable polysaccharides

Dextran with labile cationic group was prepared by a 2 steps coupling reaction using 1,1'-carbonyldiimidazole (CDI) **8** as a coupling agent. *N,N'*-dimethylaminoethanol (DMAE) **9** was firstly activated by CDI **8**, and then grafted onto the hydroxyl groups of dextran **5** as shown in **Scheme 4.1**^{32,36}.



Scheme 4.1: Synthesis of dextran modified with labile cationic groups.

The residue of CDI **8** used in the first step must be completely removed to avoid the production of the chemical cross-linking of dextran in the following step. The final product, dextran-DMAE **12**, was purified by dialysis at 4°C against NH_4OAc buffer (pH 5.0) due to the slower hydrolysis rate of the carbonate esters under such conditions³². We used the FT-IR spectroscopy to confirm the introduction of DMAE groups onto the chain of dextran by the appearance of the absorbance from the carbonate groups around 1264 cm^{-1} (C-O) and 1755 cm^{-1} (C=O) (**Figure 4.3**). 1H NMR spectroscopy was applied to verify the purity of products as well as to determine the degree of substitution (**Figure 4.4A, B**). To avoid the degradation of cationic dextran derivative, the mixture of D_2O and DCl was chosen as the solvent of dextran-DMAE. No signal of CDI was found in the spectrum of DMAE-CI **10** and about 100% of DMAE was successfully activated with CDI within 1 hour. The degree of substitution of dextran-DMAE was found to be 0.7 by integration of the methyl protons of DMAE and anomeric protons of dextran.

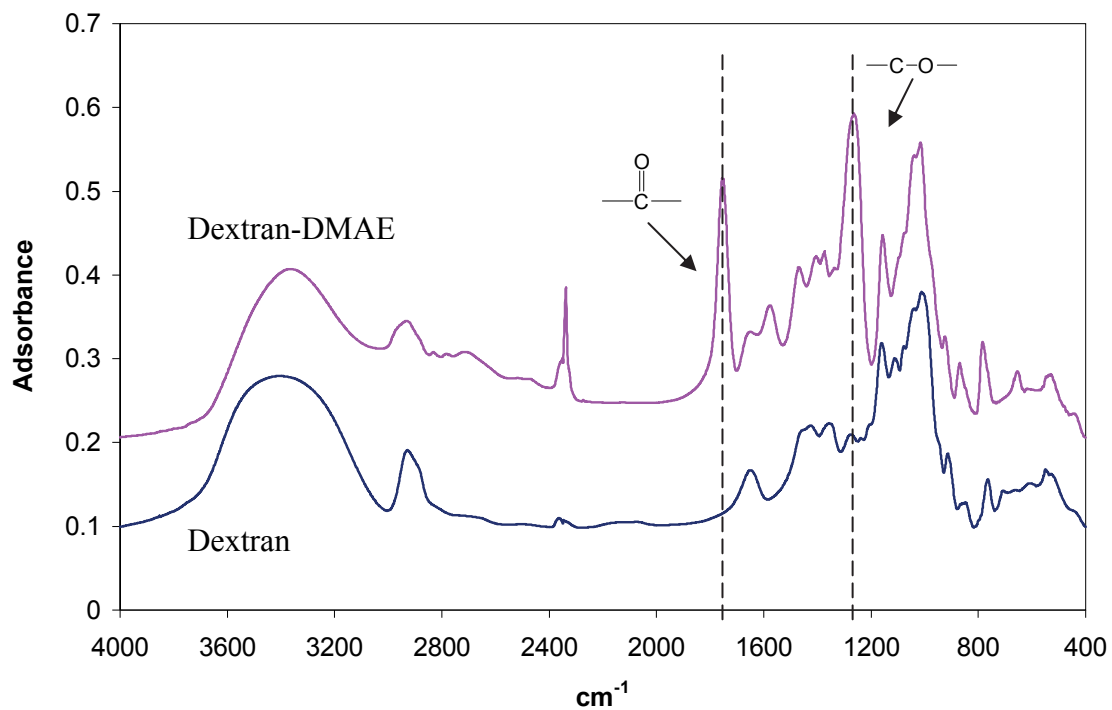
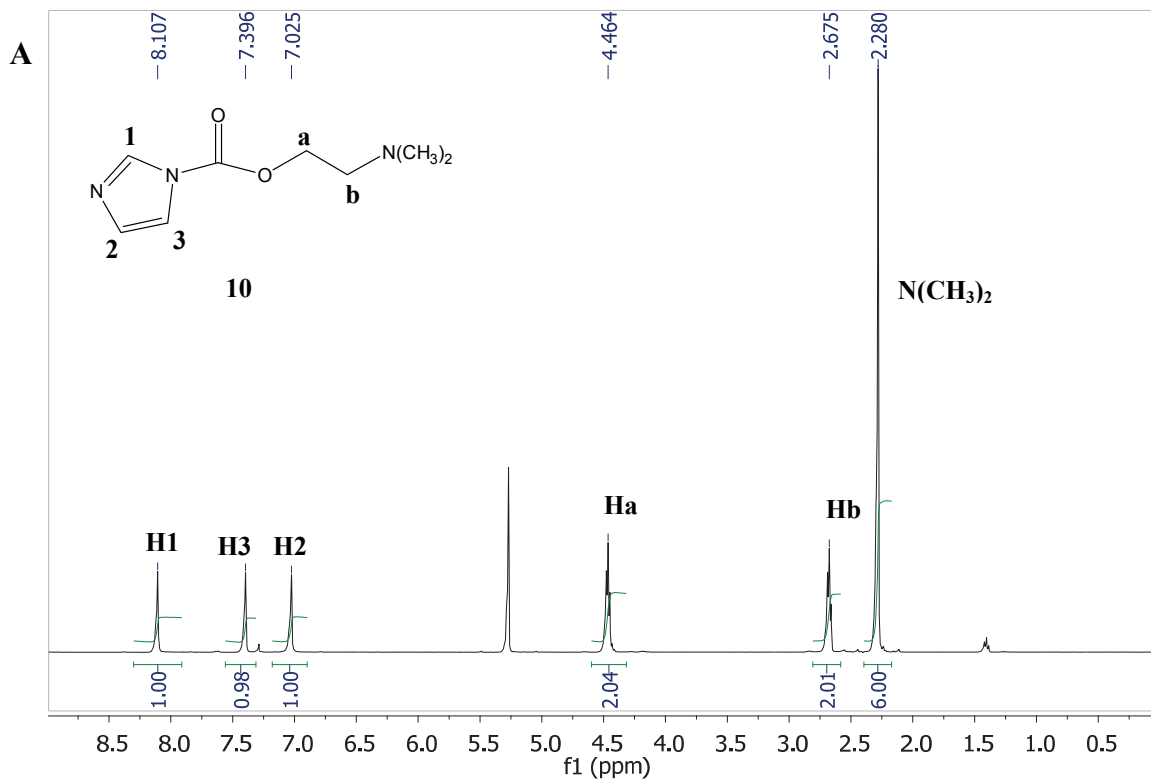


Figure 4.3: FT-IR spectra of dextran and its cationic derivatives (dextran-DMAE).



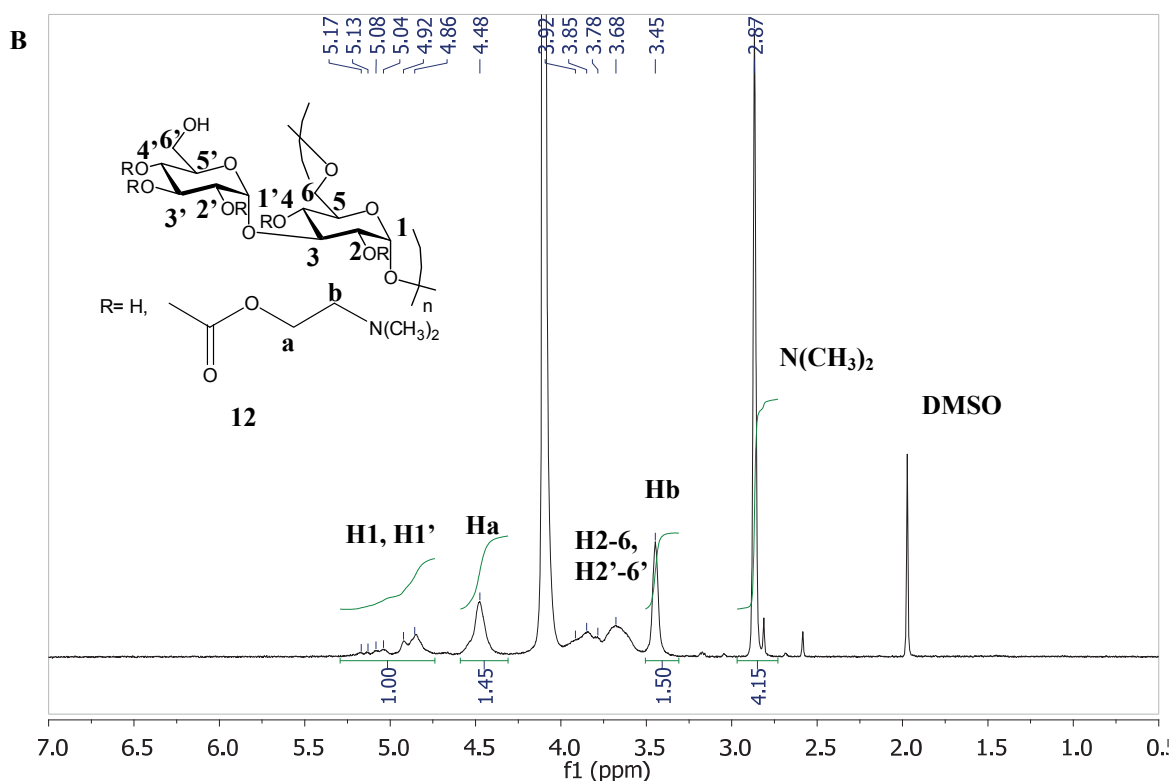


Figure 4.4: ^1H NMR spectra of A) DMAE-CI dissolved in CDCl_3 at 25°C and B) dextran-DMAE dissolved in $\text{D}_2\text{O}+\text{DCl}$ at 80°C .

DMAE was also grafted on other polysaccharides under the same conditions, i.e. HEC **6** and guar **7**. ^1H NMR spectroscopy confirmed that DMAE could be grafted on the main chains of HEC and the DS of HEC-DMAE **8** (~ 0.7) was similar to that of Dextran-DMAE **9** (~ 0.7) (Figure 4). Different to dextran-DMAE, which was soluble in a wide range of pH, this product was soluble in water at pH 2 \sim 3, but not at pH above 4.5. In contrast, we could not provide proof of the successful coupling of DMAE with guar as the purified products could not be dissolved at any pH. Up to now, no explanation has been found for the poorer solubility of modified HEC and guar compared to the initial ones. One possibility is that the cross-linking occurred during the reaction, which decreased the solubility of modified polysaccharides.

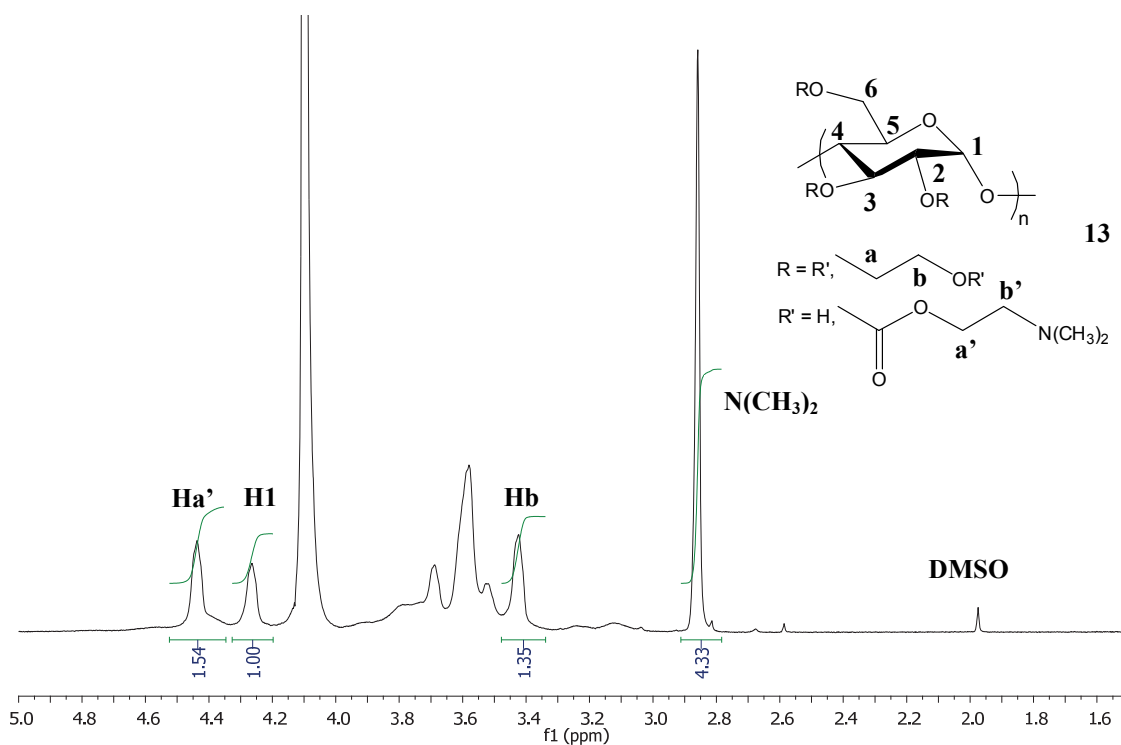
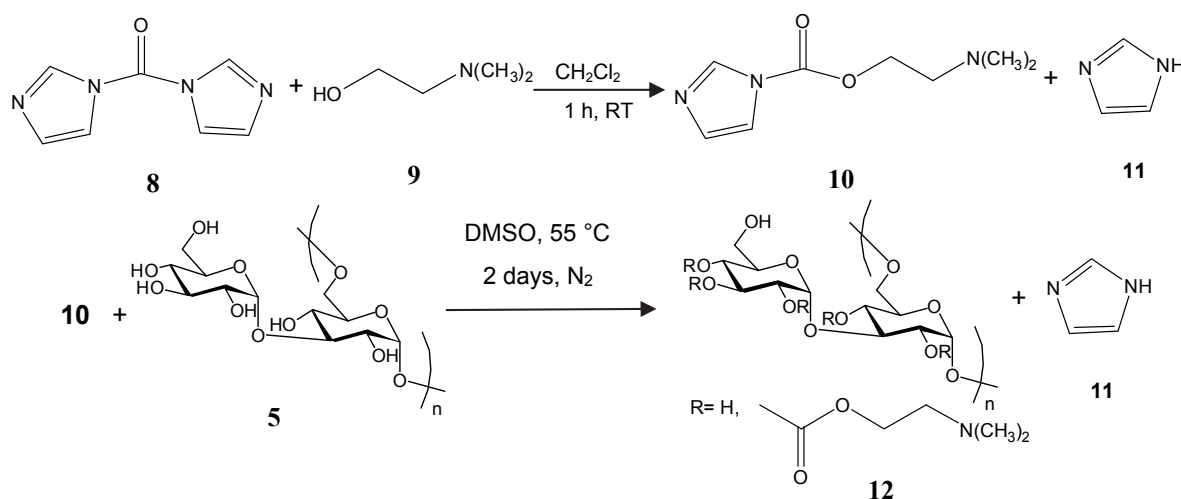


Figure 4.5: ¹H NMR spectrum of HEC-DMAE dissolved in D₂O+DCl at 80 °C.

In a second step, we investigated other reaction conditions to improve the synthesis of dextran-DMAE. The reaction was carried out at higher temperature (55 °C) without adding DMAP for a shorter time (2 days) (**Scheme 4.2**).



Scheme 4.2: Synthesis of cationic dextran derivatives.

The higher temperature was expected to increase the rate of reaction. In the first reaction condition, DMAP was added as an alkaline catalyst to increase the reactivity of DMAE-CI **10**.

In the new conditions, we did not use DMAP considering that the small imidazole **11** produced during the reaction may also act as an alkaline catalyst. We observed that the final reaction medium was much more viscous than the one obtained in the first conditions. Therefore, we collected the product by precipitation using acetone. The product was then purified by dialysis against NH₄Ac aqueous buffer at 4 °C. Interestingly, the DS of dextran-DAME prepared under these conditions was identical to that prepared in the first conditions. However, the solubility of these two products in aqueous solution was different. The dextran-DMAE prepared under the second conditions was not soluble at neutral pH in contrast to the first dextran-DMAE sample. This indicates that both temperature and DMAP influence the properties of the products, while the DS of products is controlled by the DMAE-CI/dextran molar ratio. The first reaction conditions are better than the second ones due to the good solubility over a wide range of pH. By varying the portion of Dextran to DMAE, it is possible to obtain cationic derivatives of dextran with different DS. To verify this conclusion, we synthesized dextran-DMAE with higher DS by increasing the DMAE-CI/dextran ratio from 1.33/1 to 2.7/1, dextran-DMAE with higher DS was obtained from the latter ratio. The precise reaction conditions are listed in **Table 4.1**. Here, we must emphasize that the dextran-DMAE sample used in the following studies has a DS of 0.7.

Table 4.1: Effect of the reaction conditions on DS and solubility in water at neutral pH of dextran-DMAE.

Reaction conditions	Dextran/DMAE-CI ^a	DS ^b	Solubility of product at neutral pH ^c
55 °C, 2 days without adding DMAP	1/1.33	0.7	insoluble
RT, 3 days, adding DMAP	1/1.33	0.7	soluble
RT, 3 days, adding DMAP	1/2	1	soluble
RT, 3 days, adding DMAP	1/2.7	1.2	soluble

^amolar ratio; ^bdetermined by ¹H NMR and ^cobserved by naked eyes at 25 °C (C_p ~ 2 g/L)

4.3 Hydrolysis of dextran-DMAE

As dextran-DMAE was selected for the fabrication of capsules, we investigated its sensitivity to hydrolysis at pH 6.5, which is the pH of the solvent e fused for the capsules synthesis. Moreover, considering the biomedical application of capsules, we also studied their

degradation behavior under physiological conditions (pH 7.4, 37 °C). The hydrolysis of dextran-DMAE under alkaline conditions was also determined.

Figure 4.6 shows the ^1H NMR spectra of dextran-DMAE recorded 1 h and 20 h after solubilization in phosphate buffer at pH 7.4 (25 °C). The area of peaks at ~ 4.45 , 3.25 and 2.7 ppm decreases after 20 h; in contrast that at ~ 3.83 , 3.24 and 2.85 ppm increases. The shifts of $-\text{CH}_2$ and $-\text{N}(\text{CH}_3)_2$ groups are caused by the progressive hydrolysis of dextran-DMAE at neutral pH. The mechanism of degradation of carbonate groups under acidic, neutral and alkaline conditions has been proposed by Ostergaard et al. and is described in **Scheme 4.3**.³⁷

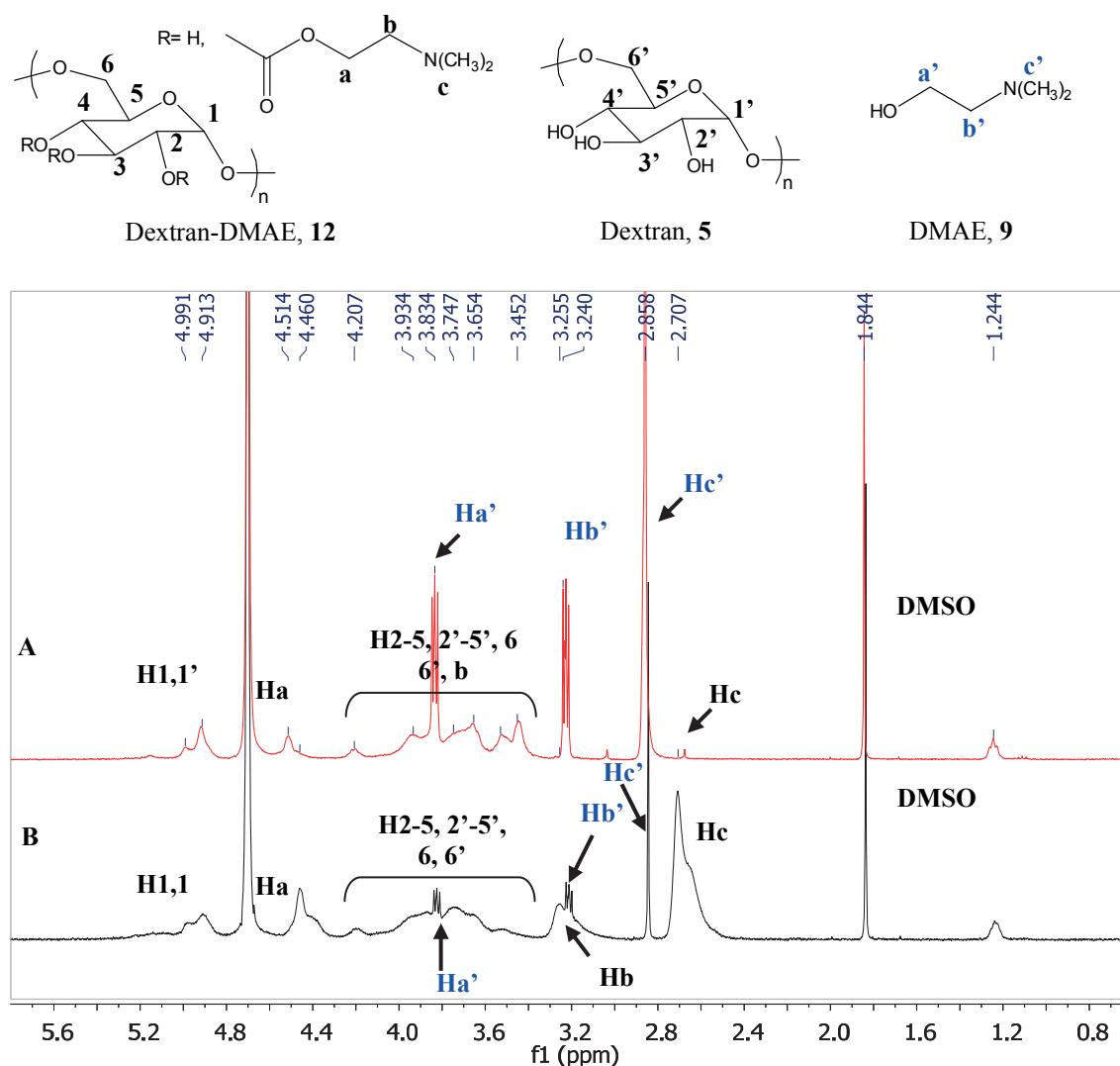
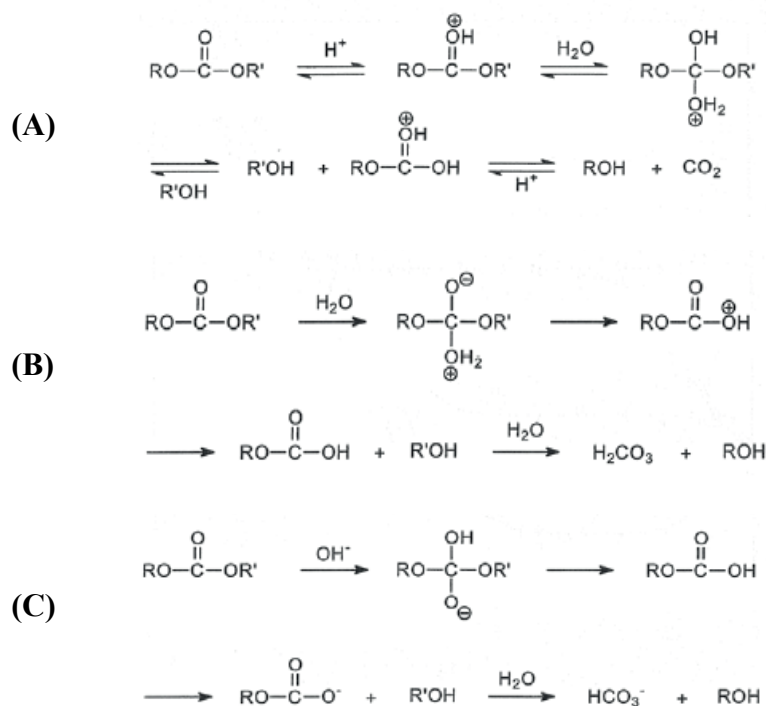


Figure 4.6: ^1H NMR spectra of dextran-DMAE (~ 6 mg/ml) in phosphate buffer (pH 7.4 at 25 °C) recorded for A) 20 h and B) 1 h after dissolution. In order to facilitate the recording, the dextran was represented in a simplified form without branched glucose moieties.



Scheme 4.3: Proposed reaction mechanisms for the (A) acid catalyzed, (B) water catalyzed and (C) base catalyzed hydrolysis of carbonate esters.

Digital integration of the NMR signals arising from the anomeric protons of dextran and –CH₂ protons of DMAE group (Ha) gave a decreasing degree of substitution with time (**Figure 4.7A**). The degree of degradation (DD) was calculated based on the value of the DS according to the equation: $DD = (DS_0 - DS_t) / DS_0$, in which, DS_0 is the DS of the initial product and DS_t is the DS of the product dissolved in the buffer after the time t (**Figure 4.7B**).

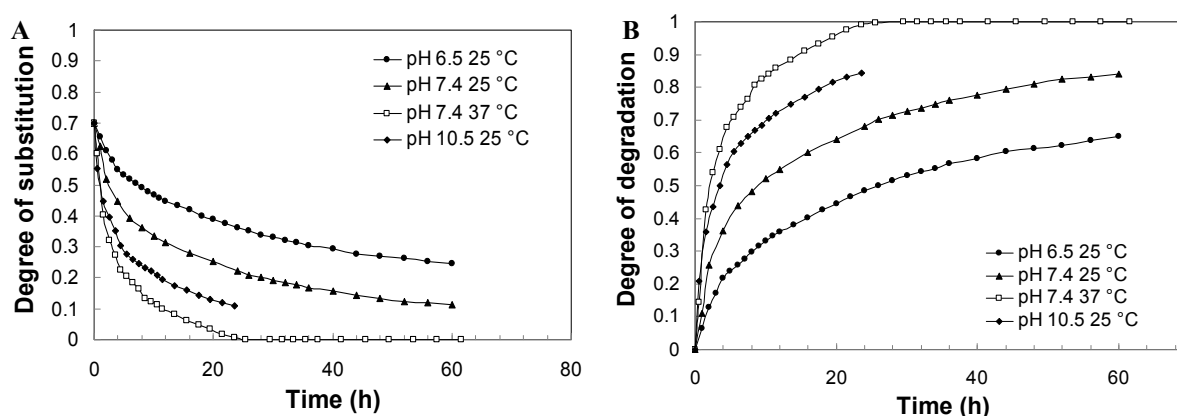


Figure 4.7: Analysis of the hydrolysis of dextran-DMAE under different conditions: A) variation of the DS as a function of time and B) variation of the DD as a function of time.

It is not surprising to find that higher temperature and higher pH result in a higher rate of degradation. At 25°C, the estimated half-time of degradation ($t_{1/2}$), defined as the time for 50 % of DD, is ~ 6 h at pH 10.5, shorter than that at pH 7.4 (~ 8 h) and at pH 6.5 (~ 23 h). When the temperature was increased to 37°C, $t_{1/2}$ reduced to ~ 2.5 hours at pH 7.4. This value is much lower than that of p(HMPA-DMAE), which requires 12 h for 50% hydrolysis under the same conditions³⁸. Since the rate of hydrolysis of dextran-DMAE is lower at pH 6.5 and at 25°C, it may be used as the cationic polyelectrolyte for the construction of multilayers. Indeed, during the time required for the multilayer build-up (4 h) the DS of dextran-DMAE dissolved in water at pH 6.5 decreased only from 0.70 to 0.55.

4.4 Polyelectrolyte complexation between dextran-DMAE and HA

a) Complexation in tubes

It was reported that the electrostatic interaction between oppositely charged PE in solution generally produces a precipitate and such precipitation of PEs is affected by the salt concentration, the Mw and the concentration of PE and other factors.³⁹⁻⁴² As the stability of the precipitate can be used to assess the feasibility to prepare multilayer capsules, we first investigated qualitatively the complexation ability between HA and dextran-DMAE in tubes. HA with a high molecule weight ($M_w = 820\,000$ g/mol) was chosen as the anionic partner of dextran-DMAE as it was previously shown to be well adapted for the capsule synthesis using CaCO_3 particles as template. Indeed, its rather high hydrodynamic radius prevents the diffusion of the PE layers in the porous CaCO_3 core and thereby allows to obtain stable capsules with good reproducibility³⁰. We chose PLL and *N*-QCHI2 as the references of dextran-DMAE. Purified HEC-DMAE and guar-DMAE solutions were also used as polycationic partners to examine the complexation ability between HA and modified polysaccharides bearing cationic DMAE groups. HA, *N*-QCHI2 and PLL were dissolved in the phosphate buffer at pH 6.5 overnight ($C_{\text{phosphate}} = 0.14$ M). Dextran-DMAE was dissolved in the same buffer for half an hour just before starting the experiments. HA and the polycations used in these essays are at 5 g/L and 2 g/L, respectively. **Table 4.2** indicates the observations performed on the initial solutions and the mixtures of in the absence and in the presence of EDTA. EDTA ($C_{\text{EDTA}} \sim 0.1$ M, pH 7.2) was added in the mixture as this chelating agent is used to dissolve the CaCO_3 core after multilayer build-up. It is therefore important to

investigate its potential effect on the polyelectrolyte complexes. Once EDTA was added, there may be a competition between polycation/HA and polycation/EDTA complexation. If the interaction of polycation/EDTA is stronger than the other one, the precipitates should disappear, as in the case of PLL/HA complex. In contrast, the precipitates would remain, as in the case of *N*-QCHI2/HA. However, the complexation of HA/Dextran-DMAE was very strange. Although a slight precipitate appeared at the beginning of the mixing process, the white precipitate converted into a transparent gel-like precipitate overnight. This phenomenon may be due to the hydrolysis of dextran-DMAE, which decreased the complexation ability between HA/dextran-DMAE. The precipitation evidenced the complexation between HA and Dextran-DMAE. The addition of EDTA made the suspension of the HA/dextran-DMAE complex less turbid. Such mixture turned to be a gel-like precipitate after overnight deposition.

Table 4.2: Investigation of the complexation of polycations with HA in tubes observed by naked eyes: ---: transparent solution; - slightly transparent gel-like precipitate; + weak turbid solution; ++ turbid solution; +++ small white precipitate and ++++ big white precipitate.

Polycations Adding solution	PLL	QCHI	Dextran -DMAE	HEC- DMAE	Guar- DMAE
Phosphate buffer (pH 6.5)	---	---	---	---	---
HA (pH 6.5) + P(+)	+++	++++	++	++	++
HA (pH 6.5) + P(+) deposited overnight	+++	++++	-	---	---
HA (pH 6.5) + P(+) + EDTA (pH 7.2)	---	++++	+	---	---
HA (pH 6.5) + P(+) +EDTA (pH 7.2) deposited overnight	---	++++	-	---	---

b) QCM

The assembly of HA and dextran-DMAE in multilayer films was confirmed by following (HA/Dextran-DMAE) films deposition on a planar solid substrate by quartz crystal microbalance (QCM). For comparison, we also followed the assembly of HA and PAH as a

reference multilayer film. Due to the hydrolysis of dextran-DMAE, the multilayer systems built on the gold coated crystal could not reach equilibrium. Thus, the resonance frequency could only be measured when the multilayer films were in the dry state. An exponential growth of the frequency changes ($-\Delta f/\nu$) with the increasing number of layers was evidenced in our working conditions, indicating the successful alternative layer-by-layer deposition of PEs (**Figure 4.8**). In addition, we found that the frequency growth of the HA/dextran-DMAE multilayer film was much higher than that of HA/PAH multilayer films. As the rapid growth (exponential vs. linear growth) is typically observed in the case of weak PE complexes, it can be assumed that the HA/dextran-DMAE interaction is weaker than that of HA/PAH.

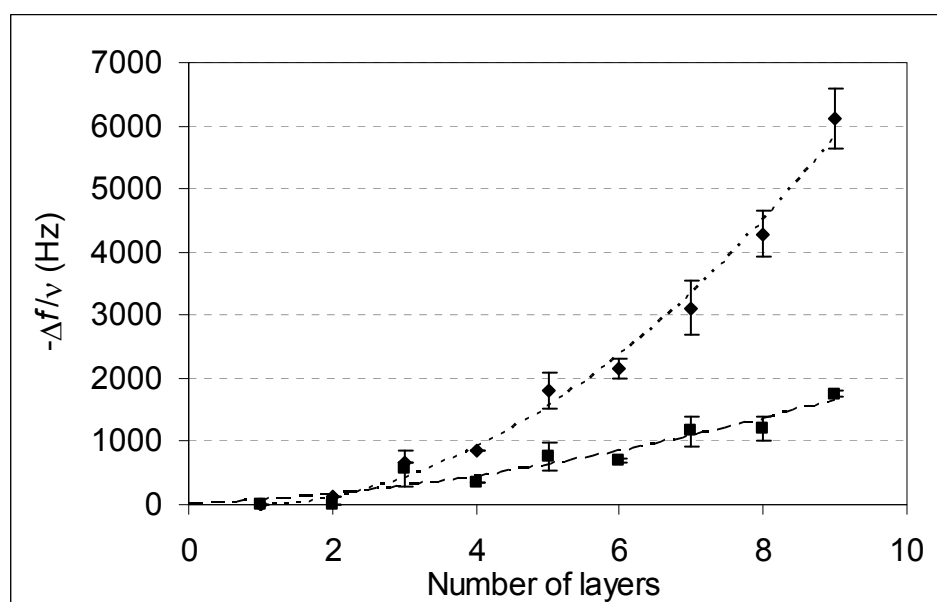


Figure 4.8: QCM frequency shift $-\Delta f/\nu$ during the alternate deposition of (◆) HA/dextran-DMAE and (■) HA/PAH obtained at harmonics 5 MHz as a function of deposited layer. HA and the polycations were used at a concentration of 5g/L and 2g/L in phosphate buffer at pH 6.5 with 0.14 M NaCl, respectively.

c) SEM

Since the QCM study suggested the possibility to deposit several bilayers on a planar substrate; we then investigated the formation of capsules. Multilayer microcapsules were fabricated by layer-by-layer assembly of HA/Dextran-DMAE onto CaCO_3 particles, followed

by a step of core removal. HA and Dextran-DMAE were dissolved at a concentration of 5 and 2 g/L in the phosphate buffer containing 0.14 M NaCl at pH 6.5, respectively. Dextran-DMAE was dissolved half an hour before the deposition in order to avoid strong degradation. The multilayers were constructed by alternatively incubating the CaCO₃ cores in HA and Dextran-DMAE solutions. Two washing steps with the phosphate buffer (pH 6.5, $C_{phosphate} = 0.01$ M, $C_{NaCl} = 0.01$ M) were carried out between each deposition to remove excess of polymers.

The surface of microparticles coated with 0.5, 2.5 and 4.5 bilayers of HA/dextran-DMAE was observed by FEG-SEM (**Figure 4.9**). As can be seen from **Figure 4.9a**, the surface of CaCO₃ microparticles is porous. After the deposition of the 1st layer of HA, the CaCO₃ particles were completely covered by HA (**Figure 4.9b**). However, after deposition of 2.5 (HA/dextran-DMAE) bilayers, a loosely porous surface appeared on the particles coated with the 2.5 (HA/dextran-DMAE) bilayers (**Figure 4.9c**), which was also observed after deposition of 4.5 (HA/dextran-DMAE) bilayers (**Figure 4.9d**).

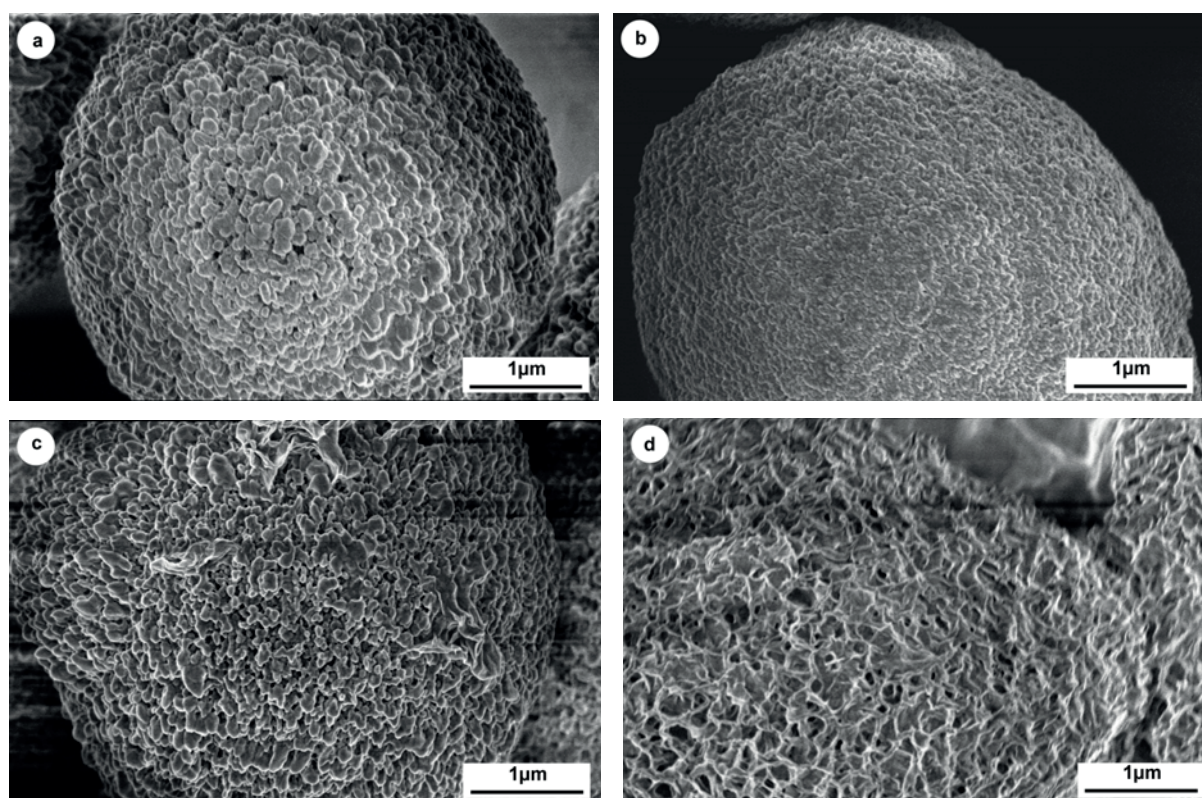


Figure 4.9: Observation of a) CaCO₃ microparticles and the particles coated with b) 0.5, c) 2.5 and d) 4.5 bilayers of HA/dextran-DMAE by FEG-SEM.

During the process of capsules preparation, we found that the particles became aggregated upon the deposition of the bilayers and such agglomeration increased with the increase number of deposition. The particles coated with 4.5 (HA/dextran-DMAE) bilayers had a rather bigger average diameter ($\sim 6 \mu\text{m}$) compared to the CaCO_3 particles ($\sim 5 \mu\text{m}$) measured from the SEM images. This means that the shell thickness of the capsules with 4.5 (HA/dextran-DMAE) bilayers in dry state is $\sim 500 \text{ nm}$. This value is much higher than those obtained from the capsules with the same number of bilayers based on HA and other polycations, such as PLL, PAH and QCHI derivatives. These thicker shells might be related to the weaker complexation of HA and Dextran-DMAE, which perhaps induced a swollen gel-like 3D structure.

After deposition of 4.5 (HA/dextran-DMAE) layer pairs, the LbL coated CaCO_3 particles were incubated in EDTA ($C_{\text{EDTA}} \sim 0.1 \text{ M}$, pH 7.2), affording hollow capsules steps. The morphology of these hollow microvectors was observed by CLSM using Dextran^{FITC}-4 (Mw 4000 g/mol) as a fluorescence dye. After 20 min of mixing, the Dextran^{FITC}-4 completely diffused inside the aqueous cavity of capsules and showed the dark irregular circle-like morphology of hollow capsules (**Figure 4.10**).

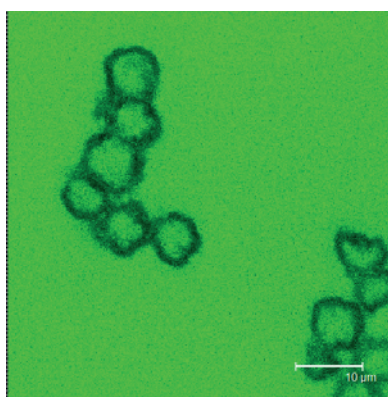


Figure 4.10: Observation of $(\text{HA/dextran-DMAE})_{4.5}$ microcapsules in PBS incubated with Dextran^{FITC}-4 (Mw $\sim 4000 \text{ g/mol}$).

4.5 Hydrolyze of capsules based on HA/Dextran-DMAE

Considering the hydrolysable property of dextran-DMAE, the microcapsules based on HA/Dextran-DMAE was expected to be degraded in aqueous solution.

4.5.1 Hydrolysis under neutral conditions

a) QCM

The first data about degradation was obtained by the measurement of QCM experiments. The crystal with the (HA/dextran-DMAE)₄ film was incubated in PBS solution at 25°C for 8 days. We took the non degradable (HA/PAH)₄ film as a reference. The frequency shift of dried crystals were regularly measured (**Figure 4.11**). The extent of degradation of multilayer films is described as the percentage of the decreased frequency shift after incubation in comparison to the beginning. As can be seen from figure 10, the degradation of PE multilayer films could be divided into 2 or 3 stages according to the nature of PE. In the first stage (Stage I), the $-\Delta f/\nu$ of multilayer films decreased fast, which can be explained by the diffusion of polysaccharides from inside of multilayer films to outside following the change of external conditions, such as pH, ion concentration, etc. In this stage, $-\Delta f/\nu$ of (HA/PAH)₄ films and (HA/Dextran-DMAE)₄ films decreased $\sim 42\%$ within one day and $\sim 26\%$ within two days, respectively. In the second stage (Stage II), since the diffusion of polysaccharides reached the equilibrium, the variation of $-\Delta f/\nu$ appeared lower. We can see that the $-\Delta f/\nu$ of (HA/PAH)₄ films kept constant in the last 7 days and that of (HA/dextran-DMAE)₄ films decreased slowly (4%) for about two days. Different to the multilayer films based on non degradable polymers, in the case of multilayer films made of labile cationic polysaccharides, dextran-DMAE, we observed the third stage of degradation. Indeed, after Stage II, $-\Delta f/\nu$ of (HA/dextran-DMAE)₄ films dramatically decreased again ($\sim 22\%$ in last 4 days). This rapid decrease of $-\Delta f/\nu$ in the third stage (Stage III) is related to the hydrolysable property of dextran-DMAE. We hypothesized that the hydrolyzed polymers were difficult to escape from the multilayer films at the beginning of test and once the decomposition of the films caused by the degradation of the polycation was strong enough, the small blocks of films dropped down. One proof to support such explanation was the variation of the surface compartment of multilayer films. It was observed by naked eyes that the smooth surface of (HA/dextran-DMAE)₄ multilayer films at the beginning turned to rough at the end of experiment, while the variation of the surface compartment of (HA/PHA)₄ films was not perceivable. The surface roughness study by AFM will be meaningful to understand the degradation process of PE multilayer films made of hydrolysable polysaccharides.

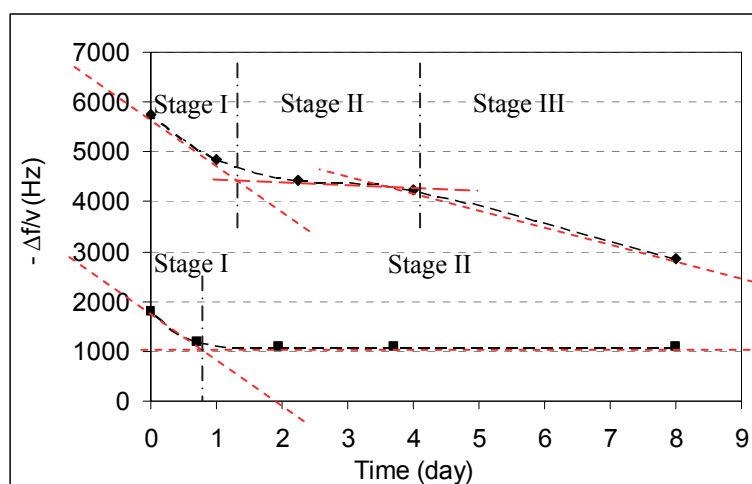


Figure 4.11: QCM-D frequency shift $-\Delta f/v$ during the degradation study of (♦) HA/Dextran-DMAE and (■) HA/PAH obtained at harmonics 5 MHz as a function of time. HA and the polycations were used at a concentration of 5g/L and 2g/L in phosphate buffer at pH 6.5 with 0.14 M NaCl, respectively.

b) CLSM

We also tried to directly investigate the degradation of the capsules in PBS at 25°C and 37 °C for a period of 7 days by CLSM. Although dextran-DMAE could 100 % hydrolyze at PBS at 37 °C within 24 hours, the capsules kept mechanically stable under the same condition. Similar results were obtained by Kris et al ¹⁸. They found that the decrease of the thickness of thin multilayer films based on heparin and the type c of poly(β-amino ester) **1c** became constant after 10 hours' immersion in the buffer at pH 7.4, although poly(β-amino ester) could be fully degraded within 3 hours. Reported by Lu et al, the multilayer film of Protein/PPE-EA degraded 55% within 25 days whereas the degradation half-time of PPE-EA is 10 hours ³⁴. In these studies, the hydrolysable polymers in solution were degraded more quickly than those used as a component of multilayer films. However, De Geest et al. reported that the degradation rate of p(HPMA-DMAE)/PSS capsules was the same to p(HPMA-DMAE) ¹⁰. These results indicate that the destruction of multilayer capsules by degradation of the hydrolysable polyelectrolyte polymers was not only dependent on the hydrolysis of polymers in the solution, but also on the structure of the PE film, the complexation ability of polyelectrolyte polymers and furthermore the thickness of multilayer. In our case, the slow decomposition rate of capsules based on fast hydrolysable polymers might be mainly related to the difficulty of polysaccharides escaping out of the PE multilayer capsules, which might

be affected by the entangled polymer chains in the multilayer capsules based on HA and Dextran-DMAE and the thicker wall of capsules.

4.5.2 Hydrolysis under alkaline conditions

Since the (HA/dextran-DMAE)_{4.5} capsules kept their mechanical stability under neutral conditions for at least one week, we tried to promote the degradation rate under alkaline conditions. To compare the effect of the pH on the degradation of capsules, the study was done in HEPES buffer at 25 °C at pH 7.4 and pH 10.5 in parallel. As can be seen from the cryo-TEM images (**Figure 4.12**), the capsule in HEPES buffer at pH 7.4 kept its hollow spherical structure after 1 day's incubation, but that at pH 10.5 was collapsed and deformed. The capsules stored at pH 7.4 kept their morphologies for the tested time (~ 1 week), while those stored at pH 10.5 were disappeared in 3 days from the observation by naked eyes.

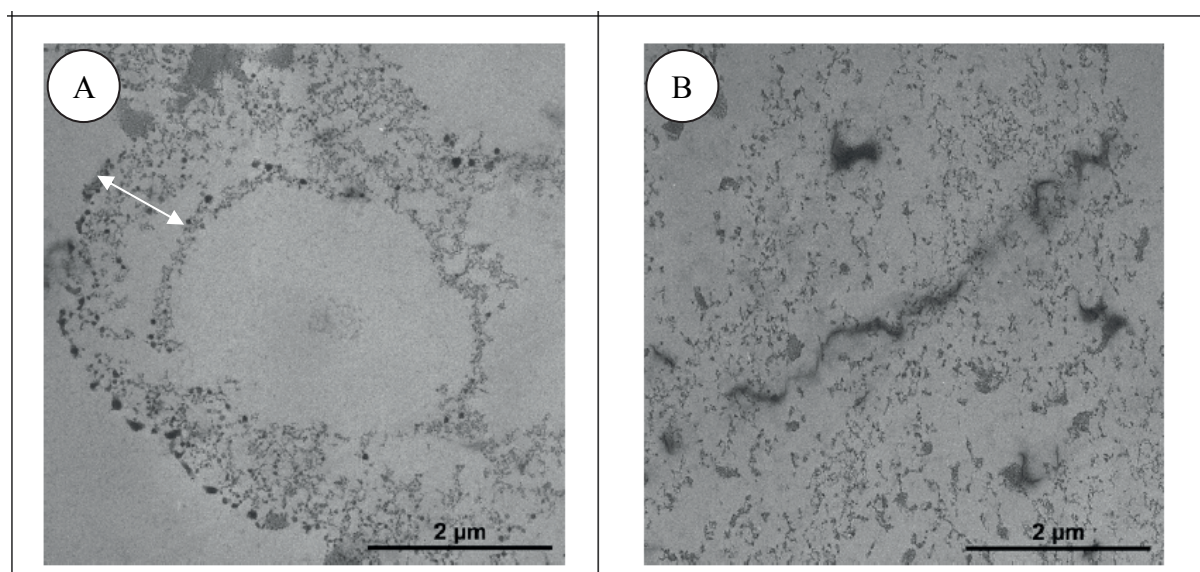


Figure 4.12: (Dextran-DAME/HA)_{4.5} capsules incubated in HEPES buffer at different pH observed par TEM after 1 day: A). at pH 7.4 and B). at pH 10.5. The white arrow in A marks the shell of hollow (dextran-DAME/HA)_{4.5} capsules.

We purified the solution of the hydrolyzed capsules (the one treated at pH 10.5) and the suspension of capsules (the one treated at pH 7.4) by dialysis against milli-Q water for three times to remove the free molecule of DMAE and the salts, and then freeze-dried the

suspensions. These products were analyzed by FT-IR. As can be seen from **Figure 4.13**, the absorbance of the carbonate ester groups at 1280 and 1740 cm^{-1} only appeared in the sample of capsules treated at pH 7.4. It demonstrates that dextran-DMAE in the solution of capsules treated at pH 10.5 was completely hydrolyzed, while that treated at pH 7.4 was not.

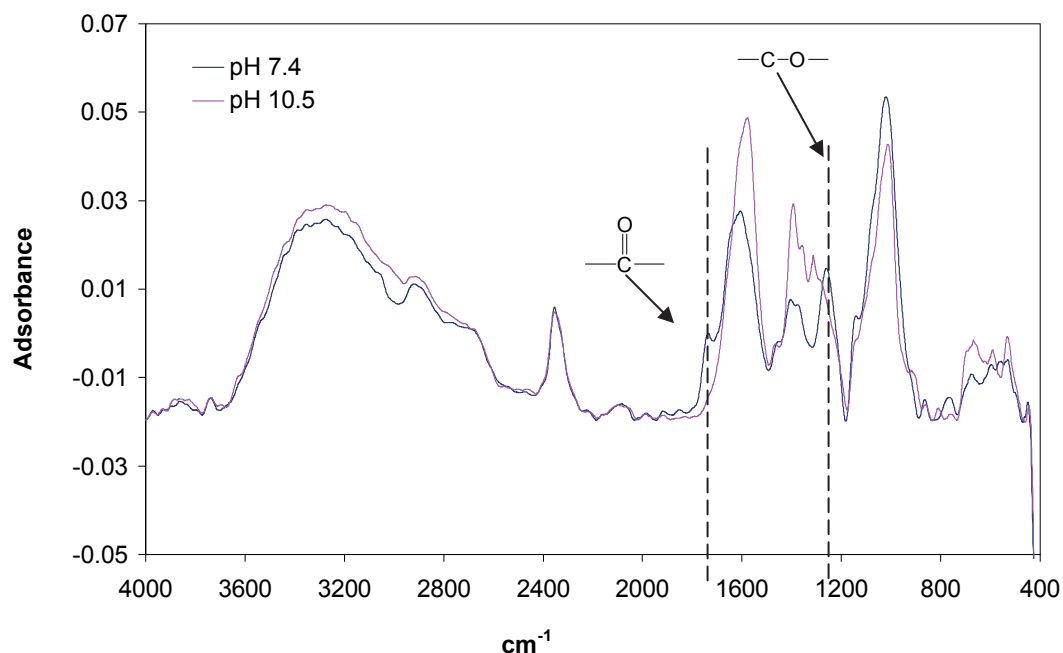


Figure 4.13: Comparison of the IR spectra of dried $(\text{HA/dextran-DMAE})_{4.5}$ capsules incubated in HEPES buffer at different pH at 25 °C after 3 days.

We summarized the results about hydrolysis study of dextran-DMAE and the capsules based on dextran-DMAE under different conditions in the table 3 and found interesting information. Although the degradation rate of dextran-DMAE at pH 10.5 at 25 °C was lower than that at pH 7.4 at 37 °C, the capsules incubated at pH 10.5 and 25 °C could be destroyed in short time while those incubated at neutral pH and 37 °C kept their mechanical stability for at least one week. Such phenomena indicate that the higher pH played an important role on the deconstruction of capsules. Since the pKa of DMAE is ~ 10 , the $-\text{N}(\text{CH}_3)_2$ groups on the chains of dextran-DMAE could be deprotonated at pH 10.5, which eliminate the electrostatic complexation between polyelectrolyte polymers. Thus, affected by both the deprotonation of cationic groups of dextran-DMAE and the degradation of labile groups, the capsules were destroyed rapidly.

Table 4.3: Comparison of the effect of pH and temperature on the degradation of dextran-DMAE in solution and on the destruction of capsules.

pH	Temperature	$t_{1/2}$ of dextran-DMAE in solution	Deconstruction of capsules
pH 10.5	25 °C	6 hours	Yes, 3 days
pH 7.4	25 °C	8 hours	No, 7 days
pH 7.4	37 °C	2.5 hours	No, 7days

4.6 Conclusion

In order to obtain rapid degradable microcapsules based fully on polysaccharides, we synthesized dextran-DMAE, a kind of labile cationic polysaccharides derivatives. Such modified polysaccharides can be hydrolyzed quickly under mild condition. The higher degradation rate was obtained at higher pH and higher temperature. Thanks to the cationic groups on the end of side chain of dextran, dextran-DMAE could form a complex with HA by electrostatic interaction, which has been confirmed by different techniques. However, the exponential growth during the build-up of multilayer films indicates the dextran-DMAE/HA complexation is not strong. Even that, we successfully prepared the hollow capsules based on dextran-DMAE and HA. The particles coated with dextran-DMAE/HA multilayers showed loosely porous surface and the average thickness of this coating (4.5 bilayers) was found to be $\sim 0.5 \mu\text{m}$. Once the core was removed, the hollow capsules were mechanically stable but exhibited irregular morphology. The degradation of these multilayer films and capsules was investigated. Although the dextran-DMAE hydrolyzes fastest at pH 7.4 at 37 °C, the capsules under such condition kept mechanical stability at least one week. However, these capsules were completely destructed within three days at pH 10.5 at 25°C. Based on the above results, it appears that the rapid degradation of capsules by using only hydrolysable polymer could be achieved at alkaline pH (pH 10.5).

4.7 Experimental part

Materials:

Hyaluronic acid under the sodium salt form, having a molar mass (M_w) of 820000 g/mol, was a gift from ARD (Pomacle, France). Hydroxyethyl cellulose (HEC) with a M_w of 104 800 g/mol and guar with a M_w of 1335 000 g/mol were purchased from Hercules and Rhodia, respectively. Dextran from *Leuconostoc* spp. with a M_w of \sim 70000 g/mol, 1,1'-carbonyldiimidazole (CDI), *N,N'*-dimethylaminoethanol (DMAE), dichloromethane (DCM), 4-dimethylaminopyridine (DMAP), dimethyl sulfoxide (DMSO), ethylenediaminetetraacetic acid (EDTA), calcium chloride (CaCl_2), sodium carbonate (Na_2CO_3), anhydrous magnesium sulphate (MgSO_4), sodium hydroxide (NaOH), hydrochloric acid (HCl), ammonium acetate (NH_4Ac), sodium chloride (NaCl), phosphate buffer saline (PBS), sodium phosphate monobasic dihydrate ($\text{NaH}_2\text{PO}_4 \cdot 2\text{H}_2\text{O}$), sodium phosphate dibasic (Na_2HPO_4), 4-(2-hydroxyethyl)piperazine-1-ethanesulfonic acid, *N*-(2-hydroxyethyl)piperazine-*N'*-(2-ethanesulfonic acid) (HEPES) and fluorescein isothiocyanate with a M_w of 4000 g/mol (dextran^{FITC}-4) were purchased from Sigma-Aldrich-Fluka. All chemicals were used without any further purification. The water used in all experiments was purified by a Millipore Milli-Q Plus purification system, with a resistivity of 18.2 M Ω cm.

Syntheses:

Synthesis of the DMAE-Cl. 6.85 g CDI (42.16 mmol) was dissolved in CH_2Cl_2 (50 ml). 2.5 ml DMAE (24.8 mmol) was added drop by drop in the yellow suspension of CDI. During the addition, the CDI dissolved and a clear yellow solution was obtained. This reaction lasted for 1 hour at room temperature. The crude product was purified by three times extraction with 20 ml distilled water, and then dried by anhydrous MgSO_4 . Finally the colorless liquid DMAE-Cl was collected by evaporation of CH_2Cl_2 under reduced pressure. (Yield: 2.8 g, 62.4%). The assigned ^1H NMR spectra is shown in **Figure 4.4A**.

Synthesis of the dextran-DMAE (Condition 1). 1.335 g dextran (8.25 mmol) was dissolved in 25 ml anhydrous DMSO overnight. 2 g DMAE-Cl (2.2 mmol) was added drop-wise in the colorless solution of dextran, and then 1.344 g DMAP (11 mmol) dissolved in 25 ml anhydrous DMSO was added. The reaction lasted for 3 days at room temperature with the protection of N_2 and was stopped by adding 40 ml 1 N HCl (final pH \sim 5.0). The product was purified by extensive dialysis (MWCO 3500 g mol⁻¹, more than 8 times, 2 hours/time) against an NH_4Ac buffer of pH 5.0 (10 mM, last step 5 mM) at 4°C and collected after freeze drying.

(Yield: 1.65 g, $DS_{\text{NMR}} = 0.70$, 85%). The assigned ^1H NMR spectra is shown in Figure 3B. The same procedure was used to synthesize the HEC-DMAE and guar HEC. The assigned ^1H NMR spectra of dextran-DMAE and HEC-DMAE are shown in **Figure 4.4B** and **Figure 4.5**, respectively.

Synthesis of the dextran-DMAE (Condition 2). 1.335 g dextran (8.25 mmol) was dissolved in 25 ml anhydrous DMSO overnight. 2 g DMAE-Cl (2.2 mmol) was added drop-wise in the colorless solution of dextran. The reaction lasted for 2 days at 55°C with the protection of N_2 and was stopped by adding 40 ml 1 N HCl (final pH ~ 5.0). The product was cooled and then purified by extensive dialysis ($\text{MWCO } 3500 \text{ g mol}^{-1}$, more than 8 times, 2 hours/time) against an NH_4Ac buffer of pH 5.0 (10 mM, last step 5 mM) at 4°C and collected after freeze drying. (Yield: 1.65 g, $DS_{\text{NMR}} = 0.70$, 85%). The assigned ^1H NMR spectrum is shown in **Figure 4.6**.

Capsule preparation. Microcapsules were prepared by layer-by-layer technique using calcium carbonate particles as a sacrificial template. CaCO_3 particles were synthesized from solutions of CaCl_2 and Na_2CO_3 as reported in the literature.⁴³⁻⁴⁴ Dextran-DMAE and HA were dissolved in the phosphate buffer with 0.14 M NaCl (pH 6.5, $C_{\text{phosphate}} = 0.01 \text{ M}$) for 30 min and overnight before the synthesis of capsules respectively. The CaCO_3 particles were coated layer-by-layer by incubating them at a concentration 2 % (w/v)⁴⁵ in solutions of dextran-DMAE (C_p at 2 g/L) and HA (C_p at 5 g/L). After shaking for 10 min, the particles were collected by centrifugation and the residual non-adsorbed polyelectrolyte was removed by washing twice with the phosphate buffer with 0.01 M NaCl (pH 6.5, $C_{\text{phosphate}} = 0.01 \text{ M}$).

After the desired number of layers was deposited, the CaCO_3 core was removed by treatment with an aqueous solution of EDTA (0.1 M, pH 7.2) for 30 min. The hollow capsules with dissolved ions were purified by dialysis ($\text{MWCO } 6000\text{-}8000 \text{ g/mol}$) against pure water.

Characterization:

NMR Spectroscopy. ^1H NMR spectra of dextran-Cl dissolved in CDCl_3 (1 drop/ml) and ^1H NMR spectra of dextran-DMAE dissolved in deuterium oxide (D_2O) with slight of deuterium chloride (DCl) (6 mg/ml) were performed at 25°C and 80°C respectively using a Bruker DRX400 spectrometer operating at 400 MHz. For Dextran-DMAE hydrolyze study, Dextran-DMAE was firstly dissolved in phosphate buffer (pH 6.5 and pH 7.4) and HEPES buffer (pH 10.5), respectively, then free-dried, redissolved in deuterium oxide, free-dried, finally redissolved in deuterium oxide.

Fourier Transform Infrared Spectroscopy (FT-IR). The freeze dried samples were milled with potassium bromide to form very fine powder. These powders were then compressed into thin pellets to be analyzed. A thin pellet of pure potassium bromide was prepared to be the background. All analyses were performed using Spectrum RX1 spectrometer, Perkin Elmer. For each sample 8 scans were recorded between 4000 and 400 cm^{-1} with a resolution of 2 cm^{-1} using Spectrum software V 5.0.0.

Films characterization by quartz crystal microbalance (QCM). The (HA/dextran-DMAE)_i and (HA/PAH)_i film were constructed by alternative incubation of the gold-coated quartz crystal in the opposite charged polyelectrolyte solution, HA (C_p at 5 g/L) and polycations (C_p at 2 g/L), which were dissolved in the phosphate buffer with 0.14 M NaCl (pH 6.5, $C_{\text{phosphate}} = 0.01$ M) overnight and for 30 min respectively before the built-up. The films were twice washed by milli-Q water after each deposition of polyelectrolyte and then dried thoroughly under a stream of dry nitrogen. For the degradation studies, the built-up multilayer films were incubated in PBS (pH7.4) at 25 °C with slightly shaking (~ 50 rpm). To well determine the frequency shift of multilayer films after degradation, the crystals coated with films were washed and dried before each measure as the same to the process used in film construction. The dried crystal was installed in *in situ* quartz crystal microbalance (QCM with dissipation monitoring, D300, Qsense, Sweden). The frequency covered with and without film was measured by its excitation at 5 and 15 MHz.

Confocal Laser Scanning Microscopy (CLSM). Capsules suspensions alone were observed with a Leica TCS SP2 AOBS (Acoustico Optical Bean Splitter) confocal laser scanning system and an inverted fluorescence microscope equipped with an oil immersion objective lens 63 \times . The capsules after 20 min immersion in the dextran^{FITC} 4000 solution (2 mg/ml) was visualized by excitation of the fluorochrome with a 488 nm Argon/krypton laser and the emitted fluorescence was collected between 497 and 576 nm, precisely defined by the AOBS.

Field Emission Gun Scanning Electron Microscopy (FEG-SEM). Drops of the capsules suspensions were deposited onto mica and allowed to air dry. The samples were sputtered with Au/pd, and observed in secondary electron imaging mode with a Jeol JSM6100 microscope using an accelerating voltage of 8kV. For high resolution SEM analysis, the specimens were coated by 2 nm of carbon, and observed in secondary electron imaging mode with a Zeiss ultra 55 FEG-SEM (CMTC-INPG, Grenoble) at an accelerating voltage of 1 kV, using an in-lens detector.

Transmission Electron Microscopy (TEM). The samples were fixed with 2.5% glutaraldehyde in 0.1M sodium cacodylate buffer at pH 7.2 for one hour at room temperature. Then the sample were post-fixed in 1% osmium tetroxide in water for one hour at 4°C, and dehydrated in graded series of ethanol and infiltrated with an ethanol/epoxy resin mixture. The samples were embedded in Epon. Ultrathin sections (60nm) were prepared with a diamond knife on an UC6 Leica ultramicrotome and collected on 400µm mesh copper grids. Ultrathin sections were post-stained with 5% uranyl acetate in water and lead citrate before examining on a Philips CM200 transmission electron microscope.

References:

- (1) Heuberger, R.; Sukhorukov, G.; Vörös, J.; Textor, M.; Möhwald, H. *Advanced Functional Materials* **2005**, *15* 357.
- (2) Zhang, F.; Wu, Q.; Chen, Z.-C.; Li, X.; Jiang, X.-M.; Lin, X.-F. *Langmuir* **2006**, *22*, 8458.
- (3) Del Mercato, L.; Rivera-Gil, P.; Abbasi, A. Z.; Ochs, M.; Ganas, C.; Zins, I.; Sönnichsen, C.; Parak, W. J. *Nanoscale* **2010**, *2*, 458.
- (4) Ibarz, G.; Dähne, L.; Donath, E.; Möhwald, H. *Adv. Mater.* **2001**, *13*, 1324.
- (5) Köhler, K.; Sukhorukov, G. B. *Advanced Functional Materials* **2007**, *17*, 2053.
- (6) Lvov, Y.; Antipov, A. A.; Mamedov, A.; Möhwald, H.; Sukhorukov, G. B. *Nano Lett.* **2001**, *1*, 125.
- (7) De Geest, B. G.; Jonas, A. M.; Demeester, J.; De Smedt, S. C. *Langmuir* **2006**, *22*, 5070.
- (8) Kreft, O.; Skirtach, A. G.; Sukhorukov, G. B.; Möhwald, H. *Adv. Mater.* **2007**, *19*, 3142.
- (9) Szarpak, A.; Cui, D.; Dubreuil, F.; De Geest, B. G.; De Cock, L. J.; Picart, C.; Auzely-Velty, R. *Biomacromolecules* **2010**, *11*, 713.
- (10) De Geest, B. G.; Vandenbroucke, R. E.; Guenther, A. M.; Sukhorukov, G. B.; Hennink, W. E.; Sanders, N. N.; Demeester, J.; De Smedt, S. C. *Advanced Materials (Weinheim, Germany)* **2006**, *18*, 1005.
- (11) De Geest, B. G.; Sukhorukov, G. B.; Möhwald, H. *Expert Opin. Drug Deliv.* **2009**, *6*, 613.
- (12) Piskin, E. *J. Biomater. Sci. Polym. Ed.* **1995**, *6*, 775.
- (13) Richert, L.; Boulmedais, F.; Lavallo, P.; Mutterer, J.; Ferreux, E.; Decher, G.; Schaaf, P.; Voegel, J.-C.; Picart, C. *Biomacromolecules* **2004**, *5*, 284.
- (14) Etienne, O.; Schneider, A.; Addei, C.; Richert, L.; Schaaf, P.; Voegel, J.-C.; Egles, C.; Picart, C. *Biomacromolecules* **2005**, *6*, 726.
- (15) Picart, C.; Schneider, A.; Etienne, O.; Mutterer, J.; Schaaf, P.; Egles, C.; Jessel, N.; Voegel, J.-C. *Advanced Functional Materials* **2005**, *15*, 1771.
- (16) Schneider, A.; Richert, L.; Francius, G.; Voegel, J. C.; Picart, C. *Biomed. Mater.* **2007**, *2*, S45.
- (17) Schneider, A.; Vodouhê, C.; Richert, L.; Francius, G.; Le Guen, E.; Schaaf, P.; Voegel, J. C.; Frisch, B.; Picart, C. *Biomacromolecules* **2007**, *8*, 139.

- (18) Wood, K. C.; Boedicker, J. Q.; Lynn, D. M.; Hammond, P. T. *Langmuir* **2005**, *21*, 1603.
- (19) Vazquez, E.; Dewitt, D. M.; Hammond, P. T.; Lynn, D. M. *Journal of the American Chemical Society* **2002**, *124*, 13992.
- (20) Fredin, N. J.; Zhang, J. T.; Lynn, D. M. *Langmuir* **2005**, *21*, 5803.
- (21) Jewell, C. M.; Zhang, J. T.; Fredin, N. J.; Lynn, D. M. *J. Control Release* **2005**, *106*, 214.
- (22) Zhang, J. T.; Chua, L. S.; Lynn, D. M. *Langmuir* **2004**, *2004*, 19.
- (23) Little, S. R.; Lynn, D. M.; Puram, S. V.; Langer, R. *J. Control Release* **2005**, *107*, 449.
- (24) Lynn, D. M. *Soft Matter* **2006**, *2*, 269.
- (25) Lynn, D. M. *Adv. Mater.* **2007**, *19*, 4118.
- (26) De Geest, B. G.; Van Camp, W.; Du Prez, F. E.; De Smedt, S. C.; Demeester, J.; Hennink, W. E. *Chemical Communications (Cambridge, United Kingdom)* **2008**, 190.
- (27) Richert, L.; Schneider, A.; Vautier, D.; Vodouhe, C.; Jessel, N.; Payan, E.; Schaaf, P.; Voegel, J. C.; Picart, C. *Cell Biochem. Biophys.* **2006**, *44*, 273.
- (28) Kadi, S.; Cui, D.; Bayma, E.; Boudou, T.; Nicolas, C.; Glinel, K.; Picart, C.; Auzély-Velty, R. *Biomacromolecules* **2009**, *10*, 2875.
- (29) Baier, L. J.; Bivens, K. A.; Patrick, C. W. J.; Schmidt, C. E. *Biotechnol. Bioeng.* **2003**, *82*, 578.
- (30) Szarpak, A.; Pignot-Paintrand, I.; Nicolas, C.; Picart, C.; Auzely-Velty, R. *Langmuir* **2008**, *24*, 9767.
- (31) Lynn, D. M.; Langer, R. *Journal of the American Chemical Society* **2000**, *122*, 10761.
- (32) Funhoff, A. M.; van Nostrum, C. F.; Janssen, A. P. C. A.; Fens, M. H. A. M.; Crommelin, D. J. A.; Hennink, W. E. *Pharmaceutical Research* **2004**, *21*, 170.
- (33) Wang, J.; Mao, H.-Q.; Leong, K. W. *Journal of the American Chemical Society* **2001**, *123*, 9480.
- (34) Lu, Z.-Z.; Wu, J.; Sun, T.-M.; Ji, J.; Yan, L.-F.; Wang, J. *Biomaterials* **2008**, *29*, 733.
- (35) Van Dijk-Violthuis, W. N. E.; J., V. S. M.; Underberg, W. J. M.; Hennink, W. E. *Journal of pharmaceutical sciences* **1997**, *86*, 413.
- (36) Van Dijk-Volthuis, W. N. E.; Tsang, S. K. Y.; Kettenes-Van Den, J. J.; Hennink, W. E. *Polymer* **1997**, *38*, 6235.
- (37) Ostergaard, J.; Larsen, C. *Molecules* **2007**, *12*, 2396.
- (38) Lutén, J.; Akeroyd, N.; Funhoff, A.; Lok, M. C.; Talsma, H.; Hennink, W. E. *Bioconjugate Chem.* **2006**, *17*, 1077.
- (39) Rodriguez-Parada, J. M.; Duran, R.; Wegner, G. *Macromolecules* **1989**, *22*, 2507.
- (40) Kudlay, A.; Olvera de la Cruz, M. *J. Chem. Phys.* **2004**, *120*, 404.
- (41) Langevin, D. *Advances in colloid and interface science* **2009**, *147-148*, 170.
- (42) Szapark, A. *Thesis* **2009**.
- (43) Antipov, A. A.; Shchukin, D.; Fedutik, Y.; Petrov, A. I.; Sukhorukov, G. B.; Mohwald, H. *Colloids and Surfaces, A: Physicochemical and Engineering Aspects* **2003**, *224*, 175.
- (44) Volodkin, D. V.; Petrov, A. I.; Prevot, M.; Sukhorukov, G. B. *Langmuir* **2004**, *20*, 3398.
- (45) Petrov, A. I.; Volodkin, D. V.; Sukhorukov, G. B. *Biotechnology Progress* **2005**, *21*, 918.

General conclusion and perspectives (*En*)

Up to now, due to the potential biomedical applications of capsules, the requirement of their biocompatibility and biodegradability raised up. Since recent researches demonstrated that capsules based partially on polysaccharides showed good biocompatibility and could be biodegraded using enzyme, in this work, we focused on the fabrication of multilayer capsules based fully on polysaccharides. These capsules were prepared by layer-by-layer deposition of oppositely charged polyelectrolytes on a sacrificial colloidal template of CaCO_3 particles, followed by a step of the core removal. As such carriers possess a fantastic multicompartemental structure with the possibility to introduce a high degree of functionality at the nanometer scale within the shell, we focused on the chemical modification of chitosan and hyaluronic acid in order to prepare polysaccharide capsules able to incorporate various types of drug and release them under well-defined stimuli.

To this end, we first modified chitosan (CHI) with quaternary ammonium groups and used the resulting quaternized chitosan (QCHI) derivatives to develop contact-killing capsules. The QCHI derivatives with various degree of substitution and grafted positions were synthesized under acidic (homogenous) and neutral (heterogeneous) conditions. These derivatives show good water-solubility at neutral pH and allowed to form stable capsules combining hyaluronic acid (HA) without chemically cross-linking the layers. The morphology and the antibacterial activity of these capsules were found to be strongly dependent on the structure (grafting positions) and the DS of QCHI derivatives. Since these capsules still retained biocompatibility towards myoblast cells, such capsules displaying effective cationic contact-killing antimicrobial abilities could offer a distinct advantage for the delivery of drugs especially for the treatment of some bacterial infections.

As the capsules based on the QCHI derivatives and HA showed good stability, the QCHI derivatives were next selected in the preparation of capsules to load hydrophobic drugs. Alkyl HA derivatives were used instead of HA for the formation of capsules since they showed good ability to incorporate the hydrophobic dyes, Nile red (NR), by hydrophobic interactions. It was found that the high degree of substitution (DS) of modified polysaccharides derivatives was essential to obtain stable capsules. The loading of NR in the nanoshell of capsules was realized by first complexing NR with alkyl HA derivatives in solution, then depositing these NR-containing solution according to the capsules formation process. Due to the high amount of NR trapped in the shell of capsules and the durability of drug entrapment under

physiological conditions, these hydrophobic polysaccharide nanoshells open new avenues for applications in nanomedicine, as hydrophobic drug-carrier systems as well as coatings of medical devices or implantable biomaterials. Current work in CERMAV concerning this part focuses on the encapsulation of various hydrophobic drugs in the shell of capsules, and furthermore, the entrapment of both hydrophobic and hydrophilic drugs in the shell and the cavity of capsules, respectively.

Although capsules based on polysaccharides can load several drugs, the release of the drugs by biodegradation was quite difficult, even using high concentration of enzyme. In order to release the payload in the capsules without suffering the external harsh stimuli, a new kind of rapidly degradable capsules was designed at the end of this work. These capsules were prepared based on HA combining the cationic labile derivatives of dextran (dextran-dimethylaminoethanol, dextran-DMAE). The results of degradation study showed that the degradation rate of multilayer assemblies based on hydrolysable polyelectrolytes was much slower than that of the polymers in solution. The rapid degradation of capsules was realized under alkaline conditions, pH 10.5, which could be attributed to the deprotonation of cationic groups and the hydrolysis of the side chain of dextran derivatives.

Overall, this work showed the ability to prepare tailor-made capsules from chemically modified polysaccharides but further improvements are required.

In our case, the capsules based solely on polysaccharides showed a high permeability in PBS towards the small hydrophilic molecules, Dextran^{FITC}-4 (Mw of Dextran^{FITC} ~ 4000 g/mol). Since the hydrodynamic radius of Dextran^{FITC}-4 (~ 2 nm) is similar to or a little smaller than that of some real hydrophilic drugs, the higher permeability of capsules indicates that these capsules were not efficient to load the hydrophilic drugs with that size. Therefore, in order to decrease the porosity of capsules wall, the built-up conditions of capsules should be optimized.

Otherwise, it was found that both the enzymatic degradation of the capsules containing polysaccharides ((HA/QCHI)_{4.5} capsules) and the hydrolysis of the capsules composed of hydrolysable polyelectrolytes ((HA/dextran-DMAE)_{4.5} capsules) at neutral pH were difficult. The slow degradation rate of these two kinds of capsules is probably attributed to the twinkled chains of oppositely charged polymers and the thicker shell of capsules, which impede the escape of degraded polymer chains. In the latter case, adding enzyme may be the other method to improve the degradability of capsules.

Additionally, considering the potential applications of capsules in drug delivery, especially in the encapsulation of anticancer drugs, the capsules should be able to circulate in the bloodstream without aggregating. However, the current systems could not satisfy these requirements. Similar to the diameter of CaCO_3 particles, the size of the capsules presented in this work is $\sim 4 - 6 \mu\text{m}$. The agglomeration of capsules was found in all cases, which was probably due to the weak complexation ability of polysaccharides. We tried to alter the size of capsules by decreasing the size of template, but the aggregation of capsules was enlarged. Thus, one of the challenges in the future is to avoid the agglomeration of capsules and at meanwhile to decrease the size of capsules.

Conclusion générale et perspectives (*Fr*)

Compte tenu de leurs applications biomédicales potentielles, les capsules multicouches supposent d'être biocompatibles et biodégradables. Dans la mesure où des travaux récents ont montré la possibilité d'obtenir des capsules biocompatibles à base de polysaccharides et potentiellement dégradables par des enzymes présentes dans le corps, nous nous sommes concentrés dans ce travail sur la fabrication de capsules multicouches constituées uniquement de polysaccharides. Ces capsules ont été préparées par dépôt couche-par-couche de polyélectrolytes de charges opposées sur des particules sacrificielles de CaCO_3 , suivie de la dissolution de ces supports. Du fait de la structure multicompartement de ces systèmes transporteurs et de la possibilité de fonctionnaliser la paroi de façon versatile, nous avons consacré une grande partie de notre travail à la modification chimique du chitosane et de l'acide hyaluronique dans l'objectif de préparer des capsules qui soient capables d'incorporer différents types de médicaments et de les libérer en réponse à des stimuli bien définis.

À cette fin, nous avons modifié le chitosane (CHI) avec des groupes ammonium quaternaire et nous avons utilisé les dérivés quaternisés résultants (QCHI) pour concevoir des capsules capables de tuer des bactéries par simple contact. Les dérivés QCHI avec différents degrés de substitution et différentes positions de greffage ont été synthétisés en milieu acide ou neutre (conditions homogènes ou hétérogènes, respectivement). Ces dérivés montrent une bonne solubilité dans l'eau à pH neutre et permettent de former des capsules stables par complexation avec l'acide hyaluronique (HA) malgré l'absence de pontages covalents entre les couches. La morphologie et l'activité antibactérienne de ces capsules se sont avérées être fortement dépendantes de la structure (positions de greffage) et du DS des dérivés QCHI. Puisque ces capsules montrent une bonne biocompatibilité vis-à-vis des cellules myoblastes, elles pourraient offrir un avantage distinct pour le traitement de certaines infections bactériennes.

Compte tenu de la bonne stabilité des capsules préparées à base de QCHI et de HA, les dérivés QCHI ont été sélectionnés dans la suite de notre travail pour préparer des capsules pouvant incorporer des principes actifs hydrophobes. Des dérivés alkylés du HA ont été utilisés pour la formation de tels capsules du fait de leur capacité à solubiliser des molécules hydrophobes par formation de nanodomains hydrophobes en milieu aqueux. Il a été constaté qu'un degré de substitution élevé des dérivés de polysaccharides modifiés est essentiel pour obtenir des capsules stables. L'insertion d'une sonde fluorescente hydrophobe, le Nile red (NR)

dans la paroi des capsules a été réalisée par pré-complexation avec les dérivés alkylés du HA en solution, avant l'étape de dépôt couche-par-couche. Ces parois hydrophobes qui sont capables de piéger une grande quantité de molécules hydrophobes dans des conditions physiologiques, ouvrent de nouvelles voies vers des applications en nanomédecine, comme systèmes transporteurs de médicaments hydrophobes ou comme revêtements de dispositifs médicaux ou biomatériaux implantables. Les travaux en cours au sein du CERMAV concernent le premier aspect ainsi que l'encapsulation simultanée de deux médicaments, hydrophobes et hydrophiles, dans la paroi et la cavité des capsules, respectivement.

Bien que les capsules à base de polysaccharides puissent encapsuler plusieurs médicaments, la libération des médicaments par biodégradation peut s'avérer difficile. Afin de libérer la charge utile dans les capsules, un nouveau type d'assemblage multicouche rapidement dégradable a été conçu à la fin de ce travail. Cet assemblage a été préparé à partir de HA et de dextrane porteur de groupements cationiques labiles (dextrane-diméthylaminoéthanol, dextrane-DMAE). Les résultats de cette étude indiquent que la vitesse de dégradation des assemblages multicouches est beaucoup plus lente que celle des dérivés de dextrane en solution. La dégradation rapide des capsules a été réalisée dans des conditions alcalines (pH 10,5), ce qui a été attribué à la déprotonation des groupements cationiques et à l'hydrolyse de la chaîne latérale des dérivés du dextrane.

Ce travail de thèse a montré la possibilité de préparer des capsules « sur mesure à base de polysaccharides chimiquement modifiés », mais des améliorations sont encore nécessaires.

Dans notre cas, les capsules à base uniquement de polysaccharides ont montré une perméabilité élevée dans le PBS vis-à-vis de petites molécules hydrophiles, telles que le Dextrane^{FITC}-4 (Mw de Dextran^{FITC} ~ 4000 g / mol). Par conséquent, afin de diminuer la porosité de la paroi des capsules, les conditions de synthèse des capsules doivent être optimisées.

En outre, tenant compte des applications potentielles des capsules pour la libération de médicaments, celles-ci doivent pouvoir circuler dans le sang. Les systèmes actuels ne peuvent pas satisfaire à ces exigences. Ayant un diamètre similaire à celui des particules CaCO₃, la taille des capsules décrites dans ce travail est d'environ 4 à 6 µm. Ces capsules ont de plus tendance à s'agréger dans certaines conditions du fait des propriétés de leur paroi, très hydrophile, stabilisée uniquement par complexation polyanion-polycation. Ainsi, l'un des défis futurs est d'éviter l'agglomération de capsules et de réduire leur taille.

Annexes

List of Figures

- Figure 1.1: The cell envelope structure of bacteria designated by a Gram strain. 18
- Figure 1.2: Three stages of the variation of the antibacterial activity of CHI as a function of the concentration changes of CHI. 21
- Figure 1.3: Structure of CHI derivatives with anionic groups (10 *O*- carboxymethyl CHI, 11, n=1 *N,O*-carboxymethyl CHI, 12, n=2 *N,O*-carboxyethyl CHI, 13, n=3 *N,O*-carboxypropyl CHI, 14, n=4 *N,O*-carboxybutyl CHI, 15 *N, O*-sulfate CHI, 16 *N*-vinylsulfate CHI, and 17 *N*-(2-methacryloyl oxyethyl) phosphate CHI). 26
- Figure 1.4: Structure of CHI derivatives with hydrophobic neutral groups (18, n=0 *N*-acetyl CHI, 19, n=1 *N*-propionyl CHI, 20, n=2 *N*-butyl CHI, 21, n=3 *N*-vinyl CHI, 22, n=4 *N*-hexanoyl CHI, 23 (*N,O*-sulfate)-*N*-propanoyl CHI, 24 (*N,O*-sulfate)-*N*-hexanoyl CHI, 25 (*N,O*-quaternized)-*N*-benzyl CHI and 26 (*N,O*-quaternized)-*N*-octyl CHI). 29
- Figure 1.5: Comparison of rheological behaviors of CHI and its *N*-acrylated CHI derivatives. (solvent: 0.3 M HAc-0.05M NaAc; T =25 °C).⁶² 30
- Figure 1.6: Schematic representation of intramolecular aggregates and intermolecular cross-links of *N*-acrylated CHIs with desired amount of hydrophobic alkyl chains (a small loop in a micelle is called “petal” and a subchain connecting two junctions on different chains is call “bridge”).⁶² 30
- Figure 1.7: Structure of CHI derivatives with hydrophilic neutral groups (27 *N*-lactosyl CHI, 28 *N*-cellobiosyl CHI, 29 *N*-maltosyl CHI, 30 *N,O*-quaternized CHI, 31 (*N,O*-quaternized)-*N*-xylosyl CHI, 32 (*N,O*-quaternized)-*N*-xylosyl CHI, 33 (*N,O*-quaternized)-*N*-arabinosyl CHI, 34 (*N,O*-quaternized)-*N*-glucosyl CHI, 35 (*N,O*-quaternized)-*N*-galactosyl CHI, 36 (*N,O*-quaternized)-*N*-lactosyl CHI, 37 (*N,O*-quaternized)-*N*-cellobiosyl CHI, 38 (*N,O*-quaternized)-*N*-melibiosyl CHI, 39 (*N,O*-quaternized)-*N*-maltosyl CHI and 40 *O*-hydroxyethyl CHI). 32
- Figure 1.8: Structure of CHI derivatives modified with amino groups (41 *O*-chitin or *O*-chitosan CHI, 42 *O*-ethyldiamine CHI and 43 (*O*-hydroxyethyl)-*N,O*-ethylamine CHI). 34
- Figure 1.9: Structure of CHI derivatives containing tertiary amide groups (44 *O*-aminoethyl CHI, 45 *O*-dimethylaminoethyl CHI and 46 *O*-diethylaminoethyl CHI). 36
- Figure 1.10: Structure of cationic CHI derivatives obtained by methylation (47 (*O*-methyl)-*N,N,N*-trimethyl CHI, 48 (*O*-methyl)-*N,N*-dimethyl-*N*-propyl CHI, 49 (*O*-methyl)-*N,N*-dimethyl-*N*-butyl CHI, 50 (*O*-methyl)-*N,N*-dimethyl-*N*-octyl CHI, 51 (*O*-methyl)-*N,N*-diimethyl-*N*-dodecyl CHI, 52 (*O*-methyl)-*N*-methyl-*N,N*-dibutyl CHI, 53 (*O*-methyl)-*N,N*-dimethyl-*N*-furfuryl CHI, 54 *O*-triethylaminoethyl CHI, 55 (*O*-methyl)-*N*-(4-

trimethylaminocinnamyl) CHI, 56 (<i>O</i> -methyl)- <i>N</i> -(4-trimethylaminobenzyl) CHI and 57 (<i>O</i> -methyl)- <i>N</i> -(4-methylpyridyl) CHI).....	37
Figure 1.11: Structure of CHI derivatives modified with quaternized groups (58 <i>N,O</i> -hydropropyltrimethyl CHI, 59 <i>N</i> -hydropropyltrimethyl CHI, 60 <i>N</i> -hydropropyltriethyl CHI, 61 <i>N</i> -hydropropyltripropyl CHI, 62 <i>N</i> -hydropropyltributyl CHI and 63 <i>N</i> -hydropropyldimethylbenzyl CHI and 64 <i>N</i> -betainate CHI).....	40
Figure 1.12: Three chief strategies to design an antibacterial surface. ⁸⁹	41
Figure 1.13: Process of the construction the polyelectrolyte multilayers (PEM) films by layer-by-layer technique. ⁸⁹	42
Figure 1.14: Structures of Keggin-type polyoxometalate (POM) (α -[SiW ₁₂ O ₄₀] ⁴⁻ (α -SiW ₁₂)). ²⁵	43
Figure 1.15: Pairs of polyelectrolyte polymers used in the PEM films showing the antibacterial activity.	44
Figure 1.16: The simulation mechanism of reversible pH-dependent transition behavior of (PAH/PAA) and (PAH/PAA) PEM films. At lower pH, the films swells due to strongly electrostatic repulsion of the protonated amino groups; at higher pH, the non-protonated amino groups form the microhydrophobic domains, which cause the formation of rather thinner films. Once these films are washed at neutral pH, the protonated amino groups highly concentrate on the surface of the films just undergoing the incubation step at lower pH and bring out the antibacterial activity. ¹⁰⁴	45
Figure 2.1: ¹ H NMR spectra of initial CHI (400 MHz, D ₂ O + DCl, 80 °C, C _p ~ 6 g/L).	57
Figure 2.2: The reduced viscosity of CHI and its derivatives determined as a function of polymer concentration in aqueous 0.3 M AcOH/0.1 M AcONa solution at 25 °C: A) initial CHI and its <i>N</i> -QCHI derivatives and B) initial CHI and its <i>N,O</i> -QCHI derivatives.	61
Figure 2.3: Plots of intrinsic viscosities of QCHI derivatives as a function of DS: A) for the <i>N</i> -QCHI derivatives and B) for the <i>N,O</i> -QCHI derivatives.	63
Figure 2.4: Simulation of the grafting position of <i>N,O</i> -QCHI3b derivatives.	65
Figure 2.5: Antibacterial activity against <i>E. coli</i> of A) the most substituted <i>N,O</i> -QCHI derivatives, <i>N,O</i> -QCHI3a (DS = 1.33) and <i>N,O</i> -QCHI3b (DS = 1.10) and B) the <i>N</i> -QCHI derivatives (the DS of <i>N</i> -QCHI2-5 correspond to 0.31, 0.39, 0.55 and 0.66, respectively). All QCHI samples were dissolved in PBS at a concentration of 1.25 mM.....	66
Figure 2.6: Hydrodynamic radius of FITC and FITC labeled dextran molecules (Dextran ^{FITC}) at different Mw. ¹⁴⁻¹⁶	94
Figure 2.7: Schematic illustration of images of a single suspended shell which can be obtained in the presence of fluorescent probes. The green colour indicates regions of lower or higher fluorescent intensity according to the local concentration distribution of the probe (outside/shell wall/inside). Black regions mean the absence of fluorescent probes. ¹⁷ ...	94

Figure 2.8: CLSM images of capsules based on HA and <i>N</i> -QCHI2 (DS = 0.31) obtained after 20 min of contact with Dextran ^{FITC} : A) Dextran ^{FITC} -4 and B) Dextran ^{FITC} -2000.....	95
Figure 2.9: Permeability of capsules based on HA and QCHI derivatives: A) effect of the salt on the permeability of capsules to Dextran ^{FITC} -4 in MES buffer (pH 6.5) and B) effect of Mw of Dextran ^{FITC} on the permeability of capsules in PBS. The <i>N</i> -QCHI derivatives with DS of 0.31, 0.39, 0.55 and 0.66 correspond to <i>N</i> -QCHI2-5, respectively.	96
Figure 2.10: Investigation of enzymatic degradation of capsules by CLSM: A) CLSM image of capsules incubated in PBS at room temperature overnight and B) CLSM image of capsules incubated in PBS with contact of hyaluronidase (500 U/mL) overnight.	97
Figure 2.11: Comparison of antibacterial activity of <i>N</i> -QCHI derivatives solutions and capsules based on HA and <i>N</i> -QCHI derivatives ended by either HA or <i>N</i> -QCHI derivatives against <i>E. coli</i> . Cap. (HA/ <i>N</i> -QCHI)4.5 and Cap (HA/ <i>N</i> -QCHI)5 mean the capsules prepared based on the pair of HA/ <i>N</i> -QCHI ended by HA and <i>N</i> -QCHI, respectively ($C_p \sim 1.25$ mM; Capsules/bacterial cells ratio ~ 100)......	98
Figure 2.12: Investigation of antimicrobial activity of (HA/ <i>N</i> -QCHI5) capsules against <i>E. coli</i> by TEM: A) <i>E. coli</i> ; B) HA-ended capsules with <i>E. coli</i> and C) <i>N</i> -QCHI5-ended capsules with <i>E. coli</i>	99
Figure 2.13: (HA/ <i>N,O</i> -QCHI) film growth monitored in situ by QCM-D. Differences in A) frequency shifts measured at 15 MHz and B) film thickness are plotted for each HA and <i>N,O</i> -QCHI derivatives deposited layer up to four layer pairs.....	100
Figure 2.14: TEM images of (HA/ <i>N,O</i> -QCHI) multilayer films coated CaCO ₃ particles: A) 4.5 (HA/ <i>N,O</i> -QCHI3a) bilayers; B) 4.5 (HA/ <i>N,O</i> -QCHI3b) bilayers.	100
Figure 2.15: Observation of capsules based on HA and <i>N,O</i> -QCHI derivatives with 4.5 bilayers by SEM and CLSM.	101
Figure 2.16: AFM images of dried (HA/ <i>N,O</i> -QCHI) _{4.5} capsules with corresponding profiles: A) and C) correspond to the (HA/ <i>N,O</i> -QCHI3a) _{4.5} capsules and B) and D) (HA/ <i>N,O</i> -QCHI3b) _{4.5} correspond to capsules.....	102
Figure 2.17: SEM images of capsules with 4.5 bilayers prepared based on HA and QCHI derivatives with different DS: A-C). <i>N,O</i> -QCHIa and D-E). <i>N,O</i> -QCHIb.	104
Figure 2.18: Permeability of capsules with 4.5 bilayers prepared based on HA and <i>N,O</i> -QCHI derivatives. A) effect of the salt on the permeability of capsules to Dextran ^{FITC} -4 in MES buffer (pH 6.5); B) effect of Mw of Dextran ^{FITC} on the permeability of capsules in PBS. The <i>N,O</i> -QCHI derivatives with DS of 1.33 and 1.10 correspond to <i>N,O</i> -QCHI3a and <i>N,O</i> -QCHI3b, respectively.	105
Figure 2.19: Comparison of antibacterial activity of <i>N,O</i> -QCHI derivatives solutions and capsules based on HA and <i>N,O</i> -QCHI derivatives ended by either HA or <i>N,O</i> -QCHI derivatives against <i>E. coli</i> . (HA/ <i>N,O</i> -QCHI) _{4.5} capsules and (HA/ <i>N,O</i> -QCHI) ₅ capsules are terminated by HA and <i>N,O</i> -QCHI, respectively. ($C_p \sim 1.25$ mM; Capsules/bacterial cells ratio ~ 100).	106

Figure 2.20: Investigation of antimicrobial activity of capsules based on HA and N,O-QCHI derivatives by CLSM and TEM (capsules/bacterial cells ratio ~ 1).....	107
Figure 3.1: Comparison of ¹ H spectra of HA18C10 and HA20C10 (400 MHz, D ₂ O, 80 °C, C _p ~ 6 g/L).....	132
Figure 3.2: Comparison of the storage and loss moduli as a function of frequency for the solutions of HA18C10 and HA20C10 (10 g/L in PBS at 25 °C).....	134
Figure 3.3: SEM and CLSM images of capsules based on N,O-QCHI3a and decyl-grafted HA derivatives with different DS. In all cases, NR was loaded in the nanoshell during the process of capsules construction by pre-complexation with decyl-grafted HA derivatives. .	134
Figure 3.4: Permeability of capsules based on HA20C10 combining N,O-QCHI derivatives, A) N,O-QCHI3a and B) N,O-QCHI3b, respectively, towards Dextran ^{Fluorescein} with different Mw in the phosphate buffer (at pH 6.5, C _{phosphate} ~ 0.01M) with and without the adding of NaCl (C _{NaCl} ~ 0.14 M).....	135
Figure 3.5: Comparison of antibacterial activity of capsules based on N,O-QCHI derivatives combining A) HA20C10 and B) HA ended by against <i>E. coli</i> (Capsules/bacterial cells ratio ~ 100).	137
Figure 3.6: Investigation of antibacterial activity of capsules based on HA and N,O-QCHI derivatives by CLSM (capsules/bacterial cells ratio ~ 1): A) (HA20C10/N,O-QCHI3a) ₅ capsules and B) (HA20C10/N,O-QCHI3b) ₅ capsules.....	137
Figure 4.1: Structure of hydrolysable polymers used for the fabrication of multilayer films and capsules: 1a, 1b and 1c belong to the family of poly(β-amino ester), 2 and 3 are the polymers containing carbonate ester groups and 4 is poly(2-aminoethyl propylene phosphate) (PPE-EA).	145
Figure 4.2: Structure of the neutral polysaccharides used to prepare hydrolysable polycations: 5 dextran, 6 HEC and 7 Guar.....	147
Figure 4.3: FT-IR spectra of dextran and its cationic derivatives (dextran-DMAE).	149
Figure 4.4: ¹ H NMR spectra of A) DMAE-CI dissolved in CDCl ₃ at 25 °C and B) dextran-DMAE dissolved in D ₂ O+DCl at 80 °C.....	150
Figure 4.5: ¹ H NMR spectrum of HEC-DMAE dissolved in D ₂ O+DCl at 80 °C.	151
Figure 4.6: ¹ H NMR spectra of dextran-DMAE (~ 6 mg/ml) in phosphate buffer (pH 7.4 at 25 °C) recorded for A) 20 h and B) 1 h after dissolution. In order to facilitate the recording, the dextran was represented in a simplified form without branched glucose moieties.....	153
Figure 4.7: Analysis of the hydrolysis of dextran-DMAE under different conditions: A) variation of the DS as a function of time and B) variation of the DD as a function of time..	154
Figure 4.8: QCM frequency shift -Δf/v during the alternate deposition of (◆) HA/dextran-DMAE and (■) HA/PAH obtained at harmonics 5 MHz as a function of deposited layer.	

HA and the polycations were used at a concentration of 5g/L and 2g/L in phosphate buffer at pH 6.5 with 0.14 M NaCl, respectively.....	157
Figure 4.9: Observation of a) CaCO ₃ microparticles and the particles coated with b) 0.5, c) 2.5 and d) 4.5 bilayers of HA/dextran-DMAE by FEG-SEM.....	158
Figure 4.10: Observation of (HA/dextran-DMAE) _{4.5} microcapsules in PBS incubated with Dextran ^{FITC} -4 (Mw ~ 4000 g/mol).	159
Figure 4.11: QCM-D frequency shift $-\Delta f/v$ during the degradation study of (◆) HA/Dextran-DMAE and (■) HA/PAH obtained at harmonics 5 MHz as a function of time. HA and the polycations were used at a concentration of 5g/L and 2g/L in phosphate buffer at pH 6.5 with 0.14 M NaCl, respectively.....	161
Figure 4.12: (Dextran-DAME/HA) _{4.5} capsules incubated in HEPES buffer at different pH observed par TEM after 1 day: A). at pH 7.4 and B). at pH 10.5. The white arrow in A marks the shell of hollow (dextran-DAME/HA) _{4.5} capsules.....	162
Figure 4.13: Comparison of the IR spectra of dried (HA/dextran-DMAE) _{4.5} capsules incubated in HEPES buffer at different pH at 25 °C after 3 days.....	163

List of Schemes

Scheme 1.1: Synthetic pathway of <i>O</i> -chitin/chitosan CHI. ⁶⁴	35
Scheme 2.1: Strategies for the synthesis of QCHI derivatives reported in the literature (1 chitosan (CHI), 2 and 3 quaternized chitosan derivatives (QCHI derivatives) prepared by different ways).....	56
Scheme 4.1: Synthesis of dextran modified with labile cationic groups.	148
Scheme 4.2: Synthesis of cationic dextran derivatives.	151
Scheme 4.3: Proposed reaction mechanisms for the (A) acid catalyzed, (B) water catalyzed and (C) base catalyzed hydrolysis of carbonate esters.....	154

List of Tables

Table 1.1: Structures of polysaccharides used for the synthesis of multilayer assemblies via electrostatic interaction and the pK _a values of their functional groups.....	14
Table 1.2: Gram bacteria applied in the test of antibacterial activity of CHI.....	18
Table 1.3 : The effect of molar mass on the antibacterial activity of CHI against <i>E. coli</i> according to different authors. (M _w : weight average molar mass; M _v : viscosity average molar mass)	24
Table 2.1: QCHI derivatives with different DS and water-solubility prepared under different reaction conditions.....	59
Table 2.2: The intrinsic viscosities [η] and Huggins constant k_H derived from the measurement of reduced viscosities of the <i>N</i> -QCHI derivatives.	62
Table 2.3: The intrinsic viscosities [η] and Huggins constant k_H derived from the measurement of reduced viscosities of the <i>N</i> -QCHI derivatives.	62
Table 2.4: The degree of substitution (DS), humidity, weight-average molar mass (M _w), molar mass of the repeating units (M _{RU}), theoretical molar mass (theoretical M _w), weight-average degree of polymerization (DP _w) and weight-average intrinsic viscosity ([η] _w) of CHI and its derivatives.....	64
Table 2.5: The MIC and MBC of QCHI derivatives against <i>B.cereus ATCC 14579</i>	67
Table 2.6: Comparison of the thickness of (HA/ <i>N,O</i> -QCHI) coatings measured by different techniques.....	103
Table 3.1: Decyl-grafted HA derivatives with different DS synthesized by varying the molar ratio of HA/decanal.....	133
Table 4.1: Effect of the reaction conditions on DS and solubility in water at neutral pH of dextran-DMAE.....	152
Table 4.2: Investigation of the complexation of polycations with HA in tubes observed by naked eyes: ---: transparent solution; - slightly transparent gel-like precipitate; + weak turbid solution; ++ turbid solution; +++ small white precipitate and ++++ big white precipitate.....	156
Table 4.3: Comparison of the effect of pH and temperature on the degradation of dextran-DMAE in solution and on the destruction of capsules.....	164

Abbreviations

CHI	Chitosan
DA	Degree of acetylation
DD	Degree of degradation
Dextran-DMAE	Dextran-dimethylaminoethanol
Dextran^{FITC}	FITC labelled dextran
DP_w	Weight-average degree of polymerization
DS	Degree of substitution
HA	Hyaluronic acid
HA^{FITC}	FITC labelled HA
HAxC10	Decylamino hydrazide hyaluronic acid
HEC	Hydroxyethyl cellulose
HEC-DMAE	Hydroxyethyl-dimethylaminoethanol
LbL	Layer-by-Layer
MIC	Minimum inhibitory concentration
MBC	Minimum bactericidal concentration
M_w	Weight-average molar mass
M_{RU}	Molar mass of repeating units
N-QCHI	N-substituted quaternized chitosan
N,O-QCHI	N,O-substituted quaternized chitosan
NR	Nile red
PBS	Phosphate buffer saline
PEM	Polyelectrolyte multilayers
QCHI	Quaternized chitosan
OD	Optical density

Symbols

Δf	Frequency shift
$[\eta]$	Intrinsic viscosity
R_h	Hydrodynamic radius
V_h	Apparent hydrodynamic volume

List of Instruments

AFM	Atomic Force Microscopy
CLSM	Confocal Laser Scanning Microscopy
FEG-SEM	Field Emission Gun Scanning Electron Microscopy
FT-IR	Fourier Transform Infrared Spectroscopy
ITC	Isothermal Titration Calorimetry
NMR	Nuclear Magnetic Resonance Spectroscopy
SEC	Size Exclusion Chromatography
SEM	Scanning Electron Microscopy
TEM	Transmission Electron Microscopy
QCM-D	Quartz Crystal Microbalance with Dissipation

Synthesis and characterization of functional multilayer capsules based on chemically modified polysaccharides

Abstract

This work focused on the design of functional capsules made of chemically modified polysaccharides. The layer-by-layer capsules have attracted great interest due to their advanced multifunctionality, which can be advantageously used for pharmaceutical and biomedical applications. Polysaccharides, which are generally biocompatible and biodegradable, are very attractive materials for the construction of bio-related multilayer systems. Considering the intrinsic antibacterial properties of chitosan (CHI), this polysaccharide was selected and quaternized to prepare in physiological conditions contact-killing capsules by combination with hyaluronic acid (HA). The relationship between the antibacterial activity of the quaternized chitosan derivatives (QCHI) and that of QCHI-based capsules was investigated. Then, in order to encapsulate small hydrophobic drugs within the wall of capsules, alkylated derivatives of HA were used as the negatively charged partner of QCHI for the capsules formation. The encapsulation of the hydrophobic dye, Nile red (NR), in the hydrophobic shell of capsules was determined. At last, to release the payload under mild conditions was studied by synthesizing rapidly degradable capsules composed of hydrolysable cationic dextran derivatives and HA. The degradation of the layer-by-layer assemblies, both multilayer films and microcapsules is discussed.

Key words: layer-by-layer, polysaccharides, microcapsules, antibacterial activity, hydrophobic drug encapsulation, biodegradability

Résumé

Ce travail de thèse porte sur la conception de capsules fonctionnelles à base de polysaccharides chimiquement modifiés. Les capsules couche par couche connaissent actuellement un essor important lié à leur multifonctionnalité pouvant être avantageusement mise à profit dans les domaines pharmaceutique et biomédical. Les polysaccharides, généralement biocompatibles et biodégradables, constituent des matériaux de choix pour la construction de systèmes multicouches. Compte tenu des propriétés antibactériennes intrinsèques du chitosane (CHI), ce polysaccharide a été choisi puis quaternisé afin de préparer dans des conditions physiologiques des capsules par complexation avec l'acide hyaluronique (HA), capables de tuer les bactéries par simple contact. La relation entre l'activité antibactérienne des dérivés quaternisés du chitosane (QCHI) et celle des capsules préparées à partir de QCHI a été étudiée. En outre, afin d'encapsuler des médicaments hydrophobes dans la paroi des capsules, des dérivés alkylés du HA ont été utilisés en tant que partenaire chargé négativement du QCHI pour la formation des capsules. L'encapsulation d'une sonde fluorescente hydrophobe, le Nile rouge (NR), dans le réservoir hydrophobe des capsules a été réalisée avec succès. Enfin, pour libérer des médicaments encapsulés dans des capsules dans des conditions douces, des capsules rapidement dégradables comprenant des dérivés cationiques hydrolysables du dextrane et de HA ont été préparées. La dégradation des assemblages couches par multicouches a été analysée par différentes approches à la fois à partir de capsules et de films plans.

Mots clés: Déposition couche par couche, polysaccharides, microcapsules, activité antibactérienne, encapsulation de médicaments hydrophobes, biodégradabilité